Department of Organic and Medicinal Chemistry

Department of Pharmacy, Health and Nutritional Sciences

NOVEL ANTI-ADENOVIRUS AGENTS BASED ON AMINOGLYCEROL AND PIPERAZINE SCAFFOLDS: DESIGN, SYNTHESIS AND *IN VITRO* BIOLOGICAL EVALUATION

PhD Thesis in joint supervision

Sarah Mazzotta

Seville, September 2020

Department of Organic and Medicinal Chemistry

Department of Pharmacy, Health and Nutritional Sciences

NOVEL ANTI-ADENOVIRUS AGENTS BASED ON AMINOGLYCEROL AND PIPERAZINE SCAFFOLDS: DESIGN, SYNTHESIS AND *IN VITRO* BIOLOGICAL EVALUATION

PhD Thesis in joint supervision

Sarah Mazzotta

Seville, September 2020

Supervisors (University of Seville)

Margarita Vega Holm

Fernando Iglesias Guerra

José Manuel Vega Pérez

Supervisor (University of Calabria)

Francesca Aiello

Departamento de Química Orgánica y Farmacéutica

Dipartimento di Farmacia e Scienze della Salute e della Nutrizione

NOVEL ANTI-ADENOVIRUS AGENTS BASED ON AMINOGLYCEROL AND PIPERAZINE SCAFFOLDS: DESIGN, SYNTHESIS AND *IN VITRO* BIOLOGICAL EVALUATION

Tesis Doctoral en Cotutela

Sarah Mazzotta

Sevilla, septiembre 2020

Directores (Universidad de Sevilla)

Margarita Vega Holm (Tutora)

Fernando Iglesias Guerra

José Manuel Vega Pérez

Directora (Università della Calabria)

Francesca Aiello

Margarita Vega Holm, Fernando Iglesias Guerra, José Manuel Vega Pérez and Francesca Aiello.

Hereby certify:

That Sarah Mazzota has carried out under our direction, and under joint supervision, in the Department of Organic and Medicinal Chemistry of the Faculty of Pharmacy of the University of Seville, and in the Department of Pharmacy, Health and Nutritional Sciences, University of Calabria, the research leading to the Doctoral Thesis entitled: NOVEL ANTI-ADENOVIRUS AGENTS BASED ON AMINOGLYCEROL AND PIPERAZINE SCAFFOLDS: DESIGN, SYNTHESIS AND IN VITRO BIOLOGICAL EVALUATION.

Once this manuscript has been drafted, it has been supervised by us and we find it compliant with the requirements to be presented as a thesis to aspire to the degree of Doctor by the University of Seville and the University of Calabria, before the committee that is duly appointed in its day.

And for the record, in compliance with current provisions, we issue this in Seville on July 16, 2020.

Signed: Margarita Vega Holm

Signed: Fernando Iglesias Guerra

Signed: José Manuel Vega Pérez

Signed: Francesca Aiello

When someone you love becomes a memory,
the memory becomes a priceless treasure.

ABSTRACT

HAdV is a non-enveloped virus that has progressively been recognized as significant viral pathogen. It traditionally causes self-limited respiratory, gastrointestinal and conjunctival infections, mainly in immunocompromised patients. HAdV-induced infections are associated with significant morbidity and mortality, both in immunosuppressed and otherwise healthy individuals. At present, there are no effective and specific antiviral drugs approved for HAdV infections. The current and non-specific therapeutic options provide no satisfactory results in terms of efficacy and safety. Cidofovir is the drug of choice for the treatment of severe HAdV infections, but display low oral bioavailability and nephrotoxicity that limit its use in therapy. Consequently, there is an urgent need to identify new anti-HAdV agents with suitable therapeutic index. In this work, we report the design, synthesis, structural characterization and biological evaluation of new compound libraries as novel anti-HAdV infection inhibitors. Piperazine and aminoalcohols scaffolds were selected to generate new molecules, introducing most common functions present in reported anti-adenovirus agents.

A set of piperazine derivatives (67 compounds) were designed through an optimization process starting from our previous work. Twelve derivatives were identified with significant inhibition of HAdV infections at nanomolar and low micromolar concentrations (IC_{50} from 0.6 μM to 5.1 μM) with low or no cytotoxicity. These compounds were selected for further biological analysis in order to explore their potencial mechanism of action. Our studies suggested that most active compounds inhibited HAdV replicative cycle through different mechanisms of action.

A small library of serinol derivatives (37 compounds) was designed and synthesized in order to evaluate acyclic scaffolds and develop new effective anti-HAdV agents. Four compounds inhibited HAdV infection in a dose-dependent manner, reducing HAdV infection at low micromolar concentrations (from 2.82 to 5.35 μM). Their IC_{50} values were lower compared to that of cidofovir, the current drug of choice. All compounds significantly reduced HAdV DNA replication process.

Finally, a collection of 3-amino-1,2-propanediol (55 compounds) derivatives was designed to further explore the potential of aminoalcohol scaffolds in providing effective antiviral agents. Different synthetic methodologies were employed for the introduction of the acyl/triazole functions at primary or secondary position of the aminoalcohol skeleton. Six derivatives demonstrated a significant inhibition of HAdV infection and displayed IC_{50} values at low micromolar concentration (2.47-4.19 μM). At present these compounds are being submitted to further biological assays in order to select compounds with suitable selectivity index and investigate their potential mechanism of action.

The new data indicate that these new scaffolds may represent a potential tool useful for the development of effective anti-HAdV drugs.

TABLE OF CONTENTS

LIST OF ABBREVIATIONS

A

- AA: arachidonic acid
- ADME: absorption, distribution, metabolism, and excretion
- ADP: adenovirus death proteins
- AEA: arachidonoyl ethanolamide
- AGE: acute gastroenteritis
- ANK: ankyrin
- ANPs: acyclic nucleoside phosphonates
- ATCC: american type culture collection
- AVP: adenovirus protease

B

- BAA: bisandrographolide
- BCV: brincidofovir
- BOILED-egg: brain or intestinal estimated permeation method

C

- CaM: calmodulin
- CAR: coxsackievirus and adenovirus receptor
- CC_{50}: cytotoxic concentration 50%
- CDV: cidofovir
- CI: chemical Ionization
- CMV: cytomegalovirus
- COSY: correlation spectroscopy
- CPE: cytopathic effect
- CuAAC: copper(I)-catalyzed azide alkyne cycloaddition

D

- DBP: DNA-binding protein
- DCM: dichloromethane
- DEPT: distortionless enhancement by polarization transfer

- DIBAL-H: diisobutylaluminium hydride
- DMAP: 4-dimethylaminopyridine
- DMEM: dulbecco/vogt modified eagle's minimal essential
- DMF: dimethylformamide
- DMSO: dimetilsulfoxide
- DSG-2: desmoglein-2

E

- ECGC: epigallocatechin gallate
- EDCI: 1-ethyl-3-(3-dimethylaminopropyl)carbodiimide
- EMEM: minimum essential medium eagle
- ESI: electrospray ionization

F

- FAB: fast atom bombardment
- FBS: fetal bovine serum
- FDA: food and drug administration

G

- GAPDH: glyceraldehyde 3-phosphate dehydrogenase
- GCV: ganciclovir
- GI: gastrointestinal

H

- HadV: human Adenoviruses
- HATs: histone acetyltransferases
- HBV: hepatitis B virus
- HCV: hepatitis C virus
- HDACs: histone deacetylases
- HEPES: 4-(2-hydroxyethyl)-1-piperazineethanesulfonic acid
- HIV: human immunodeficiency virus
- HMBC: heteronuclear multiple bond correlation
- HRMS: high resolution mass spectrometry
- HSCT: hematopoietic stem cell transplantation

- HSPGs: heparan sulfate proteoglycans
- HSQC: heteronuclear single quantum correlation

I

- IAV: influenza A virus
- IC_{50}: half maximal inhibitory concentration
- IP_3: inositolo trifosfato
- ITRs: inverted terminal repeats
- IVIg: intravenous immunoglobulin

L

- LC-MS: liquid chromatography–mass spectrometry

M

- *m*CPBA: *meta*-chloroperoxybenzoic acid
- MLTU: major late transcriptional unit
- MOI: multiplicity of infection
- MRM: multiple reaction monitoring

N

- NA: not active
- NE: nuclear envelope
- NMR: nuclear magnetic resonance
- NO: nitric oxide
- NOESY: nuclear overhauser effect spectroscopy

O

- ODE: octadecyloxyethyl

P

- PCR: polymerase chain reaction
- PKC: protein kinase C

- PRD: `proline-rich domains
- pTP, preterminal protein

R

- RAR: retinoic acid receptor
- RT: renal transplantation
- rt: room temperature
- RT-PCR: reverse transcription polymerase chain reaction

S

- SAHA: suberoylanilide hydroxamic acid
- SAR: structure–activity relationship
- SD: standard deviation
- SI: selectivity index
- SOT: solid organ transplantation

T

- TCID50: 50% tissue culture infective dose
- THF: tetrahydrofuran
- TLC: thin-layer chromatography
- TLR: toll-like receptor
- TMD: transmembrane domain
- TMS: tetramethylsilane
- TP: terminal protein
- TRP: transient receptor potential cation channels

U

- UV: ultraviolet

V

- VPA: valproic acid
- VSLD: voltage sensor-like domai

CHAPTER 1
AN OVERVIEW OF ADENOVIRUS BIOLOGY AND DISEASES

Human adenovirus (HAdV) is a DNA virus that causes severe diseases in immunocompromised hosts [1]. It was isolated from human adenoids in the 1953 and was associated with some respiratory infections [2]. HAdVs belong to the *Mastadenovirus* genus of the family *Adenoviridae* and include more than 80 serotypes classified into 7 species (HAdV A-G**).** Among these, 2 and 5 (species C) are the most common studied, though many types belong to the species D [3]. Species designation depends on several features such as genome organization of E3 region, phylogenetic distance, nucleotide composition, oncogenicity in rodents, host range, crossneutralization, recombine capacity [4]. The diversity of species is the result of the recombination between capsid protein genes and this factor improves the pathogenicity and virulence of the new viruses [3,5].

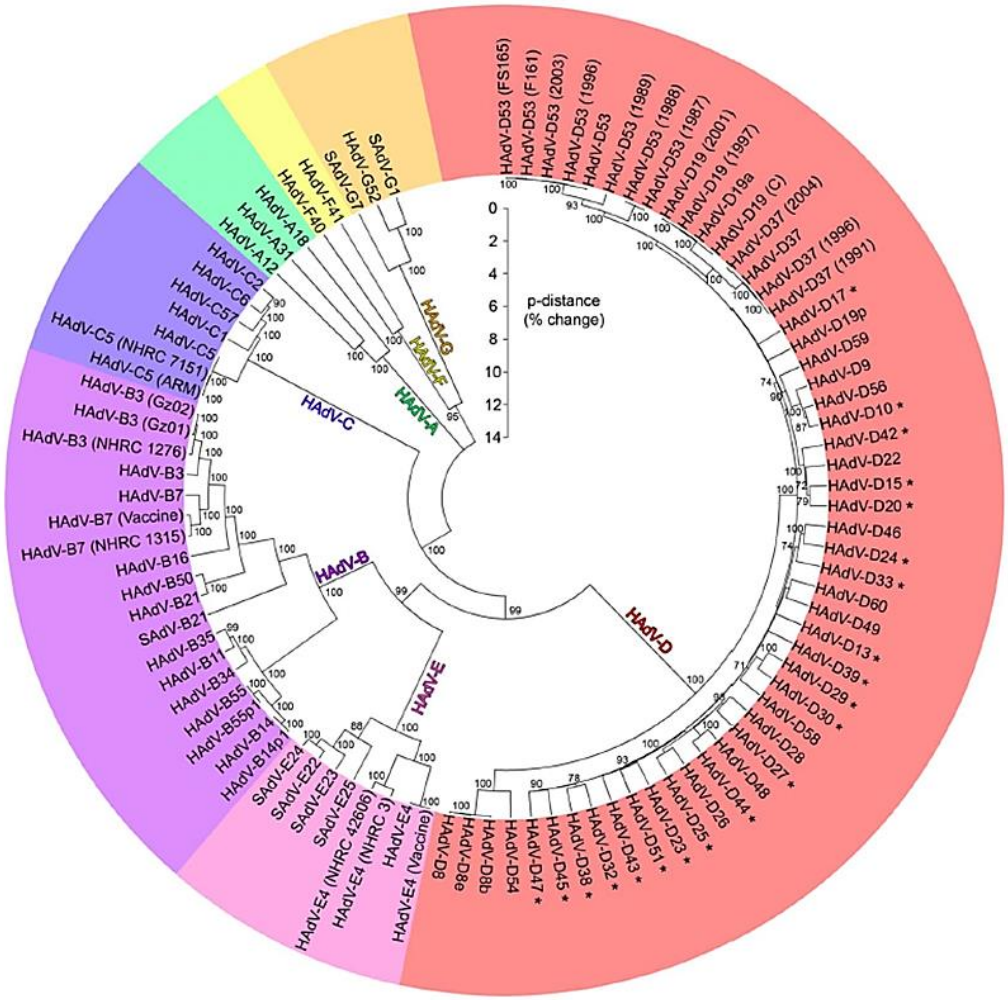

Figure 1. Adenovirus diversity [5].

1.1 Viral genome

HAdVs present an icosahedral capsid including a linear and double-stranded DNA genome of 26-45 kb depending on the serotype. In particular, HAdV type 5 has a ~36 kb genome which encodes more than 40 proteins in its transcription units [5]. During Adenovirus lytic infections, HAdV genome encodes at least 25 early gene products and 15 late gene products before and after the viral DNA replication (B, Figure 1) [6]. The proteins from the early regions E1, E2, E3, E4 (Figure 2) are involved in the beginning of viral replication; in particular, immediate-early E1A proteins are the first to be transcribed and activate the transcription of the delayed-early genes and re-programme cellular gene expression in inflected cells, facilitating the viral replication [7]. The splicing process affords five several transcripts of the primary E1A. The most important forms (289R, 243R) interacting with cellular proteins is implicated in cell cycle and epigenetic regulation, transcription factors, thus increase the viral gene expression and promote the infection. E1A proteins can be identified through *in vitro* studies during the late infection [8]. Proteins from E1B regions in cooperation with E4 are involved in ubiquitination of cellular proteins, inactivation of cellular DNA damage response and viral mRNAs transport [9].

The early region E2 consists of two transcriptional units, E2A and E2B, which different polyadenylation sites. They code for the three proteins required for viral DNA replication: E2A codes for the DNA-binding protein (DBP), while E2B codes for the precursor terminal protein (pTP) and the viral DNA polymerase [10,11]. E3 proteins are implicated in immunomodulatory functions in infected host cells. Furthermore, E3 region encodes the HAdV death protein (ADP); it was expressed from late promoter to improve the cell lysis and the virus release after complete replication [12]. E3 region was generally delated in order to generate viral vectors used in gene therapy [13]. E4 region encode proteins that regulate the transition to late phase of infection. They are involved in the regulation of viral transcription and RNA splicing; moreover, proteins from this region interfere with cell signaling and DNA repair, contributing to cell transformation and oncogenicity [14]. The adenovirus major late transcription unit (MLTU) encodes multiple proteins from L1 to L5 regions by an alternative splicing and polyadenylation (B, Figure 1) [15]. A L1 product (52/55K) is expressed prior to the replication and promote the expression of L1 IIIa and L2-L5, that code for structural components of the capsid. L4 promoter is important for the late gene expression [16,17].

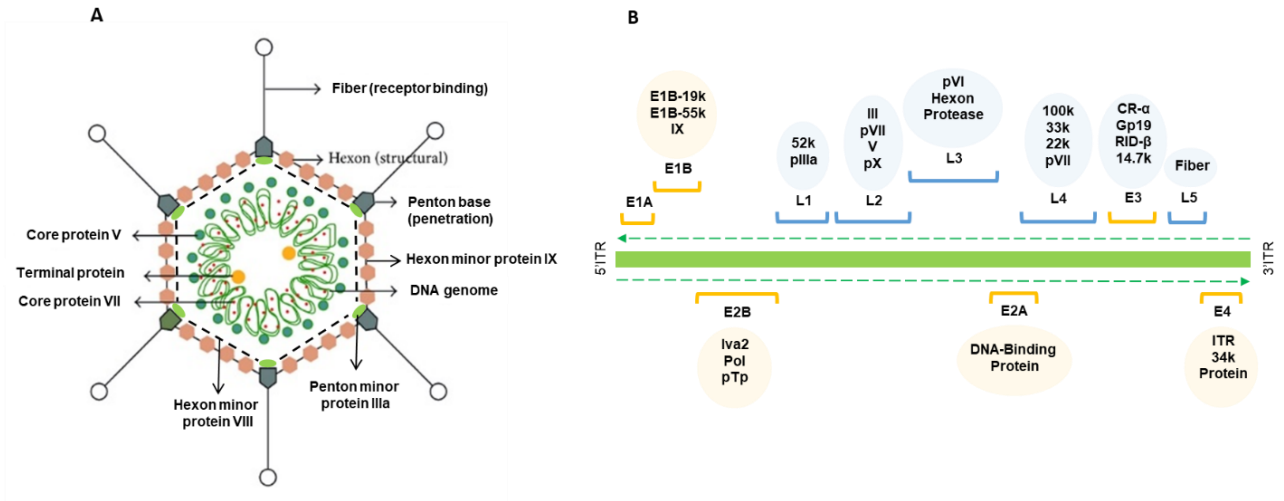

Figure 2. Adenovirus virion (A) and genome (B) [18].

1.2 Virion and life cycle

Structurally, HAdV consists of two main elements, an external capsid and an inner core which includes viral DNA genome and histone-like proteins. The HAdV icosahedral capsid with a diameter of ~70–100 nm exists in four forms (different in DNA quantity) between which only one are fully infectious. Capsid is mostly composed of three major proteins: 240 hexon trimers (protein II) that contribute to the capsid mass, 12 penton base pentamers (protein III) and 12 fiber trimers (protein IV) [19], that act in the cell internalization; and four minor proteins (IIIa, VI, VIII, IX) that preserve the capsid and connect it to a nucleoprotein core [20]. Other four proteins (VII, V, Mu, terminal protein TP) are connected with viral DNA inside de virion. (A, Figure 2); In particular, core protein VII promotes the DNA packaging and stabilize chromatin structure [21], while V represent a linker between DNA and internal capsid [22,23].

All viruses need to bind to specific receptors on cellular membranes in order to infect the host. In particular, HAdV life cycle begin with the cellular entry through two receptor interactions. Primarily, the terminal knob domain of viral fibers binds the coxsackie and adenovirus receptor (CAR). Next, an Arg-Gly-Asp (RGD) motif of penton base engages cellular integrins (αvβ3 and αvβ5), promoting the virus internalization by clathrin-mediated endocytosis [24]. In this process, fibers are dissociated and penton bases changes its conformation, weakening interactions with the capsid [25]. The uncoating proceeds with the vertex and V proteins release from early endosome. Protein VI liberation plays a key role in the subsequent viral particles secretion into the cytosol [26]. HAdV causes a progressive disruption of cell endosome in a mild acid pH condition in order to release the virion,

that migrates to the cell nucleus associated to the cellular microtubule network through the hexons [27]. The virion transport terminates on the nuclear envelope (NE) that is not only a barrier, but it is also involved in the exchange of information and matter between nucleus and cytoplasm. HAdV connects with the nucleus surface by an interaction between the hexon shell and Nup214, promoting the final uncoating and the internalization of DNA and protein VII into de nucleus [26]. The "chromatinization" of genome is essential for the transition to a transcriptionally active state and to start the transcription of early genes [28]. This transport occurs because of the interaction of protein VII to nuclear transport. HAdV genome also associates with histones (H3 preferentially) during the first hours of infection, and adopts a nucleosome-like structure similar to the host DNA. The literature reported that the virus may needs a temporal histone acetylation to obtain an efficient early promoter function [29]. E1A is able to interact with multiple histone acetyltransferase complexes and recruit these to viral or selected cellular promoters [30]. Replication starts when the primer pTP links DNA polymerase forming a complex at the origin of replication in terminal repeats (ITRs) of genome. After the onset of replication major late promoter (MLP) are activated and the late genes are expressed. Meanwhile, the new synthesized capsid with core proteins are translocated to the nucleus from cytosol for their assembly with new viral DNA through pre-pVII. The packaging of new genomes involves several viral proteins from L1, L4, IIIa and IVa2 and generate the young virions, which than evolve by maturation processes to obtain final and infectious AdV particles [31]. If resulted HAdv particles are defective in uncoating, they remain trapped and are eliminated in the lysosomes aborting the infection. In conclusion, as other viruses, HAdV uses cellular proteins to complete its life cycle, hijacking cellular pathways to allow viral gene expression and replication. This produces modification of the cellular gene expression and protein functions leads to the cell death due to cytopathic effects and the release of virion progeny (Figure 3) [32].

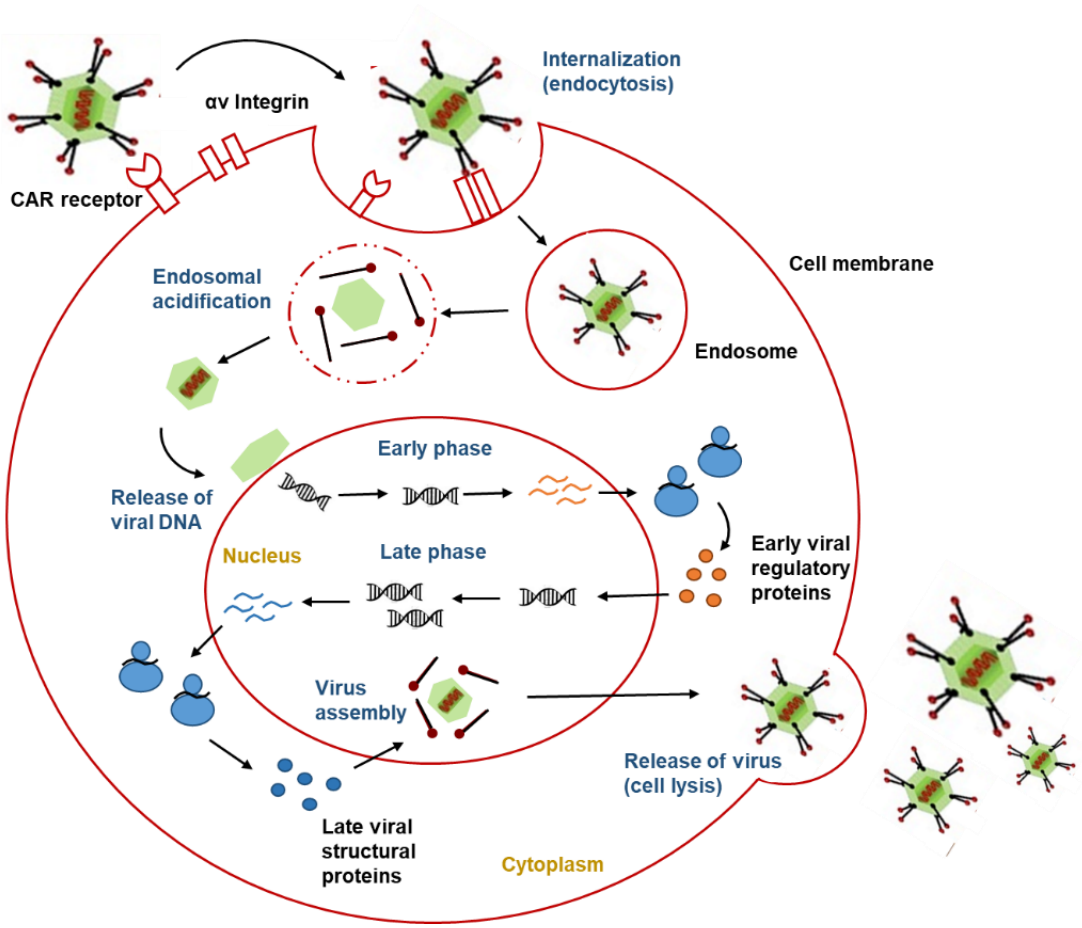

Figure 3. HAdV life cycle in host cells.

1.3 HAdV-induced infections

HAdV is an opportunistic pathogen responsible for a wide range of global clinical diseases in immunocompromised patients; instead is not typically associated with severe clinical manifestations in healthy individuals [5,33]. HAdV infections can be asymptomatic or be accompanied with clinical symptoms. Young children and immunosuppressed adult patients are more susceptible to serious HAdV infections; indeed, the mortality rate in children (less than 4 years) and neonates are of 40% and 80% respectively for pneumonia or disseminated diseases [34]. During the years, the incidence of sever HAdV infections has gradually increased because of the high number of transplantation and its related immunosuppressive therapy [4]. In fact, stem cell or solid organ transplantation (SOT) represent the highest risk factors that predispose individuals to invasive HAdV infectious diseases, followed by congenital or acquired immunodeficiencies, lymphopenia and chemotherapy [35]. The infections can be acquired from transplanted organ or by the reactivation of a latent infection. In the first case, the primary site of infection is often the transplanted organ and the typical symptoms such

as fever or enteritis can be observed 2 or 3 months after the transplantation [36]. pediatric hematopoietic stem cell transplantation (HSCT) patients the percentage range of HAdV infections is 15-44%, accompanied by high mortality rate for patients with other disseminated diseases. HAdV is able to avoid host immune responses through the inhibition of cellular apoptosis in infected cells or by the inhibition of interferon action. In addition, it's well demonstrated that T cells surveillance represent an important defence towards HAdV viremia. Therefore, a T cell deficiency lead to a major susceptibility to the infection [37].

HAdVs generally infect the epithelium of respiratory tract, but it is also associated with ocular, urinary, gastrointestinal diseases and several multi-organ failures [33]. Among these, pneumonia and hemorrhagic cystitis result the most relevant complications, with incubation periods between 2 and 14 days. In some instance, hepatitis, meningoencephalitis, myocarditis or nephritis are also observed [38]. After acute primary infection, serotypes as 1,2 and 5, may persist in stool for a long time due to their diffusion, although the immune response protect towards reinfection. In fact, some infections keep in a latent phase especially in tonsils, adenoids, intestine and urinary tract epithelial cells, but relative mechanisms are not yet clearly defined [36]. Epithelial cells is the favorite site for HadV replication [13]. HAdV infections are highly contagious, and the transmission occurs by respiratory route with aerosol inhalation, tissue contact with infected individuals, direct conjunctival inoculation, fecal-oral route [4]. The virus demonstrates to be resistant to lipid disinfectants due to its nonenveloped nature and can survive on environmental surfaces for a large period. However, it is neutralized using formaldehyde, bleach or heat [35].
Symptomatic HAdV infections are associated with one third of whole known HAdV serotypes. The type and tissue tropism of HAdV-induced diseases depend of involved serotypes [33,36].

-*Respiratory tract infections.* HAdV-related respiratory illness are generally associated with human B, C and E species (serotype 1-3, 5, 7). In particular, serotypes of C species (1, 2 and 5) are responsible of mild respiratory infections in children, whereas serotypes 3, 7, 14, 21 (species B) and 4 (species E) produce serious infections in children and adults. [36] It is reported that HAdV causes 5% of all respiratory tract infections and 4-10% of pneumonias [39]. Adenoviral pneumonia represents an important problem in clinical setting; it is associated with serotypes 3, 7, 14, and 21. Patients with Ad pneumonia present symptoms like fever, malaise, myalgia, cough, that worsen until dyspnea. In children pneumonia is generally associated with lethargy, diarrhea and vomiting. The typical extrapulmonary complications associated with viral pneumonia consist of meningoencephalitis, myocarditis, nephritis, hepatitis [40]. Furthermore, due to the hyperactivating immune response

during the infection, hemophagocytic lymphohistiocytosis can be also observed. In the most serious cases, patients need extracorporeal membrane oxygenation (ECMO) support because of unsatisfactory results of conventional mechanical ventilation [41]. In the last few years, severe cases of respiratory failure with death cases were documented [42].

-*Ocular infections.* Serotypes from species D are implicated in ocular diseases, between which epidemic keratoconjunctivitis represent the most frequent infections; but also pharyngoconjunctival fever and nonspecific conjunctivitis is observed. Epidemic keratoconjunctivitis (shipyard conjunctivitis) is mainly associated with serotypes 8, 19 and 37, but also with 3, 4, 53 and 54. HAdV-induced keratoconjunctivitis represents from 65% to 90% of all viral conjunctivitis [43]. Typical ocular symptoms include irritation, soreness, red eye, accompanied with ocular pain, and but also general malaise and fever. More serious complications involve cornea and conjunctiva, with a progressive reduction of visual acuity. Pharyngoconjunctival fever (PCF) is associated with serotypes 3, 4, 7, 11 and 14 and is also characterized by viral conjunctivitis, upper respiratory disorders and the contemporary presence of bacterial superinfections. Ocular infections are highly contagious, and the virus can spread through direct contact with contaminated items, fingers or medical instruments [35].

-*Enteric infections.* HAdV induces enteric disorders generally associated with species A and F (serotypes 40, 41). Among these, acute gastroenteritis (AGE) resulted to be the most frequent enteric outbreaks, mainly in infant and young children which could be easily infected in schools or nursery. Adenovirus was responsible for 5–15% of all gastroenteritis cases. The symptoms associated includes diarrhea, nausea and vomiting, abdominal cramps and pain [35,44].

-*Urinary tract infections.* Urogenital diseases are more observed in children than adults. Serotypes 11 and 21 from species D cause acute hemorrhagic cystitis; in addition, 11, 34 and 35 cause also tubulointerstitial nephritis. Typical symptoms are hematuria, urinary incontinence, painful urination, abdominal pain. Although hemorrhagic cystitis in children can be alarming, it is usually self-limiting and without severe systemic manifestations [35]. On the other hand, urinary infection after renal transplantation (RT) often produced graft loss and acute organ rejection, that may result in recipient death, due to co-presence of nephropathy and systemic diffusion [45].

1.4 Current anti-HAdV therapies

At present, there is no specific approved antiviral drugs for the treatment of HAdV infections. Main adopted measures consist in symptomatic treatment, thus analgesic, antipyretics, antiemetics and the oxygen supplementation when it is required; whereas nonspecific antiviral therapies are generally limited for immunosuppressed patients or for organ and stem cell transplantation recipients [35]. Today, the reduction of immunosuppressive therapy, immunotherapy and antiviral therapy resulted to be the most relevant clinical strategies available for severe HAdV infections [46]. The already mentioned role of T-cells in effective clearance of the virus suggests that a decrease of immune suppression should be a useful support to antiviral therapy. In some instances, mainly in pediatric HSCT, the reduction of immunosuppressive therapy alone led to a whole resolution of Ad infection. Adoptive immunotherapy is an alternative and innovative immunologic approach for immune reconstitution. The intravenous administration of antibody preparations demonstrated satisfactory results in T-cell-depleted HSCT recipients [47]. Among 30 HSTC patients with HAdV infections treated with an adoptive T-cell transfer (ACT), the 86% showed a complete elimination of viremia. Moreover, the use of ACT was well tolerated without acute toxicity [46]. treatment with intravenous immune globulin (IVIG) as additive therapy also displayed promising results [48].

With regard to the antiviral therapy, despite the high number of reported compounds showing *in vitro* HAdV activity, there is no approved specific drugs by Food and drug Administration (FDA) for these infections. Usually, drugs approved to treat other viral infection are used off-label to inhibit serious HAdV-induced diseases, such as ganciclovir, ribavirin, cidofovir and brincidofovir, but they afford no suitable clinical results in the terms of efficacy or safety [49,50].

-*Ganciclovir (GCV).* GCV is an acyclic analogue of guanosine that is approved for the treatment of herpesvirus infections (**1**, Figure 4). It is converted in GCV monophosphate and then in GCV triphosphate by viral kinase; in this form it is able to inhibit DNA replication acting as false substrate for the viral DNA polymerase. Ad genome do not code for a kinase, GCV showed *in vitro* inhibition activity of many types of HAdV, with EC_{50} range from 26 to 206 µM. In particular, GCV inhibits HAdV5 DNA synthesis and late gene expression. Moreover, the preventive treatment of transplant patients with GCV decreased the frequency of severe HAdV infections [51]. Replication Unfortunately, its use is limited due to poor available clinical data [52].

-*Ribavirin.* Ribavirin is a nucleoside analogue of guanosine and an antiviral agent used in the treatment of chronic hepatitis C (**2**, Figure 4). Several mechanisms have been reported in relation to its antiviral activity: the depletion of intracellular levels of guanosine triphosphate by the inhibition

of inosine monophosphate dehydrogenase and the improvement of T-cell response are proposed as indirect mechanisms. Direct mechanisms consist in inhibition of viral polymerase, inhibition of RNA capping and induction of mutation due to the insertion of ribavirin in nascent viral genomes [50]. Ribavirin showed *in vitro* activity against HAdV serotypes of species C (1, 2, 5, and 6) [48], even if the therapeutic effect of ribavirin in patients are debated. In some cases of immunocompromised patients with Ad infections, the treatment with ribavirin resulted effective, but no significant evidence was observed in several arger-scale studies [49]. In another studies, among patients treated with ribavirin by intravenous or oral administration, no significantly decrease of Ad viremia was observed [46].

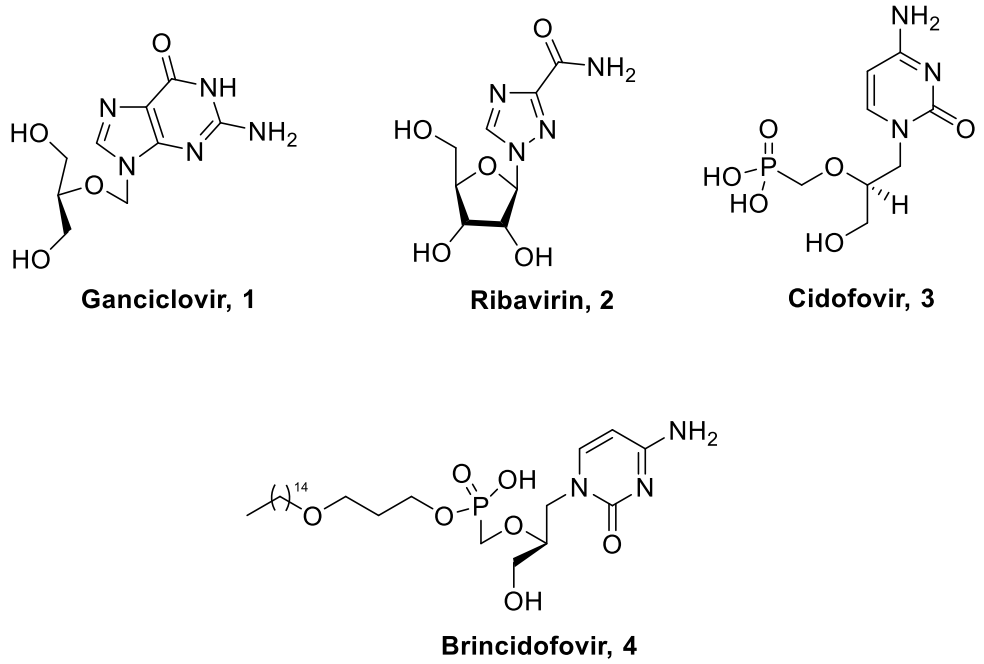

Figure 4. Current drugs employed for invasive HAdV infections.

-*Cidofovir (CDV).* CDV is an acyclic analogue of cytosine with a broad spectrum anti-viral activity against DNA viruses (**3**, Figure 4). It is an approved antiviral agent for the treatment of cytomegalovirus (CMV) retinitis. CDV is converted in the active form (CDV diphosphate) by kinase and inhibits replication by competitive incorporation in viral DNA genome and inhibition of DNA polymerase [35,53]. *In vitro* studies to evaluate its antiviral properties against HAdV species highlighted an inhibitory activity towards Ad serotypes 2, 9, 10, 14, 23, 25, 28, 33 [48]. Furthermore, *in vivo* studies demonstrated the efficacy of CDV in invasive adenoviral diseases; for these reasons CDV represents the most commonly used anti-HAdV agents in current clinical setting. Administering CDV in HSCT patients produced a clinical improvement in association with a reduction of mortality

rate from HAdV infections (less than 20%) [54,55]. Levels Clinical studies displayed the efficacy of CDV in the treatment of acute adenoviral keratoconjunctivitis in immunocompromised patients, especially when its administration was associated with immunotherapy [49]. Unfortunately, low oral bioavailability, nephrotoxicity and myelosuppression are limiting factors for CDV clinical use. Of an intravenous dose of CDV only 10% of drug is absorbed, while the remaining part (90%) is expelled in the urine by filtration and tubular secretion processes. Despite its rapid excretion, CDV is absorbed by proximal tubular cells through organic anion transporters and secreted into the lumen. The resulting improvement of intracellular levels of CDV causes tubular necrosis. For this reason, the hydratation before and after the CDV therapy promotes the drug elimination and prevents the nephrotoxicity [56].

-*Brincidofovir (BCV).* BCV is a lipid ester conjugate of CDV, with improved oral bioavailability and reduced toxicity (**4**, Figure 4) compared to CDV. The presence of a lipid moiety allows an efficient absorption through lipid uptake pathways of enterocytes simulating the endogenous lipid lysophosphatidylcholine [57]. Thus a high intracellular concentration of BCV achieves suitable antiviral activity by its conversion in CDV diphosphate. In particular, it demonstrated *in vitro* inhibitory activity against double-strand DNA viruses such as herpes simplex virus, polyomaviruses, papillomaviruses, poxviruses, cytomegalovirus (CMV) and adenovirus (serotypes 3, 5, 7, 8, 31) [49,58]. BCV results to be effective in immunosuppressed animal models with HAdV infections. Administration of BCV in HAdV-infected patients, for which the CDV therapy failed, provided better results in terms of efficacy and toxicity. Nephrotoxicity are not observed during BCV therapy (Phase II clinical trial-NCT01231344) because of its low plasma levels and weak propensity for renal storage [58]. At present, it is subjected to Phase III of clinical trials (NCT02087306) but significant gastrointestinal (GI) disorders including diarrhea, nausea, vomiting and pain have been observed in HSCT patients, limiting its use in therapy [59,60].

-*Anti-HAdV vaccines.* A live oral vaccine against HAdV type 4 and 7 was approved from 1971 to 1997 for the use in US military units. This vaccine resulted to be safe and effective in several clinical trials, reaching a 100-fold reduction of HAdV diseases, mainly respiratory ones. Nevertheless, this vaccine never was available to the general public and there are no vaccines approved today for adenoviral infections [61].

The unsatisfactory results of current antiviral drugs highlight the need of new effective anti-HAdV agents for clinical use in association to immune system reconstitution therapy.

CHAPTER 2

NEW PERSPECTIVES IN ADENOVIRUS DRUG DISCOVERY

2.1 Potential targets useful in HAdV drug discovery

Over the years, many researchers discovered novel compounds with inhibitory activity against HAdV serotypes in cell culture and animal model. Different targets could be considered useful in the design of specific anti-HAdV agents, especially proteins involved in critical roles of viral entry, replication or maturation processes [62]. HAdV cell entry in host cells implicates the attachment of virions to several cellular receptors. The most common receptors used by HAdV serotypes are CAR, CD46 and desmoglein 2 (DSG-2), although serotype D typically use sialic acid as entry receptor and heparan sulfate proteoglycans (HSPGs) mediate HAdV-C (2 and 5) cell entry [63]. Other potential targets are integrins, whose inhibition provide a block of viral internalization by clathrin-mediated endocytosis, or virus microtubule transport to the nucleus. The Ad replication proteins are the major explored targets for the development of new antiviral drugs. Among them are included E1A protein, an important regulator of other early genes expression [64], and proteins implicated in viral replication: DNA polymerase, pTP and DBP. HAdV proteases such as adenain (AVP) constitute additional potential targets due to their role in viral maturation process [62]. Many current antiviral therapies are directed to viral proteins or enzymes, although host targets have been identified in order to avoid the development of resistance mechanisms. Since HAdV associates with nucleosomes in the host nucleus, the viral gene expression is also affected by cellular epigenetic regulator proteins such as histone acetyltransferases (HATs) and histone deacetylases (HDACs), suggesting that these proteins could be represent interesting host targets for the development of new anti-HAdV candidates [65]. Protein p21 have an important role in the termination of cell cycle; it also promotes cells resistance to Adenovirus infection. Indeed, the upregulation of p21 expression may lead to viral replication inhibition. Toll-like receptors (TLR) pathways are activated by viruses and promote an increase of pro-inflammatory cytokines, in the case of HAdV B and C. The use of TLR pathways ligands could be an efficient approach to control HAdV infections [66]. Also retinoic acid receptor (RAR) represents a potential host target for anti-HAdV agents. A downregulation of RARβ mRNA was observed during Ad infections; on the contrary, the RARβ overexpression was associated with a decreased of virus spread. For this reason, RAR agonist could be effective in the treatment of HAdV infections [67].

2.2 Drug repositioning

Drug repurposing is an effective strategy to detect new uses of existing drugs that are approved for other pharmacological indication, allowing low risks about safety and reduced development costs. Several drugs have been identified as inhibitors of HAdV infections.

Valproic acid (VPA) is a medication employed in the treatment of epilepsy or bipolar disorder and the first reported HDAC inhibitor with demonstrated anti-HAdV activity (**5**, Figure 5). In a reported study, typical cytopathic effects (CPE) of infected cells were observed in absence of VPA, while no CPE occurred in the presence of this drug. It significantly affected viral replication and spread in cell culture. The majority of its effects seems to be related to VPA-induced upregulation of p21 expression with subsequent cell-cycle arrest, but also to the dysfunctional upregulation of viral E1A expression, that resulted in a block of late promoter induction. The role of HDACs in HAdV infection still must be clarify [68]. Also the suberoylanilide hydroxamic acid vorinostat (SAHA) is a member of HDAC inhibitors with antiviral properties (**6**, Figure 5). It is approved for the use in refractory or relapsed cutaneous T cell lymphoma, but showed also a broad spectrum of epigenetic activities. Since HDACs are associated with reduction of gene expression and cell cycle, an HDAC inhibitor should provide reverse effects due to an increase of histone acetylation. Unexpectedly, **6** achieved a significant decrease of HAdV5 gene expression and of E1A protein levels in cell cultures, influencing negatively several steps of virus cycle and virus yield at nanomolar concentration. Other HDAC inhibitors such as apicidin and panobinostat demonstrated antiviral activity, besides **6** [65]. Modulators of RNA splicing, such as cardiotonic steroids digoxin (**7**) and digitoxin (**8**) used for the heart failure, have been described as anti-HAdV agents (Figure 5). Both drugs inhibited several steps of viral replication in serotype 5, 31, 35 by alteration of E1A RNA splicing and resulted impairment of major late genes expression [69].

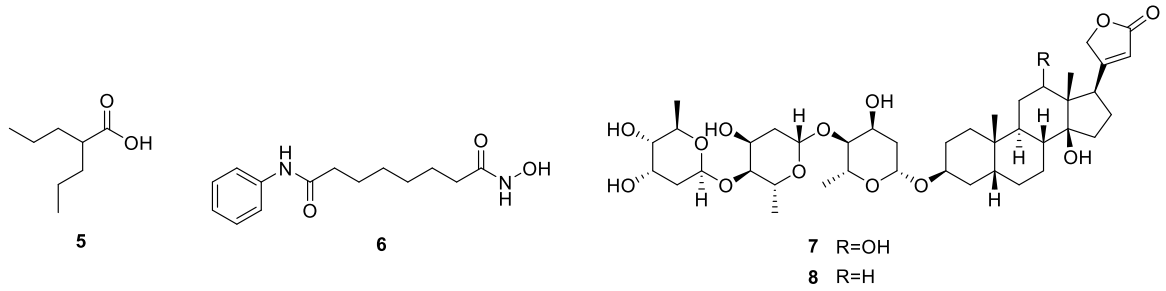

Figure 5. HDAC inhibitors and cardiotonic steroids with HAdV activity.

Mifepristone is an another commercially available steroid drug. It is approved by FDA for the medical termination of intrauterine pregnancy but it should be formally assessed as repurposed drug for the treatment of HAdV-induced diseases (**9**, Figure 5), due to its reported inhibition of HAdV infections in cells and mice. It showed *in vitro* activity against HAdV-5 at low micromolar concentration (EC_{50} =1.9 μM) with low cytotoxicity, interfering with virus translocation into de nucleus and with the replication of viral genome [70]. Among the RAR agonists potentially useful in antiviral therapy, tazarotene is a retinoid approved for the topic treatment of psoriasis, that was able to inhibit HAdV infection *in vitro* (**10**, Figure 6), with IC_{50} values of 8.34 μM for Ad5, 13.75 μM for Ad7 and 11.36 μM for Ad55. This effect was mediated by the binding of tazarotene to RARβ, with subsequent reduction of viral DNA replication and late hexon protein expression in a dose-dependent manner [67]. Polyphenolic compounds, especially from green tea, have been found to have antiviral activity. Among catechins, epigallocatechin gallate (EGCG) is the best broad-spectrum compound (**11**, Figure 6), showing activity against several viruses such as human immunodeficiency virus (HIV), adenovirus (AdV), influenza A virus (IAV), hepatitis B (HBV) and hepatitis C (HCV) virus. EGCG interacted with viral glycoproteins, interfering with the attachment of virus on host cell membrane. In particular, the competition between EGCG and virions for the binding to heparan sulfate or sialic acid glycoproteins have been observed, displayed IC_{50} values of 3.7 μM for HAdV binding inhibition [63].

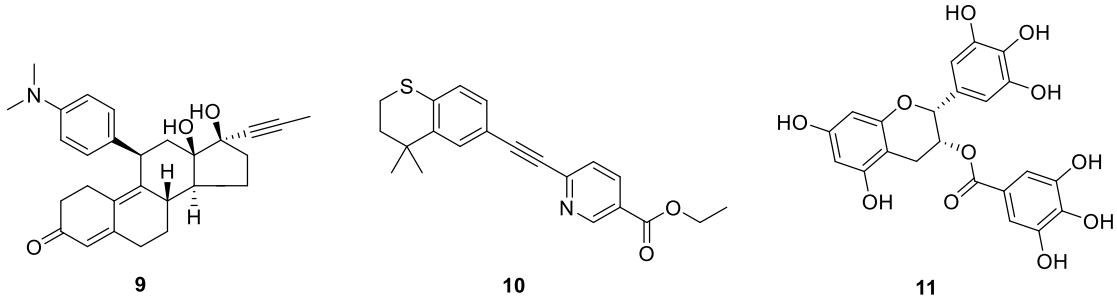

Figure 6. Diversified potential repurposed drugs for the treatment of HAdV infections.

The salicylanilide antielminting drugs niclosanide (**12**), oxyclozanide (**13**), and rafoxanide (**14**) displayed significant anti-adenovirus activity by suggested different ways (Figure 7). Niclosamide and rafoxanide interfered with the virus transport to the nucleus, whereas oxyclozanide inhibited HAdV early gene E1A transcription. The IC_{50} range for all compounds against HAdV5 and HAdV16 was from 0.45 μM to 2.3 μM with low cytotoxicity. Furtheromore, salicylanilide drugs caused a virus yeld reduction from 10 to 186 fold [71].

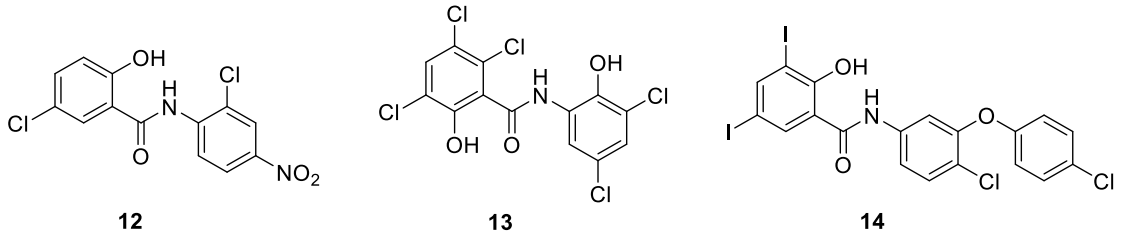

Figure 7. Salicylanilide drugs with anti-HAdV activity.

2.3 Novel nucleoside or nitrogen bases analogues

Considering that current drugs CDV, GCV and ribavirin are moderately effective to arrest Ad infections but provide no satisfactory results in terms of safety, many novel synthetic nucleoside or nitrogen bases analogues have been developed in order to reach better activity and reduced adverse effects *in vitro* and *in vivo* models [72]. Sets of ether lipid-ester of CDV and of (S)-9-(3-hydroxy-2-phosphonylmethoxypropyl)adenine (HPMPA) were evaluated against five HAdV serotypes (3, 5, 7, 8, 31). These acyclic nucleoside phosphonates (ANPs) presented several linkers and alkyl chain lengths on phosphonate group, resulting orally bioavailable and from 15 to 2500-fold more active than the parent compounds in *in vitro* experiments. Among best active compounds, **15** (hexadecyloxypropyl CDV, HDP-CDV) and **16** (octadecyloxyethyl HPMPA, ODE-HPMPA) (Figure 8) showed low IC_{50} values (from 0.009 to 0.28 mmol/L) towards all HAdV serotypes. In animal experiments these compounds demonstrated an efficacy similar to CDV, thus requesting further modifications for their use as anti-HAdV agents [73]. Based on these *in vitro* promising results, other octadecyloxyehtyl derivatives (ODE) of acyclic nucleoside phosphonates was prepared to evaluate the effect of different nitrogen bases. All compounds were able to inhibit HAdV14 and one of them, the octadecyloxyethyl derivative of 2,6-diaminopurine (ODE-HPMP-DAP, **17**, Figure 8) resulted to be the most effective compound, with IC_{50} value of 1.7 nM and a virus yield reduction of 90% at 4.1 nM [74]. This compound could be further investigated to evaluate its efficacy in the treatment of Ad infections.

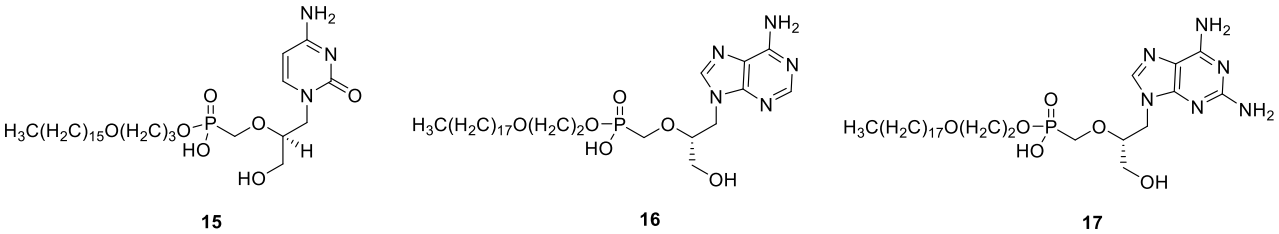

Figure 8. Ether lipid-esters of acyclic nucleoside phosphonates with HAdV activity.

6-Azacytidine derivatives were described by I. Alexeeva *et al* as new potential antiviral agents against HAdV types 2 and 5. Several substituents on N-4 of azacytidine nucleus were evaluated as well as the functionalization of hydroxyl groups. The thio-analogue **18** and *N,O*-tetracylated compound **19** (Figure 9) demonstrated the most potent anti-viral effect against HAdV2, with IC_{50} values of 0.8 μM and 0.3 μM respectively. Compounds **19**, the tetracetylated derivative, presented high selectivity index. Further studies demonstrated that these molecules can inhibit the formation of intranuclear DNA-containing inclusion bodies, suggesting that they could be interfere with the viral genome expression [75].

A series of new 5-aminouracil derivatives were synthesized and *in vitro* evaluated against HAdV5. The effect of several substitutents on the aromatic moiety as well as on the uracil scaffold were explored. Compound with a morpholine ring (**20**, Figure 9) afforded the best inhibitory activity (IC_{50} = 0.5 μM) and a suitable selectivity index. Additional investigation highlighted the ability of these molecules to block viral replication thorough the inhibition of DNA polymerase and E1A gene expression [76]. The main advantage of DNA/RNA component analogues potentially used as antiviral agent is that they can be easily inserted into the viral genome suspending the replication.

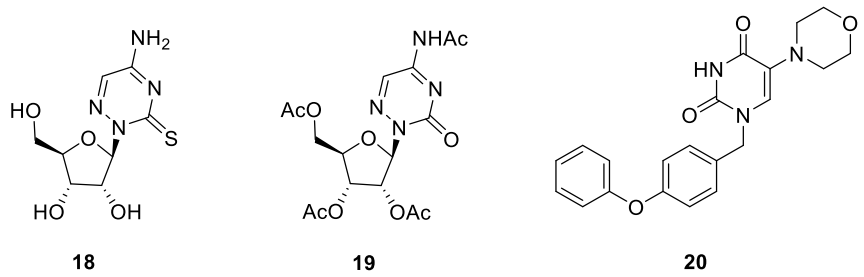

Figure 9. 6-Azacytidine- and 5-aminouracil-derived compounds as new potential HAdV agents.

2.4 Novel non-nucleoside small molecules

Over the years, structural diversified small molecules with non-nucleoside core have been described in order to obtain new effective antiviral candidates useful in the management of HAdV-induced diseases. Common features were present in a lot of new described compounds, mainly amide/urea functions and aromatic moieties.

Many benzoic acid derivatives were found to inhibit Ad infections *in vitro*. In a study, three generations of 2-[2-benzoylamino)benzoylamino]benzoic acids were prepared and the structure-activity relationships were identified. Changes in the position of carboxylic acid moiety resulted to decrease the activity against HAdV 5, while electron-withdrawing substituents such as chlorine or

fluorine on terminal and central aromatic rings were well tolerated. The most active compounds **21** and **22** (Figure 10) inhibited viral replication with IC_{50} values of 0.57 μM and 0.58 μM respectively and low cytotoxicity [77]. A set of optimized salicylamide derivatives as potent anti-HAdV agents was recently described. The effect of several modifications on both aromatic moieties as well as a linker insertion between the benzamide and the other phenyl ring were evaluated through *in vitro* assay. Many halogenated molecules showed an improved antiviral activity against HAdV5 compared to lead compound niclosamide (600 nM). Compound **23** and **24** were the best of the series (Figure 10), reaching IC_{50} values of nanomolar concentrations (50 nM and 80 nM respectively) and high selectivity index. The proposed mechanism for compound **24** was the inhibition of viral replication whereas **23** affected later steps. A di-amide series was also prepared but resulted to be less active than mono-amide ones. Compounds **23** and **24** are suitable candidates to evaluate their efficacy in animal model and develop an alternative antiviral therapy for HAdV infections [78]. Benzoic acid esters with anti-HAdV activity were also developed. This compounds demonstrated inhibition of cytopathic effect of HAdV7 in host cell and reduction of virus progeny production. Moreover, they were able to block apoptosis of host cell caused by virus. For compound **25** (Figure 10) the inhibition rate was 82.4 % at 40 μg / mL [79].

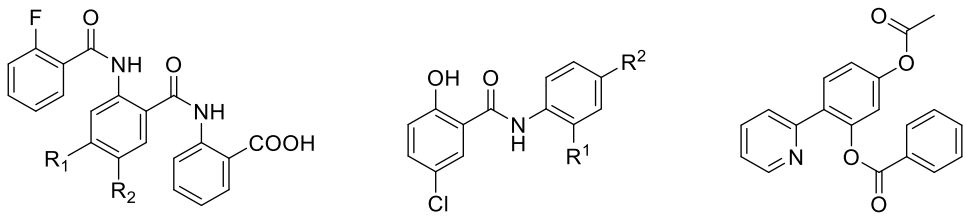

21 R^1=H R^2=Cl
22 R^1=F R^2=F
23 R^1=F; R^2=NO_2
24 R^1=Cl; R^2=CF_3
25

Figure 10. Benzoic acid amides and esters with anti-HAdV activity.

Several new biologically active compounds with nitrogen heterocycle scaffolds were discovered as anti-HAdV agents. Hamdy *et al* developed different sets of pyrazoles, pyrazolopyridazines, enaminones, and sulphonamides and examined their antiviral activity against adenovirus and rotavirus. Among the modification at N-1 of pyrazolo-pyridazine core, compound with a methoxy group on the aryl moiety resulted to be the most active (**26**, Figure 11), while the presence of electron withdrawing groups suppressed the activity. Compound **26** displayed an IC_{50} value of 0.06 mg/mL and suitable therapeutic index. Further investigations are needed to identify the mechanism of action of these new molecules [80]. Since there are no small molecules described as adenain inhibitors, a

set of pyrimidine nitrile derivatives was developed by a molecular hybridization strategy from two lead compounds. Compound **27** demonstrated to be the most effective inhibitor (Figure 11) toward adenovirus protease 8 and 5 (AVP), achieving IC_{50} values of 0.003 μM and 0.002 μM respectively. High-resolution X-ray co-crystal structures of these derivatives in complex with adenain illustrated that a nitrile group covalently connected with Cys122 and all amide functions were implicated in non-covalent hydrogen bonds with several protease residues [81]. In another study, privileged structure-guided scaffold refining strategy was used to prepare new triazolyl-quinazoline-diones with *in vitro* activity towards vaccinia virus and HAdV2 (**28**, **29**, Figure 11). The most active compounds were those with a methoxy group at *para* position or a fluorine atom at *orto* position of the phenyl ring conneted to triazol moiety. Active compounds presented IC_{50} values ranging from 6.2 μM to 13 μM exhibiting no cytotoxicity [82].

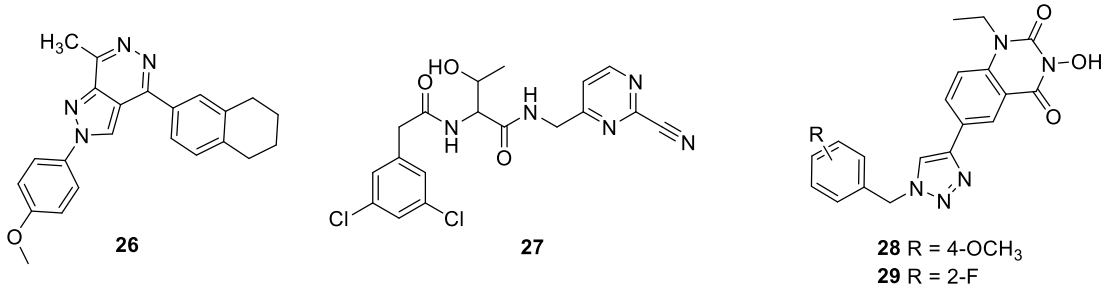

Figure 11. Several nitrogen heterocycle derivatives with anti-HAdV activity.

A tri-substituted piperazin-2-one derivative (**30**, Figure 12) was identified among more than 25.000 synthetic small molecules screened against Ad infections, using high-throughput screening (HTS). Compound **30** inhibited HAdV 5 in a dose-dependent manner, reaching 100% *in vitro* inhibition at concentrations higher than 3 μM and a virus yield reduction of 12–17-fold. Mechanistic studies suggested that **30** affected viral replication, possibly targeting DNA–VII complex or involved replication proteins [83]. Starting from this selected hit compound, a new set of piperazine derivatives have been designed and synthesized by our research group to obtain new effective agents. Several substituents were evaluated on both nitrogen atoms, introducing urea and amide functions. From the structure-activity relationship point of view, the presence of a benzofuran group on amide function seemed to be relevant for the antiviral activity against HAdV5; in addition, halogen substituents on the urea phenyl ring generally increased the infection inhibition. In particular, compound **31** influenced later steps of viral DNA replication (Figure 12) and resulted to be the best compound of

the series (IC_{50} = 1.1 μM) with no cytotoxicity. These compounds represent suitable candidate for further *in vivo* experiments and development of new potential anti-HAdV agents [84,85].

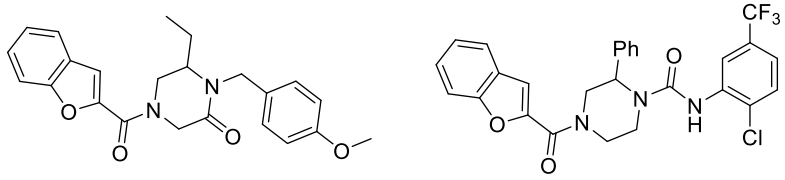

30 **31**

Figure 12. Piperazine-derived compounds with HAdV-activity.

AIMS OF THE WORK

HAdV usually infects the epithelium of respiratory tract causing severe pneumonia and other infections, mostly in immunosuppressed patients and young children. Despite its clinical relevance, there is no approved antiviral therapy for the treatment of HAdV infections and repurposed nonspecific antiviral drugs reached no satisfactory results. Since the find of novel specific anti-HAdV is an important topic for the medicinal chemistry, this PhD thesis aimed to discover new structural diversified small molecules useful for HAdV-induced diseases. This project was carried out in the University of Seville and was focused on the preparation of new nitrogen compounds based on cyclic and acyclic scaffolds as direct inhibitors of HAdV infection. The main tasks were:

1) Design of new small molecules based on piperazine and aminoalcohol scaffolds. An optimization process of piperazine-derived ureas privileged structures, by introducing slight modifications in the general piperazine backbone (amide and urea/thiourea functions), has been developed in order to improve the inhibition of HAdV infection and the safety profile. Since our interest in the discovery of new interesting structures with antiviral activity, the acyclic scaffolds 2-amino-1,3-propanediol and 3-amino-1,2-propanediol have also been employed. Firstly, a set of symmetric esters and carbamates from 2-amino-1,3-propanediol (serinol) have been designed, based on the typical features of reported antiviral agents. Serinol has been then replaced with its positional isomer 3-amino-1,2-propanediol. In order to introduce diversified functionalization of hydroxyl and amino groups, urea, ester, carbamate, triazole derivatives have been planned.

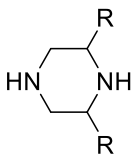

substistuted piperazine

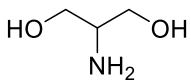

2-amino-1,3-propanediol (serinol)

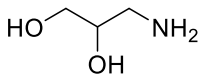

3-amino-1,2-propanediol

Figure 13. Cyclic and acyclic scaffolds employed for the development of new anti-HAdV agent.

2) Synthesis and **structural characterization** of designed compound libraries. A short and high yielded synthetic methodology has been employed for most compounds of these series. The selective *O*-acylation reactions of primary/secondary alcohol group (3-amino-1,2-propanediol) and the introduction of triazole moiety (click chemistry) have been performed through a multi-step synthesis.

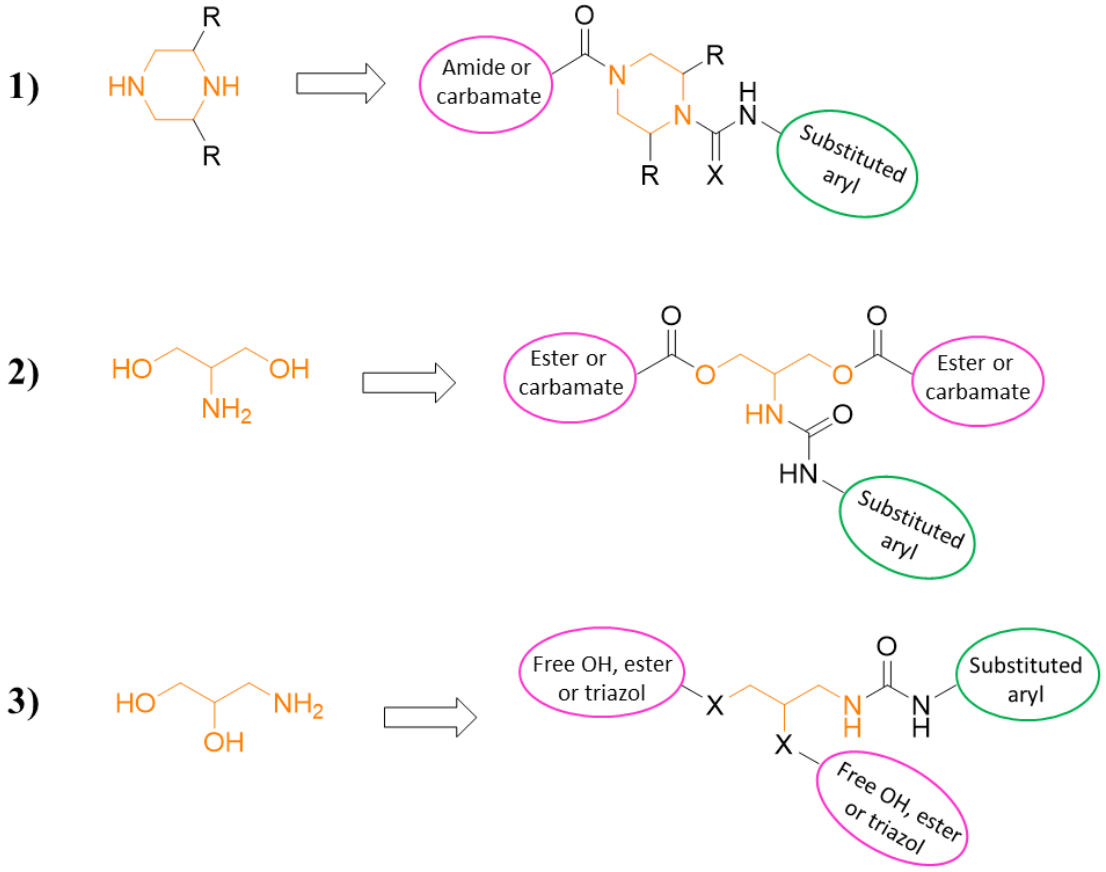

Figure 14. General backbone of new synthesized compounds.

3) *In vitro* biological evaluation. The ability of new sets of compounds to inhibit HAdV5 infection and their effect on cellular viability has been examined through *in vitro* assays. For selected compounds, studies to gain some knowledge regarding their potential mechanism of action have also been performed.

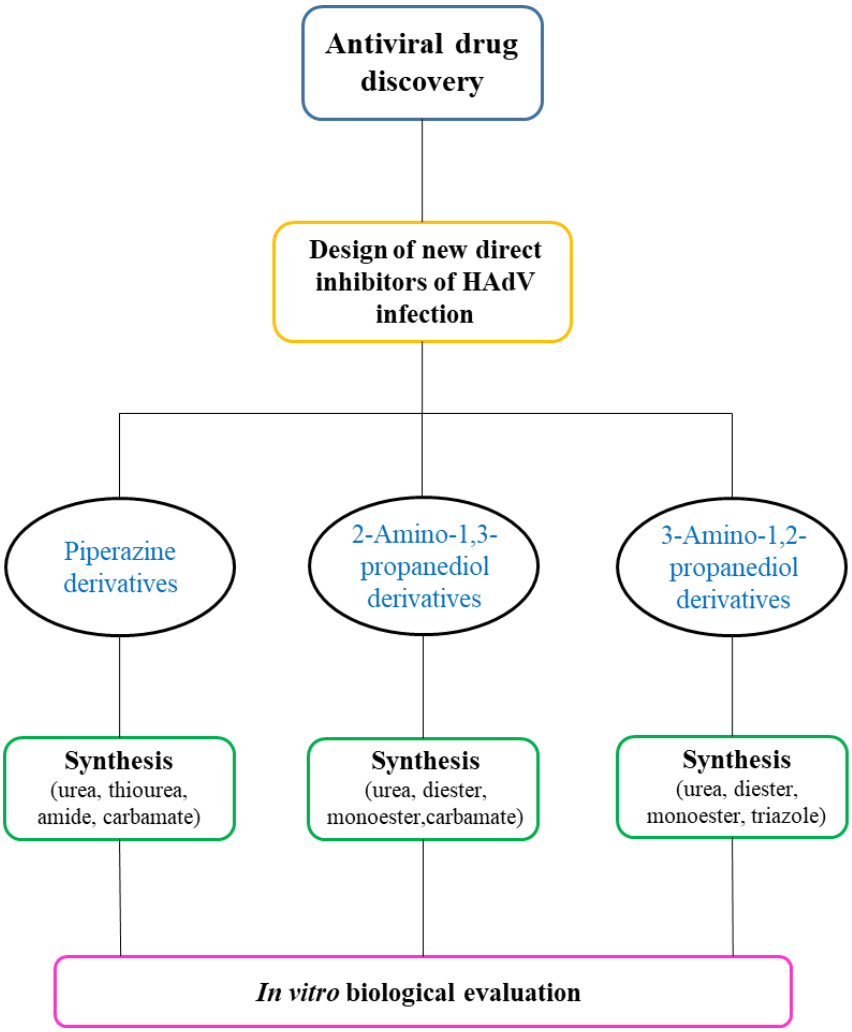

Figure 15. General aims of the work.

CHAPTER 3

4-ACYL-1-PHENYLAMINO(THIO)CARBONYL PIPERAZINE DERIVATIVES

3.1 Chemistry

3.1.1 Design of optimization process

Since the promising results obtained in our just mentioned work [84], the piperazine scaffold was further investigated in order to obtain new effective anti-HAdV agents. Nowadays, the development of new potential drugs is mainly directed to find novel lead compounds rather than the employing synthesis or creative discovery technologies. For this reason, the privileged structure-guided scaffold re-evolution/refining is an interesting strategy to identify novel interesting compounds with therapeutic applications by modifications of already active molecules. This strategy is commonly used in the antiviral drug discovery [86]. In this context, our purpose was to identify optimized piperazine derivatives starting from compounds **31-36** from our previous work (Figure 16), that can be considered as potential strong candidates for the development of a new class of antivirals.

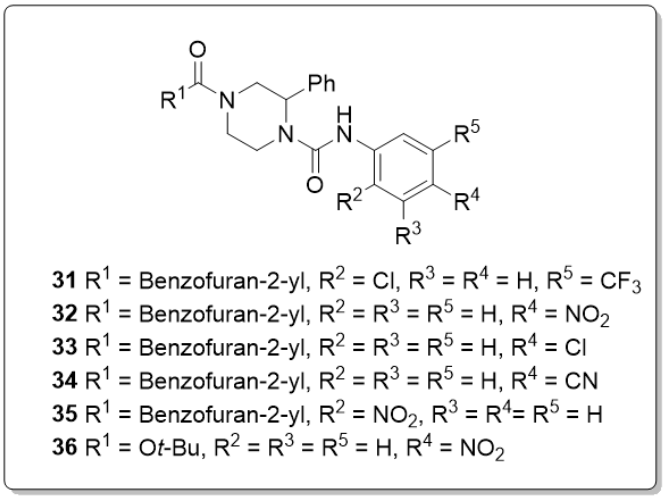

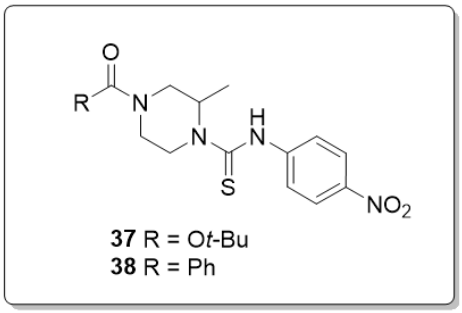

Figure 16. Lead compounds from previous work.

We decided to explore several structural modifications of lead compounds (pathways A, B and C), preserving three moieties of the general backbone: the piperazine core, the urea function at N-1, and the amide group at N-4 (Figure 17). In the pathway **A**, the replacement of the urea function with a thiourea one (Figure 17) was performed. This modification was realized due to results of two previous derivatives (**37, 38,** Figure 16), which demonstrated suitable anti-HAdV activity (100% and 94% inhibition at 10 μM in the plaque assay) but low CC_{50} values. Keeping the methyl piperazine core

with the thiourea function at N-1, the effect on activity and cytotoxicity profile of several substituents on the phenyl ring of the thiourea function (electron-withdrawing or donating groups) as well as different acyl functions at N-4 were examined. With regard to acyl function, subsequent changes were performed: firstly, the *tert*-butyloxycarbonyl (Boc) was replaced with 2-*tert*-butyl acetyl (as a bioisosteric modification); secondly, several bulkier groups (2-cyclohexyl, 2-phenyl) were introduced. Since the importance of the benzofuran moiety in our lead compounds, the thiourea analogues of benzofuran -2-carbonyl derivatives **31-35** were also prepared, preserving *p*-NO2, *p*-CN, *p*-F and *p*-CF3 substituted phenyl amine thiocarbonyl group at N-1. As our initial prototypes (**31-35**) were based on a phenyl piperazine backbone, the subsequent preparation of 2-phenyl piperazine-derived thiourea analogues was a natural evolution in the optimization process.

In the pathway **B** the major change concerned the acyl group at N-4, preserving the 2-phenyl piperazine core and the urea function at N-1 (Figure 17). Compound **31**, **32** and **35** (Figure 16) were chosen as a model to perform this structural modification due to these compounds showed lowest IC_{50} values. 2-*tert*-butyl acetyl, 2-cyclohexylacetyl and 2-phenylacetyl groups were incorporated at N-4 together with *p*-NO_2, *o*-NO_2, and 2-Cl-5-CF_3 substituents on the phenyl ring of the urea function. Another two phenyl piperazine derivatives with benzofuranlyl di-amide moiety or di-urea 2-Cl-5-CF_3 substituted were prepared in order to evaluate the relevance of these groups in the biological activity. Lastly, the pathway **C** included modifications of piperazine skeleton (Figure 17). To evaluate the effect of an additional substituent and the absence of substituents, analogues of compounds **31-36** (benzofuranyl and Boc derivatives) with 2,6-dimethylpiperazine and unsubstituted piperazine scaffolds were generated. In addition to already used electron-withdrawing groups on the phenyl amine thiocarbonyl group, some electron-donating groups (Me, OMe) were evaluated.

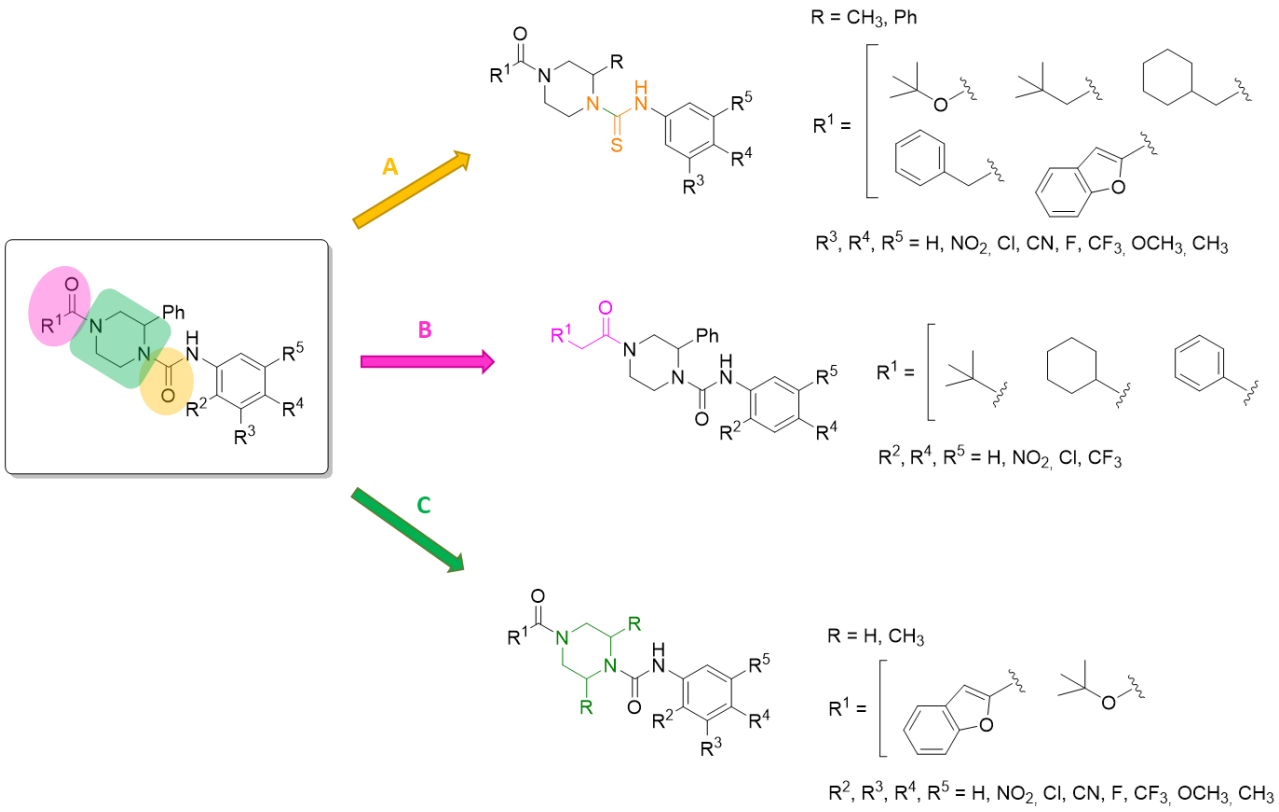

Figure 17. Optimization process of piperazine derivatives privileged structures for the inhibition of HAdV infection.

3.1.2 Synthesis

All piperazine derivatives were obtained following a short and high-yielding synthetic methodology that involved few reactions in order to functionalize both nitrogen atoms of piperazine core.

-Pathway A: replacement of the urea function with a thiourea one (50–92).

Thiourea derivatives **50–92** were obtained following the general synthetic route depicted in the Scheme 1. The 2-methylpiperazine (**39**) and 2-phenylpiperazine (**40**) were employed as precursors of new compounds. In the first step, a chemoselective N-acylation reaction (at low temperature) on the less hindered nitrogen (N-4) of 2-substituted piperazine core provided amide or urethane derivatives (**41–49**). Compounds **39** and **40** reacted with corresponding acylating agent (di-*tert*-butyl dicarbonate or 2-tert-butyl acetyl, 2-cyclohexylacetyl, 2-phenylacetyl, benzofuran-2-carbonyl chlorides) in DCM in the presence of pyridine.

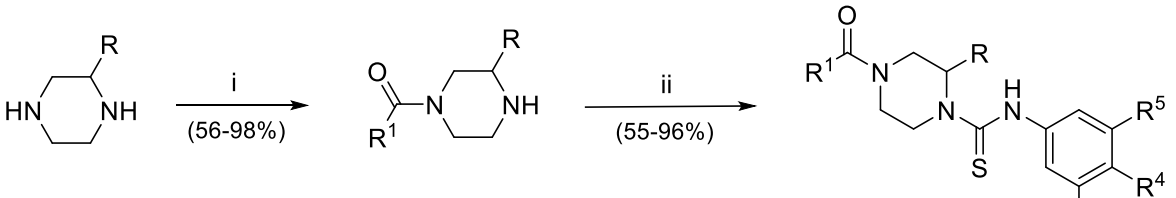

39 R = Me
40 R = Ph

41 R = Me, R^1 = O*t*-Bu
42 R = Me, R^1 = CH_2*t*-Bu
43 R = Me, R^1 = CH_2*c*-Hex
44 R = Me, R^1 = CH_2Ph
45 R = Me, R^1 = Benzofuran-2-yl
46 R = Ph, R^1 = O*t*-Bu
47 R = Ph, R^1 = CH_2*t*-Bu
48 R = Ph, R^1 = CH_2*c*-Hex
49 R = Ph, R^1 = CH_2Ph

50-92

i: Acyl halyde or anhydride 1 eq, pyridine 1.5 eq, DCM, 0-25 ºC, 12 h

ii: Isothiocyanate 1.2 eq, DCM, rt, 24 h

Scheme 1. Chemical synthesis of 4-acyl-2-substituted piperazine thiourea derivatives (**50–92**).

The thiourea function was introduced at N-1 in a second reaction between the monoacylated compound (**41–49**) and the corresponding phenyl isothiocyanate, which proceeded in DCM at rt (Scheme 1). Due to the variability of employed substituted phenyl isothiocyanates, a collection of 43 thiourea derivatives were generated (**50–92**, Table 1)

Table 1. 4-Acyl-2-substituted-piperazine thiourea derivatives from pathway A.

Comp	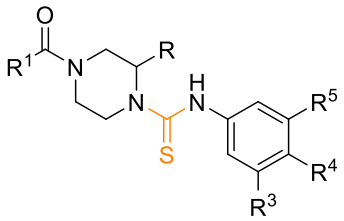					
	R	**R^1**	**R^3**	**R^4**	**R^5**	**Yield (%)**
50	Me	O*t*-Bu	H	Cl	H	73
51	Me	O*t*-Bu	H	CN	H	76
52	Me	O*t*-Bu	H	F	H	79
53	Me	O*t*-Bu	H	CF_3	H	73
54	Me	O*t*-Bu	H	OCH_3	H	75
55	Me	O*t*-Bu	H	CH_3	H	75
56	Me	O*t*-Bu	CF_3	H	CF_3	71

Comp	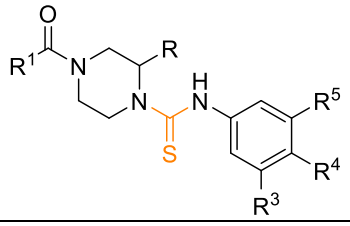					
	R	**R^1**	**R^3**	**R^4**	**R^5**	**Yield (%)**
57	Me	CH_2*t*-Bu	H	NO_2	H	68
58	Me	CH_2*t*-Bu	H	Cl	H	70
59	Me	CH_2*t*-Bu	H	CN	H	66
60	Me	CH_2*t*-Bu	H	F	H	60
61	Me	CH_2*t*-Bu	H	CF_3	H	73
62	Me	CH_2*t*-Bu	H	OCH_3	H	62
63	Me	CH_2*t*-Bu	H	CH_3	H	76
64	Me	CH_2*t*-Bu	CF_3	H	CF_3	68
65	Me	CH_2*c*-Hex	H	NO_2	H	76
66	Me	CH_2*c*-Hex	H	Cl	H	75
67	Me	CH_2*c*-Hex	H	CN	H	73
68	Me	CH_2*c*-Hex	H	F	H	77
69	Me	CH_2*c*-Hex	H	CF_3	H	68
70	Me	CH_2*c*-Hex	H	OCH_3	H	70
71	Me	CH_2*c*-Hex	H	CH_3	H	66
72	Me	CH_2*c*-Hex	CF_3	H	CF_3	78
73	Me	CH_2Ph	H	NO_2	H	57
74	Me	CH_2Ph	H	Cl	H	61
75	Me	CH_2Ph	H	CN	H	67
76	Me	CH_2Ph	H	F	H	56
77	Me	CH_2Ph	H	CF_3	H	70
78	Me	CH_2Ph	H	OCH_3	H	55
79	Me	CH_2Ph	H	CH_3	H	62
80	Me	CH_2Ph	CF_3	H	CF_3	65
81	Me	Benzofuran-2-yl	H	NO_2	H	92
82	Me	Benzofuran-2-yl	H	CN	H	72
83	Me	Benzofuran-2-yl	H	F	H	85
84	Me	Benzofuran-2-yl	H	CF_3	H	84
85	Ph	O*t*-Bu	H	F	H	70
86	Ph	CH_2*t*-Bu	CF_3	H	CF_3	96

Comp	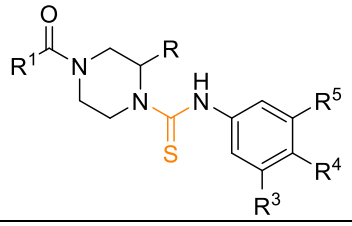					
	R	**R^1**	**R^3**	**R^4**	**R^5**	**Yield (%)**
87	Ph	CH_2*c*-Hex	H	CN	H	65
88	Ph	CH_2*c*-Hex	H	F	H	60
89	Ph	CH_2*c*-Hex	H	CH_3	H	60
90	Ph	CH_2Ph	H	NO_2	H	65
91	Ph	CH_2Ph	H	CN	H	72
92	Ph	CH_2Ph	CF_3	H	CF_3	93

-Pathway B: Exchange the acyl groups at N-4 in 2-phenyl piperazine urea derivatives (93–101). The preparation of compounds **93–99** (Scheme 2, Table 2) followed the previously described short synthetic route. The formation of urea function at N-1 occurred due to the reaction between 2-phenyl piperazine mono-amide **47–49** (2-tert-butyl acetyl, 2-cyclohexylacetyl, 2-phenylacetyl) and *p*-NO_2, *o*-NO_2 or *o*-Cl-*m*-CF_3 phenyl isocyanate.

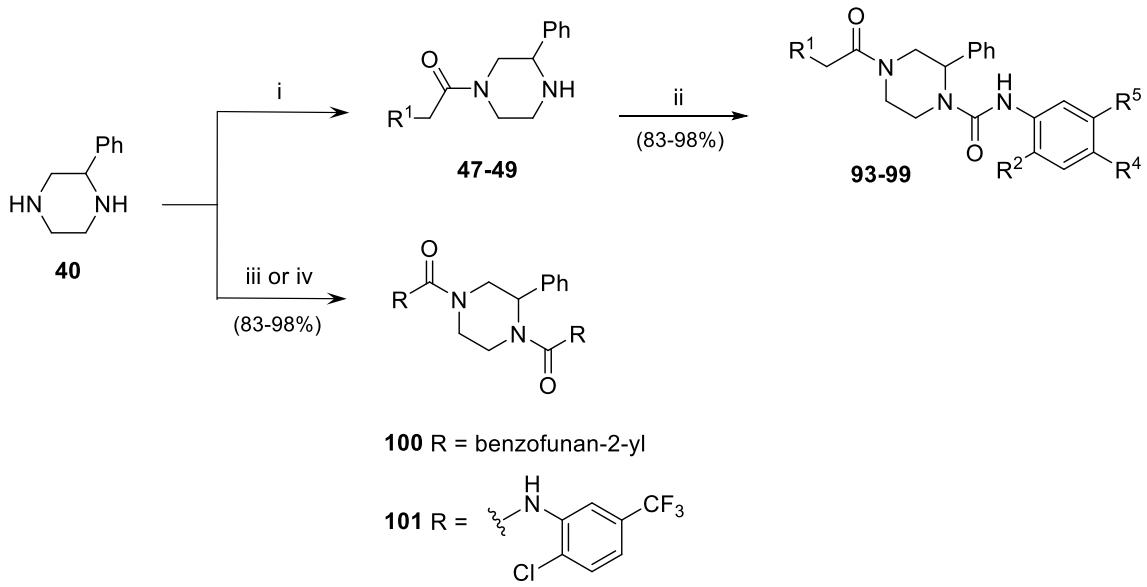

i: Acyl halyde 1 eq, pyridine 1.5 eq, DCM,0-25 ºC, 12 h

ii: Isocyanate 1.2 eq, DCM, rt, 24 h

iii: Acyl halyde 2.4 eq, pyridine 1.5 eq, DCM, 24 h

iv: Isocyanate 2.4 eq, DCM, 12 h

Scheme 2. Chemical synthesis of 4-acyl-2-phenylpiperazine urea derivatives (**93–101**).

Compounds **100** (di-amide derivative) and **101** (di-urea derivative) were synthesized directly from 2-phenyl piperazine, using an excess of reactive agent (acyl chloride/pyridine or isocyanate, respectively) in DCM at rt (Scheme 2).

Table 2. 4-Acyl-2-phenylpiperazine urea derivatives from pathway B.

Comp.	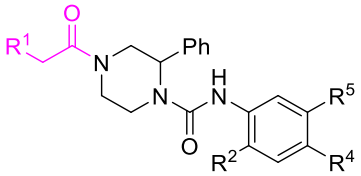				
	R^1	**R^2**	**R^4**	**R^5**	**Yield (%)**
93	*t*-Bu	H	NO_2	H	90
94	*t*-Bu	NO_2	H	H	88
95	*c*-Hex	H	NO_2	H	83
96	*c*-Hex	NO_2	H	H	88
97	Ph	H	NO_2	H	98
98	Ph	NO_2	H	H	96
99	Ph	Cl	H	CF_3	96
100	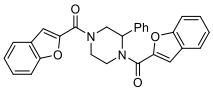				83
101	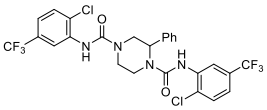				90

-Pathway C: Replacement of 2-substituted piperazine core with 2,6-dimethylpiperazine and unsubstituted piperazine (104–110, 112–114, 118–121).

A series of benzofurane-2-carbonyl-derived ureas (**104–110**, Table 3) with 2,6-dimethylpiperazine central ring were prepared as analogues of lead compounds **31–35,** through the same procedure used for the other substituted piperazine derivatives. NO_2, CN, Cl, CF_3, CH_3 substituted phenylisocyanates were implicated in the urea formation together with the intermediate **103** (Scheme 3).

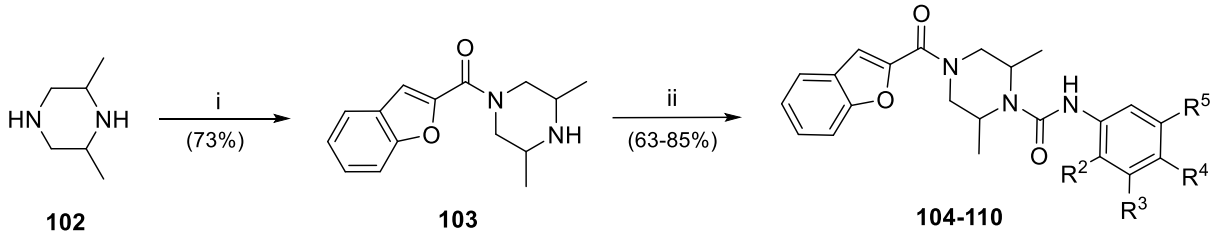

i: Acyl halyde 1 eq, pyridine 1.5 eq, DCM, 0-25 ºC, 24 h

ii: Isocyanate 1.2 eq, DCM, rt, 12 h

Scheme 3. Chemical synthesis of 4-(benzofurane-2-carbonyl)-2,6-dimethylpiperazine urea derivatives (**104–110**).

To prepare those analogues with an unsubstituted piperazine core, the Boc-piperazine, commercially available, was employed as the starting material. Firstly, the urea function was introduced by reaction with appropriate isocyanates, afforded compounds **112–114** which were deprotected in acid condition (CF_3COOH) at rt, using DCM as solvent. The intermediates **115** and **116** reacted with the acylating agent (benzofuran-2-carbonyl chloride) to obtain final products **118** and **119**. Finally, piperazine derivatives **120** (di-amide) and **121** (di-urea) were prepared through the same reaction used for 2-methyl piperazine analogues (**100**, **101**) (Scheme 4, Table 3).

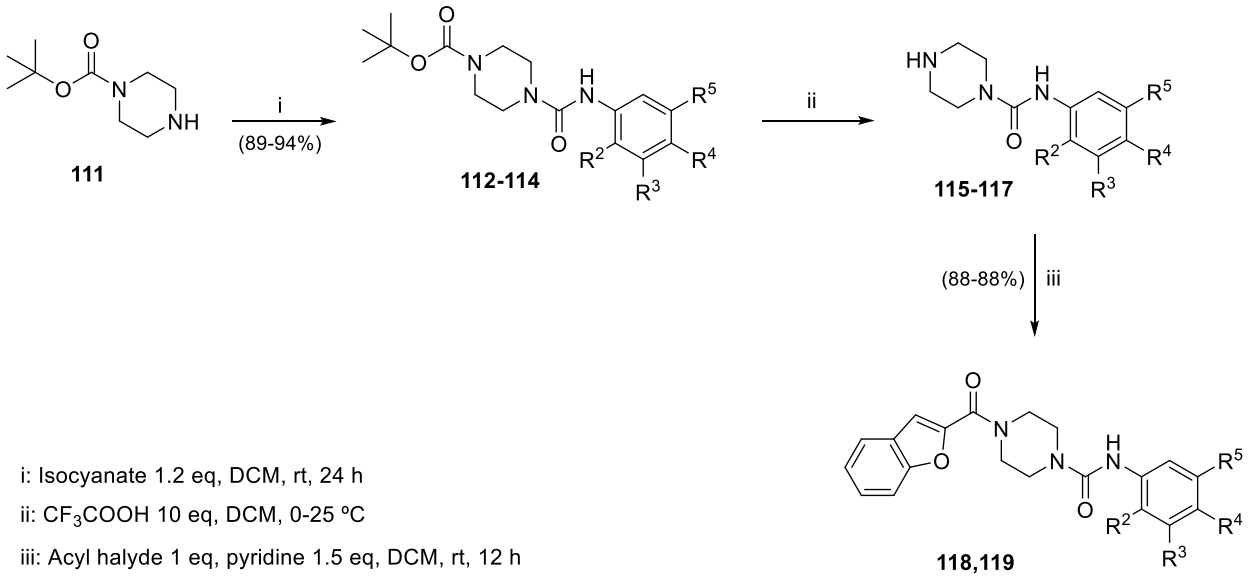

i: Isocyanate 1.2 eq, DCM, rt, 24 h

ii: CF_3COOH 10 eq, DCM, 0-25 ºC

iii: Acyl halyde 1 eq, pyridine 1.5 eq, DCM, rt, 12 h

Scheme 4. Chemical synthesis of 4-acyl-piperazine urea derivatives (**112–114**, **118**, **119**).

Table 3. 2,6-disubstituted and unsubstituted piperazine urea derivatives from pathway C.

Comp	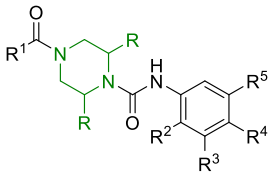						
	R	**R^1**	**R^2**	**R^3**	**R^4**	**R^5**	**Yield (%)**
104	Me	Benzofuran-2-yl	H	H	NO_2	H	75
105	Me	Benzofuran-2-yl	H	H	Cl	H	70
106	Me	Benzofuran-2-yl	H	H	CN	H	85
107	Me	Benzofuran-2-yl	NO_2	H	H	H	85
108	Me	Benzofuran-2-yl	H	H	CH_3	H	63
109	Me	Benzofuran-2-yl	Cl	H	H	CF_3	69
110	Me	Benzofuran-2-yl	H	CF_3	Cl	H	70
112	H	O*t*-Bu	H	H	NO_2	H	94
113	H	O*t*-Bu	NO_2	H	H	H	89
114	H	O*t*-Bu	Cl	H	H	CF_3	92
118	H	Benzofuran-2-yl	H	H	NO_2	H	80
119	H	Benzofuran-2-yl	NO_2	H	H	H	88
120	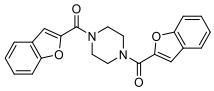						91
121	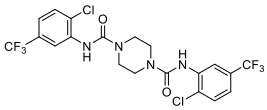						98

All new piperazine-derived compounds were characterized by NMR and Mass Spectrometry and through the determination of melting points. Representative resonance assignments from ^{1}H NMR and ^{13}C NMR of some selected compounds were illustrated in the Table 4.

Table 4. Selected piperazine derivatives and some representative resonance assignments (^{1}H NMR and ^{13}C NMR).

Compound		^{1}H NMR[a] (ppm)			^{13}C NMR[b] (ppm)		
		N*H*SO	C*H*CH$_3$/C*H*Ph	C*H*$_2$CO/ C(C*H*$_3$)$_3$[a]	C=O/C=S	*C*HCH$_3$/*C*HPh	CH$_3$/OCH$_3$
52	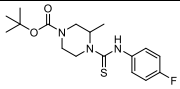	7.10	5.14-4.75	1.47[a]	183.6, 155.0	52.3	15.1
67	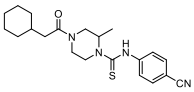	9.59	5.11	2.38-2.15	181.3, 170.7	51.7	15.1
68	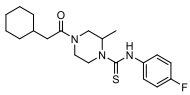	9.23	5.06	2.40-2.11	181.9, 170.7	51.3	15.1
71	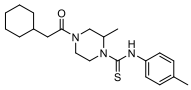	9.19	5.18-4.97	2.26-2.14	181.9, 170.7	51.2	20.5, 15.1
73	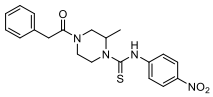	9.76-9.74	5.13	3.26-3.14, 3.08-2.86	181.2, 169.7	51.9	15.0
75	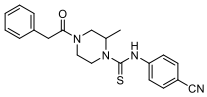	9.59-9.57	5.14	3.32-3-15, 3.08-2.89	181.3,169.7	51.7	15.0
80	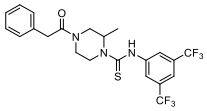	9.72-9.69	5.12	3.29-3.17, 3.06-2.94	180.9,169.8	51.6	15.1
92	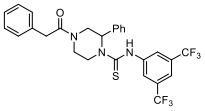	9.88	4.94	3.21-3.12	181.9,169.5	58.4	-
96	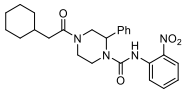	9-42-9.35	5.43-5.33	3.22-3.16	170.5,154.2	54.3	-
98	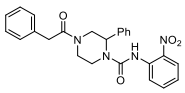	9.40	5.47	3.02-2.94	169.5,154.2	54.0	-
112	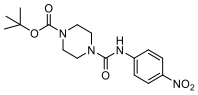	9.28	-	1.42[a]	153.9,153.8	-	-
114	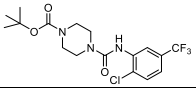	8.49	-	1.43[a]	154.5,153.8	-	-

[a]500 MHz, DMSO-d_6;

[b]125MHz, DMSO-d_6

3.2 Biological evaluation

New synthesized compounds were assessed for their antiviral activity against HAdV5 as well as for their cytotoxicity.

3.2.1. *In vitro* antiviral activity and effect on cellular viability

Firstly, the anti-HAdV activity of the new piperazine derivatives at 10 μM was evaluated in plaque assay (*293β5* cell line). Since cidofovir current represent the only therapeutic option for HAdV infection, it was also evaluated and compared to our results. The effect on cellular viability was examined in A549 cell line and the 50% cytotoxic concentration (CC_{50}) was determined for those compounds that reached a percentage of inhibition in the plaque assay >80%, in order to ascertain their safety profile. Among the compounds included in the pathway A (**50–92**) we have identified many piperazine thiourea derivatives which reached HAdV5-GFP plaque-formation inhibition >80% together with low cytotoxicity (CC_{50} > 100 μM) (Table 5). Compounds containing electron-withdrawing substituents (NO_2, Cl, CN, CF_3) in *para* position on the phenyl ring showed greater inhibition (**51**, **52**, **65**, **66**, **67**, **68**, **69**, **73**, **74**, **75** and **76**); NO_2 and Cl resulted to be the most present groups. Also the presence of two trifluoromethyl groups in 3 and 5 positions (not previously evaluated) increased the activity (**72** and **80**), while compound **71** with p-CH_3 represented an exception of the series (Table 5). With regard to the acyl function at N-4, compounds with 2-*tert*-butyl group did not achieve a percentage of inhibition more than 80%. On the contrary, the major part of highly active compounds contained 2-cyclohexylacetyl moiety (**65–69**, **71** and **72**). Thiourea derivatives with benzofuran-2-carbonyl group at N-4 (**81**, **82** and **84**) did not represent potentially interesting analogues. They displayed high inhibition (100%), but showed low CC_{50} values. Neither 2-phenyl piperazine analogues have demonstrated high percentage of plaque-formation inhibition, with the exception of **86**, **87** and **92** that showed better anti-HAdV activity (percentage range 80-100 %). It is important to note that compound **86** (2-*tert*-butylacetyl derivative from 2-phenyl piperazine) was an analogue of **64** (2-*tert*-butylacetyl derivative from 2-methy piperazine) which inhibited 4.8% of HAdV plaque formation. In this case, the presence of phenyl group in position 2 of piperazine core improved the antiviral activity profile.

Table 5. Inhibition of HAdV infection in the plaque assay and effects on cellular viability for compounds **50-92** from pathway A.

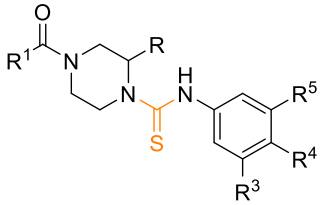

Comp	% of plaque-formation inhibition[a]	CC_{50}[b]	Comp.	% of plaque-formation inhibition[a]	CC_{50}[b]
50	73.43 ± 4.19	-	**72**	100.00 ± 0.0	82.4 ± 5.5
51	88.91 ± 15.92	175.0 ± 8.8	**73**	98.21 ± 3.57	210.4 ± 17.8
52	92.91 ± 3.82	200.0 ± 10.8	**74**	84.56 ± 15.72	175.0 ± 10.2
53	73.43 ± 22.49	-	**75**	98.36 ± 2.13	174.7 ± 4.8
54	36.55 ± 30.13	-	**76**	100 ± 0.0	26.3 ± 1.6
55	49.11 ± 4.73	-	**77**	73.43 ± 4.19	-
56	11.11 ± 19.25	-	**78**	88.91 ± 15.92	175.0 ± 8.8
57	76.23 ± 22.02	-	**79**	92.91 ± 3.82	200.0 ± 10.8
58	61.64 ± 25.29	-	**80**	73.43 ± 22.49	-
59	51 ± 4.13	-	**81**	100 ± 0.0	20.0 ± 15.5
60	7.50 ± 15.00	-	**82**	100 ± 0.0	25.5 ± 10.0
61	36.33 ± 32.43	-	**83**	85.0 ± 6.10	75.4 ± 22.8
62	58.11 ± 17.20	-	**84**	100 ± 0.0	46.3 ± 20.8
63	76.83 ± 13.56	-	**85**	27.5 ± 10.6	-
64	4.81 ± 9.34	-	**86**	100.0 ± 0.0	91.8 ± 0.9
65	82.56 ± 15.63	148.1 ± 12.5	**87**	80.0 ± 7.1	65.3 ± 10.5
66	89.33 ± 10.08	200.0 ± 0.0	**88**	5.0 ± 6.3	-
67	100.00 ± 0.0	193.0 ± 4.9	**89**	15.0 ± 8.5	-
68	100.00 ± 0.0	143.4 ± 6.6	**90**	5.5 ± 7.8	-
69	88.94 ± 10.32	142.2 ± 7.9	**91**	64.0 ± 12.7	-
70	25.53 ± 36.11	-	**92**	100.0 ± 0.0	104.3 ± 15.4
71	95.79 ± 4.82	122.2 ± 12.5	**Cidofovi**[c]	3.51 ± 4.97	50.6 ± 9.8

[a] Percentage of control HAdV5-GFP inhibition in a plaque assay at 10 mM using the 293β5 cell line
[b] Cytotoxic concentration 50%. The results represent means ± SD of triplicate samples from three independent experiments
[c] Data of cidofovir, as positive clinical drug candidate, have been list.

The effect of different acyl groups at N-4 keeping the presence of the urea function at N-1 in 2-phenyl piperazine was examined (Table 6). Compounds **93–99** from pathway B were all active, with

percentages of plaque-formation inhibition ranging from 74% to 100%, independently of the acyl nature (2-*tert*-butylacetyl, 2-cyclohexylacetyl, 2-phenylacetyl) and of the phenylaminocarbonyl substituents (*p*-NO2, *o*-NO2, *o*-Cl-*m*-CF_3) Compounds **100** (di-amide derivative) showed a weak antiviral activity (19% inhibition in plaque assay), whereas compound **101** (di-urea derivative) resulted to be a good inhibitor of HAdV infection (90.4%). These results suggest the relevance of the urea function for the antiviral activity.

Table 6. Inhibition of HAdV infection in the plaque assays and effects on cellular viability for compounds **93-101** from pathway B.

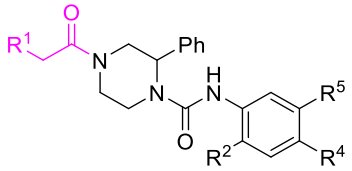

Comp.	% of plaque-formation inhibition[a]	CC_{50}[b]
93	74.4 ± 29.0	72.0 ± 9.2
94	100 ± 0.0	63.3 ± 5.7
95	98.9 ± 1.5	71.8 ± 5.0
96	100 ± 0.0	112.1 ± 10.1
97	82.6 ± 12.3	174.0 ± 12.8
98	96.9 ± 1.4	120.5 ± 10.6
99	100 ± 0.0	64.5 ± 5.3
100	19.4 ± 6.4	-
101	90.4 ± 12.4	200 ± 0.0
Cidofovir[c]	3.51 ± 4.97	50.6 ± 9.8

[a] Percentage of control HAdV5-GFP inhibition in a plaque assay at 10 mM using the 293b5 cell line
[b] Cytotoxic concentration 50%. The results represent means ± SD of triplicate samples from three independent experiments
[c] Data of cidofovir, as positive clinical drug candidate, have been list.

The impact of an additional substituent on the piperazine scaffold and of the use of unsubstituted piperazine core was also analysed (pathway C). Among the 2,6-dimetilpiperazine urea derivatives with benzofuranyl acyl group, only compounds **105** and **107** (*p*-Cl and *o*-NO_2 respectively) displayed

moderate percentages of plaque-formation inhibition (81.1% and 72.2% respectively), indicating that more substituents on this scaffold were not generally well tolerated (Table 7). Conversely, two piperazine derivatives (**112**, **114**), with *tert*-butyloxycarbonyl group at N-1, inhibited plaque-formation with a percentage >90% and CC_{50} >100 µM. Both di-amide **120** and di-urea **121** derivatives (analogues of **100** and **101** respectively) were poorly active (Table 7).

Table 7. Inhibition of HAdV infection in the plaque assays and effects on cellular viability for compounds **104-110, 112-114, 118-121** from pathway C.

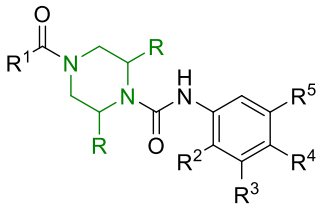

Comp.	% of plaque-formation inhibition[a]	CC_{50}[b]
104	12.2 ± 17.3	-
105	81.1 ± 4.7	113.3 ± 12.5
106	10.0 ± 12.2	-
107	72.2 ± 4.4	-
108	0.0 ± 0.0	-
109	0.0 ± 0.0	-
110	0.0 ± 0.0	-
112	91.5 ± 5.5	118.1 ± 1.7
113	15.0 ± 16.9	-
114	95.0 ± 7.1	200 ± 0.0
118	0.0 ± 0.0	-
119	41.5 ± 4.9	-
120	51.5 ± 4.3	-
121	33.9 ± 9.7	-
Cidofovir[c]	3.51 ± 4.97	50.6 ± 9.8

[a] Percentage of control HAdV5-GFP inhibition in a plaque assay at 10 mM using the 293b5 cell line
[b] Cytotoxic concentration 50%. The results represent means ± SD of triplicate samples from three independent experiments
[c] Data of cidofovir, as positive clinical drug candidate, have been list.

Compounds with percentage of inhibition >90% in the plaque assay and CC_{50} values >100 µM were selected for further evaluation. Twelve compounds demonstrated to have selectable profiles, eight

from pathway A (**52**, **67**, **68**, **71**, **73**, **75**, **80** and **92**), **96** and **98** from pathway B, **112** and **114** from pathway C.

3.2.2. Determination of IC_{50} values and fold-reduction in virus yield

The half maximal inhibitory concentration (IC_{50}) for selected compounds was measured and the selectivity index was calculated. Selected compounds demonstrated to block HAdV infection in a dose-dependent manner (Figure 18) and their IC_{50} values ranging from 0.6 μM to 5.1 μM (Table 8). This new set of piperazine derivatives resulted in a slight optimization of activity compared to lead compounds from the previous work (**31–36**); two compounds showed anti-HAdV activity at nanomolar concentrations (**68** and **92**) and eight compounds presented IC_{50} < 2.5 μM.

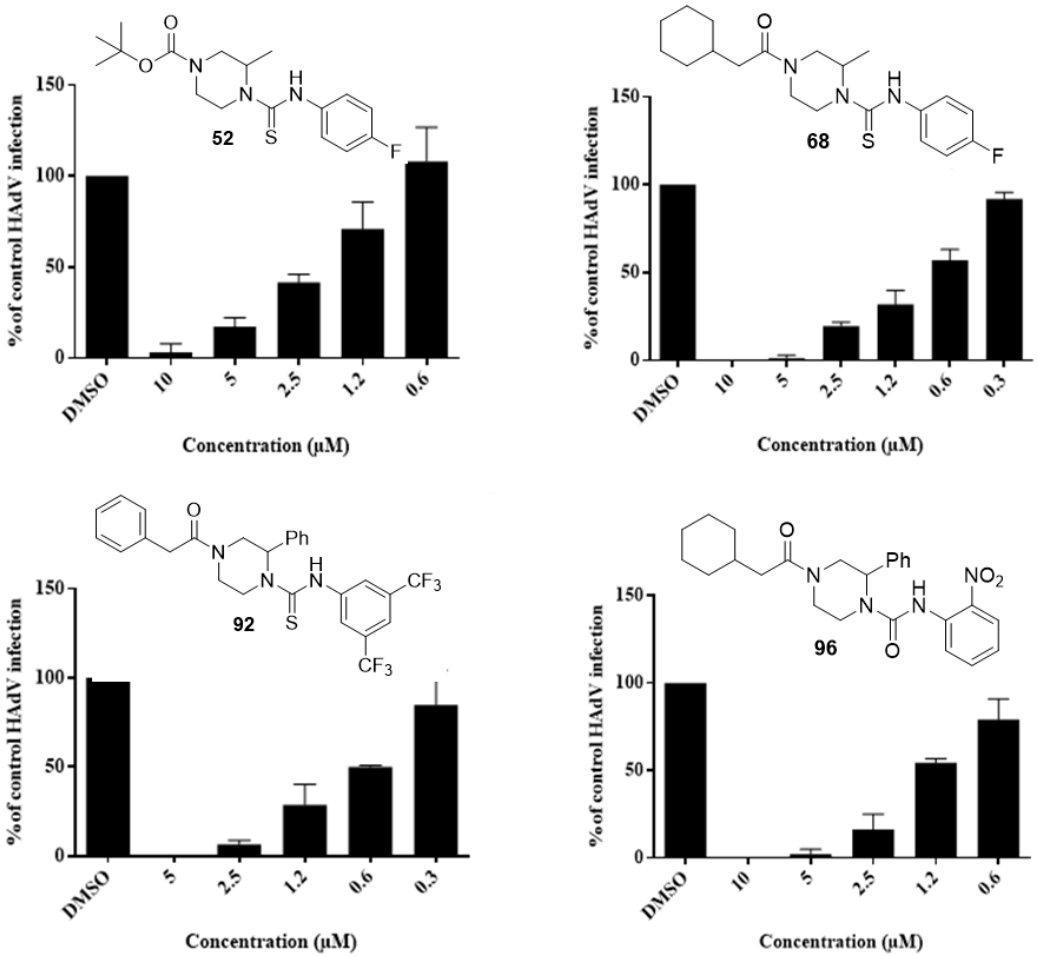

Figure 18. Dose-dependent activity of representative selected derivatives in a plaque assay. For all panels, the DMSO control is a positive control with cells infected at the same MOI (multiplicity of infection) but in the absence of drugs. The results represent means ± SD of triplicate samples from three independent experiments.

Compounds from 2-phenyl piperazine *o*-NO_2 substituted on the phenyl ring (**96**, **98**) and with 2-cyclohexylacetyl or 2-phenylacetyl at N-4, resulted to be more active than the benzofuran analogue **35** (IC_{50} = 1.4-2.1 μM vs 2.5 μM). On the contrary, compounds with the *p*-NO_2 substituent (**73** and **112**) preserved similar activity to previous compound **32** (IC_{50} range = 2.0-2.7 μM), but less than compound **36** (Boc-derivative). The presence of *p*-CN group together with an aromatic moiety at N-4 (**75**) gave comparable activity to lead compound **34** (benzofuran derivative), with IC_{50} of 4.6 μM and 4.7 μM respectively, while the 2-cyclohexylacetyl derivative **67** increased the activity (IC_{50} = 2.5 μM). In addition, the determined IC_{50} values of cidofovir from our studies (24.06 μM) were significantly higher than values showed by piperazine derivatives. These selected derivatives also presented a better safety profile (CC_{50} range 104.3-201.4 μM) compared to previous compounds **37** and **38** (CC_{50} 26.3 and 21.4 μM respectively) and similar to lead compounds **31–36** (CC_{50} range 130.8-199.8 μM) (Table 8).

Compound **68** demonstrated to be the most effective anti-HAdV agent (IC_{50} = 0.6 μM). It was a methyl piperazine derivative with a *p*-F phenyl urea at N-1 and a cyclohexylacetyl group at N-4. Since the structure-activity relationship point of view, the replacement of cyclohexyl substituent with *tert*-butoxy one (**52**) decreased the antiviral activity (IC_{50} = 1.8 μM) as well as the presence of *p*-CN (**67**) or *p*-CH_3 (**71**) on phenyl ring (IC_{50} values higher than 2 μM) (Table 8). Also compound **92** resulted to be one of best active compounds (IC_{50} = 0.7 μM); the thiourea function, decorated with two CF_3 group on the aromatic ring, was connected to a 2-phenyl piperazine central core, while a phenylacetyl function is located at N-4. A reduction in antiviral activity was observed by exchanging the bis-CF_3 group with *p*-CN or *o*-NO_2 (**90** and **91**). The replacement of 2-phenylpiperazine with the methyl one (**80**) also reduced the inhibition of HAdV infection (IC_{50} =5.1 μM) (Table 8).

The antiviral effect of selected derivatives was subsequently examined using a virus burst assay in order to quantity their block of the production of new virus particles. These compounds were associated with virus yield reductions comparable with prototypes **31–36.** One of them (**92)** presented an impressive reduction of HAdV yield (1690-fold) (Table 7).

Table 8. IC_{50}, CC_{50}, SI and virus yield reduction values for selected compounds compared to prototypes **31–36** and drug cidofovir.

Compound		IC_{50} (µM)[a]	CC_{50} (µM)[b]	Selectivity Index (SI)[c]	Yield reduction (fold-reduction)[d]
52	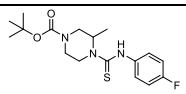	1.8±0.9	200.0±10.8	111.1	12.1±2.8
67	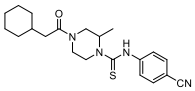	2.5±0.8	193.0±4.9	77.2	9.3±2.9
68	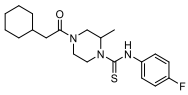	0.6±0.2	143.4±6.6	238.3	30.5±12.9
71	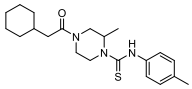	2.1±0.4	122.2±12.5	58.19	39.1±15.9
73	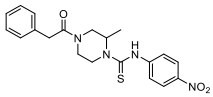	2.0±0.4	210.4±17.8	105.2	25.6±10.5
75	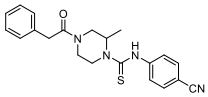	4.6±0.1	174.7±4.8	38.0	18.4±5.4
80	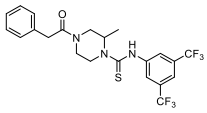	5.1±0.5	129.7±3.8	25.4	33.4±10.2
92	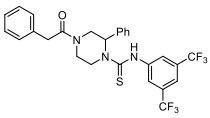	0.7±1.3	104.3±15.4	149.0	1,690±271.7
96	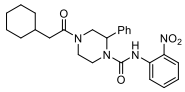	1.4±0.4	112.1±10.1	80.1	15.2±4.5
98	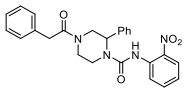	2.1±0.7	120.5±10.6	57.4	32.9±12.8
112	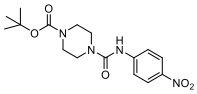	2.7±0.9	118.1±1.7	43.7	21.2±10.1
114	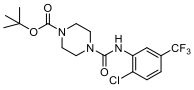	2.3±0.7	200±0.0	87.0	18.7±9.7
31[e]	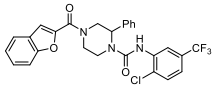	3.4±0.96	161.3±45.18	47.3	211.7±44.1
32[e]	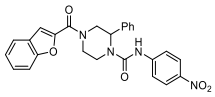	2.1±0.10	193.9±1.68	93.5	35.7±13.5
33[e]	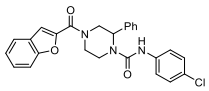	2.5±1.17	193.5±9.19	79	9.9±3.4

Compound		IC_{50} (µM)[a]	CC_{50} (µM)[b]	Selectivity Index (SI)[c]	Yield reduction (fold-reduction)[d]
34[e]	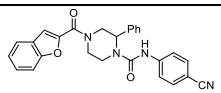	4.7±0.11	199.8±0.26	42.7	16.9±5.2
35[e]	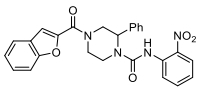	2.5 ± 0.0	131.8 ± 6.0	53.3	34.5 ± 12.6
36[e]	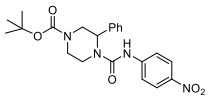	1.1±0.05	130.8±17.79	116.2	60.3±15.2
Cidofovir[e]		24.06 ± 5.9	50.6 ± 9.8	7.5	82.5 ± 21.4

[a] Inhibitory concentration 50 at low MOI in a plaque assay.
[b] Cytotoxic concentration 50.
[c] Selectivity Index value was determined as the ratio of cytotoxic concentration 50 (CC_{50}) to inhibitory concentration 50 (IC_{50}) in a plaque assay for each compound.
[d] Fold-reduction in virus yield as the ratio of particles produced in the presence of DMSO divided by the yield in the presence of each of compounds (50 µM).
[e] Data of lead compounds from previous work and cidofovir as positive clinical drug candidate.
The results represent means ± SD of triplicate samples from three independent experiments.

3.2.3. Insights into the antiviral mechanism of action

For selected compounds further studies were performed to gain some knowledge regarding their potential mechanism of action.

Impact on HAdV entry

After the attachment of HAdV virions to host cellular receptors through the fibre, they are internalized by clathrin-mediated endocytosis. Inside the endosome the progressive uncoating expose the membrane lytic viral protein VI with consequent endosomolysis and release of viral particles into the cytoplasm. [24] Then, the translocation of virus to the cell nucleus occurs through the association to cellular microtubule network. Since HAdV genomes generally accumulated into the nucleus, we have examined the potential ability of selected compounds to inhibit the HAdV entry by quantifying the number of HAdV genomes that reach the host nucleus after the infection. From our study, a significant inhibition of the HAdV genome accumulation at the nucleus of the host cell was observed for compounds **96**, **98** and **114** (Figure 19), suggesting that their antiviral activity was associated with some steps of HAdV entry. Other compounds did not demonstrate to influence this phase of viral life cycle.

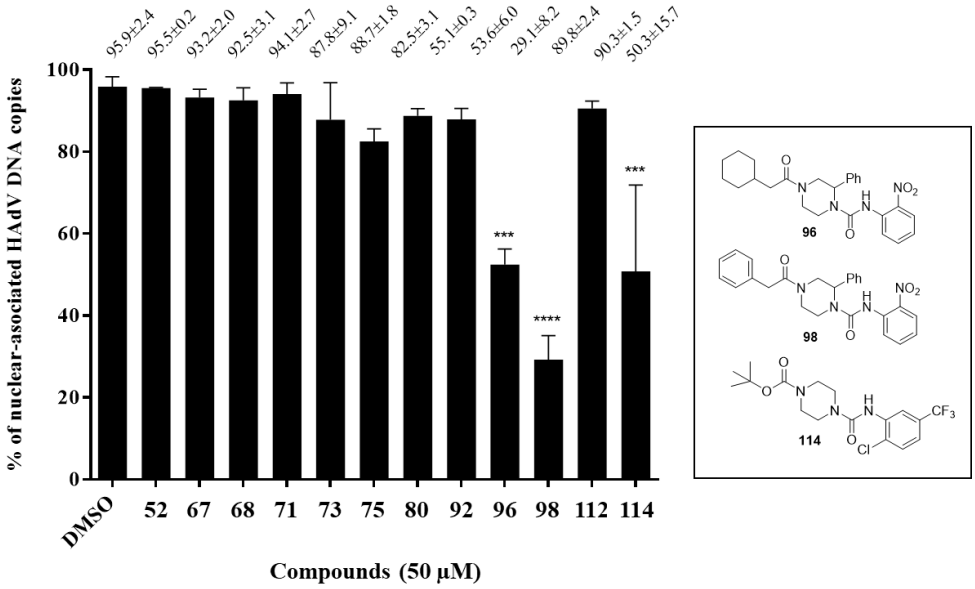

Figure 19. Effect of the selected compounds on nuclear association of HAdV5 genomes. Bars represent means ± SD of triplicate samples from two independent experiments. *P<0.05.

Impact on HAdV DNA replication

The influence on viral DNA replication of new piperazine derivatives was primarily examined by measuring the production of HAdV DNA copies through quantitative polymerase chain reaction (PCR) assay. Our results demonstrated an inhibition of HAdV DNA replication by compounds **71**, **73**, **75**, **80**, and **112**. They significantly reduced HAdV DNA copies after 24 hours of infection compared to the positive control. (Figure 20A). These compounds could directly inhibit viral proteins involved in DNA replication (DNA polymerase), or may interfere with a previous step, such as the transcription of the immediate early gene E1A. In the nucleus, the transcription of the viral early gene E1A by cellular RNA polymerase II is necessary for the subsequent expression of the early genes E1B, E2, E3, and E4 and to trigger the HAdV DNA replication [7]. Compound **71**, **73**, **112** and especially compound **80** provided a reduction of E1A cDNA copies (Figure 20B). The α-amanitin, a cyclic peptide toxin derived from the mushroom *Amanita phalloides*, is able to block the activity of the RNA polymerase II and thus the generation of new HAdV particles [87]. Compound **80** showed a dose-dependent activity similar to α-amanitin, so it could be target RNA polymeras II. Alternatively, compound **80** may interact with HAdV early transactivator E1A, the DNA-pVII complex or other proteins implicated in the regulation of E1A transcription. To evaluate if the potential target of new compounds was the viral DNA polymerases, the effect on the *in vitro* amplification efficiency of the DNA polymerase from bacteriophage Phi29 was examined. Phi29 is

a closely-related DNA polymerase belonging to the same family of viral DNA polymerase, the family B. Compound **71** showed significant inhibition of the Phi29 DNA polymerase activity (Figure 20C), suggesting that its preferential target may be the HAdV DNA polymerase. Compounds **52**, **67**, **68**, **92** and **98** did not demonstrate inhibition of the HAdV genome accessibility to the nucleus or of the HAdV DNA production. The mechanism of action for these compounds may be related to later steps in the HAdV replicative cycle, such as assembly, maturation or release of the new viral particles.

The twelve derivatives influenced different steps in the HAdV life cycle such as the HAdV entry process, the transcription of the E1A gene, viral DNA replication or later steps. Additional studies are needed to clarify the specific mechanisms for the inhibition of HAdV infection by these seven compounds. Since they have shown high variability regarding their potential mechanism of action, these compounds could be useful as a tool to clarify the complex events involved in the HAdV replicative cycle.

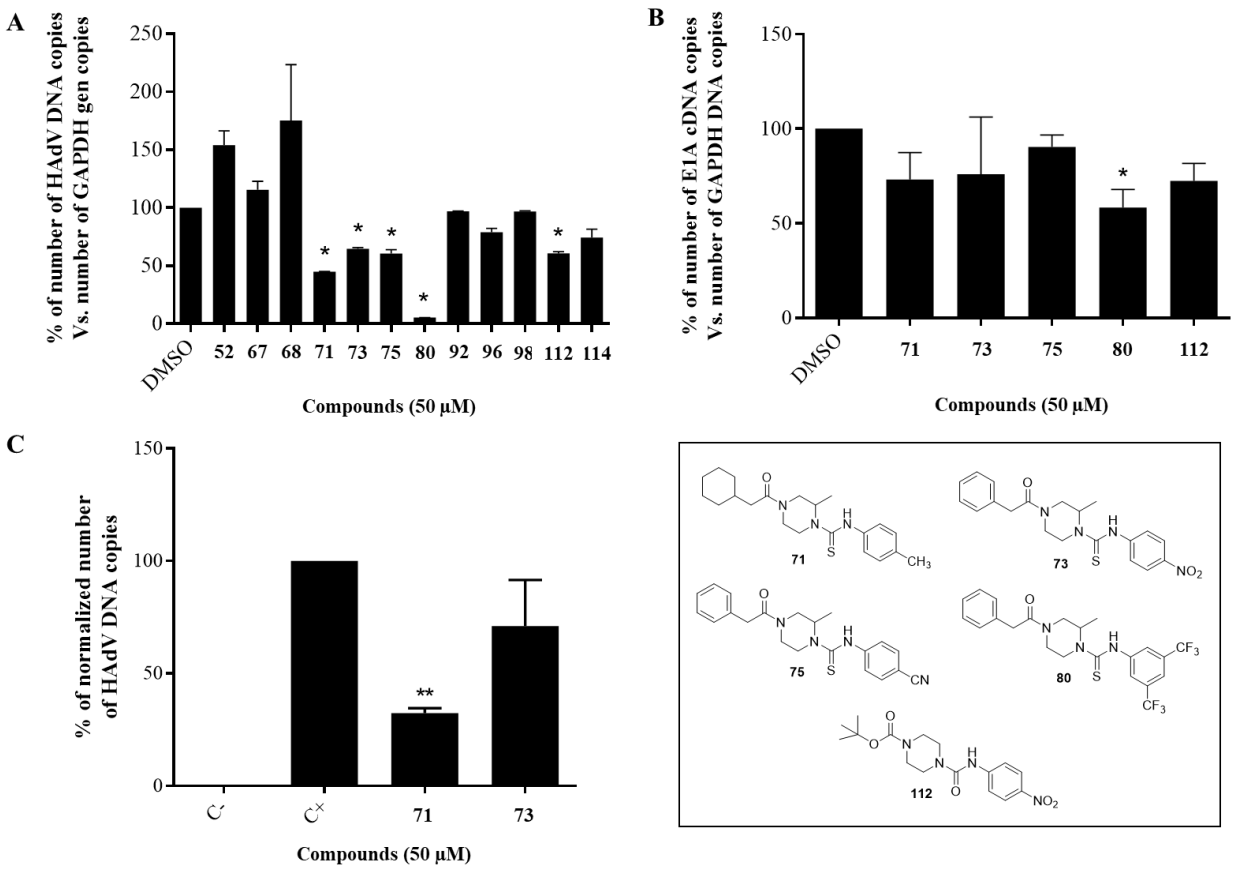

Figure 20. Effect of the selected compounds on HAdV DNA replication. (A) De novo production of HAdV DNA copies compared to the positive control 24-h post-infection in a quantitative PCR assay. (B) Expression of the immediate early gene E1A compared to the positive control 6-h post-infection in a quantitative PCR assay. (C) Impact on the amplification efficiency of the Phi29 DNA polymerase. The results are expressed as the relative copy number of HAdV DNA and E1A mRNA normalized to GAPDH copy number, and they are presented as the mean ± SD of triplicate assays. *P < 0.05.

3.2.4. Synergistic activity evaluation

Since these new compounds presented different ways to explicate their activity, the effect on the HAdV infection inhibition of compound combinations with diversified mechanisms of action was investigated. A representative piperazine derivative for each mechanism type was selected to perform a combination study based on the Chou-Talalay method, using the CalcuSyn software [88]. Compound **68** was selected due to its action in later steps after DNA replication, compound **71** as an inhibitor of the HAdV DNA replication process (DNA polymerase) and compound **80** as inhibitor of the E1A transcription. All compounds were 4-acyl-1-phenylaminothiocarbonyl-2-methylpiperazine derivatives from pathway A. The ratio for each combination was selected based on IC_{50} values of selected derivatives. All the combinations demonstrated good conformity to the mass-action law as shown in Table 9 (r ranged from 0.937 to 0.967). A very strong synergism was observed for the combination **68** + **71** (1:4) at all three levels of inhibition (IC_{50}, IC_{75} and IC_{90}) and for **68 +71 + 80** (1:4:8) at IC_{90}. The combination **71** + **80** (1:2) at IC_{90}, **68** + **80** (1:8) at all the levels of inhibition and **68 + 71 + 80** (1:4:8) at IC_{50} and IC_{75} levels were considered synergism (Table 9). The different proposed ways of action of these compounds were supported by the significant combinatory index values CI (a pharmacological interaction estimation which uses the IC_{50} and the dose-response curve's shape of each individual compound and their combinations) obtained using the CalcuSyn software for all the combinations.

Table 9. Synergistic activity of different combinations three selected anti-HAdV compounds.

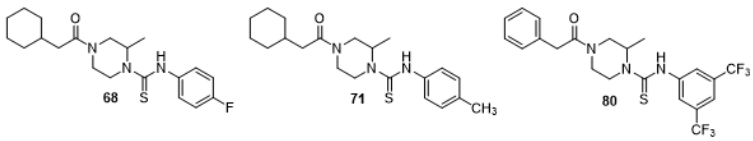

Comp ratio	Combinatory index (CI) values at			r[a]
	IC_{50}	IC_{75}	IC_{90}	
68 + 71 (1:4)	0.095	0.092	0.091	0.937
68 + 80 (1:8)	0.359	0.350	0.353	0.959
71 + 80 (1:2)	0.202	0.254	0.319	0.939
68 +71 + 80 (1:4:8)	0.443	0.474	0.091	0.937

[a] The r value for each combination is also reported to indicate the correlation coefficient of the data to the mass-action law.

3.2.5. Hamster serum stability

We examined the stability of selected compounds in Syrian hamster serum as a previous step to the evaluation of their efficacy and safety in the Syrian hamster model of HAdV infection. This assay allowed to select the antiviral compounds with structural moieties resistant to degradation by serum proteins and with low binding to serum proteins. Compounds included in this test were those SI values >100 and with different modes of action to block HAdV infection (**52**, **68**, **73** and **92**), together with **80** due to its ability to inhibit the E1A transcription. A significant degradation significant degradation after 2 hours of incubation in hamster serum was observed for compounds **52** and **68**, tertbutoxycarbonyl and 2-cyclohexylacetyl derivatives respectively, with percentages of remaining compound <70%. Compounds **73** and **92** didn't incur in any degradation after 2 hours of incubation, displaying percentages of remaining compound of 106.7 and 100.0 respectively. At last, compound **80** showed a percentage of remaining compound of 92.8% (Table 10).

Table 10. Selected derivatives serum stability in a graphical representation of the percentage of the derivatives remaining at different incubation time points.

Time	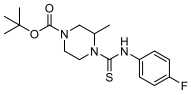	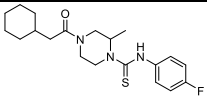	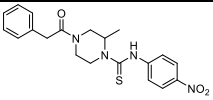	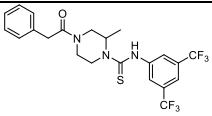	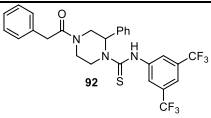
	52	**68**	**73**	**80**	**92**
0	100.0±8.6[a]	100.0±25.3	100.0±11.2	100.0±3.0	100.0±8.4
15	97.8±6.0	116.7±20.5	142.7±8.5	108.9±6.2	97.2±3.6
30	102.4±14.3	96.4±31.2	139.4±2.3	106.6±4.2	109.6±13.5
60	86.5±30.3	85.0±24.1	114.2±6.5	96.5±3.6	90.5±16.9
120	75.4±5.0	67.3±27.7	106.7±3.8	92.8±13.3	100.0±9.2

[a] Percentages of remaining compound at different time points (minutes). The results represent means ± SD from three independent experiments.

3.3 *In silico* prediction of physicochemical properties: drug-likeness evaluation

During the drug discovery and the development of compounds with biological activity, the preliminary estimation of the absorption, distribution, metabolism and excretion (ADME) properties for potential drug candidates reduces pharmacokinetic-related failures in the later phases of the development [89]. Some physicochemical properties of twelve selected compounds were predicted using a free online software (http://www.molinspiration.com) to assess their compliance with the Lipinski's rule of five [90]. Eleven compound resulted well conformed to the Lipinski's rule of five,

while compound **92** failed with two violations, LogP and Molecular Weight values that surpassed the accepted ranges (Table 11).

The bioavailability is mainly related to gastrointestinal absorption. Drug-likeness is a concept used in drug discovery to identify and exclude compounds with an inadequate pharmacokinetic profile. it is based on the analysis of the physicochemical properties and structural features of drug candidates and allows to evaluate if a molecule can become an oral drug with respect to their bioavailability [91]. Also the freely accessible web tool SwissADME (http://www.swissadme.ch) was employed to evaluate pharmacokinetics and drug-likeness of these small molecules [92]. Also in this case, compound **92** showed the same Lipinski's rules violations; in addition, the Bioavailability Radar, a rapid drug-likeness evaluation based on physicochemical properties lipophilicity, size, polarity, solubility, flexibility and saturation, predicted only compound **92** as no orally bioavailable due to be too lipophilic, insoluble and high sized. On the contrary, other compounds conformed to both Lipinski's and Veber's rules. According to Brain Or IntestinaL EstimateD permeation method (BOILED-egg) [92] the predicted human gastrointestinal absorption was high for all compounds except for compound **92**.

Table 11. Prediction of physicochemical properties of selected compounds.

N°	**NViol[a]**	**Natoms[b]**	**miLogP[c]**	**MW/Da[d]**	**nON[e]**	**nOHNH[f]**	**Nrotb[g]**	**TPSA/A^{2}, [h]**	**MV[i]**
AR[l]			<5	<500	<10	<5	≤10	<140	
52	0	24	3.01	356.46	5	1	5	44.81	321.91
67	0	27	3.63	384.55	5	1	5	59.37	365.47
68	0	26	4.04	377.53	4	1	5	35.57	353.54
71	0	26	4.33	373.57	4	1	5	35.57	365.17
73	0	28	2.90	398.49	7	1	6	81.40	353.36
75	0	27	2.69	378.50	5	1	5	59.37	346.88
80	0	33	4.66	489.49	4	1	7	35.57	392.62
92	2	38	5.91	551.56	4	1	8	35.57	447.46
96	1	33	5.14	450.54	8	1	5	98.47	417.91
98	0	33	4.20	444.49	8	1	5	98.47	399.32
112	0	25	2.58	350.38	9	1	4	107.70	314.85
114	0	27	4.12	407.82	6	1	4	61.868	336.35

[a] nViol: no. of violations; [b] natoms: no. of atoms; [c] miLogP: molinspiration predicted LogP; [d] MW: molecular weight; [e] nON: no. of hydrogen bond acceptors; [f] nOHNH: no. of hydrogen bond donors; [g] nrotb: no. of rotatable bonds; [h] TPSA: topological polar surface area; [i] MV: molar volume; [l] AR: accepted range

These results have been recently published [93].

CHAPTER 4

O-ACYL-*N*-PHENYLAMINOCARBONYL SERINOL DERIVATIVES

4.1 Chemistry

4.1.1 Design

With the aim to identify novel privileged structures for the development of potential anti-adenovirus agents, our interest was focused on aminoalcohols as employed scaffolds for the preparation of new compounds libraries. In the first place, we have selected the symmetric aminoalcohol serinol as central backbone and precursor on new molecules. Many of reported antiviral acyclic nucleoside analogues presented an aminoalcohol or glycerol skeleton, such as cidofovir and ganciclovir (**1**, Figure 21), that represent the current therapeutic options for severe HAdV infections acting as inhibitors of viral DNA replication; even if they resulted not very effective and associated with several adverse effects (section 1.4)[56]. Also the antiviral drug penciclovir (**122**, Figure 21), used for the treatment of various herpesvirus infections, consist of a guanine base connected to an aminoalcohol five-carbon chain [94].

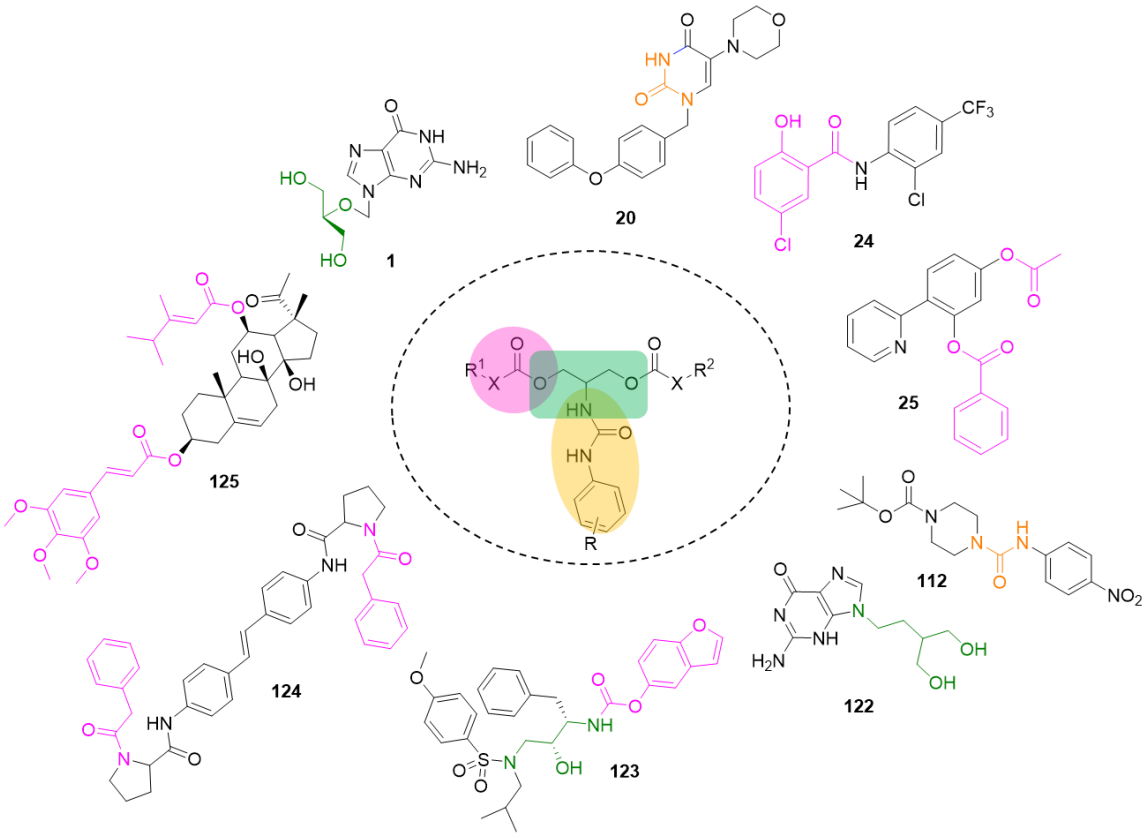

Figure 21. Design of new set of serinol derivatives.

In this context, non-nucleoside compounds with isopropanolamine core and a simple heterocyclic structure have been discovered as antiviral agents against HIV (**123**, Figure 21) [95]. An important structural consideration that prompted us to choose this scaffold consists in the symmetry. Diversified symmetric compounds have been described as potential antiviral candidates, such as novel symmetrical phenylenediamines targeting the viral HCV NS3 helicase[96], symmetrically disposed stilbenes as potent inhibitors of NS5A proteins (**124**, Figure 21) [97], and complex homodimeric structures derived from daclastavir and other related symmetric compounds [98,99]. In this field, no symmetric compounds have been described as potential anti-HAdV agents. From a chemical point of view, serinol scaffold allow us to quickly design and generate new molecules keeping some important features present in reported anti-adenovirus compounds, mainly urea [76,84] and amide/ester [78,79,81] functions that have been identified as relevant for the antiviral activity (**20**, **24**, **25**, **112**, Figure 21).

The general structure of new compounds shared the urea function at position 2 of serinol chain and an aromatic moiety connected to both primary hydroxyl groups through an acyl function (ester or carbamate, Figure 22). The points of structural variability that have been investigated regarded the introduction of several substituents on the phenyl ring of the ester function as well as of the phenylaminocarbonyl group, in order to assess different electronic properties, and the replacement of the ester moiety with a carbamate one. The *N*-aryl urea function was decorated with three different groups (*p*-CF_3, *p*-CH_3, 3-CF_3-4-Cl), in order to evaluate the effect of mono and di-substitutions as well as different electronic behaviours. In the collection of diester derivatives, we have explored the presence of a wider variety of substituents on the phenyl ring, having electron-withdrawing (CN and NO_2) or donating properties (CH_3, $N(CH_3)_2$, OCH_3). In particular, our attention was focused on methoxy groups (mono, di and trimethoxy), due to these benzoyl derivatives represent interesting scaffolds found in several anticancer and antiviral compounds, in the form of amides or esters [82,100,101]. In this field and aimed to further explore the presence of methoxy groups, a trimethoxycynnamic moiety was also inserted, in order to examine the presence of a spacer between the acyl function and the terminal 3,4,5-trimetoxyphenyl ring (Figure 22). Over the years, several reported antiviral natural products and molecular hybrids with trimethoxycynnamic portions have been discovered, such as compound **125** (Figure 21) which demonstrated *in vitro* anti-hepatitis B activity [102]. Some monoester serinol derivatives were also designed (Figure 22) considering that many antiviral acyclic nucleosides displayed at least one free primary hydroxyl group. Finally, we performed a change in the acyl function, introducting a carbamate in the pleace of the ester. These

compounds were prepared due to their potential to engage in additional hydrogen interactions through both urethane functions.

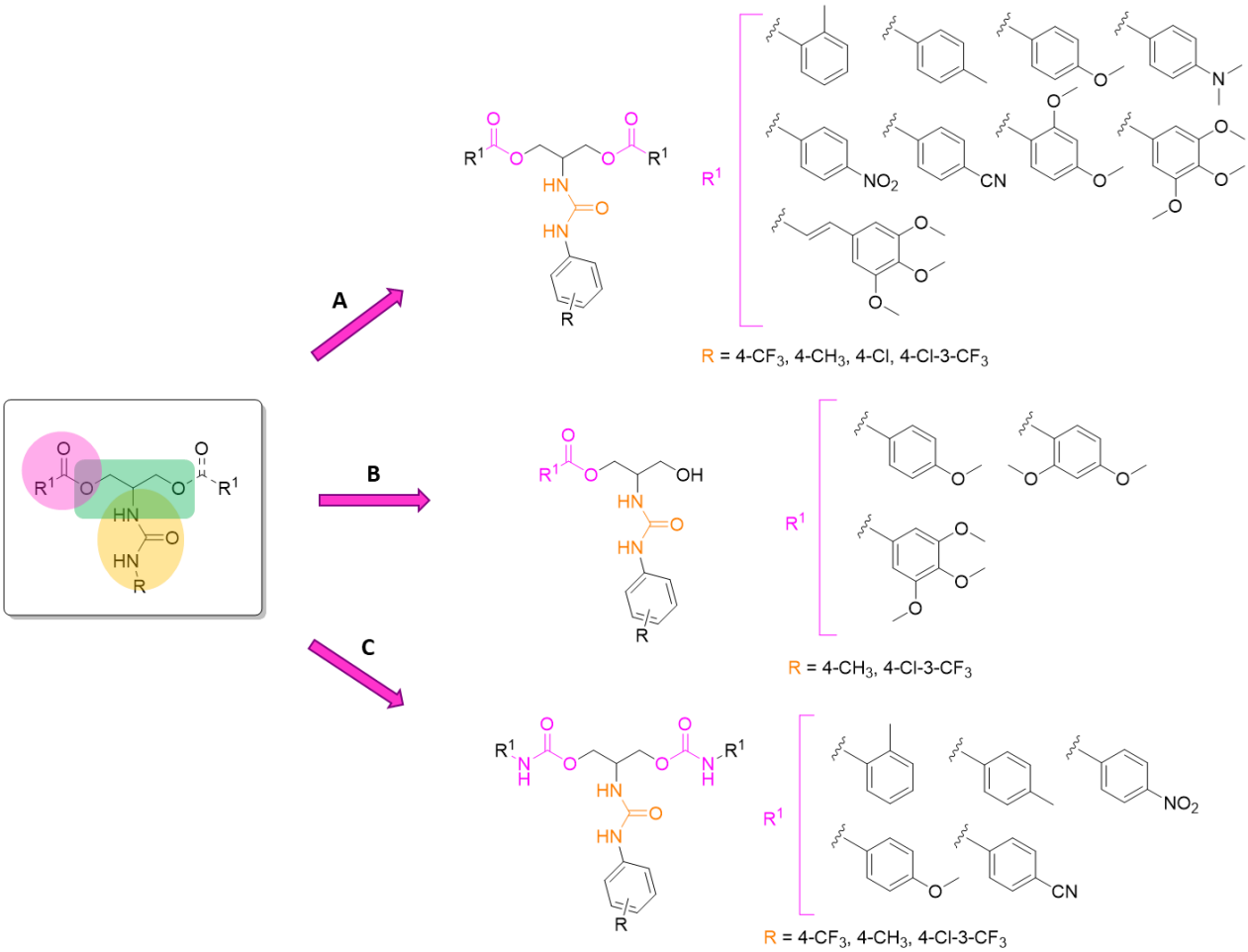

Figure 22. General structures of new designed diester, dicarbamate and monoester derivatives from serinol.

4.1.2 Synthesis

The synthetic pathways for the preparation of new set of serinol-derived diesters, monoesters and dicarbamates included two reaction starting from commercially available 2-amino-1,3-propanediol (serinol), which shared the first step providing the insertion of urea function, while they differed in the second one (ester/carbamate formation).

-Pathway A: Synthesis of N-phenylaminocarbonyl serinol diester derivatives (131–155)

Diester derivatives of serinol (**131–135**) were obtained following the synthetic route depicted in the Scheme 5. Primarily, the urea function was introduced an N-2 of serinol skeleton by the reaction of **126** with appropriate substituted phenyl isocyanate (*p*-CF_3, *p*-CH_3, 3-CF_3-4-Cl, *p*-Cl) in DCM at rt (**127–130**). Subsequently, aromatic esters **131–152** were synthesized by an acylation reaction of both primary hydroxyl groups, using corresponding acyl chloride and DMAP, in DCM at rt. At this step, the diversity was introduced on the phenyl ring through substituents with different electronic properties (CN, NO_2, CH_3, $N(CH_3)_2$, OCH_3, di-OCH_3, tri-OCH_3).

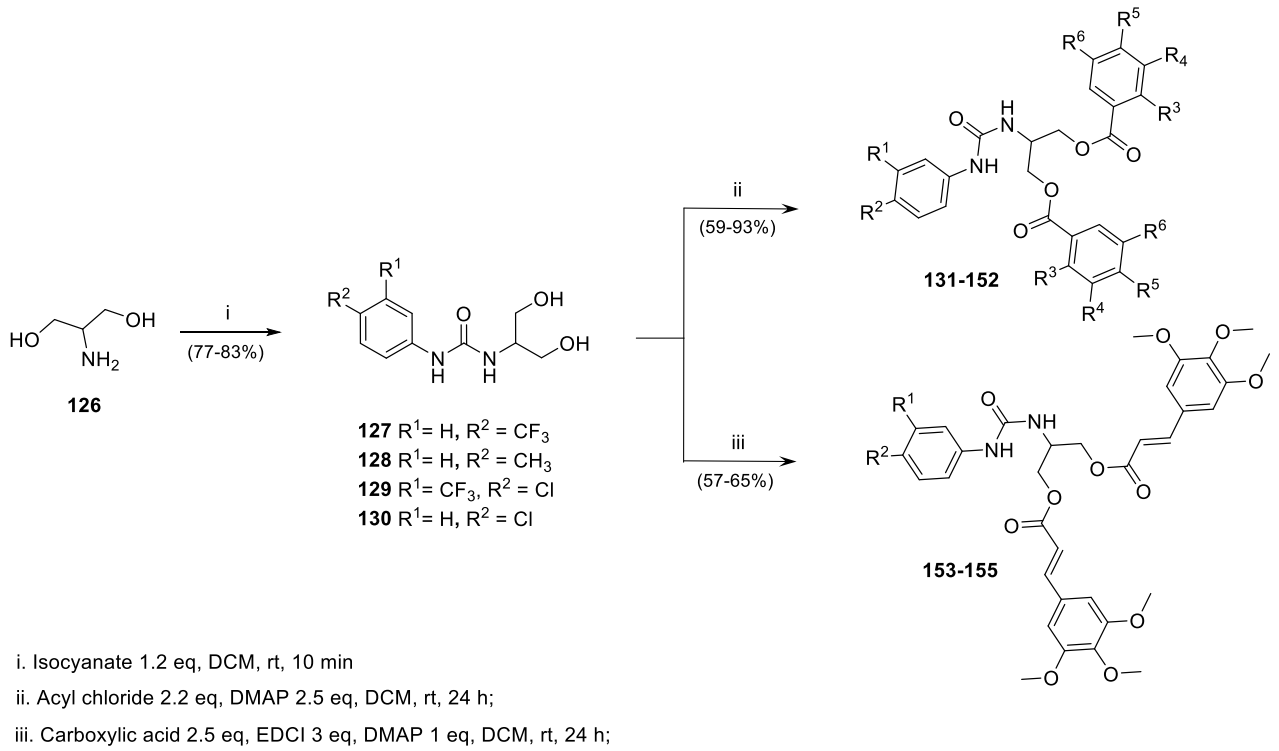

Scheme 5. Synthetic routes for the preparation of *N*-phenylaminocarbonyl diesters derivatives from serinol (**131–155**).

For the preparation of trimethoxycynnamic ester derivatives **153–155** the condensation occurred using carboxylic acid as acylating in DCM and following Steglich condition (EDCI, DMAP, Scheme 5) [103].

Table 12. Serinol-derived aromatic esters and cynnamic acid esters from pathway A.

Comp	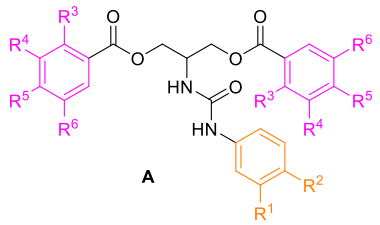 A	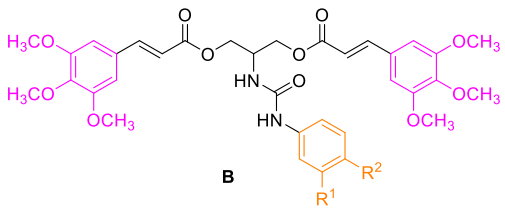 B					
	R^1	**R^2**	**R^3**	**R^4**	**R^5**	**R^6**	**Yield (%)**
131 (A)	H	CF_3	H	H	CH_3	H	75
132 (A)	H	CF_3	CH_3	H	H	H	68
133 (A)	H	CF_3	H	H	OCH_3	H	67
134 (A)	H	CF_3	H	H	CN	H	65
135 (A)	H	CF_3	H	H	NO_2	H	71
136 (A)	H	CF_3	OCH_3	H	OCH_3	H	70
137 (A)	H	CF_3	H	OCH_3	OCH_3	OCH_3	82
138 (A)	H	CH_3	H	H	CH_3	H	66
139 (A)	H	CH_3	CH_3	H	H	H	92
140 (A)	H	CH_3	H	H	OCH_3	H	79
141 (A)	H	CH_3	H	H	NO_2	H	62
142 (A)	H	CH_3	OCH_3	H	OCH_3	H	65
143 (A)	H	CH_3	H	OCH_3	OCH_3	OCH_3	61
144 (A)	CF_3	Cl	H	H	CH_3	H	85
145 (A)	CF_3	Cl	CH_3	H	H	H	62
146 (A)	CF_3	Cl	H	H	OCH_3	H	56
147 (A)	CF_3	Cl	H	H	CN	H	70
148 (A)	CF_3	Cl	H	H	NO_2	H	68
149 (A)	CF_3	Cl	OCH_3	H	OCH_3	H	74
150 (A)	CF_3	Cl	H	OCH_3	OCH_3	OCH_3	76
151 (A)	CF_3	Cl	H	H	$N(CH_3)_2$	H	67
152 (A)	H	Cl	H	H	OCH_3	H	86
153 (B)	CF_3	Cl	-	-	-	-	57
154 (B)	H	CF_3	-	-	-	-	61
155 (B)	H	CH_3	-	-	-	-	64

-Pathway B: Synthesis of N-phenylaminocarbonyl serinol monoester derivatives (156–158)

For the preparation of monoester derivatives **156–158,** the urea intermediates **128** and **129** was previously prepared with the same procedure described above. A selective *O*-acylation reaction of serinol ureas with the corresponding acyl chloride (mono, di and trimethoxy substituted) in DCM and

pyridine afforded the monoester derivative by strict controlling the reaction time (1h), stechiometric (0.9 eq) and temperature (-15 ºC) (Scheme 6, Table 13). Despite this reaction conditions, compound yields were not very high and a moderate percentage of diacylated compounds was isolated.

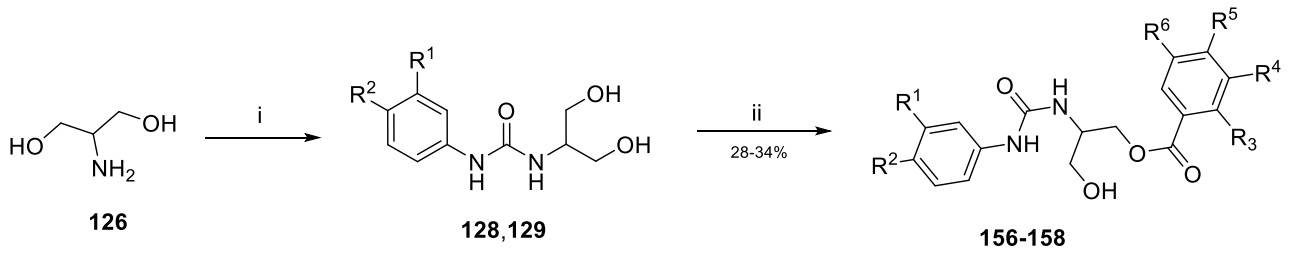

i. Isocyanate 1.2 eq, DCM, rT, 10 min;
ii. Acyl chloride 0.9 eq, pyridine, DCM, -15 °C, 1 h.

Scheme 6. Synthetic route for the preparation of *N*-phenylaminocarbonyl monoesters derivatives from serinol (**156–158**).

Table 13. Serinol-derived aromatic monoesters from pathway B.

Comp

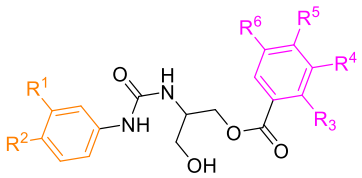

	R^1	R^2	R^3	R^4	R^5	R^6	Yield (%)
156	CF_3	Cl	H	H	OCH_3	H	30
157	H	CH_3	OCH_3	H	OCH_3	H	34
158	H	CH_3	H	OCH_3	OCH_3	OCH_3	28

-Pathway C: Synthesis of N-phenylaminocarbonyl serinol dicarbamate derivatives (159–167)

Dicarbamate derivatives **159–167** were prepared by reaction between the alcohol groups of the urea derivatives (**127–129**) and substituted phenyl isocyanate. With commercial phenyl isocyanates (*p*-CH_3, *p*-OCH_3, *p*-CN, *p*-NO_2) the reaction proceeded at 110 °C in toluene [104]. For the synthesis of compounds **160** and **165**, the corresponding phenyl isocyanate (*o*-CH_3) was previously prepared from *o*-toluidine through the reaction with triphosgene in basic condition (Na_2CO_3) [105]. Dicarbamate was then generated in milder conditions, using DMAP in DCM at rt (Scheme 7, Table 14). In the case of compound **163**, the monoderivative were also isolated (**168**).

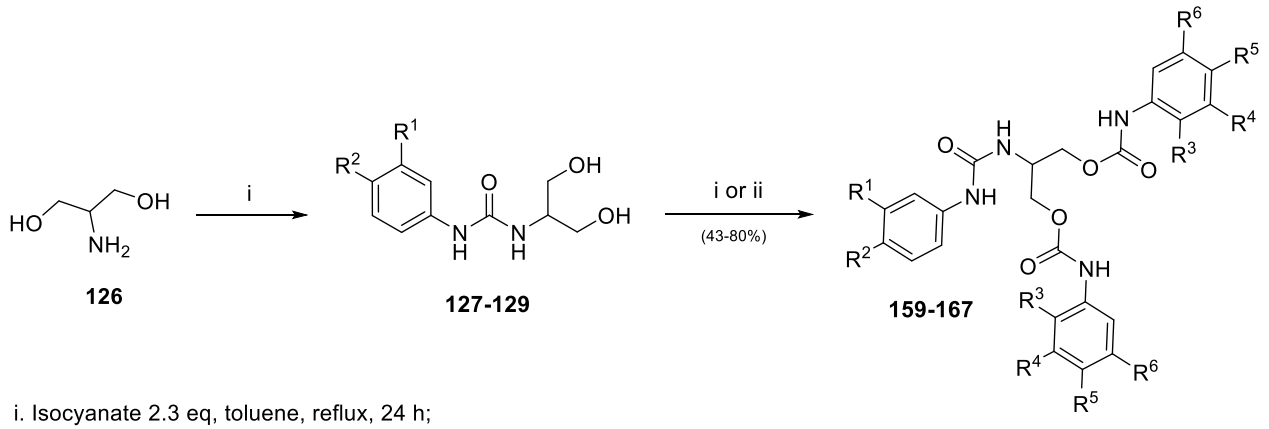

i. Isocyanate 2.3 eq, toluene, reflux, 24 h;
ii. Isocyanate 2.5 eq, DMAP 2.5 eq, DCM, rt, 48 h.

Scheme 7. Synthetic route for the preparation of *N*-phenylaminocarbonyl dicarbamate derivatives from serinol (**159–167**).

Table 14. Serinol-derived dicarbamates from pathway C.

Comp	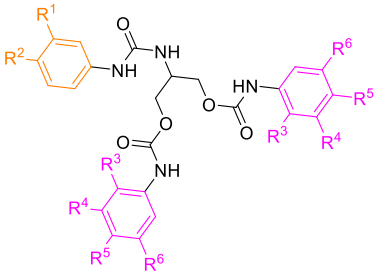						
	R^1	R^2	R^3	R^4	R^5	R^6	Yield (%)
159	H	CF_3	H	H	CH_3	H	66
160	H	CF_3	CH_3	H	H	H	43
161	H	CF_3	H	H	OCH_3	H	50
162	H	CF_3	H	H	CN	H	60
163	H	CF_3	H	H	NO_2	H	50
164	CF_3	Cl	H	H	CH_3	H	80
165	CF_3	Cl	CH_3	H	H	H	48
166	CF_3	Cl	H	H	NO_2	H	65
167	H	CH_3	H	H	CH_3	H	46
168[a]	H	CF_3	H	H	NO_2	H	24

[a] Monoderivative.

New synthesized diesters, monoesters and dicarbamates compounds were characterized by NMR Spectroscopy, Mass Spectrometty and melting points determination. Representative resonance

assignments from ^{1}H NMR and ^{13}C NMR of some selected compounds are illustrated in the Table 15.

Table 15. Representative resonance assignments (^{1}H NMR and ^{13}C NMR) of some serinol-derived compounds.

Compound		^{1}H NMR[a] (ppm)			^{13}C NMR[b] (ppm)		
		N*H*Ar urea/-N*H*CO carb[c]	OC*H*$_2$C*H*C*H*$_2$O/ C*H*$_2$OH[d]	C*H*$_3$/OC*H*$_3$	C=O	*C*H	CH$_3$/OCH$_3$
133	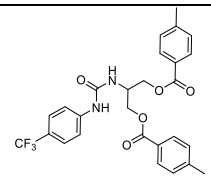	9.04	4.52-4.35	3.81	165.2, 154.6	47.4	55.5
134	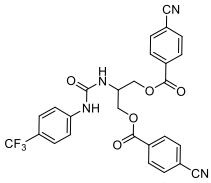	8.98	4.58-4.47	-	164.4, 143.4	47.1	-
138	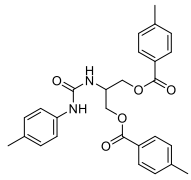	8.50	4.63-4.50	2.49, 2.32	165.5, 154.9	47.2	21.1, 20.2
141	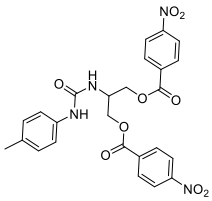	8.48	4.59-4.49	2.22	164.1, 154.9	47.0	20.2
145	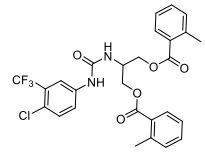	9.06	4.54-4.48, 4.45-4.49	2.49	166.7, 154.6	47.4	20.9
149	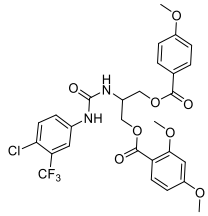	9.11	4.43-4.29	3.87-3.76	164.6, 154.5	47.4	55.5, 55.4
154	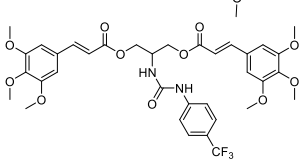	9.03	4.40-4.30	3.79, 3.69	166.2, 154.4	47.5	60.0, 56.0

Compound		^{1}H NMR[a] (ppm)			^{13}C NMR[b] (ppm)		
		N*H*Ar urea/-N*H*CO carb[c]	OC*H*$_2$C*H*C*H*$_2$O/ C*H*$_2$OH[d]	C*H*$_3$/OC*H*$_3$	C=O	*C*H	CH$_3$/OCH$_3$
156	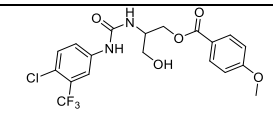	9.10	3.67-3.60[d]	3.83	165.3, 154.6	49.9	55.5
161	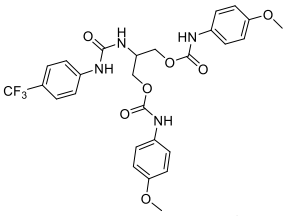	9.52[c], 9.08	4.30-4.15	3.71	153.4, 153.4	48.1	55.1
168	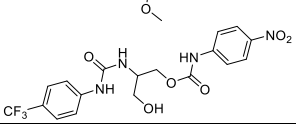	10.40[c], 9.02	4.33-4.10[d]	-	154.5, 153.2	49.9	-

[a]500 MHz, DMSO-d_6

[b]125MHz, DMSO-d_6

4.2 Biological evaluation

As for previous piperazine derivatives (**section 3.2**), new compounds were submitted to biological assays.

4.2.1. *In vitro* antiviral activity and effect on cellular viability

The antiviral activity of synthesized compounds **131–168** was firstly evaluated in plaque assay (*293β5* cell line) by the quantification of HAdV plaque formation in the presence of molecules at concentrations of 10 μM.

Among the serinol-derived diester **131–155**, the subfamily with a methyl group on the phenylurea function showed poor or any inhibition of viral plaque formation (**138–141**,**155**, Table 16). Only compounds **142** and **143** (dimethoxy and trimethoxy benzoyl derivatives), reached a moderate activity (41.48% and 34.58% respectively). On the contrary, the analogues with 4-CF_3 or 3-CF_3-4-Cl substituents on the urea phenyl ring (**131–137** and **144–151)** afforded higher levels of inhibition. Depending of the substituent on the benzoyl moiety different behaviours were observed. In particular, the presence of electron-withdrawing groups (*p*-CN, *p*-NO_2) were not tolerated; in fact, compounds **134**, **135**, **141**, **147** and **148** displayed percentages of plaque formation inhibition ranging from 0% to 7.66% (Table 16). Conversely, compounds with electron-donating substituents in several positions on the aromatic ester (*p*-CH_3, *o*-CH_3, *p*-OCH_3, 2,4-di-OCH_3 and 3,4,5-tri-OCH_3) showed better

inhibitory activity (plaque formation inhibition range of 66-97%). *o*-CH_3 and *p*-OCH_3 substituted esters with *p*-CF_3 and 3-CF_3-4-Cl phenyl ureas (**132**, **133**, **145** and **146**) demonstrated to be the most active compounds (>90% of inhibition), together with compound **150**, the trimethoxy derivative with a disubstituted urea (97.58% of inhibition) (Table 16). Since both *p*-methoxy diester **133** and **146** showed a suitable antiviral activity, their analogue with *p*-Cl substituted urea were prepared (**152**) but it resulted less active. Similarly, the introduction of a different electron donor such as *p*-dimethylamino group (compound **151**) also led a reduction of activity (44.76 % of inhibition). The trimethoxycinnamic derivatives (**153–155**) did not improve the activity compared to trimethoxy benzoyl analogues **150**, **137** and **143** (58.79%, 0%, 0% vs 97.58%, 47.33%, 34.58% respectively). As depicted in the Table 16, also in the case of monoester derivatives, a decrease of the plaque formation inhibition was observed for compounds **156-158** in comparison with their diacylated analogues **146, 142** and **143** (30.0 %, 34.93%, 27.51% vs 91.51 %, 41.48%, 34.58%).

The dicarbamate derivatives offered different results in the terms of structure-activity relationship. Compounds with the *p*-CF_3 substituted urea and electron-withdrawing substituents on the aromatic carbamate function (**162** *p*-CN and **163** *p*-NO_2) displayed high percentage of inhibition (98.59 % and 99.45% respectively). Moreover, both *orto* methyl derivatives from *p*-CF_3 and disubstituted phenyl urea (**160** and **165**) inhibited 99.4% and 100% of plaque formation respectively. Finally, the monocarbamate derivative **168**, isolated during the synthetic preparation of compound **163**, was also evaluated for its antiviral activity and demonstrated to be the only active monoacyl compounds (99.45% inhibition, Table 16). It is important to note that precursors **127–129** were also assessed in plaque assay, giving 6%, 0% and 58% respectively and suggesting that the presence of acyl functions on primary hydroxyl groups could be important for the antiviral activity.

The effect on cellular viability in A549 cell line was examined for those compounds with percentage of inhibition in the plaque assay >60% (eleven compounds) in order to evaluate their safety profile determining the 50% cytotoxic concentration (CC_{50}). (Table 16)

Table 16. Inhibition of HAdV infection in the plaque assay for compounds **131-168**.

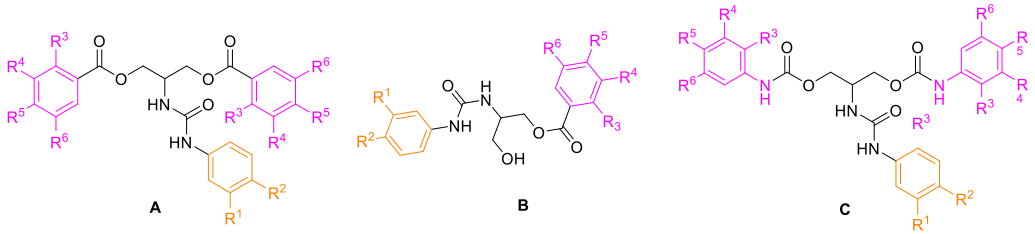

Comp.	% of plaque-formation inhibition[a]	CC_{50}[b]	Comp.	% of plaque-formation inhibition[a]	CC_{50}[b]
131 (A)	66.33±2.49	93.24 ± 7.7	**151 (A)**	44.76±2.69	-
132 (A)	89.69±7.13	200.00 ± 33.87	**152 (A)**	43.29±11.86	-
133 (A)	97.17±0.77	11.73 ± 0.26	**153 (A)**	58.79 ± 3,43	-
134 (A)	7.66±10.83	-	**154 (A)**	0.00±0.00	-
135 (A)	0.00±0.00	-	**155 (A)**	0.00±0.00	-
136 (A)	55.83±4.31	-	**156 (B)**	30.0±27.85	-
137 (A)	47.33±38.86	-	**157 (B)**	34.93±16.67	-
138 (A)	9.40±13.29	-	**158 (B)**	27.51±59.28	-
139 (A)	0.00±0.00	-	**159 (C)**	0.00±0.00	-
140 (A)	6.78±13.90	-	**160 (C)**	99.74 ± 0,36	19.8 ± 0.16
141 (A)	0.00±0.00	-	**161 (C)**	0.00±0.00	-
142 (A)	41.48±1.23	-	**162 (C)**	98.59 ± 2,00	14.4 ± 0.63
143 (A)	34.58±6.23	-	**163 (C)**	99.45±0.77	11.56 ± 4.30
144 (A)	25.68±36.31	-	**164 (C)**	0.00±0.00	-
145 (A)	98.25±2.48	25.10 ± 0.16	**165 (C)**	100 ± 0.00	18.4 ± 0.60
146 (A)	91.51±11.9	11.24 ± 4.48	**166 (C)**	37.43 ± 3.12	-
147 (A)	6.25±8.84	-	**167 (C)**	0.00±0.00	-
148 (A)	5.81±8.22	-	**168 (C)**	99.45±0.77	41.16 ± 3.17
149 (A)	0.00±0.00	-	**Cidofovir**[c]	3.51 ± 4.97	50.6 ± 9.8
150 (A)	97.58±4.73	63.73 ± 0.50			

[a] Percentage of control HAdV5-GFP inhibition in a plaque assay at 10 μM using the 293β5 cell line
[b] Cytotoxic concentration 50%. The results represent means ± SD of triplicate samples from three independent experiments
[c] Data of cidofovir as positive clinical drug candidate.

4.2.2. Determination of IC_{50} values and fold-reduction in virus yield

The half maximal inhibitory concentration (IC_{50}) for selected compounds was determined through plaque assay and the selectivity index was calculated. All eleven compounds inhibited HAdV5

infection in a dose-dependent manner (Figure 23) showing IC_{50} values ranging from 2.05 µM to 9.74 µM (Table 17).

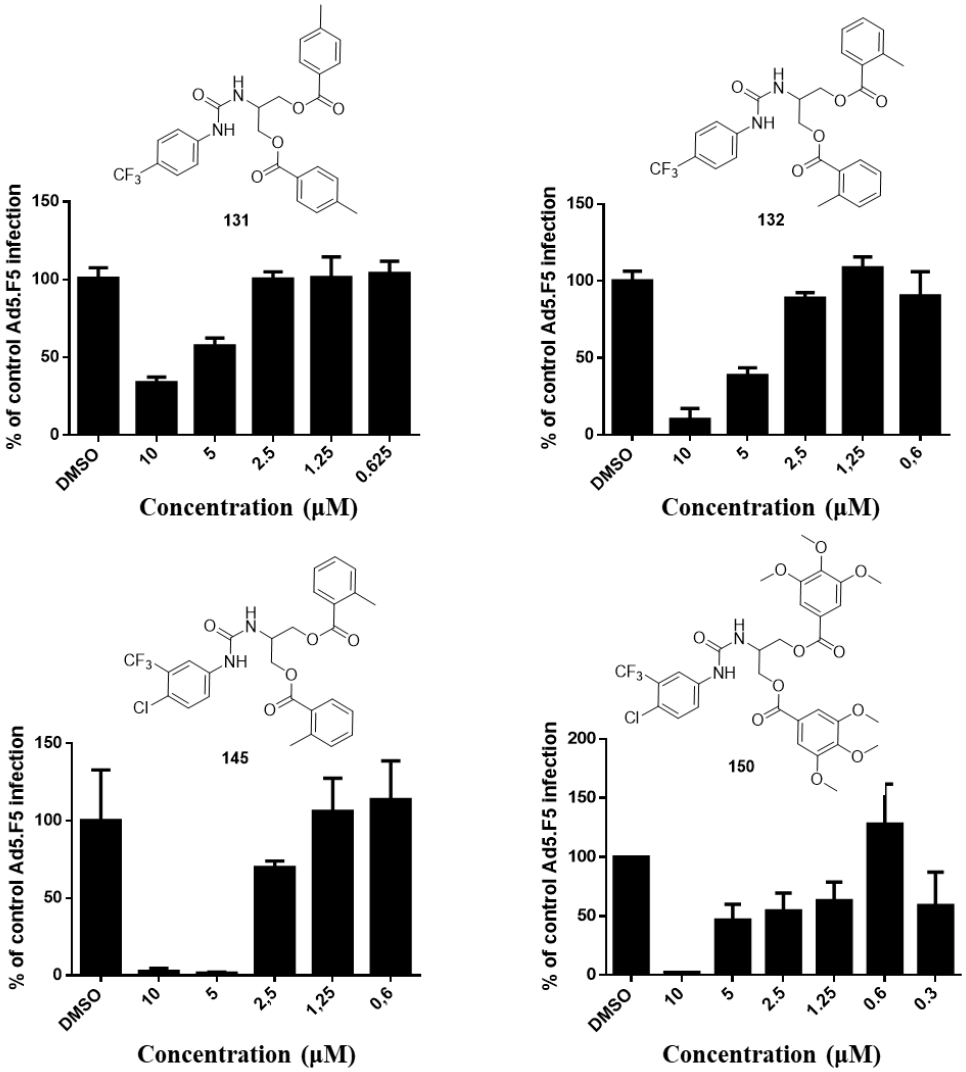

Figure 23. Dose-dependent activity of representative compounds in a plaque assay. For all panels, the DMSO control is a positive control with cells infected at the same MOI but in the absence of drugs. The results represent means ± SD of triplicate samples from three independent experiments.

IC_{50} values for cidofovir from previously reported studies [106] and from our methodology were significantly higher than those shown by our compounds, as it can be observed in the Table 17. Among selected active diesters with *p*-CF_3 phenyl urea (**131–133**), compound **133** (*p*-methoxybenzoyl derivative) showed the lowest IC_{50} value (2.63 µM), whereas the presence of methyl group in *para* (**131**) or *orto* (**132**) position reduced the activity (5.35 µM and 4.53 µM respectively). In the case of compound **132**, if an additional substituent was introduced on the phenyl urea (3-CF_3-4-Cl, analogue **145**), an increased inhibition was observed (2.82 µM). Compound **146** (4-

methoxybenzoyl derivative) with the same urea function, showed IC_{50} value of 8.96 µM, whereas the trimetoxybenzoyl analogue (**150)** showed better inhibitory activity (3.67 µM). Among the small set of active carbamate derivatives, **163** reached the best results with an IC_{50} value of 2.05 µM.

Table 17. IC_{50}, CC_{50}, SI and virus yield reduction values for selected compounds compared to drug cidofovir.

Comp		IC_{50} (µM)[a]	CC_{50} (µM)	Selectivity Index (SI)[b]	Yield reduction (fold-reduction)[c]
131	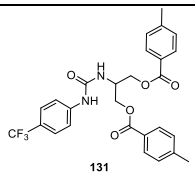	5.35 ± 0.66	93.24 ± 7.7	17.42	7.23 ± 5.38
132	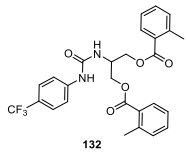	4.53 ± 0,64	200.00 ± 33.87	44.15	92.28 ± 33.77
133	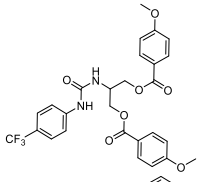	2.63 ± 0.26	11.73 ± 0.26	4.46	-
145	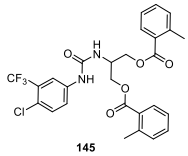	2.82 ± 0.31	25.10 ± 0.16	8.90	42.83 ± 15.68
146	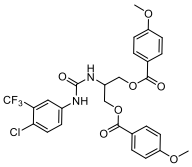	8.96 ± 1.12	11.24 ± 4.48	1.25	-
150	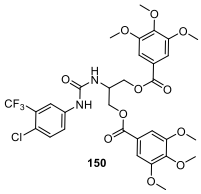	3.67 ± 1.46	63.73 ± 0.50	17.37	1.22 ± 0.63
160	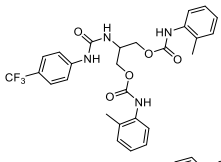	3.76 ± 0.23	19.8 ± 0.16	5.27	-
162	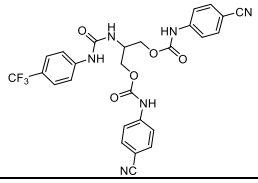	7.05 ± 2.65	14.4 ± 0.63	2.04	-

Comp		IC_{50} (µM)[a]	CC_{50} (µM)	Selectivity Index (SI)[b]	Yield reduction (fold-reduction)[c]
163	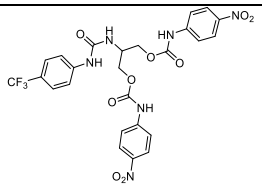	2.05 ± 0.02	11.56 ± 4.30	5.64	-
165	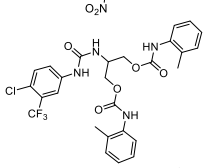	7.78 ± 2.02	18.4 ± 0.60	2.37	-
168	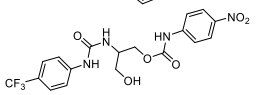	9.74 ± 0.90	41.16 ± 3.17	4.23	-
Cidofovir[d]		24.06 ± 5.9	50.6 ± 9.8	7.5	82.5 ± 21.4

[a]Inhibitory concentration 50 at low MOI in a plaque assay.
[b]Selectivity Index value was determined as the ratio of cytotoxic concentration 50 (CC_{50}) to inhibitory concentration 50 (IC_{50}) in a plaque assay for each compound.
[c]Fold-reduction in virus yield as the ratio of particles produced in the presence of DMSO divided by the yield in the presence of each of compounds (50 µM). The results represent means ± SD of triplicate samples from three independent experiments
[d]Data of cidofovir as positive clinical drug candidate.

Compounds with selectivity index SI >10 were selected for further evaluation to obtain some knowledge regarding their potential mechanism of action. Only compounds **131**, **132**, **145** and **150** showed a CC_{50} value at least 10-times over their IC_{50}, with selectivity indexes ranging from 8.9 to 44.15 (Table 17)

The anti-HAdV potency were assessed using a virus burst assay, measuring their efficacy in blocking the production of new HAdV particles. The presence of these compounds was associated with reductions in virus yield (from 1.22-fold tu 92.3-fold), similar to cidofovir (82.5-fold). (Table 17).

4.2.3. Insights into the antiviral mechanism of action

Impact on HAdV entry

To explore if selected compounds interfere with some steps of HAdV entry and HAdV DNA transport into the nucleus, we carried out a nuclear association assay to quantify the HAdV genome accessibility to the host nucleus. If the mechanism of action of these molecules was directed to HAdV entry this would be reflected in the amount of HAdV genomes that reach the nucleus. As depicted in Figure 24, the treatment with selected compounds did not show a significant difference in the number of HAdV genomes into the nucleus compared with those treated with DMSO. This study suggests that any of selected compounds interfered with the entry phase of the HAdV viral particles.

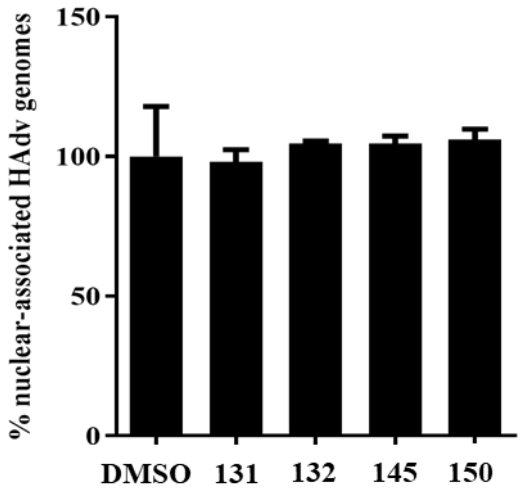

Figure 24. Effect of the selected compounds on nuclear association of HAdV5 genomes. Results are expressed as the mean ± SD of duplicate assays.

Impact on HAdV DNA replication

The DNA copy number of the cellular housekeeping gene GAPDH in both the nucleus and the cytoplasm were also measured as a control for the purity of nuclear isolation, indicating that we were specifically measuring the HAdV genomes that reached the nuclear membrane. This study confirms that any of selected compounds affected the early steps that span the entry phase of the HAdV viral particles.

Since the mechanism of action of these four compounds seems to be related with early steps after HAdV entry into the nucleus we next evaluate the capacity of these compounds to block the HAdV entry or the DNA replication process. A real-time PCR was carried out to evaluate the HAdV DNA replication efficiency in the presence of these compounds, in a single round of infection for 24 h. Compound **132** blocked 99.2% of the synthesis of new HAdV DNA copies, while compounds **131** and **145** showed slight lower inhibitions, 95.1% and 92.1%, respectively. Compound **150** also showed a significant inhibition of HAdV DNA replication (73.5%), even if less then the other ones (Figure 25A).

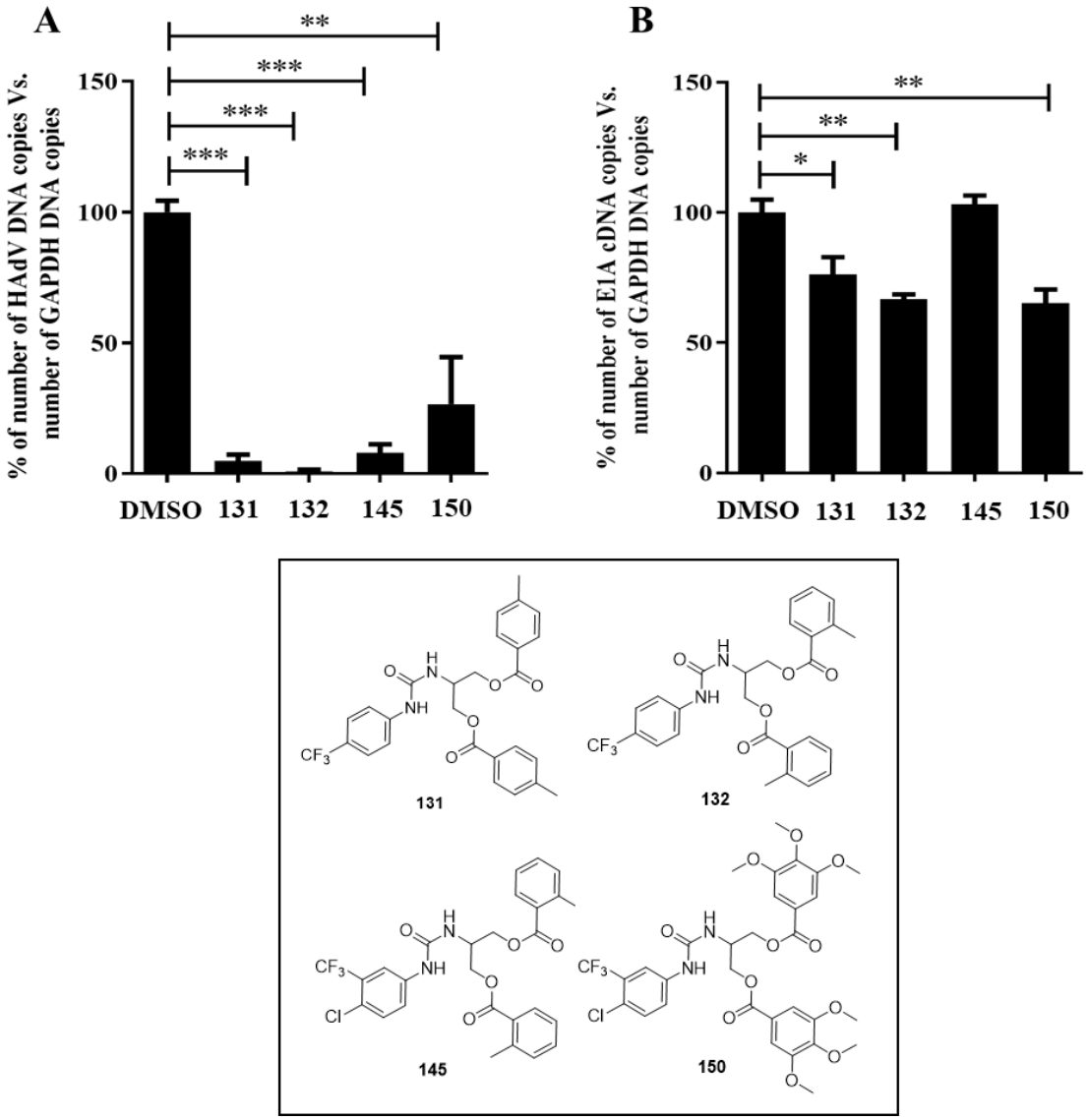

Figure 25. Effect of the selected compounds on HAdV DNA replication. A) HAdV copies number; B) Expression of the E1A gene. Results are expressed as the relative copy number of HAdV DNA and E1A mRNA normalized to GAPDH copy number, and they are presented as the mean ± SD of duplicate assays. * $p \leq 0.05$, ** $p \leq 0.01$, *** $p \leq 0.001$.

We also quantified the mRNA copy number of the E1A gene using quantitative reverse transcription (RT-PCR). As shown in Figure 25B, **131**, **132** and**150** significatly blocked the expression of the E1A gene in a 6 h assay. Compound **145** did not show any decrease in the expression of the E1A gene compared with a control treated with DMSO. The ability of compounds **131**, **132** and**150** to interfere HAdV early gene transcription may be the cause of the inhibition of the DNA replication showed by these compounds. On the other hand, since any inhibition of the early gene transcription was observed

by compound **145**, this compound could interact with viral proteins essential for HAdV DNA replication, including the HAdV DNA polymerase, the precursor of the terminal protein (pTP), or the DNA-binding protein (DBP). Further studies will be needed to clarify their specific mechanism for antiviral activity.

CHAPTER 5

3-PHENYLAMINOCARBONYL-1,2-PROPANEDIOL DERIVATIVES

5.1 Chemistry

5.1.1 Design

Due to the preliminary and promising results demonstrated by some serinol-derived aromatic diesters in the inhibition of HAdV infection, our interest was focused in the replacement of serinol scaffold (2-amino-1,3-propanediol) with its regioisomer, 3-amino-1,2-propanediol (Figure 26) to identify the largest number of lead compounds for further optimization processes. This skeleton has been found in several antiviral acyclic nucleoside and non-nucleoside analogues. CDV (**3**, Figure 26) can be considered as constituted by an aminopropanediol central core, with a phosphonate group on the secondary alcohol and a cytosine base at N-3. Other acyclic nucleoside phosphonate analogues with aminoalcohol skeleton have been discovered as potent and selective inhibitors of herpesvirus replication [107].

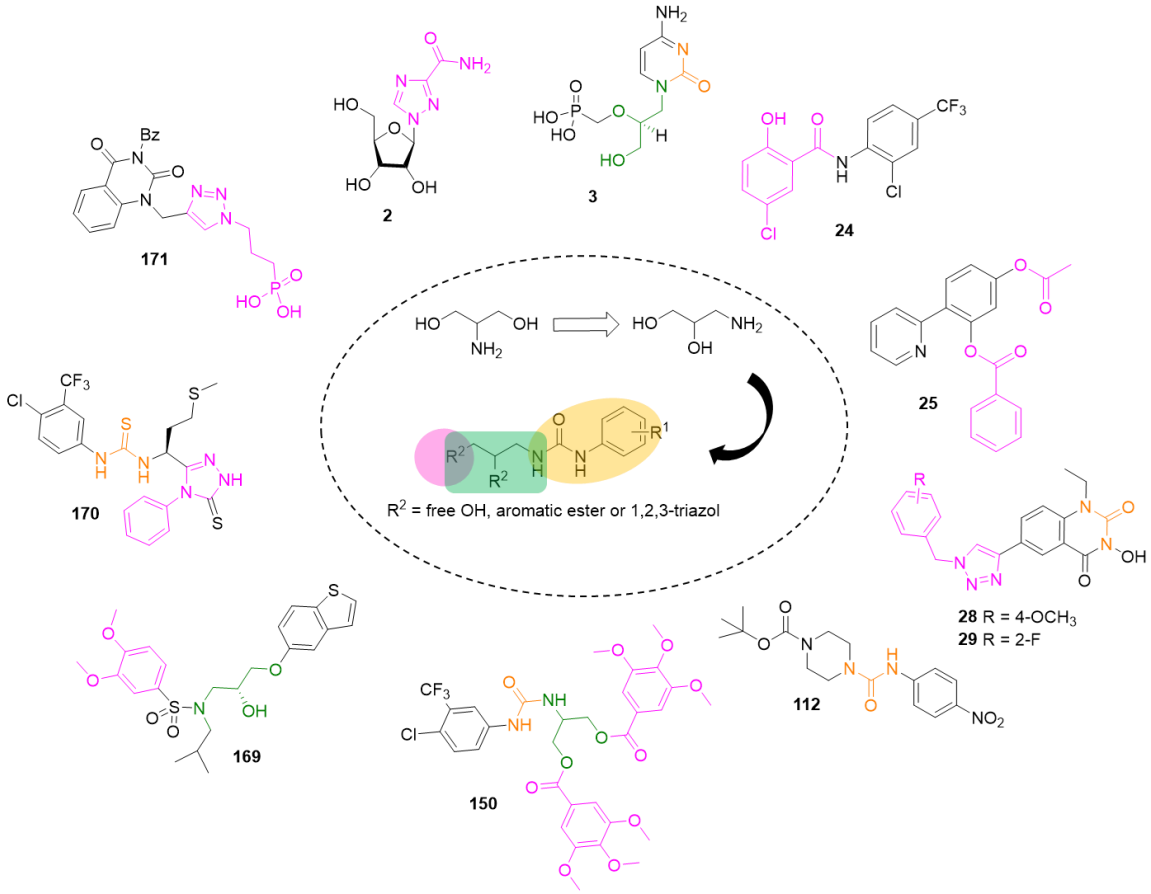

Figure 26. Design of new 3-amino-1,2-propanediol derivatives.

Among non-nucleoside compounds, a series of novel aminopropanediol-derived small molecules have been described as inhibitors of human immunodeficiency virus 1 (HIV-1). In these molecules the propyl chain linked the sulphonamide function with an heterocyclic moiety (**169,** Figure 26) [108]. Also in this case, we designed a set of new compounds preserving the urea function as in many antiviral agents [76,84], including our piperazine and serinol derivatives (**112**, **150**, Figure 26). Firstly, keeping in mind the antiviral effect of some serinol-derived aromatic diesters (IC_{50} from 2.05 μM to 9.74 μM) and other described compounds with acyl moieties in their structures (**24**, **25**, Figure 26) [78,79,81], a set of diester derivatives from 3-amino-1,2-propanediol were designed in order to explore the effect of this functionality (Figures 26 and 27). Regarding the aromatic acyl moiety, the same structural variability was examined on the new scaffold: methyl and methoxy as representative electron releasing substituents due to their presence in most active serinol diesters (**131–133**, **145**, **146**, **150**); CN and NO_2 were selected as electron-withdrawing groups, with the addition of CF_3 (**A**, Figure 27).

The next step of our design was directed to a small set of monoester derivatives in order to evaluate the presence of a free hydroxyl group (primary or secondary, as in the case of cidofovir). Variously substituted aromatic acyl function was located at the position 1 or 2 of the three-carbon chain, preserving the urea function at N-3 (**B**, Figure 27).

At last, we have explored the effect of 1,2,3-triazole ring into the structure; this interesting heterocycle is associated with a wide range of biological targets due to its ability to establish hydrogen-bonding and dipole interactions [109]. Furthermore, 1,2,3-triazole resulted stable in acidic and basic hydrolytic conditions as well as in oxidative and reductive ones, demonstrating a suitable resistance to metabolic degradation [110]. Many compounds with antiviral properties presented a triazole moiety in their structure; the drug ribavirin (**2**, Figure 26) and other synthetic compounds identified as inhibitors of influenza A virus were decorated with a 1,2,4-triazole ring (**170**, Figure 26) [111]. In other instances, the triazole ring represented a passive linker between the pharmacophore and other portions of the molecule. The antiviral set of 3-hydroxyquinazolinedione derivatives described by Kang *et al* consisted of a 1,2,3-triazole connecting units between the quinazoline core and a substituted aromatic moiety (**28**, **29**, Figure 26) [82]. Other studies on compounds with 1,2,3-triazole nucleus bearing a phosphate group have been reported [112], such as compound **171** (Figure 26) which demonstrated moderate activity against herpes simplex viruses [113]. In our subset of aminopropanediol-derived 1,2,3-triazoles we introduced several functions at position 4 of the heterocyclic nucleus in order to verify their impact on the antiviral activity. In addition to a phosphonate group, other polar and non-

polar functionalities were evaluated such as a short alcohol chain, aromatic aldehyde or acid and substituted phenyl rings (**C**, Figure 27).

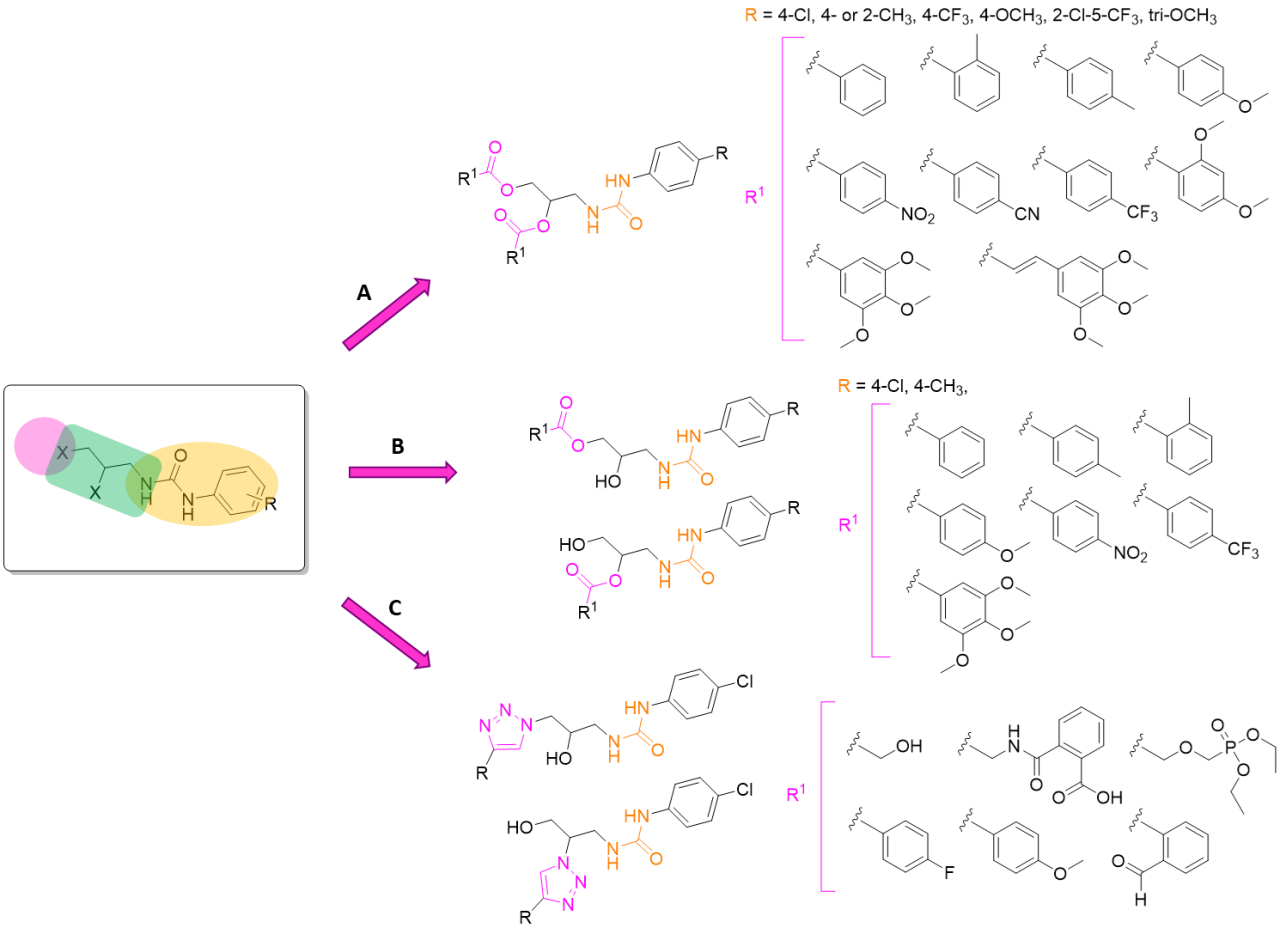

Figure 27. General structures of new designed diester, monoester and 1,2,3-triazole derivatives of 3-amino-1,3-propanediol.

5.1.2 Synthesis

For the preparation of new set of diester, monoester and triazole derivatives several synthetic strategies consisting of two or more reaction steps were employed starting from 3-amino-1,2-propanediol.

-Pathway A: Synthesis of N-phenylaminocarbonyl diester derivatives from 3-amino-1,2-propanediol (180–211)

Diester derivatives **180–211** were synthesized following the same procedures employed for serinol-derived diesters and depicted in Scheme 8. The introduction of urea function at primary amine was carried out using *p*-Cl, *p*-CH_3 and *p*-CF_3 substituted phenyl isocyanates (**173–175**); in addition, *o*-CH_3, *p*-OCH_3, 2-Cl-5-CF_3 and trimethoxy substituted phenyl ureas (**176–179**) were prepared in a subsequent optimization process. In the case of compounds **177** and **179**, without availabe commercial isocyanate, the urea function was generated starting from appropriate aniline (*o*-methyl and 3,4,5-trimethoxy aniline), using Na_2CO_3 and triphosgene in a biphasic aqueous-organic system (H_2O-DCM) [105]. The urea derivatives (**173–179**) then reacted with the corresponding acyl chloride or carboxylic acid to give the final product in a good yield (Table 18).

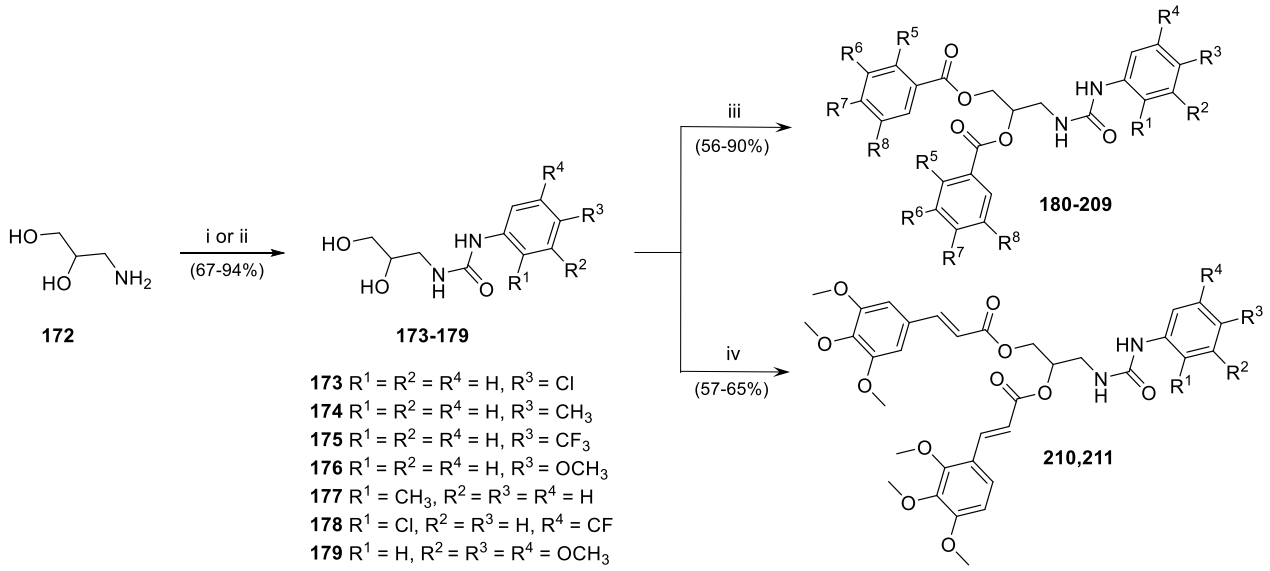

i: Isocyanate 1.2 eq, DCM, rt, 10 min

ii: Aniline 1 eq, Na_2CO_3 1.6 eq, triphosgene 0.33 eq, DCM:H_2O, rt, 2 h

iii: Acyl chloride 2.2 eq, DMAP 2.5 eq, DCM, 25 °C, 48 h

iv: Carboxylic acid 2.5 eq, EDCI 3 eq, DMAP 0.5 eq, DCM, rt, 24 h;

Scheme 8. Synthetic routes for the preparation of *N*-phenylaminocarbonyl diesters derivatives from 3-amino-1,3-propanediol (**180–211**).

Table 18. Aromatic diesters and cynnamic acid diesters of 3-amino-1,2-propanediol from pathway A.

Comp	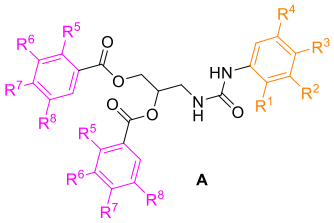 A						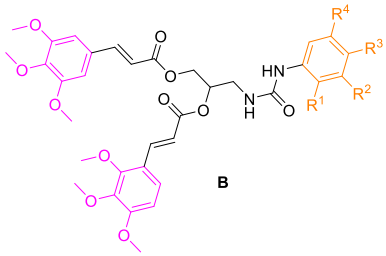 B		
	R^1	R^2	R^3	R^4	R^5	R^6	R^7	R^8	Yield (%)
180 (A)	H	H	Cl	H	H	H	H	H	70
181 (A)	H	H	Cl	H	H	H	CH_3	H	85
182 (A)	H	H	Cl	H	CH_3	H	H	H	90
183 (A)	H	H	Cl	H	H	H	OCH_3	H	74
184 (A)	H	H	Cl	H	H	H	CN	H	60
185 (A)	H	H	Cl	H	H	H	NO_2	H	90
186 (A)	H	H	Cl	H	H	H	CF_3	H	67
187 (A)	H	H	Cl	H	OCH_3	H	OCH_3	H	82
188 (A)	H	H	Cl	H	H	OCH_3	OCH_3	OCH_3	78
189 (A)	H	H	CH_3	H	H	H	CH_3	H	84
190 (A)	H	H	CH_3	H	CH_3	H	H	H	74
191 (A)	H	H	CH_3	H	H	H	OCH_3	H	61
192 (A)	H	H	CH_3	H	H	H	CN	H	64
193 (A)	H	H	CH_3	H	H	H	NO_2	H	62
194 (A)	H	H	CH_3	H	H	H	CF_3	H	63
195 (A)	H	H	CH_3	H	OCH_3	H	OCH_3	H	61
196 (A)	H	H	CH_3	H	H	OCH_3	OCH_3	OCH_3	87
197 (A)	H	H	CF_3	H	H	H	CH_3	H	84
198 (A)	H	H	CF_3	H	CH_3	H	H	H	73
199 (A)	H	H	CF_3	H	H	H	OCH_3	H	71
200 (A)	H	H	CF_3	H	H	H	CN	H	76
201 (A)	H	H	CF_3	H	H	H	NO_2	H	68
202 (A)	H	H	CF_3	H	H	H	CF_3	H	76
203 (A)	H	H	CF_3	H	OCH_3	H	OCH_3	H	56
204 (A)	H	H	CF_3	H	H	OCH_3	OCH_3	OCH_3	82
205 (A)	Cl	H	H	CF_3	CH_3	H	H	H	74
206 (A)	CH_3	H	H	H	H	OCH_3	OCH_3	OCH_3	77
207 (A)	H	H	OCH_3	H	H	OCH_3	OCH_3	OCH_3	90
208 (A)	Cl	H	H	CF_3	H	OCH_3	OCH_3	OCH_3	71
209 (A)	H	OCH_3	OCH_3	OCH_3	H	OCH_3	OCH_3	OCH_3	78

Comp	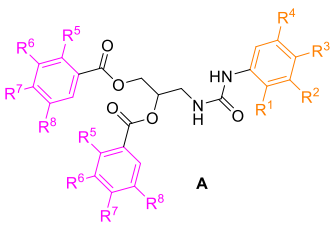 A								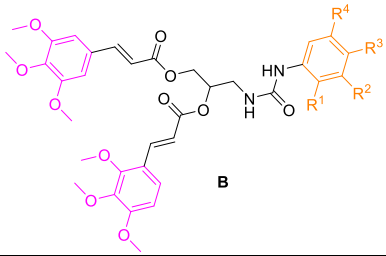 B
	R^1	R^2	R^3	R^4	R^5	R^6	R^7	R^8	Yield (%)
210 (B)	H	H	Cl	H	-	-	-	-	69
211 (B)	H	H	CH_3	H	-	-	-	-	60

-Pathway B: Synthesis of N-phenylaminocarbonyl monoester and carbamate derivatives from 3-amino-1,2-propanediol (212–215, 225–231)

Two different synthetic approaches were employed for the generation of monoester derivatives from ureas **173** and **174**, depending of the position of the acyl function on the aminoalcohol skeleton. For the preparation acylated derivatives at position one (**212–215**, Table 20**)**, a selective *O*-acylation reaction of primary alcohol group of **173–174** was performed. The reaction occurred in DCM at –40 ºC by controlling the stechiometric conditions, using the appropriate acylating agent (unsubstituted, *p*- or *o*-CH_3, *p*-CF_3 benzoyl chlorides) and pyridine (Scheme 9). Better yields have been achieved for these derivatives compared to serinol ones (48–60% *vs* 28–34% respectively), and a minor amount of diacylated compound were obtained due to the presence of a secondary hydroxyl in the 3-amino-1,2-propanediol scaffold.

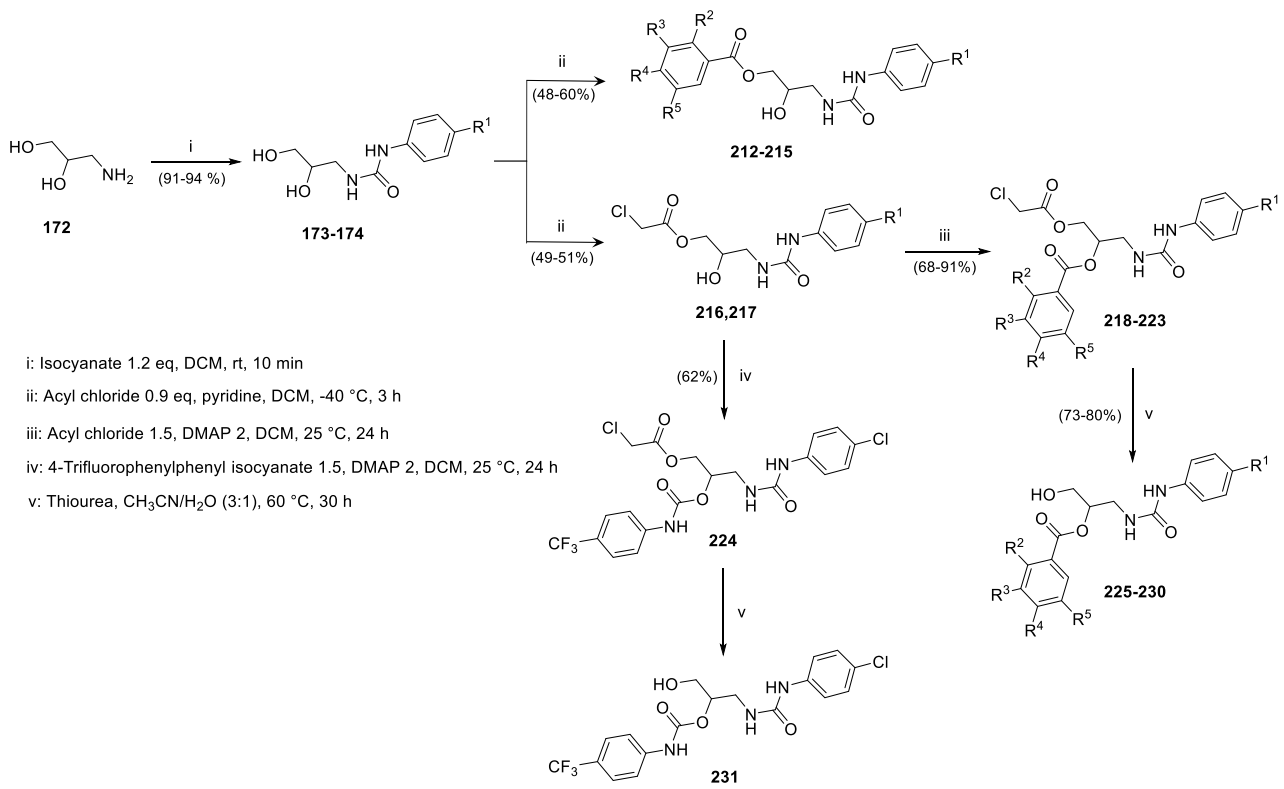

Scheme 9. Synthetic routes for the preparation of *N*-phenylaminocarbonyl monoester and monocarbamate derivatives from 3-amino-1,3-propanediol (**212–215**, **225–231**).

The introduction of the ester function on the secondary alcohol required an acyl protection and deprotection strategy (Scheme 9). In the first step, the monoacylation of primary hydroxyl of the urea derivative (**173**, **174**) proceeded following the same reaction condition described above, but using chloroacetyl chloride as protecting group (**216–217**). During the subsequent step the intermediates **218–223** were generated. Finally, the deprotection on position 1 through the reaction with thiourea in CH_3CN-H_2O at 60 ºC removed the chloroacetyl ester, giving the monoacylated compounds **225–230** (Table 20) in good yields. For the synthesis of monocarbamate **231** the same synthetic methodology was employed, exept for the acylation of secondary alcohol that was performed using phenyl isocyanate in the presence of DMAP (Scheme 9, Table 19).

Table 19. Aromatic monoesters of 3-amino-1,2-propanediol from pathway B.

Comp	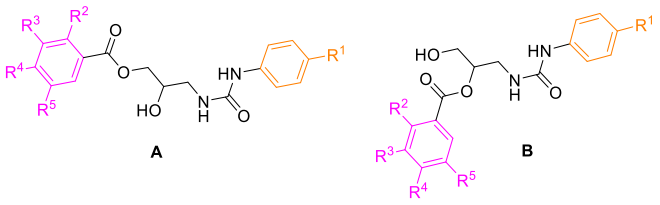					
	R^1	**R^2**	**R^3**	**R^4**	**R^5**	**Yield (%)**
212 (A)	Cl	H	H	H	H	58
213 (A)	Cl	H	H	CH_3	H	57
214 (A)	Cl	CH_3	H	H	H	60
215 (A)	Cl	H	H	CF_3	H	48
225 (B)	Cl	H	H	CH_3	H	76
226 (B)	Cl	H	H	CF_3	H	73
227 (B)	Cl	H	H	NO_2	H	73
228 (B)	Cl	H	OCH_3	OCH_3	OCH_3	77
229 (B)	CH_3	H	H	CF_3	H	80
230 (B)	CH_3	H	OCH_3	OCH_3	OCH_3	73
231 (B)[a]	Cl	H	H	CF_3	H	64

[a] Monocarbamate

New synthesized diesters, monoesters and dicarbamate were characterized by NMR Spectroscopy, Mass Spectrometty and melting points determination. Representative resonance assignments from ^{1}H NMR and ^{13}C NMR of some selected compounds are illustrated in the Table 20.

Table 20. Representative resonance assignments (^{1}H NMR and ^{13}C NMR) of some aromatic diester, monoester and monocarbamate derivatives from 3-amino-1,3-propanediol.

Compound		^{1}H NMR[a] (ppm)			^{13}C NMR[b] (ppm)		
		N*H*Ar/ N*H*CO carb[b]	C*H*$_2$O/C*H*$_2$OH	C*H*$_3$/OC*H*$_3$	C=O	CH	CH$_3$/OCH$_3$
182	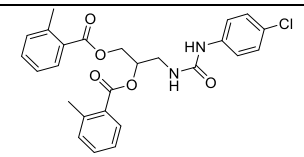	8.72	4.63, 4.48	2.48	167.0, 166.8, 155.6	71.8	21.5, 21.4
185	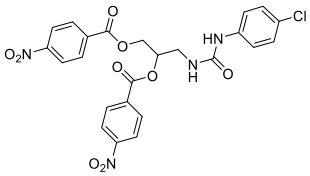	8.70	4.74, 4.60	-	164.1, 163.0, 155.2,	72.5	-
192	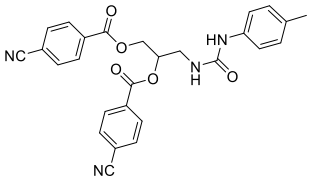	8.40	4.69, 4.56	2.22	164.3, 164.2, 155.3	72.4	20.2
204	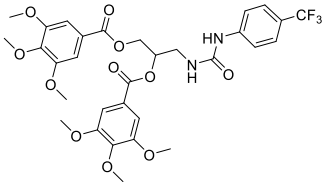	9.03	4.68, 4.49	3.82-3.73	165.0, 165.1, 155.0	71.6	55.9, 55.8
214	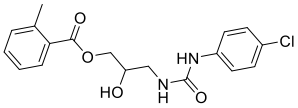	8.73	4.23-4.17, 3.92-3.87	2.54	166.8, 155.2	67.6	21.1
228	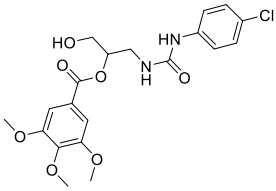	8.67	3.57-3.52, 3.47-3.41	3.83-3.79, 3.75-3.72	165.3, 155.2	74.9	60.4, 60.1
231	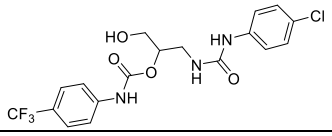	10.11[b], 8.70	3.62-3.49	-	155.1, 153.1	74.5	-

[a]500 MHz, DMSO-d_6

[b]125MHz, DMSO-d_6

-Pathway C 1: Synthesis of 1,2,3-triazole derivatives at primary position (236-241)

We generated a set of triazole derivatives with different substitutents at the position four of the triazole ring. For the preparation of compounds **236–241**, in which the heterocyclic nucleus is located at primary position, we have employed allylamine as the starting material for the synthetic procedure

(**232**). Once the *p*-Cl substituted urea derivative **223** has been prepared, an oxidation reaction of olefin, using *meta*-chloroperbenzoyc acid (*m*CPBA) in dry DCM, furnished the corresponding oxirane **234** (Scheme 10). In the next step the acid-catalysed ring opening reaction using NH_4Cl and sodium azide under EtOH reflux, gave the azide derivatives **235**. Finally, the synthesis of 1,2,3-triazole ring (1,4 adduct) was performed through a click chemistry approach, the copper(I)-catalysed alkyne-azide 1,3-dipolar cycloaddition (CuAAC) reaction. The reaction proceeded using the appropriate terminal alkyne, $CuSO_4$ as a source of pre-catalyst Cu^{II} and sodium ascorbate as reducing agent, in *t*-BuOH-H_2O at room temperature. This reaction represents the most used "click" reaction to obtain 1,2,3 triazole, due to its reliability, specificity, and biocompatibility [114,115]. Compounds **236-241** were characterised by NMR Spectroscopy (Table 22), Mass Spectrometry and melting points determination

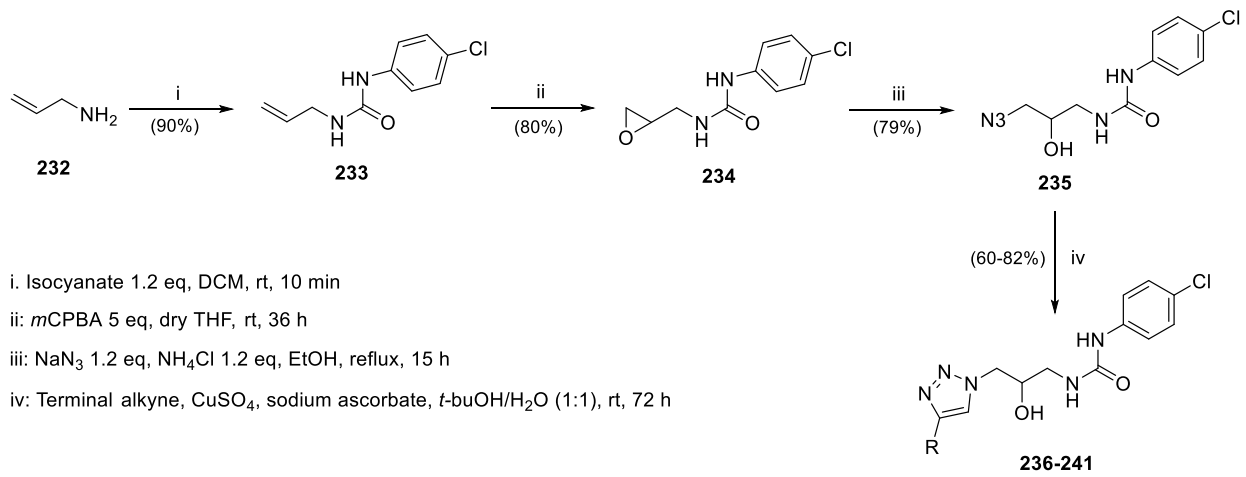

Scheme 10. Synthetic route for the preparation of *N*-phenylaminocarbonyl-1,2,3-triazole derivatives **236–241**.

The mechanism proposed by Sharpless and co-workers for the CuAAC is illustrated in the Figure 28. The reaction requires copper at the oxidation state 1; the pre-catalyst could be a Cu^{II} salt such as $CuSO_4$ and it needs the presence of a reducing agent (sodium ascorbate), or a Cu^{I} compound (CuBr/CuOAc) with a base and a reducing agent to avoid the oxidation to Cu^{II}. It started with the formation of a copper (I) acetylide and subsequent coordination of substituted azide to copper (I) at the alkylated nitrogen atom and the formation of a ternary complex (azide-alkyne-copper(I), **A**, step 1). The intermediate **A** involved into a six-membered metallacycle, in wich the copper was oxidized to the state 3, and provided the first covalent C-N bond (**B**, step 2). The reductive ring contraction

afforded the triazole nucleus with the contemporary reduction of copper (III) to copper (I) (**C**, step 3). Finally, the triazolide captures a proton from an alkyne molecule to ultimate its formation [116].

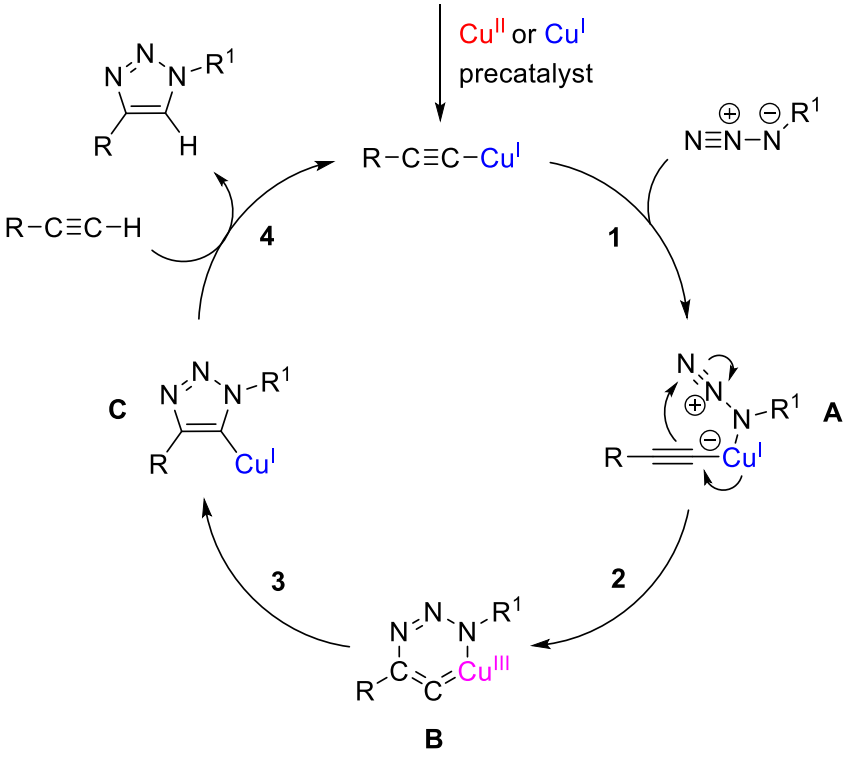

Figure 28. The mechanism of CuAAC proposed by Sharpless and co-workers.

-Pathway C 2: Synthesis of 1,2,3-triazole derivatives at secondary position (245–250)

For the introduction of the triazole ring at secondary position more steps are required and depicted in Scheme 11. From the urea derivative (*p*-Cl, **137**) the first step involves the selective protection of primary alcohol with the benzoyl group (**212**). The acylated product **212** was mesyled in THF (**242**) for the subsequent nucleophilic substitution with sodium azide (in DMF at 85 ºC), furnishing the introduction of the azide group in position 2 (**243**, Scheme 11). The click chemistry reaction between azide derivative **243** and the appropriate substituted alkyne, in the same conditions described above, afforded final 1,2,3-triazole derivatives **245–250**, that were characterised by NMR Spectroscopy (Table 21), Mass Spectrometry and melting points determination.

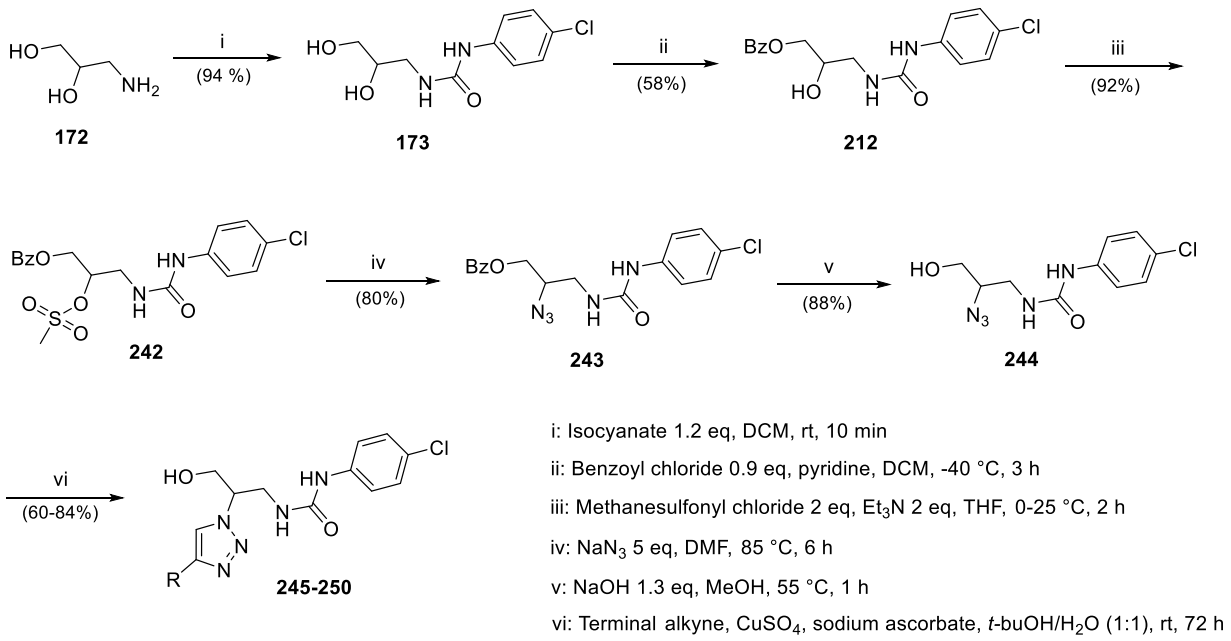

Scheme 11. Synthetic route for the preparation of *N*-phenylaminocarbonyl 1,2,3-triazol derivatives **245–250**.

Table 21. 1,2,3-Triazole derivatives and representative resonance assignments (^{1}H NMR and ^{13}C NMR).

Comp	R	Yield (%)	^{1}H NMR[a] (ppm)			^{1}C NMR[c] (ppm)		
			N*H*Ar	CH triaz	OH	C=O	CH triaz	CH prop
236 (A)[b]		79	-	7.95	-	158.2	128.3	70.7
245 (B)[b]		64	-	8.02	-	158.2	128.4	70.6
237 (A)	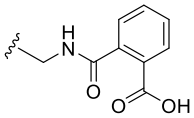	82	8.03	7.79	5.10	155.2	130.6	68.3
246 (B)		69	8.10	7.93-7.87	5.10	154.9	128.4	69.8
238 (A)	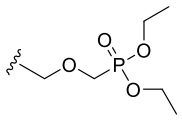	81	8.78	8.17	5.46	155.2	128.4	65.1
247 (B)		72	8.71	8.18	5.16	155.5	128.9	65.7

Comp	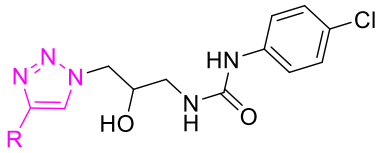 A	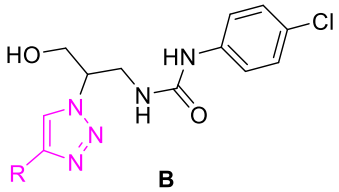 B						
	R	Yield (%)	^{1}H NMR[a] (ppm)			^{1}C NMR[c] (ppm)		
			N*H*Ar	CH triaz	OH	C=O	CH triaz	CH prop
239 (A)	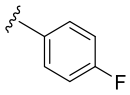	60	8.80	8.52	5.47	155.2	128.5	68.7
248 (B)		84	8.70	8.65	5.21	155.0	128.4	63.1
240 (A)	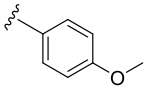	71	8.80	8.41	5.47	155.2	128.4	68.7
249 (B)		64	8.70	8.51	5.22	155.2	128.3	68.7
241 (A)	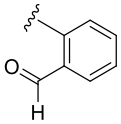	62	8.87	7.83-7.78	5.22	155.7	128.9	69.1
250 (B)		60	8.82	8.62	5.13	155.7	128.9	69.1

[a]500 MHz, DMSO-d_6

[b]500 MHz, $MeOD_4$

[c]125MHz, DMSO-d_6

The formation of 1,4-adduct in the click chemistry reaction was confirmed by 2D NMR techniques HSQC and HMBC.

-Synthesis of terminal akynes used for the click chemistry reaction (253, 254)

For the synthesis of 1,2,3-triazole derivatives (1,4 adduct), six different terminal alkynes were employed but only four of them were commercially available (propargyl alcohol, 4-ethynylanisole, 1-ethynyl-4-fluorobenzene and 2-ethynylbenzaldehyde). With the aim to introduce an aromatic acid function, the ring-opening of phthalic anhydride were performed by an aminolysis reaction with propargyl amine, in THF at room temperature (**253**, Scheme 12). For the preparation of alkynyl phosphonate **254** the propargyl alcohol reacted with the diethyl(tosyloxy)methyl phosphonate in basic condition of NaH at 25 ºC. Both compounds were characterised by NMR Spectroscopy (experimental section 6.1.4).

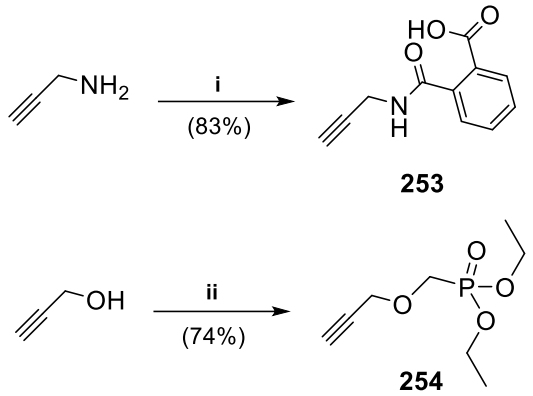

i: Phthalic anhydride 1 eq, dry THF, rt, 18 h

ii: NaH 1.1 eq, diethyl (tosyloxy)methyl phosphonate 1.3 eq, dry THF, 0-25 °C, 24 h

Scheme 12. Synthesis of terminal alkynes **253** and **254**.

5.2 Biological evaluation

As for previous synthesized derivatives (**sections 3.2** and **4.2**), new compounds were submitted to biological assays.

5.2.1. *In vitro* antiviral activity and effect on cellular viability

From a structure-activity relationship point of view, similar results to previous serinol-derived diacylated compounds were obtained by new set of diester derivatives of 3-amino-1,2-propanediol. The impact of electron-withdrawing substituents of the aromatic acyl moiety (CN, NO_2, CF_3) was generally detrimental for the antiviral activity. In fact, the plaque formation inhibition range were from 0% to 25.83 %, with the exception of compounds **193** (*p*-NO_2 with *p*-CH_3 substituted phenyl urea) and **200** (*p*-CN with CF_3 substituted phenyl urea), which showed a moderate activity (44.65% and 40.41% respectively). Conversely, electron donor groups (methyl and methoxy) achieved hiher levels of inhibition (46.69–81.29%). However, *p*-CH_3 derivatives (**181**, **189** and **197**) gave low inhibtion values (Table 23). Specifically, compounds with a methyl group in *orto* position on the aromatic ester with *p*-Cl and *p*-CH_3 phenyl urea (**182** and **190**), demonstrated significant antiviral activity (75.08% and 60.70% respectively). The dimethoxybenzoyl derivatives (**187**, **195** and **203**) gave similar percentage of plaque formation inhibition (29.70%, 47.01%, 46.69% respectively), regardless of the type of substituent on the phenylaminocarbonyl function. The introduction of an additional methoxy group (**188**, **196** and **204**, trimetoxybenzoyl derivatives) provided an improved antiviral activity, inhibiting plaque formation from 57.85% to 81.29% (Table 23). Compound **196**

resulted the most active diester derivative (81.29% of plaque formation inhibition), demonstrating the relevance of methoxy groups. On the other hand, the alternative presence of trimethoxycinnamoyl function **210** and **211** abolished the activity (0% plaque formation).

Considering the *in vitro* inhibition demonstrated by compounds **182** and **196**, their analogues with different substituted phenyl ureas were generated, in order to attempt an improvement of the antiviral activity. For compound **182** (*o*-CH_3 benzoyl derivative with *p*-Cl phenyl urea), the effect of an additional electron-withdrawing substituent (2-Cl-5-CF_3, **205**) was evaluated and resulted in a totally loss of the activity (0% in plaque assay). With regard to the compound **196** (trimethoxybenzoyl derivative with *p*-CH_3 substituted phenyl urea function), the alternative presence of the methyl group in *orto* position (**206**, 20.29 %) decreased the activity as well as a disubstitution 2Cl-5-CF_3 (**208**, 0% respectively). On the contrary, compound with the trimethoxy benzoyl group in combination with trimethoxy phenyl urea (**209**) resulted less active then **196 (**44.11 % vs 81.29**)**, while **207** (*p*-OCH_3 phenyl urea) resulted in an almost complete inhibition (99%). These results suggest the importance of an electron donor group in *para* position of the phenyl urea. Table 22.

Table 22. Inhibition of HAdV infection in the plaque assay for diester, monoester, monocarbamate and triazole derivatives (**180–211**, **212–215**, **225–231**, **236–241**, **245–250**).

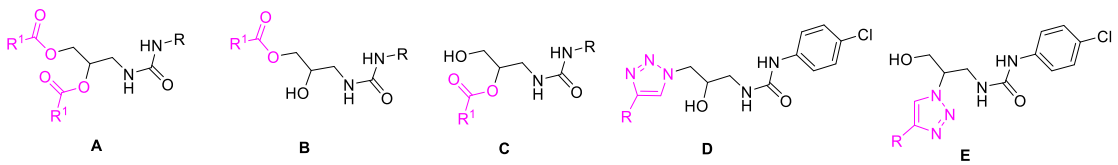

Comp.	% of plaque-formation inhibition[a]	CC_{50}[b]	Comp.	% of plaque-formation inhibition[a]	CC_{50}[b]
180 (A)	0.00 ± 0.00	-	**208 (A)**	0.00 ± 0.00	-
181 (A)	0.00 ± 0.00	-	**209 (A)**	44.11 ± 1.70	-
182 (A)	75.08 ± 15.71	28.70 ± 3.10	**210 (A)**	0.00 ± 0.00	-
183 (A)	0.00 ± 0.00	-	**211 (A)**	0.00 ± 0.00	-
184 (A)	0.00 ± 0.00	-	**212 (B)**	0.00±0.00	-
185 (A)	0.00 ± 0.00	-	**213 (B)**	15.2 ± 1.39	-
186 (A)	26.47 ± 8.32	-	**214 (B)**	25.99 ± 3.65	-
187 (A)	49.70 ± 6.77	-	**215 (B)**	5.70 ± 8.06	-
188 (A)	60.22 ± 8.43	97.25 ± 16.56	**225 (C)**	20.92 ± 10.17	-
189 (A)	31.00 ± 10.43	-	**226 (C)**	100	>200

190 (A)	60.70 ± 16.65	51.33 ± 19.04	**227 (C)**	0.00 ± 0.00	-
191 (A)	53.07 ± 16.18	-	**228 (C)**	48.03 ± 6.79	-
192 (A)	4.43 ± 6.26	-	**229 (C)**	40.21 ± 7.11	-
193 (A)	44.65 ± 18.79	-	**230 (C)**	0.00 ± 0.00	-
194 (A)	21.79 ± 30.81	-	**231 (C)**[d]	19.57 ± 2.84	-
195 (A)	47.01 ± 8.79	-	**236 (D)**	10.77 ± 15.23	-
196 (A)	81.29 ± 1.10	175.16 ± 2.97	**237 (D)**	4.78 ± 74.93	-
197 (A)	0.00 ± 0.00	-	**238 (D)**	33.33 ± 6.10	-
198 (A)	7.30 ± 11.04	-	**239 (D)**	21.54 ± 26.11	-
199 (A)	18.51 ± 1.92	-	**240 (D)**	0.00 ± 0.00	-
200 (A)	40.41 ± 13.31	-	**241 (D)**	0.00 ± 0.00	-
201 (A)	2.12 ± 3.00	-	**245 (E)**	5.80 ± 15.48	-
202 (A)	26.83 ± 24.33	-	**246 (E)**	0.00 ± 0.00	-
203 (A)	46.69 ± 3.36	-	**247 (E)**	0.00 ± 0.00	-
204 (A)	57.85 ± 22.21	-	**248 (E)**	37.45 ± 0.56	-
205 (A)	0.00 ± 0.00	-	**249 (E)**	21.57 ± 4.21	-
206 (A)	20.29 ± 2.82	-	**250 (E)**	12.63 ± 7.36	-
207 (A)	99.86 ± 0.13	136.62 ± 6.54	**Cidofovir**[c]	3.51 ± 4.97	50.6 ± 9.8

[a] Percentage of control HAdV5-GFP inhibition in a plaque assay at 10 μM using the *293β5* cell line
[b] Cytotoxic concentration 50%. The results represent means ± SD of triplicate samples from three independent experiments
[b] Data of cidofovir as positive clinical drug candidate.
[d] monocarbamate

To evaluate the presence of a free hydroxyl group on the antiviral activity a small collection of monoester derivatives of 3-amino-1,2-propanediol, in both position 1 and 2, were prepared. Two representative electron-withdrwing and donating groups were selected for the aromatic acyl moiety (CH_3 and CF_3), with the *p*-Cl phenyl urea (**212–215**). The monoester derivatives on the primary alcohol were not well tolerated, giving percentages of plaque formation inhibition from 0% to 25.99%, regardless of the electronic properties of the aromatic ester function (Table 23). When the acyl moiety is located on the secondary alcohol, the presence of a methyl group (**225**) furnished similar results to its analogue **213** (20.92% vs 15.2% respectively), while the trifluoromethyl group in *para* position (**226**) reached a complete plaque formation inhibition (100%). Other electron-attracting groups such as NO_2 (**227**) did not give active compounds (0%), while the presence of a trimethoxy group (**228**) achived a moderate activity (48.03%). For compound **226**, which demonstrated the highest level of inhibition, the analogue with *p*-CH_3 phenyl urea (**229**) were prepared but it was less active than **226** (40.21%). In the similar way, the replacement of the ester function with a carbamate one (**231**) decreased the antiviral activity (19.57%).

Finally, the biological evaluation of the synthesized of 1,2,3-triazole derivatives (at both positions) did not offered a suitable inhibitory activity (Table 23). Among triazole derivatives at position 1, compound **238** (phosphonate group) showed a moderate activity, with 33.33% of plaque formation inhibition, and compound **239** (p-F phenyl ring) with 21.54% of inhibition. Its analogue from the serie of triazole derivatives at position 2 (compound **248**) showed higher level of inhibition (37.45%). The p-OMe phenyl ring triazole derivative **249** gave 21.57% of inhibition. In spite of not displaying high levels of inhibion, four of them offered moderate activity, and become interesting compounds for further optimization process, searching for new scaffolds.

The effect on cellular viability in A549 cell line was examined for those compounds with percentage of inhibition in the plaque assay >60% (six compounds) in order to evaluate their safety profile determining the 50% cytotoxic concentration (CC_{50}) (Table 22).

5.2.2. Determination of IC_{50} values

At the time to present this manuscript the selected six compounds are being submitted to further biological assays. Firstly, the determination of their half maximal inhibitory concentration, in order to calculate the SI and to chose compounds with SI > 10. The data available showed that these compounds dose-dependently reduced HAdV5 infection (Figure 29) showing IC_{50} values ranging from 2.47 μM to 4.19 μM and SI > 10 (Table 23). Also in this instance, new compounds resulted to be more active than cidofovir.

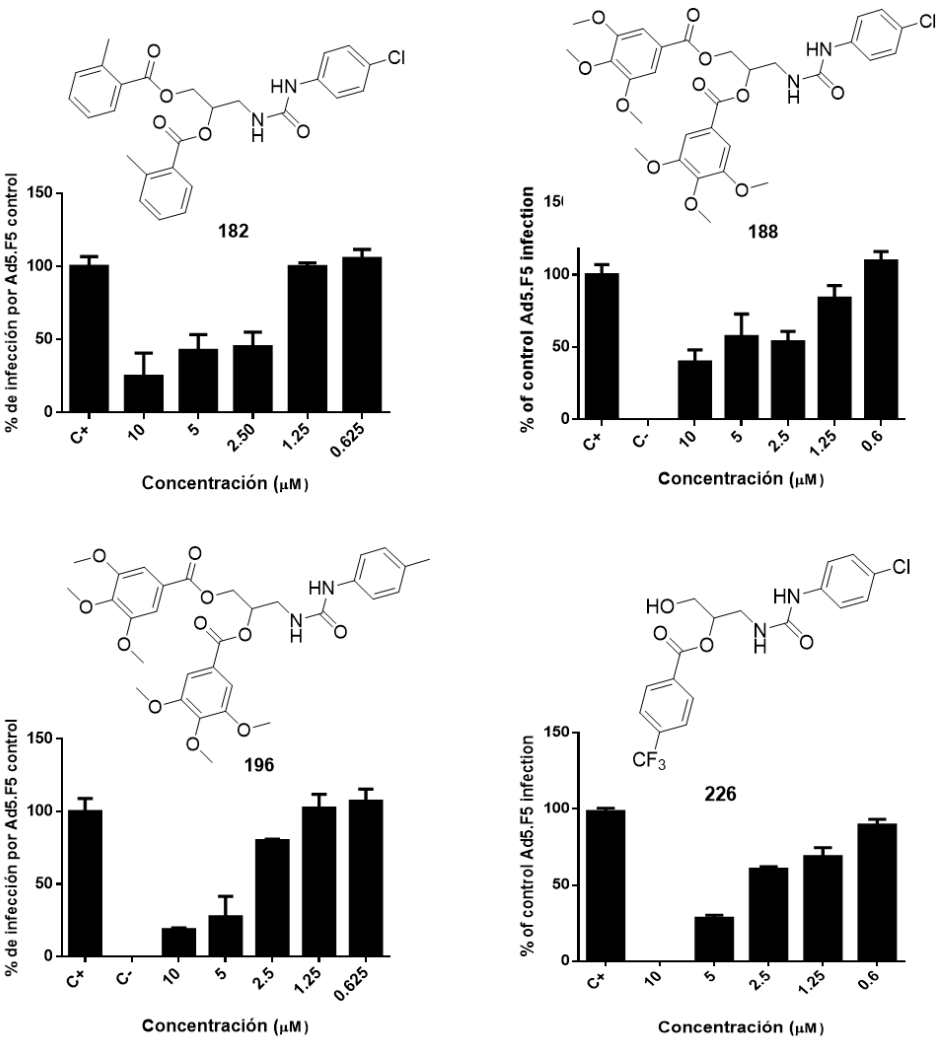

Figure 29. Dose-dependent activity of representative compounds in a plaque assay. For all panels, the DMSO control is a positive control with cells infected at the same MOI but in the absence of drugs. The results represent means ± SD of triplicate samples from three independent experiments.

Table 23. IC_{50}, CC_{50}, SI values for selected compounds compared to drug cidofovir.

Comp		IC_{50} (μM)[a]	CC_{50} (μM)[b]	Selectivity Index (SI)[c]
182	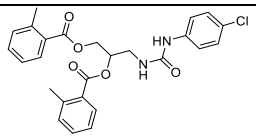	2.47 ± 0.07	28.70 ± 3.10	11.63
188	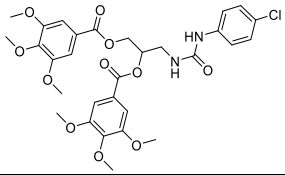	4.19 ± 2.59	97.25 ± 16.56	23.21

190	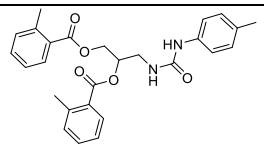	NE[d]	51.33 ± 19.04	NE
196	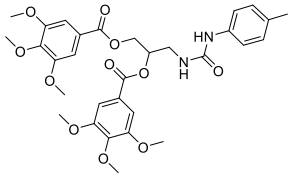	2.82 ± 0.31	175.16 ± 2.97	62.68
207	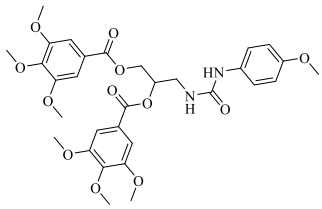	NE	136.62 ± 6.54	-
226	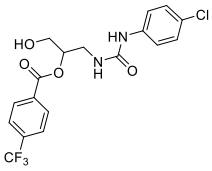	3.02 ± 0.08	>200	66.23
Cidofovir	-	24.06 ± 5.9	50.6 ± 9.8	7.5

[a]Inhibitory concentration 50 at low MOI in a plaque assay.
[b]Cytotoxic concentration 50.
[c]Selectivity Index value was determined as the ratio of cytotoxic concentration 50 (CC_{50}) to inhibitory concentration 50 (IC_{50}) in a plaque assay for each compound.
[d] Not yet evaluated.

Secondly, biological assays to explore their mechanism of action are being carried out as for previously studied libraries. The main goal it is to contribute to improve the structural diversity of this novel class of antiadenovirus agents.

One consideration should be metioned. In spite of the fact that these selected 3-amino-1,3-propanediol derivatives did not show percentages of plaque inhibition as high as those from our previous scaffolds (piperazine and serinol derivatives), they are an important contribution in the development of new antiadenovirus agents. They displayed promising IC_{50} for lead compounds (2.47-4.19 μM), they could inhibit virus replication through different ways to our other compounds (data from studies wil clarify this aspect) so they can be considered promising initial point to obtain optimized analogues with increased biological properties.

CHAPTER 6
EXPERIMENTAL SECTION

6.1 General chemical methods

All reagents, solvents, and starting materials were obtained from commercial suppliers and used without further purification. The crude reaction mixtures were concentrated under reduced pressure by removing the organic solvents in a rotary evaporator. Reactions were monitored by thin layer chromatography (TLC) using Kieselgel 60 F254 (E. Merck) plates and UV detector for visualization. Flash column chromatography was performed on Silica Gel 60 (E. Merck). All reported yields are of purified products. Melting points were obtained on a Stuart Melting Point Apparatus SMP 10 and are uncorrected. Mass spectra were recorded on a Micromass AUTOSPECQ mass spectrometer: EI at 70 eV and CI at 150 eV, HR mass measurements with resolutions of 10,000. FAB mass spectra were recorded using a thioglycerol matrix. NMR spectra were recorded at 25 °C on a Bruker AV500 spectrometer at 500 MHz for 1H and 125 MHz for 13C. COSY, DEPT, HSQC, HMBC and NOESY experiments were performed to assign the signals in the NMR spectra. The chemical shifts (δ) reported are given in parts per million (ppm) on the δ scale relative to TMS, and the coupling constants (J) are in hertz (Hz). ^{1}H chemical shift values (δ) are referenced to the residual non-deuterated components of the NMR solvents (δ = 2.54 ppm for DMSO, δ = 3.31 ppm for MeOD). The ^{13}C chemical shifts (δ) are referenced to deuterated solvent (central peak, δ = 39.5 ppm for DMSO and 49.15 ppm for MeOD) as the internal standard. The spin multiplicities are reported as s (singlet), d (doublet), t (triplet), q (quadruplet), quint (quintuplet), sex (sextet), m (multiplet), or br s (broad singlet). The purity of final compounds was evaluated by C, H and N analysis through Leco Trunspec CHNS Micro elemental system.

NMR Spectroscopy, Mass Spectrometry and Micro elemental analysis were performed by Servicios Generales de Investigación, CITIUS (Centro de Investigación, Tecnología e Innovación de la Universidad de Sevilla)

6.1.1 4-Acyl-1-phenylamino(thio)carbonylsubstituted piperazine derivatives

-General Procedure 1. Acylation reaction of amines from 2-substituted piperazine or 2,6-disubstituted piperazine (41-49, 103, 100, 120)

*A) Chemoselective N-acylation reaction of 2-substituted piperazine or 2,6-disubstituted piperazine (**41-49**, **103**).*2-Substituted piperazine or 2,6-disubstituted piperazine (5.0 mmol) was dissolved in dry DCM (100 mL) and pyridine (7.5 mmol) cooled to 0 ºC. A solution of the appropriate acylating agent (5.0 mmol) in DCM (20 mL) was added dropwise in 30 minutes. The reaction mixture was kept into an ice-water bath with stirring 6 hours and left at rt until TLC showed that all the starting material had reacted (12 hours). The reaction mixture was evaporated to dryness to obtain the corresponding monoacylderivative. The compound was further purified by flash column chromatography on silica gel using the appropriate eluent.

1-*tert*-Butoxycarbonyl-3-methylpiperazine (41) [84]. The product was obtained as a syrup and purified by column chromatography using dichloromethane-methanol (15:1) as eluent (750 mg, 75% yield). MS (CI): *m/z* 201 (20%) $[M+H]^+$. ^{1}H NMR (500 MHz, DMSO-d_6) δ 3.75–3.71 (m, 2H), 2.85–2.82 (m, 1H), 2.75–2.69 (m, 1H), 2.60–2.54 (m, 3H), 2.39–2.34 (m, 1H), 1.41 (s, 9H), 0.96 (d, J = 6.3 Hz, 3H). ^{13}C NMR (125 MHz, DMSO-d_6) δ 154.5, 79.3, 51.2, 50.5, 45.5, 44.4, 28.6, 19,3. HRMS (*m/z*): calcd for $C_{10}H_{20}N_2O_2$ 200.1528 $[M]^{+\cdot}$; found 200.1525.

1-(3,3-Dimethylbutanoyl)-3-methylpiperazine (42). The product was obtained as a syrup and purified by column chromatography using ethyl acetate-methanol (3:1) as eluent (792 mg, 80% yield). MS (CI): *m/z* 199 (100%) $[M+H]^+$. ^{1}H NMR (500 MHz, $CDCl_3$) δ 4.57 (d, J = 12.4 Hz, 1H), 3.85 (m, 1H), 3.52–3.08 (m, 2H), 3.06–2.62 (m, 3H), 2.23 (s, 2H), 1.33 (br s, 3H), 1.02 (s, 9H). ^{13}C NMR (125 MHz, $CDCl_3$) δ 170.3, 51.4, 45.8, 44.6, 44.5, 39.3, 31.5, 30.0, 17.3. HRMS (*m/z*): calcd for $C_{11}H_{22}N_2ONa$ 222.1624 $[M+Na]^+$; found 222.1619.

1-(2-Cyclohexylacetyl)-3-methylpiperazine (43). The product was obtained as a syrup and purified by column chromatography using ethyl acetate-methanol (4:1) as eluent (1.1 g, 97% yield). ^{1}H NMR (500 MHz, DMSO-d_6) δ 4.26 (d, J = 11.7 Hz, 1H), 3.76 (d, J = 11.4 Hz, 1H), 3.05–2.88 (m, 2H), 2.70–2.58 (m, 3H), 2.26–2.14 (m, 3H), 1.75–1.60 (m, 6H), 1.30–1.10 (m, 3H), 1.05–0.91 (m, 5H). ^{13}C NMR (125 MHz, DMSO-d_6) δ 169.7, 52.0, 50.8, 50.3, 47.7, 45.4, 44.8, 41.0, 34.4, 32.7, 25.8, 25.6, 18.7, 18.4. HRMS (*m/z*): calcd for $C_{13}H_{25}N_2O$ 225.1961 $[M+H]^{+\cdot}$; found 225.1964.

3-Methyl-1-(2-phenylacetyl)piperazine (44). The product was obtained as a syrup and purified by column chromatography using ethyl acetate-methanol (4:1) as eluent (1.1 g, 98% yield). ^{1}H NMR (500 MHz, DMSO-d_6) δ 7.33–7.22 (m, 5H), 4.25 (d, J = 12.7 Hz, 1H), 3.09–2.62 (m, 3H), 2.58–2.53 (m, 1H), 2.49–2.34 (m, 1H), 1.75-1.60 (m, 6H), 1.03, 0.99 (2s, J = 6.4 Hz, 3H). ^{13}C NMR (125 MHz, DMSO-d_6) δ 168.7, 135.9, 135.8, 128.9, 128.8, 128.3, 128.2, 126.3, 51.5, 50.5, 50.1, 47.1, 45.0, 44.6, 44.2 40.6, 18.1, 17.7. HRMS (*m/z*): calcd for $C_{13}H_{19}N_2O$ 219.1492 $[M+H]^+$; found 219.1486.

1-(Benzofuran-2-carbonyl)-3-methylpiperazine (45). The product was obtained as a solid and purified by column chromatography using dichloromethane-methanol (40:1) as eluent (903 mg, 74% yield), mp 101–103 ºC. ^{1}H NMR (500 MHz, DMSO-d_6) δ 7.7–7.5 (m, 5H), 4.47 (br s, 2H), 3.10 (d, J = 11.4 Hz, 1H), 2.94–2.86 (m, 2H), 1.97 (br s, 2H), 1.13 (d, J = 5.0 Hz, 3H). ^{13}C NMR (125 MHz, DMSO-d_6) δ 159.8, 154.6, 149.1, 127.0, 126.4, 123.6, 122.2, 111.9, 111.8, 51.1, 46.1, 19.4. Anal. Calcd $C_{14}H_{16}N_2O_2$: C, 68.55; H, 6.99; N, 11.42. Found: C, 68.32; H, 6.62; N, 11.22.

1-*tert*-Butoxycarbonyl-3-phenylpiperazine (**46**) [84]**.**The product was obtained as a syrup and purified by column chromatography using hexane−ethyl acetate (2:1) as eluent (864 mg, 66% yield), mp 103−105 °C. MS (CI): *m/z* 263 (100%) $[M+H]^+$. 1H NMR (500 MHz, $CDCl_3$) δ 7.4−7.3 (m, 5H), 4.05 (br s, 2H), 3.70 (dd, J = 2.4 Hz, J = 10.5 Hz, 1H,), 3.07 (m, 1H), 2.9−2.8 (m, 2H), 2.72 (br s, 1H), 1.90 (br s, 1H), 1.47 (s, 9H). ^{13}C NMR (125 MHz, $CDCl_3$) δ 154.8, 141.5, 128.5, 127.8, 127.0, 79.7, 60.3, 51.5, 46.1, 43.4, 28.5. HRMS (*m/z*): calcd for $C_{15}H_{23}N_2O_2$ 263.1754 $[M+H]^+$; found 263.1748.

1-(3,3-Dimethylbutanoyl)-3-phenylpiperazine (47). The product was obtained as a syrup and purified by column chromatography using ethyl acetate-methanol (20:1) as eluent (1.0 g, 77% yield). MS (CI): *m/z* 261 (100%) $[M+H]^+$. ^{1}H NMR (500 MHz, DMSO-d_6) δ 7,45–7,27 (m, 5H), 4,44–4.39 (m, 1H), 3,94–3,85 (m, 1H), 3,58 (dd, J = 2.3 Hz, J = 10.3 Hz, 1H), 3,31 (br s, 1H), 3,11–2,99 (m, 2H), 2,91–2,68 (m, 1H), 2,61–2,57 (m, 1H), 2,31–2,20 (m, 2H), 1,02, 1,00 (2s, 9H). ^{13}C NMR (125 MHz, DMSO-d_6) δ 169.3, 169.2, 142.2, 141.9, 128.2, 128.1, 127.4, 127.3, 127.0, 126.9, 60.1, 59.4, 53.5, 48.1, 46.4, 45.9, 45.5, 43.8, 43.6, 41.1, 40.1, 30.9, 29.8. HRMS (*m/z*): calcd for $C_{16}H_{25}N_2O$ 261.1961 $[M+H]^+$; found 261.1956.

1-(2-Cyclohexylacetyl)-3-phenylpiperazine (48). The product was obtained as a syrup and purified by column chromatography using ethyl acetate-methanol (30:1) as eluent (815 mg, 57% yield). MS (CI): *m/z* 287 (100%) $[M+H]^+$. ^{1}H NMR (500 MHz, $CDCl_3$) δ 7.40–7.27 (m, 5H), 4.67–4.63 (m, 1H), 3.84–3.79 (m, 1H), 3.69–3.67 (m, 1H), 3.26–3.02 (m, 2H), 2.91–2.83 (m, 1H), 2.59–2.54 (m, 1H),

2.29–2.16 (m, 2H), 2.10–1.91 (m, 1H), 1.85–1.65 (m, 5H), 1.33–1.21 (m, 2H), 1.18–1.10 (m, 1H), 1.02–0.92 (m, 2H). ^{13}C NMR (125 MHz, $CDCl_3$) δ 170.9, 141.3, 141.1, 128.7, 128.5, 128.2, 127.8, 127.0, 126.9, 61.4, 60.2, 53.6, 48.8, 46.7, 46.3, 46.1, 41.8, 40.8, 40.7, 35.3, 35.2, 33.5, 33.4, 33.3, 26.3, 26.2. HRMS (*m/z*): calcd for $C_{18}H_{27}N_2O$ 287.2118 $[M+H]^+$; found 287.2111.

3-Phenyl-1-(2-phenylacetyl)piperazine (49). The product was obtained as a syrup and purified by column chromatography using ethyl acetate-methanol (100:1) as eluent (784 mg, 56% yield). ^{1}H NMR (500 MHz, $CDCl_3$) δ 7.39–7.12 (m, 10H), 4.68–4.59 (m, 1H), 3.83–3.62 (m, 3H), 3.29–3.13 (m, 1H), 3.11–2.92 (m, 2H), 2.84–2.56 (m, 2H), 2.18 (br s, 1H). ^{13}C NMR (125 MHz, $CDCl_3$) δ 169.5, 169.4, 141.0, 140.8, 135.3, 135.1, 128.9, 128.7, 128.6, 128.5, 128.0, 127.9, 127.0, 126.9, 126.8, 60.8, 60.0, 53.8, 48.9, 46.5, 46.2, 45.9, 42.0, 41.4, 41.2. HRMS (*m/z*): calcd for $C_{18}H_{21}N_2O$ 281.1648 $[M+H]^+$; found 281.1644.

1-(Benzofuran-2-carbonyl)-3,5-dimethylpiperazine (103). The product was obtained as a syrup and purified by column chromatography using dichloromethane-methanol (20:1) as eluent (942 mg, 73% yield). ^{1}H NMR (500 MHz, $CDCl_3$) δ 7.76 (d, J = 7.8 Hz, 1H), 7.68 (dd, J = 8.1 Hz, J = 0.6 Hz, 1H), 7.48–7.44 (m, 1H), 7.41 (s, 1H), 7.37–7.33 (m, 1H), 4.46–4.10 (m, 2H), 2.98–2.75 (m, 3H), 1.16–0.94 (m, 6H). ^{13}C NMR (125 MHz, $CDCl_3$) δ 158.6, 153.9, 148.2, 126.7, 126.4 123.6, 122.4, 111.8, 110.7, 54.9, 18.2. HRMS (*m/z*): calcd for $C_{15}H_{19}N_2O_2$ 259.1441 $[M+H]^+$; found 259.1444.

*B) N,N'-Diacylation reaction of 2-phenylpiperazine or piperazine (**100** and **120**).* To a solution of 2-phenylpiperazine or piperazine (1 mmol) in DCM (30 mL), pyridine (3.0 mmol) and then benzofurane-2-carbonyl choride (2.4 mmol) were added. The reaction mixture was stirring at rt until TLC showed that all the starting material had reacted (24 hours). The reaction mixture was evaporated to dryness to obtain the corresponding diacylderivative. The compound was further purified by flash column chromatography on silica gel using the appropriate eluent.

1,4-Bis(benzofurane-2-carbonyl)-2-phenylpiperazine (100). The product was obtained as a solid and purified by column using chromatography dichloromethane-methanol (60:1) as eluent (374 mg, 83% yield), mp 159–162 ºC. ^{1}H NMR (500 MHz, DMSO-d_6) δ 7.79–7.74 (m, 2H), 7.69–7.64 (m, 2H), 7.54–7.24 (m, 11H), 5.98–5.74 (m, 1H), 5.01–4.75 (m, 1H), 4.55–4.38 (m, 1H), 4.36–4.08 (m, 2H), 3.88–3.42 (m, 2H). ^{13}C RMN (125 MHz, DMSO-d_6) δ 160.0, 159.3, 154.0, 153.9, 147.8, 128.6, 127.3, 126.7, 126.6, 126.5, 123.7, 122.5, 111.8, 111.3. HRMS (*m/z*): calcd for $C_{28}H_{22}N_2O_4Na$ 473.1472 $[M+Na]^+$; found 473.1464.

1,4-Bis(benzofurane-2-carbonyl)piperazine (120). The product was obtained as a solid and purified by column using chromatography hexane-ethyl acetate (1:1) as eluent (388 mg, 91% yield), mp 240–241 ºC. ^{1}H NMR (500 MHz, DMSO-d_6) δ 7.78 (d, J = 7.8 Hz, 2H), 7.69 (d, J = 8.4 Hz, 2H), 7.50–7.46 (m, 4H), 7.36 (d, J = 7.6 Hz, 2H), 3.98–3.79 (m, 8H). ^{13}C RMN (125 MHz, DMSO-d_6) δ 159.1, 154.0, 148.0, 126.7, 126.6, 123.7, 122.5, 118.8, 111.2. HRMS (*m/z*): calcd for $C_{22}H_{18}N_4O_2Na$ 397.1159 $[M+Na]^+$; found 397.1153. Anal. Calcd $C_{22}H_{18}N_4O_2$: C, 70.58; H, 4.85; N, 7.48. Found: C, 70.71, H, 5.09; N, 7.19.

-General Procedure 2. Synthesis of thiourea/urea derivatives from monoacyl piperazines or piperazine (50-99, 104-110, 112-114, 101, 121).

*A) Synthesis of thiourea/urea derivatives from monoacyl piperazines (**50-99**, **104-110**, **112-114**).* To a solution of the monoacyl derivative (**41-49, 103** and **111**) (0.75 mmol) in DCM (10 mL) was added the corresponding isothiocyanate/isocyanate (0.9 mmol). The reaction mixture was stirred at rt until TLC revealed that all the starting material had reacted (24 hours) and then was evaporated to dryness**.** The compound was purified by flash chromatography on silica gel using the appropriate eluent.

4-*tert*-Butoxycarbonyl-1-[(4-chlorophenyl)aminothiocarbonyl]-2-methylpiperazine (50). The product was obtained as a solid and purified by column chromatography using hexane-ethyl acetate (2:1) as eluent (202 mg, 73% yield), mp 143–144 ºC. MS (FAB): *m/z* 392 (100%) $[M+Na]^+$. ^{1}H NMR (500 MHz, $CDCl_3$) δ 7.30 (d, J = 8.4 Hz, 2H), 7.16–7.33 (m, 3H), 5.13–4.76 (m, 1H), 4.45–3.79 (m, 3H), 3.39–3.32 (m, 1H), 3.21 (dd, J = 3.5 Hz, J = 13.5 Hz, 1H), 3.12–2.91 (m, 1H), 1.48 (s, 9H), 1.28 (d, J = 6.7 Hz, 3H). ^{13}C NMR (125 MHz, $CDCl_3$) δ 183.3, 155.0, 138.5, 131.0, 129.8, 129.2, 126.9, 125.4, 80.5, 52.4, 43.8, 28.4, 15.1. HRMS (*m/z*): calcd for $C_{17}H_{24}ClN_3O_2SNa$ 392.1170 $[M+Na]^+$; found 392.1163. Anal. Calcd $C_{17}H_{24}ClN_3O_2S$: C, 55.20; H, 6.54; N, 11.36; S, 8.67. Found: C, 55.48; H, 6.67; N, 11.44, S, 9,01.

4-*tert*-Butoxycarbonyl-1-[(4-cyanophenyl)aminothiocarbonyl]-2-methylpiperazine (51). The product was obtained as a solid and purified by column chromatography using hexane-ethyl acetate (3:1) as eluent (205 mg, 76% yield), mp 132–134 ºC. MS (FAB): *m/z* 383 (100%) $[M+Na]^+$. ^{1}H NMR (500 MHz, $CDCl_3$) δ 7.61 (d, J = 8.4 Hz, 2H), 7.32 (d, J = 8.4 Hz, 2H), 7.22 (br s, 1H), 5.18–4.86 (m, 1H), 4.40–3.73 (m, 4H), 3.44–3.37 (m, 1H), 3.26–3.19 (m, 1H), 3.14–2.90 (m, 1H), 1.48 (s, 9H), 1,32 (d, J = 6.8 Hz, 3H). ^{13}C NMR (125 MHz, $CDCl_3$) δ 182.5, 154.9, 144.0, 133.2, 126.5, 122.7, 118,6. 80.5, 52.8, 44.1, 28.4, 15.3. HRMS (*m/z*): calcd for $C_{18}H_{24}N_4O_2SNa$ 383.1512 $[M+Na]^+$; found

383.1500. Anal. Calcd $C_{18}H_{24}N_4O_2S$: C, 59.97; H, 6.71; N, 15.54; S, 8.90. Found: C, 60.03; H, 6.81; N, 15.20; S, 9.15.

4-*tert*-Butoxycarbonyl-1-[(4-fluorophenyl)aminothiocarbonyl]-2-methylpiperazine (52). The product was obtained as a solid and purified by column chromatography using hexane-ethyl acetate (3:1) as eluent (209 mg, 79% yield), mp 74–76 ºC. MS (FAB): *m/z* 376 (100%) $[M+Na]^+$. ^1H NMR (500 MHz, $CDCl_3$) δ 7.22–7.14 (m, 2H), 7.10 (s, 1H), 7.06–7.02 (m, 2H), 5.14–4.75 (m, 1H), 4.51–3.69 (m, 3H), 3.41–3.32 (m, 1H), 3.24–3.16 (m, 1H), 3.14–2.75 (m, 1H), 1.47 (s, 9H), 1.28 (d, J = 6.8 Hz, 3H). ^{13}C NMR (125 MHz, $CDCl_3$) δ 183.6, 155.0, 135.9, 126.6, 115,9. 80.4, 52.3, 43.6, 28.4, 15.1. HRMS (*m/z*): calcd. for $C_{17}H_{24}FN_3O_2SNa$ 376.1465 $[M+Na]^+$; found 376.1456. Anal. Calcd $C_{17}H_{24}FN_3O_2S$: C, 57.77; H, 6.84; N, 11.89; S, 9.07. Found: C, 58.00; H, 6.82; N, 11.68; S, 9.48.

4-*tert*-Butoxycarbonyl-2-methyl-1-[(4-trifluoromethylphenyl)aminothiocarbonyl]piperazine (53). The product was obtained as a solid and purified by column chromatography using hexane-ethyl acetate (4:1) as eluent (220 mg, 73% yield), mp 141–143 ºC. MS (FAB): *m/z* 426 (100%) $[M+Na]^+$. ^1H NMR (500 MHz, DMSO-d_6) δ 9.52 (s, 1H), 7.65 (d, J = 8.3 Hz, 2H), 7.55 (d, J = 8.3 Hz, 2H), 5.11 (br s, 1H), 4.45–4.38 (m, 1H), 3.98–3.84 (m, 1H), 3.82–3.75 (m, 1H), 3.25–3.12 (m, 1H), 3.09–2.93 (m, 1H), 1.45 (s, 9H), 1,20 (d, J = 6.7 Hz, 3H). ^{13}C NMR (125 MHz, DMSO-d_6) δ 181.7, 154.2, 144.9, 125.1, 125.0, 124.5, 79.2, 51.4, 42.7, 28.0, 14.8. HRMS (*m/z*): calcd for $C_{18}H_{24}F_3N_3O_2SNa$ 426.1434 $[M+Na]^+$; found 426.1428. Anal. Calcd $C_{18}H_{24}F_3N_3O_2S$: C, 53.58; H, 6.00; N, 10.41. Found: C, 53.12; H, 6.41; N, 10.31.

4-*tert*-Butoxycarbonyl-1-[(4-methoxyphenyl)aminothiocarbonyl]-2-methylpiperazine (54). The product was obtained as a solid and purified by column chromatography using hexane-ethyl acetate (3:1) as eluent (205 mg, 75% yield), mp 127–129 ºC. MS (FAB): *m/z* 388 (100%) $[M+Na]^+$. ^1H NMR (500 MHz, DMSO-d_6) δ 9.15 (s, 1H), 7.16 (d, J = 9.0 Hz, 2H), 6.89 (d, J = 9.0 Hz, 2H), 5.05 (br s, 1H), 4.48–4.38 (m, 1H), 3.95–3.80 (m, 1H), 3.76 (s, 3H), 3.28–2.92 (m, 3H), 1.44 (s, 9H), 1,16 (d, J = 6.8 Hz, 3H). ^{13}C NMR (125 MHz, DMSO-d_6) δ 182.0, 156.6, 154.3, 133.8, 127.6, 113.2, 79.1, 55.2, 50.8, 42.1, 28.0, 14.8. HRMS (*m/z*): calcd for $C_{18}H_{27}FN_3O_3SNa$ 388.1665 $[M+Na]^+$; found 388.1669.

4-*tert*-Butoxycarbonyl-2-methyl-1-[(4-methylphenyl)aminothiocarbonyl]piperazine (55). The product was obtained as a solid and purified by column chromatography using hexane-ethyl acetate (6:1) as eluent (149 mg, 75% yield), mp 155–157 ºC. MS (FAB): *m/z* 372 (100%) $[M+Na]^+$. ^1H NMR (500 MHz, DMSO-d_6) δ 9.18 (s, 1H), 7.15 (d, J = 8.4 Hz, 2H), 7.11 (d, J = 8.4 Hz, 2H), 5.06 (br s, 1H), 4.46–4.37 (m, 1H), 3.95–3.81 (m, 1H), 3.79–3.72 (m, 1H), 3.21–2.88 (m, 2H), 2.29 (s, 3H), 1.44

(s, 9H), 1,16 (d, J = 6.6 Hz, 3H). ^{13}C NMR (125 MHz, DMSO-d_6) δ 181.9, 154.2, 138.4, 133.7, 128.5, 125.8, 79.1, 50.9, 42.2, 28.0, 20.5, 15.1. HRMS (*m/z*): calcd for $C_{18}H_{27}N_3O_2SNa$ 372.1716 [M+Na]$^+$; found 372.1710.

1-[{3,5-Bis(trifluoromethyl)phenyl}aminothiocarbonyl]-4-*tert*-butoxycarbonyl-2-methylpiperazine (56). The product was obtained as a solid and purified by column chromatography using hexane-ethyl acetate (7:1) as eluent (251 mg, 71% yield), mp 134–136 ºC. MS (FAB): *m/z* 494 (100%) [M+Na]$^+$. ^{1}H NMR (500 MHz, DMSO-d_6) δ 9.72 (s, 1H), 8.09 (s, 2H), 7.78 (s, 1H), 5.10 (br s, 1H), 4.55–4.42 (m, 1H), 4.04–3.74 (m, 2H), 3.26–2.91 (s, 2H), 1.45 (s, 9H), 1,21 (d, J = 6.7 Hz, 3H). ^{13}C NMR (125 MHz, DMSO-d_6) δ 181.0, 154.2, 143.1, 130.1, 129.8, 129.5, 129.3, 126.5, 124.8, 124.4, 122.2, 116.7, 79.2, 51.5, 42.7, 28.0, 14.9. HRMS (*m/z*): calcd for $C_{19}H_{23}F_6N_3O_2SNa$ 494.1307 [M+Na]$^+$; found 494.1300. Anal. Calcd $C_{19}H_{23}F_6N_3O_2S$: C, 48.40; H, 4.92; N, 8.91. Found: C, 48.56; H, 4.64; N, 8.88.

4-(3,3-Dimethylbutanoyl)-2-methyl-1-[(4-nitrophenyl)aminothiocarbonyl]piperazine (57). The product was obtained as a solid and purified by column chromatography using hexane-ethyl acetate (1:1) as eluent (193 mg, 68% yield), mp 195–198 ºC. MS (FAB): *m/z* 401 (100%) [M+Na]$^+$. ^{1}H NMR (500 MHz, DMSO-d_6) δ 9.76 (s, 1H), 8.18 (d, J = 8.8 Hz, 2H), 7.61 (d, J = 8.8 Hz, 2H), 5.12 (br s, 1H), 4.48–4.43 (m, 1H), 4.27 (d, J = 13.5 Hz, 1H), 4.08–3.88 (m, 1H), 3.02–2.85 (m, 1H), 2.42–2.08 (m, 2H), 1,22, 1,15 (2d, J = 6.7 Hz, 3H), 1.03, 1.02 (2s, 9H). ^{13}C NMR (125 MHz, DMSO-d_6) δ 181.5, 170.4, 170.3, 147.8, 142.2, 123.9, 123.0, 52.1, 51.8, 49.1, 45.1, 44.4, 43.6, 43.4, 43.1, 40.7, 31.0, 30.9, 29.7, 15.1, 14.7. HRMS (*m/z*): calcd for $C_{18}H_{26}N_4O_3SNa$ 401.1618 [M+Na]$^+$; found 401.1615. Anal. Calcd $C_{18}H_{26}N_4O_3S$: C, 57.12; H, 6.92; N, 14.80. Found: C, 57.47; H, 7.07; N, 14.56.

1-[(4-Chlorophenyl)aminothiocarbonyl]-4-(3,3-dimethylbutanoyl)-2-methylpiperazine (58). The product was obtained as a solid and purified by column chromatography using hexane-ethyl acetate (2:1) as eluent (193 mg, 70% yield), mp 77–80 ºC. MS (FAB): *m/z* 390 (100%) [M+Na]$^+$. ^{1}H NMR (500 MHz, DMSO-d_6) δ 9.76 (s, 1H), 8.18 (d, J = 8.8 Hz, 2H), 7.61 (d, J = 8.8 Hz, 2H), 5.12 (br s, 1H), 4.48–4.43 (m, 1H), 4.27 (d, J = 13.5 Hz, 1H), 4.08–3.88 (m, 1H), 3.02–2.85 (m, 1H), 2.42–2.08 (m, 2H), 1,22, 1,15 (2d, J = 6.7 Hz, 3H), 1.03, 1.02 (2s, 9H). ^{13}C NMR (125 MHz, DMSO-d_6) δ 181.6, 181.4, 170.4, 170.2, 128.4, 127.8, 127.2, 51.5, 51.2, 49.1, 45.6, 44.4, 43.6, 43.2, 43.0, 42.6, 40.7, 31.0, 30.9, 29.7, 15.1, 14.7. HRMS (*m/z*): calcd for $C_{18}H_{26}ClN_3OSNa$ 390.1377 [M+Na]$^+$; found 390.1373. Anal. Calcd $C_{18}H_{26}ClN_3OS$: C, 58.76; H, 7.12; N, 11.42. Found: C, 58.45; H, 7.03; N, 11.12.

1-[(4-Cyanophenyl)aminothiocarbonyl]-4-(3,3-dimethylbutanoyl)-2-methylpiperazine (59). The product was obtained as a solid and purified by column chromatography using hexane-ethyl acetate (1:1) as eluent (177 mg, 66% yield), mp 158–160 ºC. MS (FAB): *m/z* 381 (100%) $[M+Na]^+$. ^{1}H NMR (500 MHz, DMSO-d_6) δ 9.59 (s, 1H), 7.76–7.72 (m, 2H), 7.58–7.53 (m, 2H), 5.10 (br s, 1H), 4.46–4.33 (m, 1H), 4.26 (d, J = 13.3 Hz, 1H), 4.04–3.87 (m, 1H), 3.02–2.87 (m, 1H), 2.42–2.08 (m, 2H), 1,22, 1,15 (2d, J = 6.2 Hz, 3H), 1.03, 1.02 (2s, 9H). ^{13}C NMR (125 MHz, DMSO-d_6) δ, 170.0, 145.6, 132.2, 123.9, 119.1, 105.3, 51.9, 51.6, 49.1, 45.1, 44.6, 43.6, 43.4, 42.9, 40.7, 31.0, 30.9, 29.7, 15.2, 14.8. HRMS (*m/z*): calcd for $C_{19}H_{26}N_4OSNa$ 381.1720 $[M+Na]^+$; found 381.1714. Anal. Calcd $C_{19}H_{26}N_4OS$: C, 63.65; H, 7.31; N, 15.63. Found: C, 63.28; H, 7.35; N, 15.24.

1-[(4-Fluorophenyl)aminothiocarbonyl]-4-(3,3-dimethylbutanoyl)-2-methylpiperazine (60). The product was obtained as a solid and purified by column chromatography using hexane-ethyl acetate (1:1) as eluent (158 mg, 60% yield), mp 76–80 ºC. MS (FAB): *m/z* 374 (100%) $[M+Na]^+$. ^{1}H NMR (500 MHz, DMSO-d_6) δ 9.26 (br s, 1H), 7.33–7.26 (m, 2H), 7.18–7.11 (m, 2H), 5.06 (br s, 1H), 4.51–4.38 (m, 1H), 4.22 (d, J = 13.5 Hz, 1H), 4.05–3.84 (m, 1H), 3.06–2.88 (m, 1H), 2.43–2.09 (m, 2H), 1,20, 1,14 (2d, J = 6.6 Hz, 3H), 1.04, 1.02 (2s, 9H). ^{13}C NMR (125 MHz, DMSO-d_6) δ 181.9, 170.4, 170.2, 160.3, 158.3, 137.3, 128.0, 127.9, 114.7, 114.5, 51.4, 51.1, 49.2, 45.1, 44.4, 43.6, 43.4, 43.0, 42.3, 40.7, 31.0, 30.9, 29.7, 15.2, 14.8. HRMS (*m/z*): calcd. for $C_{18}H_{26}FN_3OSNa$ 374.1673 $[M+Na]^+$; found 374.1670. Anal. Calcd $C_{18}H_{26}FN_3OS$: C, 61.51; H, 7.46; N, 11.96. Found: C, 61.30; H, 7.29; N, 11.69.

4-(3,3-Dimethylbutanoyl)-2-methyl-1-[(4-trifluoromethylphenyl)aminothiocarbonyl] piperazine (61). The product was obtained as a solid and purified by column chromatography using hexane-ethyl acetate (2:1) as eluent (220 mg, 73% yield), mp 79–82 ºC. MS (FAB): *m/z* 424 (100%) $[M+Na]^+$. ^{1}H NMR (500 MHz, DMSO-d_6) δ 9.53 (s, 1H), 7.66 (d, J = 8.6 Hz, 2H), 7.56 (d, J = 8.4 Hz, 2H), 5.12 (br s, 1H), 4.49–4.36 (m, 1H), 4.25 (d, J = 13.3 Hz, 1H), 4.05–3.87 (m, 1H), 3.05–2.86 (m, 1H), 2.45–2.08 (m, 2H), 1,22, 1,16 (2d, J = 6.7 Hz, 3H), 1.04, 1.03 (2s, 9H). ^{13}C NMR (125 MHz, DMSO-d_6) δ 181.6, 181.4, 170.4, 170.2, 144.9, 125.5, 125.0, 124.6, 124.5, 124.0, 123.8, 123.3, 51.8, 51.5, 49.1, 45.1, 44.4, 43.6, 43.4, 43.3, 42.8, 40.7, 31.0, 30.9, 29.7, 15.2, 14.8. HRMS (*m/z*): calcd for $C_{19}H_{26}F_3N_3OSNa$ 424.1641 $[M+Na]^+$; found 424.1631. Anal. Calcd $C_{19}H_{26}F_3N_3OS$: C, 56.84; H, 6.53; N, 10.47. Found: C, 56.86; H, 6.33; N, 10.12.

4-(3,3-Dimethylbutanoyl)-1-[(4-methoxyphenyl)aminothiocarbonyl]-2-methylpiperazine (62). The product was obtained as a solid and purified by column chromatography using hexane-ethyl

acetate (1:1) as eluent (169 mg, 62% yield), mp 138–140 ºC. ^{1}H NMR (500 MHz, DMSO-d_6) δ 9.15 (s, 1H), 7.16 (d, J = 8.5 Hz, 2H), 6.88 (d, J = 8.8 Hz, 2H), 5.05 (br s, 1H), 4.53–4.34 (m, 1H), 4.20 (d, J = 12.9 Hz, 1H), 4.01–3.83 (m, 1H), 3.76 (s, 3H), 3.04–2.87 (m, 1H), 2.41–2.08 (m, 2H), 1,19, 1,13 (2d, J = 6.4 Hz, 3H), 1.03, 1.02 (2s, 9H). ^{13}C NMR (125 MHz, DMSO-d_6) δ 182.0, 181.9, 170.4, 170.2, 156.7, 133.8, 127.6, 113.2, 55.2, 51.2, 50.9, 49.2, 45.1, 44.4, 43.6, 43.4, 42.8, 42.2, 40.7, 31.0, 30.9, 29.7, 26.8, 15.2, 14.8. HRMS (*m/z*): calcd for $C_{19}H_{29}N_3O_2SNa$ 386.1873 $[M+Na]^+$; found 386.1870. Anal. Calcd $C_{19}H_{29}N_3O_2S$: C, 62.78; H, 8.04; N, 11.56. Found: C, 62.50; H, 7.81; N, 11.25.

4-(3,3-Dimethylbutanoyl)-2-methyl-1-[(4-methylphenyl)aminothiocarbonyl]piperazine (63). The product was obtained as a solid and purified by column chromatography using hexane-ethyl acetate (3:2) as eluent (197 mg, 76% yield), mp 136–138 ºC. ^{1}H NMR (500 MHz, DMSO-d_6) δ 9.19, 9.18 (ds, 1H), 7.16 (d, J = 8.2 Hz, 2H), 7.11 (d, J = 8.2 Hz, 2H), 5.06 (bs, 1H), 4.50–4.34 (m, 1H), 4.21 (d, J = 13.0 Hz, 1H), 4.02–3.82 (m, 1H), 3.04–2.87 (m, 1H), 2.29 (s, 3H), 2.41–2.10 (m, 2H), 1.19, 1.13 (2d, J = 6.4 Hz, 3H), 1.03, 1.02 (2s, 9H). ^{13}C NMR (125 MHz, DMSO-d_6) δ 181.8, 181.6, 170.4, 170.3, 138.3, 133.7, 128.5, 125.8, 51.3, 51.0, 49.2, 48.7, 45.1, 44.4, 43.6, 43.4, 42.9, 42.3, 40.7, 31.0, 30.9, 29.7, 26.8, 20.5, 15.1, 14.8. HRMS (*m/z*): calcd for $C_{19}H_{29}N_3OSNa$ 370.1924 $[M+Na]^+$; found 370.1920. Anal. Calcd $C_{19}H_{29}N_3OS$: C, 65.67; H, 8.41; N, 12.09. Found: C, 65.38; H, 8.25; N, 11.99.

1-[{3,5-Bis(trifluoromethyl)phenyl}aminothiocarbonyl]-4-(3,3-dimethylbutanoyl)-2-methyl piperazine (64). The product was obtained as a solid and purified by column chromatography using hexane-ethyl acetate (2:1) as eluent (239 mg, 68% yield), mp 87–90 ºC. MS (FAB): *m/z* 492 (100%) $[M+Na]^+$. ^{1}H NMR (500 MHz, DMSO-d_6) δ 9.71 (s, 1H), 8.10 (br s, 2H), 7.77 (br s, 1H), 5.12 (br s, 1H), 4.59–4.42 (m, 1H), 4.26 (d, J = 13.3 Hz, 1H), 4.08–3.87 (m, 1H), 3.07–2.92 (m, 1H), 2.45–2.11 (m, 2H), 1.24, 1.18 (2d, J = 6.4 Hz, 3H), 1.04, 1.03 (2s, 9H). ^{13}C NMR (125 MHz, DMSO-d_6) δ 181.0, 180.8, 170.4, 170.3, 143.1, 130.1, 129.9, 129.5, 129.3, 124.8, 124.4, 122.2, 116.7, 51.8, 51.6, 49.1, 45.0, 44.4, 43.6, 43.4, 43.2, 40.6, 31.0, 30.9, 29.7, 15.2, 14.8. HRMS (*m/z*): calcd for $C_{20}H_{25}F_6N_3OSNa$ 492.1515 $[M+Na]^+$; found 492.1500. Anal. Calcd $C_{20}H_{25}F_6N_3OS$: C, 51.17; H, 5.37; N, 8.95. Found: C, 51.10; H, 5.17; N, 8.83.

4-(2-Cyclohexylacetyl)-2-methyl-1-[(4-nitrophenyl)aminothiocarbonyl]piperazine (65). The product was obtained as a solid and purified by column chromatography using hexane-ethyl acetate (2:3) as eluent (230 mg, 76% yield), mp 87–90 ºC. MS (FAB): *m/z* 427 (100%) $[M+Na]^+$. ^{1}H NMR (500 MHz, DMSO-d_6) δ 9.77 (s, 1H), 8.18 (d, J = 9.1 Hz, 2H), 7.61 (d, J = 9.1 Hz, 2H), 5.12 (br s,

1H), 4.46–4.34 (m, 1H), 4.30–4.20 (m, 1H), 4.08–3.81 (m, 1H), 3.03–2.85 (m, 1H), 2.37–2.14 (m, 2H), 1.79–1.58 (m, 6H), 1.31–0.90 (m, 9H). ^{13}C NMR (125 MHz, DMSO-d_6) δ 181.2, 181.1, 170.7, 147.8, 142.2, 123.9, 122.9, 59.7, 51.9, 51.8, 48.5, 44.5, 44.4, 43.7, 43.1, 34.4, 34.3, 32.6, 32.5, 25.9, 25.7, 15.1, 14.6. HRMS (*m/z*): calcd for $C_{20}H_{28}N_4O_3SNa$ 427.1774 $[M+Na]^+$; found 427.1768. Anal. Calcd $C_{20}H_{28}N_4O_3S$: C, 59.38; H, 6.98; N, 13.85. Found: C, 59.53; H, 7.09; N, 13.67.

1-[(4-Chlorophenyl)aminothiocarbonyl]-4-(2-cyclohexylacetyl)-2-methylpiperazine (66). The product was obtained as a solid and purified by column chromatography using hexane-ethyl acetate (3:2) as eluent (221 mg, 75% yield), mp 77–80 ºC. MS (FAB): *m/z* 416 (100%) $[M+Na]^+$. ^{1}H NMR (500 MHz, DMSO-d_6) δ 9.32 (s, 1H), 7.38–7.31 (m, 4H), 5.09 (br s, 1H), 4.50–4.36 (m, 1H), 4.25–4.16 (m, 1H), 3.95–3.78 (m, 1H), 3.05–2.85 (m, 1H), 2.36–2.15 (m, 2H), 1.81–1.56 (m, 6H), 1.30–0.88 (m, 9H). ^{13}C NMR (125 MHz, DMSO-d_6) δ 181.7, 181.5, 170.7, 140.0, 128.4, 127.8, 127.1, 51.4, 51.2, 44.5, 44.4, 43.1, 42.4, 40.7, 34.4, 34.3, 32.6, 32.5, 25.8, 25.7, 15.1, 14.7. HRMS (*m/z*): calcd for $C_{20}H_{28}ClN_3OSNa$ 416.1534 $[M+Na]^+$; found 416.1527. Anal. Calcd $C_{20}H_{28}ClN_3OS$: C, 60.97; H, 7.16; N, 10.67. Found: C, 60.66; H, 6.97; N, 10.28.

1-[(4-Cyanophenyl)aminothiocarbonyl]-4-(2-cyclohexylacetyl)-2-methylpiperazine (67). The product was obtained as a solid and purified by column chromatography using hexane-ethyl acetate (1:1) as eluent (210 mg, 73% yield), mp 84–87 ºC. MS (FAB): *m/z* 407 (100%) $[M+Na]^+$. ^{1}H NMR (500 MHz, DMSO-d_6) δ 9.59 (s, 1H), 7.74 (d, J = 8.4 Hz, 2H), 7.55 (d, J = 8.4 Hz, 2H), 5.11 (br s, 1H), 4.47–4.33 (m, 1H), 4.29–4.18 (m, 1H), 3.98–3.79 (m, 1H), 3.04–2.83 (m, 1H), 2.38–2.15 (m, 2H), 1.82–1.57 (m, 6H), 1.32–0.90 (m, 9H). ^{13}C NMR (125 MHz, DMSO-d_6) δ 181.3, 181.2, 170.7, 145.6, 132.2, 119.1, 105.2, 51.7, 51.6, 48.5, 44.5, 44.4, 43.5, 42.9, 40.7, 34.4, 34.3, 32.6, 32.5, 25.9, 25.7, 15.1, 14.6. HRMS (*m/z*): calcd for $C_{21}H_{28}N_4OSNa$ 407.1876 $[M+Na]^+$; found 407.1866. Anal. Calcd $C_{21}H_{28}N_4OS$: C, 65.59; H, 7.34; N, 14.57. Found: C, 65.52; H, 7.09; N, 14.15.

4-(2-Cyclohexylacetyl)-1-[(4-fluorophenyl)aminothiocarbonyl]-2-methylpiperazine (68). The product was obtained as a solid and purified by column chromatography using hexane-ethyl acetate (1:1) as eluent (218 mg, 77% yield), mp 87–90 ºC. MS (FAB): *m/z* 400 (100%) $[M+Na]^+$. ^{1}H NMR (500 MHz, DMSO-d_6) δ 9.23 (s, 1H), 7.33–7.26 (m, 2H), 7.18–7.10 (m, 2H), 5.06 (br s, 1H), 4.52–4.37 (m, 1H), 4.25–4.13 (m, 1H), 3.97–3.75 (m, 1H), 3.06–2.85 (m, 1H), 2.40–2.11 (m, 2H), 1.83–1.53 (m, 6H), 1.33–0.89 (m, 9H). ^{13}C NMR (125 MHz, DMSO-d_6) δ 181.9, 181.8, 170.7, 160.3, 158.3, 137.2, 128.0, 127.9, 114.7, 114.4, 51.3, 51.1, 48.5, 44.5, 44.4, 42.9, 42.2, 40.7, 34.4, 34.3, 32.7, 32.6, 32.5, 25.9, 25.7, 15.1, 14.7. HRMS (*m/z*): calcd for $C_{20}H_{28}FN_3OSNa$ 400.1829 $[M+Na]^+$;

found 400.1826. Anal. Calcd $C_{20}H_{28}FN_3OS$: C, 63.63; H, 7.48; N, 11.13. Found: C, 63.38; H, 7.17; N, 10.77.

4-(2-Cyclohexylacetyl)-2-methyl-1-[(4-trifluoromethylphenyl)aminothiocarbonyl] piperazine (69). The product was obtained as a solid and purified by column chromatography using hexane-ethyl acetate (1:1) as eluent (218 mg, 68% yield), mp 153–156 ºC. MS (FAB): *m/z* 450 (100%) $[M+Na]^+$. ^{1}H NMR (500 MHz, DMSO-d_6) δ 9.53 (s, 1H), 7.65 (d, *J* = 8.6 Hz, 2H), 7.55 (d, *J* = 8.4 Hz, 2H), 5.11 (br s, 1H), 4.50–4.35 (m, 1H), 4.28–4.17 (m, 1H), 3.99–3.78 (m, 1H), 3.05–2.84 (m, 1H), 2.39–2.14 (m, 2H), 1.81–1.56 (m, 6H), 1.34–0.89 (m, 9H). ^{13}C NMR (125 MHz, DMSO-d_6) δ 181.6, 181.5, 170.7, 144.9, 125.1, 125.0, 124.5, 124.0, 123.8, 123.5, 123.3, 51.6, 51.5, 48.5, 44.5, 44.4, 43.4 42.7, 40.7, 34.4, 34.3, 32.7, 32.6, 32.5, 25.9, 25.7, 15.1, 14.7. HRMS (*m/z*): calcd for $C_{21}H_{28}F_3N_3OSNa$ 450.1797 $[M+Na]^+$; found 450.1788. Anal. Calcd $C_{21}H_{28}F_3N_3OS$: C, 59.00; H, 6.60; N, 9.83. Found: C, 59.27; H, 6.35; N, 9.60.

4-(2-Cyclohexylacetyl)-1-[(4-methoxyphenyl)aminothiocarbonyl]-2-methylpiperazine (70). The product was obtained as a solid and purified by column chromatography using hexane-ethyl acetate (3:2) as eluent (204 mg, 70% yield), mp 65–68 ºC. MS (FAB): *m/z* 412 (100%) $[M+Na]^+$. ^{1}H NMR (500 MHz, DMSO-d_6) δ 9.14 (s, 1H), 7.17 (d, *J* = 8.6 Hz, 2H), 6.88 (d, *J* = 8.6 Hz, 2H), 5.16–4.97 (m, 1H), 4.57–4.36 (m, 1H), 4.29–4.14 (m, 1H), 3.95–3.78 (m, 1H), 3.75 (s, 3H), 3.07–2.83 (m, 1H), 2.37–2.17 (m, 2H), 1.81–1.56 (m, 6H), 1.32–0.89 (m, 9H). ^{13}C NMR (125 MHz, DMSO-d_6) δ 181.9, 181.8, 170.6, 156.6, 133.8, 127.7, 113.2, 55.2, 51.1, 50.9, 48.5, 44.5, 44.4, 42.8, 42.2, 40.7, 34.4, 34.3, 32.7, 32.6, 32.5, 25.8, 25.7, 15.1, 14.7. HRMS (*m/z*): calcd for $C_{21}H_{31}N_3O_2SNa$ 412.2029 $[M+Na]^+$; found 412.2025. Anal. Calcd $C_{21}H_{31}N_3O_2S$: C, 64.75; H, 8.02; N, 10.79. Found: C, 64.65; H, 7.91; N, 10.61.

4-(2-Cyclohexylacetyl)-2-methyl-1-[(4-methylphenyl)aminothiocarbonyl]piperazine (71). The product was obtained as a solid and purified by column chromatography using hexane-ethyl acetate (3:2) as eluent (185 mg, 66% yield), mp 72–75 ºC. MS (FAB): *m/z* 396 (100%) $[M+Na]^+$. ^{1}H NMR (500 MHz, DMSO-d_6) δ 9.19 (s, 1H), 7.19–7.08 (m, 4H), 5.18–4.97 (m, 1H), 4.55–4.33 (m, 1H), 4.28–4.09 (m, 1H), 3.98–3.72 (m, 1H), 3.06–2.82 (m, 1H), 2.30 (s, 3H), 2.26–2.14 (m, 2H), 1.82–1.54 (m, 6H), 1.34–0.82 (m, 9H). ^{13}C NMR (125 MHz, DMSO-d_6) δ 181.9, 181.7, 170.7, 138.3, 133.7, 128.5, 125.8, 51.2, 51.1, 48.6, 44.5, 44.4, 42.9, 42.3, 40.8, 34.4, 34.3, 32.7, 32.6, 32.5, 25.8, 25.7, 20.5, 15.1, 14.7. HRMS (*m/z*): calcd for $C_{21}H_{31}N_3OSNa$ 396.2080 $[M+Na]^+$; found 396.2075. Anal. Calcd $C_{21}H_{31}N_3OS$: C, 67.52; H, 8.36; N, 11.25. Found: C, 67.24; H, 8.16; N, 10.95.

1-[{3,5-Bis(trifluoromethyl)phenyl}aminothiocarbonyl]-4-(2-cyclohexylacetyl)-2-methyl piperazine (72). The product was obtained as a solid and purified by column chromatography using hexane-ethyl acetate (2:1) as eluent (290 mg, 78% yield), mp 156–159 ºC. MS (FAB): *m/z* 518 (90%) $[M+Na]^+$. ^{1}H NMR (500 MHz, DMSO-d_6) δ 9.71 (s, 1H), 8.09 (s, 2H), 7.77 (s, 1H), 5.12 (br s, 1H), 4.56–4.39 (m, 1H), 4.31–4.15 (m, 1H), 4.01–3.78 (m, 1H), 3.10–2.87 (m, 1H), 2.39–2.17 (m, 2H), 1.82–1.56 (m, 6H), 1.27–0.91 (m, 9H). ^{13}C NMR (125 MHz, DMSO-d_6) δ 181.0, 180.9, 170.7, 143.1, 130.1, 129.8, 129.5, 129.3, 126.5, 124.7 124.4, 122.2. 120.0, 116.7, 51.7, 51.6, 48.4, 44.4, 44.3, 43.3, 42.7, 40.7, 34.4, 34.3, 32.7, 32.6, 32.5, 25.9, 25.7, 15.1, 14.7. HRMS (*m/z*): calcd for $C_{22}H_{27}F_6N_3OSNa$ 518.1671 $[M+Na]^+$; found 518.1654. Anal. Calcd $C_{22}H_{27}F_6N_3OS$: C, 53.32; H, 5.49; N, 8.48. Found: C, 53.61; H, 5.34; N, 8.40.

2-Methyl-1-[(4-nitrophenyl)aminothiocarbonyl]-4-(2-phenylacetyl)piperazine (73). The product was obtained as a solid and purified by column chromatography using hexane-ethyl acetate (2:3) as eluent (170 mg, 57% yield), mp 81–84 ºC. MS (FAB): *m/z* 421 (100%) $[M+Na]^+$. ^{1}H NMR (500 MHz, DMSO-d_6) δ 9.76, 9.74 (2s, 1H), 8.23–8.14 (m, 2H), 7.66–7.56 (m, 2H), 7.40–7.20 (m, 5H), 5.13 (br s, 1H), 4.47–4.32 (m, 1H), 4.29–4.18 (m, 1H), 4.08–3.91 (m, 1H), 3.89–3.70 (m, 2H), 3.26–3.14 (m, 1H), 3.08–2.86 (m, 1H), 1.15–1.09 (m, 3H). ^{13}C NMR (125 MHz, DMSO-d_6) δ 181.2, 181.1, 169.7, 147.8, 142.2, 135.7, 135.6, 129.1, 128.9, 128.4, 128.3, 126.4, 123.9, 122.9, 51.9, 51.8, 48.7, 44.7, 43.4, 42.9, 40.9, 15.0, 14.4. HRMS (*m/z*): calcd for $C_{20}H_{22}N_4O_3SNa$ 421.1305 $[M+Na]^+$; found 421.1298. Anal. Calcd $C_{20}H_{22}N_4O_3S$: C, 60.28; H, 5.56; N, 14.06. Found: C, 59.99; H, 5.70; N, 13.82.

1-[(4-Chlorophenyl)aminothiocarbonyl]-2-methyl-4-(2-phenylacetyl)piperazine (74). The product was obtained as a solid and purified by column chromatography using hexane-ethyl acetate (2:3) as eluent (177mg, 61% yield), mp 168–171 ºC. MS (FAB): *m/z* 410 (100%) $[M+Na]^+$. ^{1}H NMR (500 MHz, DMSO-d_6) δ 9.31, 9.30 (2s, 1H), 7.43–7.17 (m, 9H), 5.09 (br s, 1H), 4.49–4.33 (m, 1H), 4.27–4.15 (m, 1H), 4.04–3.86 (m, 1H), 3.84–3.71 (m, 2H), 3.28–3.12 (m, 1H), 3.07–2.88 (m, 1H), 1.09 (d, J = 6.9 Hz. 3H). ^{13}C NMR (125 MHz, DMSO-d_6) δ 181.2, 181.1, 169.7, 169.6, 140.0, 135.8, 135.6, 129.1, 128.9, 128.4, 128.3, 128.2, 127.8, 127.1, 126.4, 51.3, 48.7, 44.7, 42.8, 42.3, 40.9, 15.0, 14.5. HRMS (*m/z*): calcd for $C_{20}H_{22}ClN_3OSNa$ 410.1064 $[M+Na]^+$; found 410.1059. Anal. Calcd $C_{20}H_{22}ClN_3OS$: C, 61.92; H, 5.72; N, 10.83. Found: C, 61.53; H, 5.69; N, 10.60.

1-[(4-Cyanophenyl)aminothiocarbonyl]-2-methyl-4-(2-phenylacetyl)piperazine (75). The product was obtained as a solid and purified by column chromatography using hexane-ethyl acetate (1:2) as eluent (190 mg, 67% yield), mp 79–82 ºC. MS (FAB): *m/z* 401 (100%) $[M+Na]^+$. ^{1}H NMR

(500 MHz, DMSO-d_6) δ 9.59, 9.57 (2s, 1H), 7.79–7.72 (m, 2H), 7.61–7.53 (m, 2H), 7.40–7.24 (m, 5H), 5.14 (br s, 1H), 4.47–4.33 (m, 1H), 4.31–4.22 (m, 1H), 4.09–3.71 (m, 4H), 3.32–3.15 (m, 1H), 3.08–2.89 (m, 1H), 1.12 (d, J = 6.6 Hz. 3H). ^{13}C NMR (125 MHz, DMSO-d_6) δ 181.3, 181.2, 169.7, 169.6, 145.6, 135.7, 135.6, 132.2, 129.1, 128.9, 128.4, 128.3, 126.5, 126.4, 123.9, 119.1, 105.2, 51.7, 51.6, 48.7, 44.7, 43.3, 42.8, 40.9, 15.0, 14.5. HRMS (*m/z*): calcd for $C_{21}H_{22}N_4OSNa$ 401.1407 $[M+Na]^+$; found 401.1402. Anal. Calcd $C_{21}H_{22}N_4OS$: C, 66.64; H, 5.86; N, 14.80. Found: C, 66.53; H, 5.88; N, 14.65.

1-[(4-Fluorophenyl)aminothiocarbonyl]-2-methyl-4-(2-phenylacetyl)piperazine (76). The product was obtained as a solid and purified by column chromatography using hexane-ethyl acetate (2:3) as eluent (156 mg, 56% yield), mp 132–136 ºC. MS (FAB): *m/z* 394 (100%) $[M+Na]^+$. ^{1}H NMR (500 MHz, DMSO-d_6) δ 9.25, 9.24 (2s, 1H), 7.37–7.10 (m, 9H), 5.07 (br s, 1H), 4.49–4.37 (m, 1H), 4.26–4.16 (m, 1H), 4.04–3.69 (m, 3H), 3.30–3.10 (m, 1H), 3.07–2.89 (m, 1H), 1.09 (d, J = 6.6 Hz. 3H). ^{13}C NMR (125 MHz, DMSO-d_6) δ 181.9, 181.8, 169.7, 169.6, 160.2, 158.3, 137.3, 137.2, 135.8, 135.7, 129.1, 128.9, 128.3, 128.2, 127.9, 127.8, 126.4, 126.3, 114.7, 114.5, 51.1, 48.7, 44.7, 42.7, 42.2, 40.9, 15.0, 14.5. HRMS (*m/z*): calcd for $C_{20}H_{22}FN_3OSNa$ 394.1360 $[M+Na]^+$; found 394.1355. Anal. Calcd $C_{20}H_{22}FN_3OS$: C, 64.67; H, 5.97; N, 11.31. Found: C, 64.45; H, 5.77; N, 10.95.

2-Methyl-4-(2-phenylacetyl)-1-[(4-trifluoromethylphenyl)aminothiocarbonyl]piperazine (77). The product was obtained as a solid and purified by column chromatography using hexane-ethyl acetate (2:3) as eluent (221 mg, 70% yield), mp 161–164 ºC. MS (FAB): *m/z* 444 (100%) $[M+Na]^+$. ^{1}H NMR (500 MHz, DMSO-d_6) δ 9.52, 9.51 (2s, 1H), 7.68-7.61 (m, 2H), 7.59–7.51 (m, 2H), 7.39–7.22 (m, 5H), 5.12 (br s, 1H), 4.47–4.33 (m, 1H), 4.29–4.18 (m, 1H), 4.06–3.90 (m, 1H), 3.89–3.69 (m, 2H), 3.28–3.13 (m, 1H), 3.06–2.89 (m, 1H), 1.11 (d, J = 6.4 Hz. 3H). ^{13}C NMR (125 MHz, DMSO-d_6) δ 181.6, 181.5, 169.7, 169.6, 144.9, 135.8, 135.7, 129.1, 128.9, 128.4, 128.3, 126.4, 125.1, 125.0, 124.5, 51.5, 48.7, 44.7, 43.1, 42.7, 42.2, 40.9, 26.82, 15.0, 14.5. HRMS (*m/z*): calcd for $C_{21}H_{22}F_3N_3OSNa$ 444.1328 $[M+Na]^+$; found 444.1316. Anal. Calcd $C_{21}H_{22}F_3N_3OS$: C, 59.84; H, 5.26; N, 9.97. Found: C, 59.56; H, 5.46; N, 9.68.

1-[(4-Methoxyphenyl)aminothiocarbonyl]-2-methyl-4-(2-phenylacetyl)piperazine (78). The product was obtained as a solid and purified by column chromatography using hexane-ethyl acetate (2:3) as eluent (158 mg, 55% yield), mp 70–73 ºC. MS (FAB): *m/z* 406 (100%) $[M+Na]^+$. ^{1}H NMR (500 MHz, DMSO-d_6) δ 9.14, 9.13 (2s, 1H), 7.38–7.22 (m, 5H), 7.19–7.13 (m, 2H), 6.88 (d, J = 8.0 Hz, 2H), 5.06 (br s, 1H), 4.48–4.36 (m, 1H), 4.26–4.13 (m, 1H), 4.02–3.78 (m, 2H), 3.76 (s, 3H),

3.30–3.09 (m, 2H), 3.06–2.89 (m, 1H), 1.08 (d, *J* = 6.6 Hz. 3H). ^{13}C NMR (125 MHz, DMSO-d_6) δ 181.9, 181.8, 169.7, 169.6, 156.6, 135.8, 135.7, 133.8, 129.1, 128.9, 128.3, 128.2, 127.6, 126.4, 113.2, 55.2 50.9, 48.7, 44.7, 42.6, 42.0, 40.7, 15.0, 14.5. HRMS (*m/z*): calcd for $C_{21}H_{25}N_3O_2SNa$ 406.1560 $[M+Na]^+$; found 406.1554. Anal. Calcd $C_{21}H_{25}N_3O_2S$: C, 65.77; H, 6.57; N, 10.96. Found: C, 65.52; H, 6.23; N, 10.76.

2-Methyl-1-[(4-methylphenyl)aminothiocarbonyl]-4-(2-phenylacetyl)piperazine (79). The product was obtained as a solid and purified by column chromatography using hexane-ethyl acetate (1:1) as eluent (171mg, 62% yield), mp 66–70 ºC. MS (FAB): *m/z* 390 (100%) $[M+Na]^+$. ^{1}H NMR (500 MHz, DMSO-d_6) δ 9.18, 9.17 (2s, 1H), 7.39–7.22 (m, 5H), 7.19–7.08 (m, 4H), 5.08 (br s, 1H), 4.45–4.33 (m, 1H), 4.25–4.15 (m, 1H), 4.04–3.85 (m 1H), 3.83–3.68 (m, 2H), 3.30–3.07 (m, 2H), 3.05–2.87 (m, 1H), 2.29 (s, 3H), 1.08 (d, *J* = 6.6 Hz. 3H). ^{13}C NMR (125 MHz, DMSO-d_6) δ 181.8, 181.7, 169.7, 169.6, 138.3, 135.8, 135.7, 133.7, 129.1, 128.9, 128.4, 128.3, 128.2, 126.4, 125.7, 51.0, 48.7, 44.7, 42.7, 42.2, 40.9, 20.5, 15.0, 14.5. HRMS (*m/z*): calcd for $C_{21}H_{25}N_3OSNa$ 390.1611 $[M+Na]^+$; found 390.1605. Anal. Calcd $C_{21}H_{25}N_3OS$: C, 68.63; H, 6.86; N, 11.43. Found: C, 68.33; H, 6.69; N, 11.33.

1-[{3,5-Bis(trifluoromethyl)phenyl}aminothiocarbonyl]-2-methyl-4-(2-phenylacetyl)piperazine (80). The product was obtained as a solid and purified by column chromatography using hexane-ethyl acetate (3:2) as eluent (238 mg, 65% yield), mp 178–180 ºC. MS (FAB): *m/z* 512 (100%) $[M+Na]^+$. ^{1}H NMR (500 MHz, DMSO-d_6) δ 9.72, 9.69 (2s, 1H), 8.09, 8.07 (2s, 2H), 7.79 (s, 1H), 7.37–7.24 (m, 5H), 5.12 (br s, 1H), 4.52–4.38 (m, 1H), 4.24 (t, *J* = 12.5 Hz, 1H), 4.07–3.91 (m, 1H), 3.89–3.72 (m, 2H), 3.50–3.43 (m, 1H), 3.29–3.17 (m, 1H), 3.06–2.94 (m, 1H), 1.13, 1.12 (2d, *J* = 6.5 Hz. 3H). ^{13}C NMR (125 MHz, DMSO-d_6) δ 180.9, 180.8, 169.8, 169.7, 143.0, 135.7, 135.6, 130.0, 129.8, 129.5, 129.3, 129.1, 128.9, 128.4, 128.3, 126.5, 126.4, 124.8, 124.4, 122.2, 116.8, 51.6, 48.6, 44.7, 43.0, 42.6, 40.9, 15.1, 14.6. HRMS (*m/z*): calcd for $C_{22}H_{21}F_6N_3OSNa$ 512.1202 $[M+Na]^+$; found 512.1188. Anal. Calcd $C_{22}H_{21}F_6N_3OS$: C, 53.98; H, 4.32; N, 8.58. Found: C, 53.90; H, 4.29; N, 8.67.

4-(Benzofuran-2-carbonyl)-2-methyl-1-[(4-nitrophenyl)aminothiocarbonyl]piperazine (81). The product was obtained as a solid and purified by column chromatography using hexane-ethyl acetate (1:1) as eluent (292 mg, 92% yield), mp 189–191 ºC. ^{1}H NMR (500 MHz, DMSO-d_6) δ 9.83 (s, 1H), 8.19 (d, *J* = 9.2 Hz, 2H), 7.79 (d, *J* = 7.7 Hz, 1H), 7.70 (d, *J* = 8.2 Hz, 1H), 7.64 (d, *J* = 9.1 Hz, 2H), 7.51–7.47 (m, 2H), 7.37 (t, *J* = 7.5 Hz, 1H), 5.23 (br s, 1H), 4.55–4.46 (m, 1H), 4.40–4.33 (m, 1H), 4.31–4.25 (m, 1H), 3.61–3.53 (m, 2H), 1.29 (t, *J* = 6.7 Hz, 3H). ^{13}C RMN (125 MHz, DMSO-

d_6) δ 181.3, 159.7, 154.0, 148.0, 147.7, 142.3, 126.7, 123.9, 123.7, 122.9, 122.5, 111.8, 111.4, 51.9, 15.0 HRMS (*m/z*): calcd for $C_{21}H_{20}N_4O_4SNa$ 447.1077 $[M+Na]^+$; found 447.1094. Anal. Calcd $C_{21}H_{20}N_4O_4S$: C, 59.42; H, 4.75; N, 13.20. Found: C, 59.50; H, 4.92; N, 13.12.

4-(Benzofuran-2-carbonyl)-1-[(4-cyanophenyl)aminothiocarbonyl]-2-methylpiperazine (82). The product was obtained as a solid and purified by column chromatography using hexane-ethyl acetate (1:1) as eluent (218 mg, 72% yield), mp 174–175 ºC. ^{1}H NMR (500 MHz, DMSO-d_6) δ 9.66 (s, 1H), 7.79 (d, *J* = 7.7 Hz, 1H), 7.75 (d, *J* = 8.3 Hz, 2H), 7.70 (d, *J* = 8.2 Hz, 1H), 7.59 (d, *J* = 8.4 Hz, 2H), 7.52–7.46 (m, 2H), 7.37 (t, *J* = 7.4 Hz, 1H), 5.23 (br s, 1H), 4.55–4.45 (m, 1H), 4.40–4.32 (m, 1H), 4.30–4.23 (m, 1H), 3.60–3.49 (m, 2H), 1.27 (t, *J* = 6.4 Hz, 3H). ^{13}C RMN (125 MHz, DMSO-d_6) δ 181.3, 159.7, 154.0, 147.9, 145.6, 132.2, 126.7, 123.9, 123.7, 122.5, 119.1, 111.8, 111.4, 105.3, 51.7, 15.1. HRMS (*m/z*): calcd for $C_{22}H_{20}N_4O_2SNa$ 427.1199 $[M+Na]^+$; found 427.1193. Anal. Calcd $C_{22}H_{20}N_4O_2S$: C, 65.33; H, 4.98; N, 13.85. Found: C, 65.42; H, 5.15; N, 13.91.

4-(Benzofuran-2-carbonyl)-1-[(4-fluorophenyl)aminothiocarbonyl]-2-methylpiperazine (83). The product was obtained as a solid and purified by column chromatography using hexane-ethyl acetate (2:1) as eluent (253 mg, 85% yield), mp 171–173 ºC. ^{1}H NMR (500 MHz, DMSO-d_6) δ 9.32 (s, 1H), 7.79 (d, *J* = 7.7 Hz, 1H), 7.70 (d, *J* = 8.3 Hz, 1H), 7.52–7.46 (m, 2H), 7.37 (t, *J* = 7.4 Hz, 1H), 7.34–7.29 (m, 2H), 7.15 (t, *J* = 8.8 Hz, 2H), 5.18 (br s, 1H), 4.58–4.49 (m, 1H), 4.37–4.29 (m, 1H), 4.26–4.19 (m, 1H), 3.57–3.48 (m, 2H), 1.26 (t, *J* = 6.6 Hz, 3H). ^{13}C RMN (125 MHz, DMSO-d_6) δ 181.9, 160.2, 159.6, 158.4, 154.0, 148.0, 137.2, 128.0, 127.9, 126.7, 123.7, 122.5, 114.7, 114.5, 111.8, 111.4, 51.2, 15.1. HRMS (*m/z*): calcd for $C_{21}H_{20}FN_3O_2SNa$ 420.1152 $[M+Na]^+$; found 420.1148. Anal. Calcd $C_{21}H_{20}FN_3O_2S$: C, 63.46; H, 5.07; N, 10.57. Found: C, 63.78; H, 5.20; N, 10.44.

4-(Benzofuran-2-carbonyl)-2-methyl-1-[(4-trifluoromethyl)aminothiocarbonyl]piperazine (84). The product was obtained as a solid and purified by column chromatography using hexane-ethyl acetate (2:1) as eluent (282 mg, 84% yield), mp 186–188 ºC. ^{1}H NMR (500 MHz, DMSO-d_6) δ 9.59 (s, 1H), 7.79 (d, *J* = 7.7 Hz, 1H), 7.71 (d, *J* = 8.2 Hz, 1H), 7.67 (d, *J* = 8.5 Hz, 2H), 7.58 (d, *J* = 8.2Hz, 2H), 7.52–7.46 (m, 2H), 7.37 (t, *J* = 7.4 Hz, 1H), 5.22 (br s, 1H), 4.52 (m, 1H), 4.39–4.32 (m, 1H), 4.29–4.23 (m, 1H), 3.60–3.51 (m, 2H), 1.28 (t, *J* = 6.6 Hz, 3H). ^{13}C RMN (125 MHz, DMSO-d_6) δ 181.6, 159.7, 154.0, 148.0, 144.9, 126.7, 125.0, 123.7, 122.5, 111.8, 111.3, 51.6, 15.1. HRMS (*m/z*): calcd for $C_{22}H_{20}F_3N_3O_2SNa$ 470.1121 $[M+Na]^+$; found 470.1115. Anal. Calcd $C_{22}H_{20}F_3N_3O_2S$: C, 59.05; H, 4.51; N, 9.39. Found: C, 59.20; H, 4.58; N, 9.26.

4-*tert*-Butoxycarbonyl-1-[(4-fluorophenyl)aminothiocarbonyl]-2-phenylpiperazine (85). The product was obtained as a solid and purified by column chromatography using hexane-ethyl acetate (4:1) as eluent (218 mg, 70% yield), mp 145–147 ºC. MS (FAB): *m/z* 438 (100%) $[M+Na]^+$. ^{1}H NMR (500 MHz, DMSO-d_6) δ 9.45 (s, 1H), 7.46–7.37 (m, 2H), 7.35–7.28 (m, 5H), 7.15 (t, J = 8.6 Hz, 2H), 6.33 (s, 1H), 4.51 (d, J = 12.7 Hz, 2H), 3.85–3.60 (m, 1H), 3.47 (d, J = 12.7 Hz, 1H), 3.26–3.00 (m, 1H), 1.38 (s, 9H), 1.28 (d, J = 6.8 Hz, 3H). ^{13}C NMR (125 MHz, $CDCl_3$) δ 182.9, 160.3, 158.4, 137.2, 128.4, 128.0, 127.9, 127.0, 126.4, 114.7, 114.5, 79.2, 58.0, 45.5, 43.5, 42.1, 27.9. HRMS (*m/z*): calcd for $C_{22}H_{26}FN_3O_2SNa$ 438.1622 $[M+Na]^+$; found 438.1615. Anal. Calcd $C_{22}H_{26}FN_3O_2S$: C, 63.59; H, 6.31; N, 10.11; S, 7.72. Found: C, 63.42; H, 6.30; N, 9.89; S, 7.53.

1-[(3,5-Bis{trifluoromethyl}phenyl)aminothiocarbonyl]-4-(3,3-dimethylbutanoyl)-2-phenylpiperazine (86). The product was obtained as a solid and purified by column chromatography using dichloromethane-methanol (90:1) as eluent (383 mg, 96% yield). mp 82-84 MS (FAB): *m/z* 554 (100%) $[M+Na]^+$. ^{1}H NMR (500 MHz, DMSO-d_6) δ 9.95, 9.84 (2s, 1H), 8.14, 8.08 (2s, 2H), 7.84 (br s, 1H), 7.44–7.25 (m, 5H), 6.42, 6.24 (2s, 1H), 5.02–4.95 (m, 1H), 4.61–4.66 (m, 1H), 3.93–3.73 (m, 1H), 2.40–1.96 (m, 2H), 0.96, 0.88 (2s, 9H). ^{13}C NMR (125 MHz, DMSO-d_6) δ 181.9, 170.3, 170.0, 143.0, 142.9, 137.6, 128.5, 127.2, 126.3, 124.9, 124.4, 122.2,, 116.9, 59.4, 58.6, 48.0, 45.0, 44.3, 44.1, 43.7, 43.5, 42.1, 40.7, 31.0, 30.9, 29.5. HRMS (*m/z*): calcd. for $C_{25}H_{27}F_6N_3OSNa$ 554.1671 $[M+Na]^+$; found 554.1664. Anal. calcd for $C_{25}H_{27}F_6N_3OS$: C, 56.49; H, 5.12; N, 7.91. Found: C, 56.14; H, 4.89; N, 7.54.

1-[(4-Cyanophenyl)aminothiocarbonyl]-4-(2-cyclohexylacetyl)-2-phenylpiperazine (87). The product was obtained as a solid and purified by column chromatography using hexane-ethyl acetate (1:1) as eluent (217 mg, 65% yield), mp 179–181 ºC. MS (CI): *m/z* 447 (100%) $[M+H]^+$. ^{1}H NMR (500 MHz, DMSO-d_6) δ 9.79, 9.69 (2s, 1H), 7.78–7.71 (m, 2H), 7.63–7.55 (m, 2H), 7.41–7.25 (m, 5H), 6.36, 6.24 (2s, 1H), 4.89 (d, J = 13.5 Hz, 1H), 4.57–4.42 (m, 1H), 4.36 (dd, J = 2.8 Hz, J = 14.1 Hz, 1H), 3.89–3.75 (m, 2H), 3.46–3.39 (m, 1H), 2.23–2.02 (m, 2H), 1.67–1.46 (m, 5H), 1.22–0.74 (m, 6H). ^{13}C NMR (125 MHz, DMSO-d_6) δ 182.1, 170.7, 170.6, 145.6, 145.4, 138.6, 137.8, 132.2, 128.5, 128.4, 127.1, 126.3, 124.3, 119.1, 105.5, 59.2, 58.6, 47.5, 44.4, 42.3, 41.0, 34.6, 34.1, 32.6, 32.5, 32.3, 25.8, 25.7, 25.6. HRMS (*m/z*): calcd for $C_{26}H_{31}N_4OS$ 447.2213 $[M+H]^+$; found 447.2206. Anal. Calcd $C_{26}H_{30}N_4OS$: C, 69.92; H, 6.77; N, 12.55. Found: C, 69.92; H, 6.92; N, 12.22.

4-(2-Cyclohexylacetyl)-1-[(4-fluorophenyl)aminothiocarbonyl]-2-phenylpiperazine (88). The product was obtained as a solid and purified by column chromatography using hexane-ethyl acetate

(1:1) as eluent (198 mg, 60% yield), mp 158–160 ºC. MS (CI): *m/z* 440 (100%) $[M+H]^+$. ^{1}H NMR (500 MHz, DMSO-d_6) δ 9.45, 9.33 (2s, 1H), 7.42–7.24 (m, 7H), 7.18–7.11 (m, 2H), 6.33, 6.21 (2s, 1H), 4.85 (d, J = 12.8 Hz, 1H), 4.57–4.42 (m, 1H), 4.35 (dd, J = 3.1 Hz, J = 14.1 Hz, 1H), 3.91–3.76 (m, 2H), 3.46–3.39 (m, 1H), 2.24–2.00 (m, 2H), 1.67–1.42 (m, 5H), 1.27–0.73 (m, 6H). ^{13}C NMR (125 MHz, DMSO-d_6) δ 182.6, 170.7, 170.6, 160.3, 158.4, 138.9, 138.1, 137.2, 137.1, 128.4, 128.3, 128.1, 128.0, 127.9, 127.0, 126.3, 114.7, 114.5, 58.8, 58.3, 47.6, 44.3, 43.9, 43.8, 42.4, 40.8, 34.6, 34.1, 32.6, 32.5, 32.4, 25.8, 25.7, 25.6. HRMS (*m/z*): calcd for $C_{25}H_{31}FN_3OS$ 440.2166 $[M+H]^+$; found 440.2160. Anal. Calcd $C_{25}H_{30}FN_3OS$: C, 68.31; H, 6.88; N, 9.56. Found: C, 68.19; H, 6.96; N, 9.38.

4-(2-Cyclohexylacetyl)-1-[(4-methylphenyl)aminothiocarbonyl]-2-phenylpiperazine (89). The product was obtained as a solid and purified by column chromatography using hexane-ethyl acetate (2:1) as eluent (228 mg, 70% yield). MS (FAB): *m/z* 458 (100%) $[M+Na]^+$. ^{1}H NMR (500 MHz, DMSO-d_6) δ 9.37, 9.25 (2s, 1H), 7.43–7.25 (m, 7H), 7.22–7.08 (m, 2H), 6.33, 6.23 (2s, 1H), 4.84 (d, J = 13.0 Hz, 1H), 4.57–4.42 (m, 1H), 4.34 (dd, J = 2.9 Hz, J = 14.0 Hz, 1H), 3.82–3.72 (m, 2H), 3.44–3.37 (m, 1H), 2.30, 2.28 (2s, 3H), 2.23–2.00 (m, 2H), 1.68–1.43 (m, 5H), 1.22–0.73 (m, 6H). ^{13}C NMR (125 MHz, DMSO-d_6) δ 182.5, 170.7, 170.5, 138.3, 138.2, 128.5, 128.4, 128.3, 127.0, 126.3, 125.9, 58.7, 58.1, 47.6, 44.4, 43.9, 43.8, 42.4, 40.8, 34.6, 34.1, 32.6, 32.5, 32.4, 25.9, 25.8, 25.7, 25.6, 20.5. HRMS (*m/z*): calcd for $C_{26}H_{33}N_3OSNa$ 458.2237 $[M+Na]^+$; found 458.2229. Anal. Calcd $C_{26}H_{33}N_3OS$: C, 71.69; H, 7.64; N, 9.65. Found: C, 71.42; H, 7.71; N, 9.26

1-[(4-Nitrophenyl)aminothiocarbonyl]-2-phenyl-4-(2-phenylacetyl)piperazine (90). The product was obtained as a solid and purified by column chromatography using hexane-ethyl acetate (1:1.5) as eluent (224 mg, 65% yield), mp 168–170 ºC. MS (FAB): *m/z* 483 (100%) $[M+Na]^+$. ^{1}H NMR (500 MHz, DMSO-d_6) δ 9.94, 9.87 (2s, 1H), 8.21–8.16 (m, 2H), 7.70–7.62 (m, 2H), 7.42–7.00 (m, 10H), 6.42, 6.23 (2s, 1H), 4.97–4.91 (m, 1H), 4.55–4.38 (m, 1H), 3.96–3.56 (m, 5H), 3.23–3.12 (m, 1H). ^{13}C NMR (125 MHz, DMSO-d_6) δ 182.1, 169.7, 169.4, 147.7,147.5, 142.2, 138.4, 137.6, 135.4, 135.3, 129.2, 128.6, 128.5, 128.2, 127.2, 126.4, 126.3, 126.2, 123.8, 123.3, 59.3, 58.6, 44.7, 44.3, 44.2, 42.4, 41.3, 40.7. HRMS (*m/z*): calcd for $C_{25}H_{24}N_4O_3SNa$ 483.1461 $[M+Na]^+$; found 483.1454. Anal. Calcd $C_{25}H_{24}N_4O_3S$: C, 65.20; H, 5.25; N, 12.17. Found: C, 64.85; H, 5.50; N, 11.86.

1-[(4-Cyanophenyl)aminothiocarbonyl]-2-phenyl-4-(2-phenylacetyl)piperazine (91). The product was obtained as a solid and purified by column chromatography using hexane-ethyl acetate (1:1) as eluent (238 mg, 72% yield), mp 181–183 ºC. MS (FAB): *m/z* 463 (60%) $[M+Na]^+$. ^{1}H NMR

(500 MHz, DMSO-d_6) δ 9.76, 9.69 (2s, 1H), 7.76–7.72 (m, 2H), 7.61–7.55 (m, 2H), 7.41–7.13 (m, 8H), 7.06–7.00 (m, 2H), 6.40, 6.22 (2s, 1H), 4.92 (d, J = 13.6 Hz, 1H), 4.52–4.39 (m, 1H), 3.96–3.56 (m, 4H), 3.22–3.13 (m, 1H). ^{13}C NMR (125 MHz, DMSO-d_6) δ 182.1, 169.7, 169.4, 145.5, 145.2, 138.8, 135.4, 132.2, 129.2, 128.6, 128.5, 128.2, 127.2, 126.3, 126.2 124.7, 124.2, 119.0, 105.5, 59.2, 58.4, 44.7, 44.0, 42.4, 41.2. Anal. Calcd $C_{26}H_{24}N_4OS$: C, 70.88; H, 5.49; N, 12.72; S, 7.28. Found: C, 70.81; H, 5.52; N, 12.81.

1-[{3,5-Bis(trifluoromethyl)phenyl}aminothiocarbonyl]-2-phenyl-4-(2-phenylacetyl)piperazine (92). The product was obtained as a solid and purified by column chromatography using dichloromethane-methanol (90:1) as eluent (384mg, 93% yield). mp 88–90 ºC. MS (FAB): *m/z* 574 (100%) $[M+Na]^+$. ^{1}H NMR (500 MHz, DMSO-d_6) δ 9.88, (br s, 1H), 8.11, 8.08 (2s, 2H), 7.79 (s, 1H), 7.41–7.02 (m, 10H), 6.43, 6.23 (2s, 1H), 4.99–4.92 (m, 1H), 4.53–4.39 (m, 1H), 3.97–3.53 (m, 4H), 3.22–3.14 (m, 1H). ^{13}C NMR (125 MHz, DMSO-d_6) δ 181.9, 169.4, 135.6, 129.8, 129.6, 129.3, 128.6, 128.5, 128.2, 127.2, 126.3, 126.2, 124.8, 124.3, 58.5, 44.6, 43.8, 42.3. HRMS (*m/z*): calcd for $C_{27}H_{23}F_6N_3OSNa$ 574.1358 $[M+Na]^+$; found 574.1347. Anal. Calcd $C_{27}H_{23}F_6N_3OS$: C, 58.80; H, 4.20; N, 7.62. Found: C, 58.65; H, 3.96; N, 7.35.

4-(3,3-Dimethylbutanoil)-1-[(4-nitrophenyl)aminocarbonyl]-2-phenylpiperazine (93). The product was obtained as a solid and purified by column chromatography using dichloromethane-methanol (50:1) as eluent (286 mg, 90% yield), mp 101–103 ºC. ^{1}H NMR (500 MHz, DMSO-d_6) δ 9.40, 9.29 (2s, 1H), 8.24–8.15 (m, 2H), 7.79–7.61 (m, 2H), 7.37–7.25 (m, 5H), 5.58, 5.45 (2s, 1H), 4.33–3.47 (m, 3H), 3.25–3.05 (m, 2H), 2.31–2.09 (m, 2H), 1.06–0.97 (m 1H), 0.92–0.87 (2s, 9H). ^{13}C NMR (125 MHz, DMSO-d_6) δ 181.9, 181.8, 170.4, 170.2, 156.6, 133.8, 127.6, 113.2, 55.2, 51.2, 50.9, 49.2, 45.1, 44.4, 43.6, 43.4, 42.8, 42.2, 40.7, 29.7, 15.2, 14.8. HRMS (*m/z*): calcd for $C_{23}H_{28}N_4O_4Na$ 447.2003 $[M+Na]^+$; found 447.1999. Anal. Calcd $C_{23}H_{28}N_4O_4$: C, 65.08; H, 6.65; N, 13.20. Found: C, 64.86; H, 6.60; N, 12.90.

4-(3,3-Dimethylbutanoyl)-1-[(2-nitrophenyl)aminocarbonyl]-2-phenylpiperazine (94). The product was obtained as a solid and purified by column chromatography using dichloromethane-methanol (60:1) as eluent (280 mg, 88% yield), mp 93–96 ºC. ^{1}H NMR (500 MHz, DMSO-d_6) δ 9.44, 9.39 (2s, 1H), 7.99–7.63 (m, 3H), 7.43–7.20 (m, 6H), 5.46, 5.36 (2s, 1H), 4.30–3.52 (m, 3H), 3.28–3.10 (m, 2H), 2.29–2.09 (m, 2H), 1.31–1.00 (m 1H), 0.92–0.87 (2s, 9H). ^{13}C NMR (125 MHz, DMSO-d_6) δ 170.2, 170.0, 154.4, 140.0, 139.8, 139.2, 138.4, 134.6, 134.4, 134.3, 134.1, 128.5, 128.4, 127.2, 127.1, 126.5, 126.4, 125.0, 123.9, 123.5, 123.1, 122.9, 55.2, 54.1, 48.6, 45.5, 43.6, 43.4, 42.4,

41.2, 30.9, 29.5, 13.8. HRMS (*m/z*): calcd for $C_{23}H_{28}N_4O_4Na$ 447.2003 $[M+Na]^+$; found 447.1999. Anal. Calcd $C_{23}H_{28}N_4O_4$: C, 65.08; H, 6.65; N, 13.20. Found: C, 64.99; H, 6.57; N, 12.82

4-(2-Cyclohexylacetyl)-1-[(4-nitrophenyl)aminocarbonyl]-2-phenylpiperazine (95). The product was obtained as a solid and purified by column chromatography using dichloromethane-methanol (60:1) as eluent (280 mg, 83% yield), mp 159–161 ºC. ^{1}H NMR (500 MHz, DMSO-d_6) δ 9.40, 9.32 (ds, 1H), 8.24–8.14 (m, 2H), 7.78–7.71 (m, 2H), 7.37–7.25 (m, 5H), 5.55, 5.47 (2s, 1H), 4.86–4.83 (m, 1H), 4.28–3.46 (m, 3H), 3.29–3.10 (m, 2H), 2.24–1.94 (m, 2H), 1.62–1.44 (m, 6H), 1.19–0.99 (m, 3H), 0.92–0.71 (m, 2H). ^{13}C NMR (125 MHz, DMSO-d_6) δ 170.5, 170.4, 154.4, 154.2, 147.2, 147.1, 141.0, 139.7, 138.7, 128.5, 128.4, 127.0, 126.4, 126.3, 125.0, 124.7, 118.5, 54.5, 53.8, 48.0, 44.8, 42.8, 41.2, 34.6, 34.1, 32.5, 32.4, 25.8, 25.7, 25.6, 25.5. HRMS (*m/z*): calcd for $C_{25}H_{30}N_4O_4Na$ 473.2159 $[M+Na]^+$; found 473.2147. Anal. Calcd $C_{25}H_{30}N_4O_4$: C, 66.65; H, 6.71; N, 12.44. Found: C, 66.51; H, 6.79; N, 12.22.

4-(2-Cyclohexylacetyl)-1-[(2-nitrophenyl)aminocarbonyl]-2-phenylpiperazine (96) The product was obtained as a solid and purified by column chromatography using dichloromethane-methanol (70:1) as eluent (297 mg, 88% yield), mp 139–141 ºC. ^{1}H NMR (500 MHz, DMSO-d_6) δ 9.42, 9.38 (ds, 1H), 7.98–7.96 (m, 1H), 7.84–7.64 (m, 2H), 7.43–7.21 (m, 6H), 5.45, 5.36 (2s, 1H), 4.82–4.79 (m, 1H), 4.08–3.51 (m, 3H), 3.28–3.18 (m, 2H), 2.22–1.92 (m, 2H), 1.62–1.46 (m, 6H), 1.18–1.06 (m 3H), 0.91–0.73 (m, 2H). ^{13}C NMR (125 MHz, DMSO-d_6) δ 170.6, 170.5, 154.4, 140.6,140.0, 139.3, 138.5, 134.6, 134.4, 134.3, 134.1, 128.5, 128.3, 127.1, 127.0, 126.4, 126.3, 125.0, 123.8, 123.5, 123.1, 122.9, 55.0, 54.2, 48.1, 44.7, 42.7, 41.3, 34.5, 32.5, 32.4, 32.3, 25.8, 25.7, 25.6, 25.5. HRMS (*m/z*): calcd for $C_{25}H_{30}N_4O_4Na$ 473.2159 $[M+Na]^+$; found 473.2153. Anal. Calcd $C_{25}H_{30}N_4O_4$: C, 66.65; H, 6.71; N, 12.44. Found: C, 66.28; H, 6.66; N, 12.12.

1-[(4-Nitrophenyl)aminocarbonyl]-2-phenyl-4-(2-phenylacetyl)piperazine (97) The product was obtained as a solid and purified by column chromatography using dichloromethane-methanol (60:1) as eluent (326 mg, 98% yield), mp 98–100 ºC. ^{1}H NMR (500 MHz, DMSO-d_6) δ 9.34, 9.31 (ds, 1H), 8.24–8.15 (m, 2H), 7.77–7.72 (m, 2H), 7.36–7.03 (m, 10H), 5.57–5.44 (2s, 1H), 4.90–4.87 (m, 1H), 4.36–4.10 (m, 1H), 4.00–3.94 (m, 1H), 3.83–3.45 (m, 3H), 3.31–2.89 (m, 2H). ^{13}C NMR (125 MHz, DMSO-d_6) δ 169.6, 169.4, 154.3, 154.2, 147.2, 147.1, 141.0, 139.5, 135.5, 135.4, 129.1, 128.6, 128.5, 128.4, 128.2, 128.1, 127.0, 126.4, 126.2, 124.6, 118.5, 54.5, 53.6, 48.0, 45.0, 42.7, 41.6, 28.4, 26.8. HRMS (*m/z*): calcd for $C_{24}H_{24}N_4O_4Na$ 467.1690 $[M+Na]^+$; found 467.1677.

1-[(2-Nitrophenyl)aminocarbonyl]-2-phenyl-4-(2-phenylacetyl)piperazine (98). The product was obtained as a solid and purified by column chromatography using dichloromethane-methanol (70:1) as eluent (320 mg, 96% yield), mp 55–57 ºC. ^{1}H NMR (500 MHz, DMSO-d_6) δ 9.41 (s, 1H), 8.00–7.64 (m, 3H), 7.40–7.04 (m, 11H), 5.46–5.29 (2s, 1H), 4.87–4.84 (m, 1H), 4.29–4.09 (m, 1H), 3.96–3.81 (m, 1H), 3.76–3.49 (m, 3H), 3.33–3.30 (m, 1H), 3.02–2.97 (m, 1H). ^{13}C NMR (125 MHz, DMSO-d_6) δ 169.7, 169.4, 154.4, 147.2, 140.6, 139.7, 139.1, 138.4, 135.5, 135.4, 134.6, 134.4, 134.1, 129.1, 128.6, 128.5, 128.4, 128.2, 127.2, 127.1, 126.5, 126.3, 126.2, 125.1, 125.0, 123.9, 123.4, 123.1, 122.9, 55.2, 54.0, 48.0, 45.1, 42.9, 41.7, 28.4, 28.0, 26.8. HRMS (*m/z*): calcd for $C_{24}H_{24}N_4O_4Na$ 467.1690 $[M+Na]^+$; found 467.1678.

1-[(2-Chloro-5-trifluoromethylphenyl)aminocarbonyl]-2-phenyl-4-(2-phenylacetyl)piperazine (99). The product was obtained as a solid and purified by column chromatography using dichloromethane-methanol (70:1) as eluent (360 mg, 96% yield), mp 58–61 ºC. ^{1}H NMR (500 MHz, DMSO-d_6) δ 8.37 (s, 1H), 8.11–8.02 (m, 2H), 4.00–3.81 (m, 2H), 7.70–7.05 (m, 11H), 5.46, 5.30 (2s, 1H), 4.73–4.70 (m, 1H), 4.22–4.09 (m, 1H), 3.76–3.55 (m, 3H), 3.49–3.39 (m, 2H), 3.13-3.07 (m, 1H). ^{13}C NMR (125 MHz, DMSO-d_6) δ 169.6, 169.5, 154.5, 154.4, 139.3, 138.8, 137.5 137.2, 135.5, 135.4, 130.4, 130.3, 129.1, 128.7, 128.5, 128.2, 126.5, 126.4, 126.3, 126.2, 55.6, 54.4, 48.0, 45.0, 42.9, 41.9. HRMS (*m/z*): calcd for $C_{26}H_{23}N_3ClF_3O_2Na$ 524.1323 $[M+Na]^+$; found 524.1316.

4-(Benzofuran-2-carbonyl)-2,6-dimethyl-1-[(4-nitrophenyl)aminocarbonyl]piperazine (104). The product was obtained as a solid and purified by column chromatography using dichloromethane-methanol (50:1) as eluent (237 mg, 75% yield), mp 169–172 ºC. ^{1}H NMR (500 MHz, DMSO-d_6) δ 9.10 (s, 1H), 7.79 (d, J = 7.6 Hz, 1H), 7.70 (d, J = 8.4 Hz, 1H), 7.56–7.46 (m, 4H), 7.40–7.28 (m, 3H), 4.46–4.37 (m, 2H), 4.36–4.27 (m, 2H), 1.25 (d, J = 6.8 Hz, 6H). ^{13}C RMN (125 MHz, DMSO-d_6) δ 160.0, 154.0, 153.7, 148.1, 147.3, 141.0, 126.7, 124.6, 123.7, 122.5, 118.9, 111.8, 111.4, 46.3. HRMS (*m/z*): calcd for $C_{22}H_{22}N_4O_5Na$ 445.1482 $[M+Na]^+$; found 445.1476. Anal. Calcd $C_{22}H_{22}N_4O_5$: C, 62.55; H, 5.25; N, 13.26. Found: C, 62.68; H, 5.38; N, 13.20.

4-(Benzofuran-2-carbonyl)-1-[(4-chlorophenyl)aminocarbonyl]-2,6-dimethylpiperazine (105). The product was obtained as a solid and purified by column chromatography using hexane-ethyl acetate (3:1) as eluent (216 mg, 70% yield), mp 154–155 ºC. ^{1}H NMR (500 MHz, DMSO-d_6) δ 8.53 (s, 1H), 8.21–8.15 (m, 1H), 7.83–7.67 (m, 4H), 7.54–7.34 (m, 3H), 4.51–4.41 (m, 2H), 4.39–4.30 (m, 2H), 1.27 (d, J = 6.9 Hz, 6H). ^{13}C RMN (125 MHz, DMSO-d_6) δ 160.0, 154.1, 153.9, 148.2, 139.4, 128.1, 126.6, 125.6, 122.5, 121.8, 118.9, 111.3, 46.0, 26.8, 20.1. HRMS (*m/z*): calcd for

$C_{22}H_{22}ClN_3O_3Na$ 434.1242 $[M+Na]^+$; found 434.1234. Anal. Calcd $C_{22}H_{22}ClN_3O_3$: C, 64.15; H, 5.38; N, 10.20. Found: C, 64.48; H, 5.69; N, 9.86.

4-(Benzofuran-2-carbonyl)-1-[(4-cyanophenyl)aminocarbonyl]-2,6-dimethylpiperazine (106). The product was obtained as a solid and purified by column chromatography using hexane-ethyl acetate (1:1) as eluent (256 mg, 85% yield), mp 240–242 ºC. ^{1}H NMR (500 MHz, DMSO-d_6) δ 8.53 (s, 1H), 8.21–8.15 (m, 1H), 7.83–7.67 (m, 4H), 7.54–7.34 (m, 3H), 4.51–4.41 (m, 2H), 4.39–4.30 (m, 2H), 1.27 (d, J = 6.9 Hz, 6H). ^{13}C RMN (125 MHz, DMSO-d_6) δ 160.0, 154.1, 153.9, 148.2, 139.4, 128.1, 126.6, 125.6, 122.5, 121.8, 118.9, 111.3, 46.0, 26.8, 20.1. HRMS (*m/z*): calcd for $C_{23}H_{22}N_4O_3Na$ 425.1584 $[M+Na]^+$; found 425.1578. Anal. Calcd $C_{23}H_{22}N_4O_3$: C, 68.64; H, 5.51; N, 13.92. Found: C, 68.77; H, 5.26; N, 14.05.

4-(Benzofuran-2-carbonyl)-2,6-dimethyl-1-[(2-nitrophenyl)aminocarbonyl]piperazine (107). The product was obtained as a solid and purified by column chromatography using hexane-ethyl acetate (3:1) as eluent (269 mg, 85% yield), mp 128–130 ºC. ^{1}H NMR (500 MHz, DMSO-d_6) δ 9.36 (s, 1H), 7.99 (dd, J = 8.3 Hz, J = 1.4 Hz, 1H), 7.84–7.76 (m, 2H), 7.73–7.63 (m, 2H), 7.54–7.44 (m, 2H), 7.41–7.33 (m, 1H), 7.28–7.21 (m, 1H), 4.51–4.24 (m, 4H), 1.31 (d, J = 6.7 Hz, 6H). ^{13}C RMN (125 MHz, DMSO-d_6) δ 160.0, 154.0, 153.7, 148.2, 140.5, 134.7, 134.1, 126.6, 125.0, 123.8, 122.9, 122.5, 111.8, 111.4, 40.5, 19.9. HRMS (*m/z*): calcd for $C_{22}H_{22}N_4O_5Na$ 445.1482 $[M+Na]^+$; found 445.1474. Anal. Calcd $C_{22}H_{22}N_4O_5$: C, 62.55; H, 5.25; N, 13.26. Found: C, 62.23; H, 5.46; N, 12.96.

4-(Benzofuran-2-carbonyl)-2,6-dimethyl-1-[(4-methylphenyl)aminocarbonyl]piperazine (108). The product was obtained as a solid and purified by column using chromatography hexane-ethyl acetate (2:1) as eluent (185 mg, 63% yield), mp 217–220 ºC. ^{1}H NMR (500 MHz, DMSO-d_6) δ 8.30 (s, 1H), 7.79 (d, J = 7.6 Hz, 1H), 7.70 (d, J = 8.3 Hz, 1H), 7.51–7.45 (m, 2H), 7.40–7.31 (m, 3H), 7.11–7.04 (m, 2H), 4.44–4.36 (m, 2H), 4.34–4.26 (m, 2H), 2.25 (s, 3H), 1.24 (d, J = 6.7 Hz, 6H). ^{13}C RMN (125 MHz, DMSO-d_6) δ 160.0, 154.0, 153.9, 148.2, 137.7, 130.8, 129.1, 128.6, 126.6, 123.8, 123.7, 122.5, 120.6, 118.2, 111.8, 111.4, 45.9, 20.3, 20.1. HRMS (*m/z*): calcd for $C_{23}H_{25}N_3O_3Na$ 414.1788 $[M+Na]^+$; found 414.1782. Anal. Calcd $C_{23}H_{25}N_3O_3$: C, 70.57; H, 6.44; N, 10.73. Found: C, 70.28; H, 6.63; N, 10.76.

4-(Benzofuran-2-carbonyl)-1-[(2-chloro-5-trifluoromethylphenyl)aminocarbonyl]-2,6-dimethylpiperazine (109). The product was obtained as a solid and purified by column using chromatography hexane-ethyl acetate (4:1) as eluent (249 mg, 69% yield), mp 178–180 ºC. ^{1}H NMR (500 MHz, DMSO-d_6) δ 8.38 (s, 1H), 7.93 (d, J = 1.3 Hz, 1H), 7.79 (d, J = 7.8 Hz, 1H), 7.74 (d, J =

8.5 Hz, 1H), 7.71 (d, *J* = 8.5 Hz, 1H), 7.54–7.45 (m, 3H), 7.41–7.34 (m, 1H), 4.49–4.27 (m, 4H), 1.30 (d, *J* = 6.7 Hz, 6H). ^{13}C RMN (125 MHz, DMSO-d_6) δ 160.0, 154.0, 153.9, 148.2, 137.7, 132.1, 130.5, 129.1, 126.6, 123.8, 122.8, 122.7, 122.5, 121.8, 111.8, 111.4, 46.6, 19.9. HRMS (*m/z*): calcd for $C_{23}H_{21}ClF_3N_3O_3Na$ 502.1116 $[M+Na]^+$; found 502.1110. Anal. Calcd $C_{23}H_{21}ClF_3N_3O_3$: C, 57.57; H, 4.41; N, 8.76. Found: C, 57.54; H, 4.45; N, 8.76.

4-(Benzofuran-2-carbonyl)-1-[(4-chloro-3-trifluoromethylphenyl)aminocarbonyl]-2,6-dimethylpiperazine (110). The product was obtained as a solid and purified by column using chromatography hexane-ethyl acetate (2:1) as eluent (252 mg, 70% yield), mp 218–220 ºC. ^{1}H NMR (500 MHz, DMSO-d_6) δ 8.84 (s, 1H), 8.10 (d, *J* = 2.2 Hz, 1H), 7.86 (d, *J* = 8.8 Hz, *J* = 2.2 Hz, 1H), 7.79 (d, *J* = 7.8 Hz, 1H), 7.70 (d, *J* = 8.3 Hz, 1H), 7.60 (d, *J* = 8.8 Hz, 1H), 7.53–7.45 (m, 2H), 7.40–7.34 (m, 1H), 4.49–4.38 (m, 2H), 4.37–4.28 (m, 2H), 1.27 (d, *J* = 6.7 Hz, 6H). ^{13}C RMN (125 MHz, DMSO-d_6) δ 160.0, 154.0, 153.9, 148.2, 140.1, 131.5, 126.6, 124.5, 123.7, 122.5, 121.8, 118.8, 111.8, 111.3, 46.1, 20.1. HRMS (*m/z*): calcd for $C_{23}H_{21}ClF_3N_3O_3Na$ 502.1116 $[M+Na]^+$; found 502.1111. Anal. Calcd $C_{23}H_{21}ClF_3N_3O_3$: C, 57.57; H, 4.41; N, 8.76. Found: C, 57.59; H, 4.65; N, 8.54.

1-*tert*-Butoxycarbonyl-4-[(4-nitrophenyl)aminocarbonyl]piperazine (112). The product was obtained as a solid and purified by column using chromatography dichloromethane-methanol (100:1) as eluent (247 mg, 94% yield), mp 190–192 ºC. ^{1}H NMR (500 MHz, DMSO-d_6) δ 9.27 (s, 1H), 8.17 (d, *J* = 9.5 Hz, 2H), 7.37 (d, *J* = 9.5 Hz, 2H), 3.50–3.48 (m, 4H), 3.40–3.38 (m, 4H), 1.43 (m, 9H). ^{13}C RMN (125 MHz, DMSO-d_6) δ 154.0, 153.8, 147.3, 140.9, 124.7 118.3, 79.1, 43.6, 28.0. HRMS (*m/z*): calcd for $C_{16}H_{22}N_4O_5Na$ 373.1482 $[M+Na]^+$; found 373.1476. Anal. Calcd $C_{16}H_{22}N_4O_5$: C, 54.85; H, 6.33; N, 15.99. Found: C, 54.79; H, 6.21; N, 15.87.

1-*tert*-Butoxycarbonyl-4-[(2-nitrophenyl)aminocarbonyl]piperazine (113). The product was obtained as a solid and purified by column using chromatography dichloromethane-methanol (100:1) as eluent (234 mg, 89% yield), mp 91–94 ºC. ^{1}H NMR (500 MHz, DMSO-d_6) δ 9.34 (s, 1H), 7.96 (dd, *J* = 8.2 Hz, *J* = 1.2 Hz, 1H), 7.71–7.63 (m, 2H), 7.26–7.22 (m, 1H), 3.48–3.46 (m, 4H), 3.40–3.38 (m, 4H), 1.44 (m, 9H). ^{13}C RMN (125 MHz, DMSO-d_6) δ 154,2, 153,9, 140,6, 134,5, 134,0, 125,0, 123,8, 123,0. 79.2, 43.6, 28,0. HRMS (*m/z*): calcd for $C_{16}H_{22}N_4O_5Na$ 373.1482 $[M+Na]^+$; found 373.1476. Anal. Calcd $C_{16}H_{22}N_4O_5$: C, 54.85; H, 6.33; N, 15.99. Found: C, 55.11 H, 6.46; N, 15.94.

4-*tert*-Butoxycarbonyl-1-[(2-chloro-5-trifluoromethylphenyl)aminocarbonyl]piperazine (114). The product was obtained as a solid and purified by column using chromatography dichloromethane-

methanol (150:1) as eluent (285 mg, 92% yield), mp 153–155 ºC. ^{1}H NMR (500 MHz, DMSO-d_6) δ 8.45 (s, 1H), 7.96 (dd, J = 1.9 Hz, 1H), 7.71 (d, J = 8.1 Hz, 1H), 7.49 (dd, J = 1.9 Hz, J = 8.3 Hz, 1H), 3.48–3.46 (m, 4H), 3.41–3.39 (m, 4H), 1.44 (m, 9H). ^{13}C RMN (125 MHz, DMSO-d_6) δ 154.5, 153.9, 137.6, 131.3, 130.4, 122.3, 121.5 79.1, 43.6, 28.0. HRMS (*m/z*): calcd for $C_{17}H_{21}ClF_3N_3O_3Na$ 430.1116 $[M+Na]^+$; found 430.1110. Anal. Calcd $C_{17}H_{21}ClF_3N_3O_3$: C, 50.07; H, 5.19; N, 10.30. Found: C, 50.16, H, 5.06; N, 10.27.

*B) Synthesis of diurea derivatives from 2-phenyl piperazine or piperazine (**101** and **121**)*. To a solution of 2-phenyl piperazine or piperazine (1 mmol) in dry DCM (10 mL) was added the corresponding isocyanate (2 mmol). The reaction mixture was stirred at rt until TLC showed that all the starting material had reacted (12 hours) and then it was evaporated to dryness**.** The compound was purified by flash chromatography on silica gel using the appropriate eluent.

1,4-Bis[(2-chloro-5-trifluoromethylphenyl)aminocarbonyl]-2-phenylpiperazine (101). The product was obtained as a solid and purified by column using chromatography hexane-ethyl acetate (4:1) as eluent (408 mg, 90% yield), mp 134–137 ºC. ^{1}H NMR (500 MHz, DMSO-d_6) δ 8.35 (s, 1H), 8.27 (s, 2H), 8.06 (dd, J = 1.9 Hz, 1H), 7.84 (m, 1H), 7.70 (t, J = 7.5 Hz, 2H), 7.50–7.45 (m, 4H), 7.40 (t, J = 7.5 Hz, 2H) 7.30 (t, J = 7.2 Hz, 1H), 5.45 (t, J = 4.0 Hz, 1H), 4.36 (dd, J = 4.1 Hz, J = 13.9 Hz, 1H), 4.18–4.12 (m, 1H), 3.93–3.88 (m, 1H), 3.75 (dd, J = 4.4 Hz, J = 13.9 Hz, 1H), 3.54–3.40 (m, 2H). ^{13}C RMN (125 MHz, DMSO-d_6) δ 154.5, 154.4, 139.2, 137.4, 137.3, 131.3, 130.4, 128.6, 127.3, 126.6, 122.6, 122.2, 121.6, 121.3, 54.9, 45.4, 43.5. HRMS (*m/z*): calcd for $C_{26}H_{20}Cl_2F_6N_4O_2Na$ 627.0760 $[M+Na]^+$; found 627.0752. Anal. Calcd $C_{26}H_{20}Cl_2F_6N_4O_2$: C, 51.59; H, 3.33; N, 9.26. Found: C, 51.61, H, 3.56; N, 9.06.

1,4-Bis[(2-chloro-5-trifluoromethylphenyl)aminocarbonyl]piperazine (121). The product was obtained as a solid and purified by column using chromatography hexane-ethyl acetate (3:1) as eluent (388 mg, 98% yield), mp 249–250 ºC. ^{1}H NMR (500 MHz, DMSO-d_6) δ 8.49 (s, 2H), 7.98 (d, J = 1.6 Hz, 2H), 7.73 (d, J = 8.3 Hz, 2H), 7.50 (dd, J = 8.4 Hz, J = 1.7 Hz, 2H), 3.56–3.59 (m, 8H). ^{13}C RMN (125 MHz, DMSO-d_6) δ 154.6, 137.6, 131.4, 130.5, 128.3, 128.0, 127.8, 124.8, 122.6, 122.4, 121.7, 43.6. Anal. Calcd $C_{20}H_{16}Cl_2F_6N_4O_2$: C, 46.43; H, 3.34; N, 10.31 Found: C, 46.74, H, 3.33; N, 10.45.

-General Procedure 3. Deprotection reaction and synthesis of compounds 118 and 119. According with a reported procedure [117], CF_3COOH (10 mmol) was added to a solution of **112** and **113** (1 mmol) in DCM (20 mL) at 0 ºC and the reaction mixture was warmed and stirred at rt. The reaction was concentrated under vacuum, the residue was dissolved in DCM, washed with saturated $NaHCO_3$ and brine. The organic layer was dried over Na_2SO_4 and the solvent was removed under reduced pressure, to afford *N*-deprotected compounds (**115** and **116**) which were used in the next reaction without further purification. Compounds **115** and **116** (1 mmol) were dissolved in dry DCM (30 mL) and cooled to 0 ºC, then benzofurane-2-carbonyl chloride (1 mmol) and pyridine (2.5 mmol) were added. The reaction mixture was kept into an ice-water bath with stirring 6 hours and left at rt until TLC showed that all the starting material had reacted (12 hours). The reaction mixture was evaporated to dryness to obtain the corresponding acylderivatives. The compound was further purified by flash column chromatography on silica gel using the appropriate eluent.

1-(Benzofurane-2-carbonyl)-4-[(4-nitrophenyl)aminocarbonyl]piperazine (118). The product was obtained as a solid and purified by column using chromatography dichloromethane-methanol (80:1) (315 mg, 80% yield), mp 165–167 ºC. ^{1}H NMR (500 MHz, DMSO-d_6) δ 9.34 (s, 1H), 8.19–8.15 (m, 2H), 7.81–7.65 (m, 4H), 7.52–7.45 (m, 2H), 7.38–7.33 (m, 1H), 3.93–3.75 (m, 4H), 3.52–3.22 (m, 4H). ^{13}C RMN (125 MHz, DMSO-d_6) δ 159.1, 154.1, 153.9, 148.9, 147.3, 141.0, 126.7, 126.5, 124.7, 123.7, 122.5, 118.4, 111.7, 111.1, 43.8. HRMS (*m/z*): calcd for $C_{20}H_{18}N_4O_5Na$ 417.1169 $[M+Na]^+$; found 417.1163. Anal. Calcd $C_{20}H_{18}N_4O_5$: C, 60.91; H, 4.60; N, 14.21. Found: C, 60.77, H, 4.73 N, 13.83.

1-(Benzofurane-2-carbonyl)-4-[(2-nitrophenyl)aminocarbonyl]piperazine (119). The product was obtained as a solid and purified by column using chromatography hexane-ethyl acetate (1:1) (346 mg, 88% yield), mp 105–108 ºC. ^{1}H NMR (500 MHz, DMSO-d_6) δ 9.41 (s, 1H), 8.00–7.94 (m, 1H), 7.85–7.64 (m, 4H), 7.57–7.21 (m, 4H), 3.89–3.73 (m, 4H), 3.69–3.58 (m, 4H). ^{13}C RMN (125 MHz, DMSO-d_6) δ 159.1, 154.1, 153.9, 137.6, 148.1, 147.3, 141.1, 126.7, 126.6, 124.7, 123.7, 122.5, 118.4, 111.8, 111.1, 43.8. HRMS (*m/z*): calcd for $C_{20}H_{18}N_4O_5Na$ 417.1169 $[M+Na]^+$; found 417.1164 Anal. Calcd $C_{20}H_{18}N_4O_5$: C, 60.91; H, 4.60; N, 14.21. Found:C, 60.99, H, 4.50; N, 13.97.

6.1.2 *O*-Acyl-*N*-phenylaminocarbonyl serinol derivatives

-General Procedure 4. Synthesis of urea derivatives from serinol (127-130). To a solution of appropriate isocyanate (3.6 mmol) in dry DCM (20 mL), a solution of the aminoalcohol (3 mmol) in methanol (1 mL) was added dropwise. A white precipitate appeared that was filtered at *vacuum* and washed with fresh DCM to give urea derivative.

***N*-(1,3-Dihydroxyprop-2-yl)-*N'*-[4-(trifluoromethyl)phenyl]urea (127).** The compound was obtained as a white solid (717 mg, 86% yield); mp 191–193 ºC. ^{1}H NMR (500 MHz, DMSO-d_6) δ 9.03 (s, 1H, N*H*Ar), 7.57–7.44 (bs, 4H, Ar), 6.19 (d, *J* = 8.3 Hz, 1H, CHN*H*), 4.73 (t, *J* = 5.3 Hz, 2H, OH), 3.67–3.61 (m, 1H, CH), 3.56–3.41 (m, 4H, 2CH_2OH). ^{13}C NMR (125 MHz, DMSO-d_6) δ154.6, 144.2, 126.0, 125.9, 117.1, 117.0, 60.0, 52.6. HRMS (*m*/*z*): calcd for $C_{11}H_{13}N_2F_3O_3Na$ 301.0770 [M+Na]$^+$; found 301.0770. Anal. Calcd for $C_{11}H_{13}N_2F_3O_3$: C, 47.49; H, 4.71, N, 10.07. Found: C, 47.37; H, 4.72; N.10.03.

***N*-(1,3-Dihydroxyprop-2-yl)-*N'*-(4-methylphenyl)urea (128).** The product was obtained as a white resin (511 mg; 77 % yield). ^{1}H NMR (500 MHz, DMSO-d_6) δ 8.48 (s, 1H, N*H*Ar), 7.27 (d, *J* = 8.4 Hz, 2H, Ar), 7.03 (d, *J* = 8.2 Hz, 2H, Ar), 5.99 (d, *J* = 8.0 Hz, 1H, CHN*H*), 4.69 (t, *J* = 5.1 Hz, 2H, OH), 3.65–3.58 (m, 1H, CH), 3.54–3.39 (m, 4H, 2CH_2OH), 2.22 (s, 3H, CH_3). ^{13}C NMR (125 MHz, DMSO-d_6) δ 155.0, 138.0, 129.1, 129.0, 117.5, 60.2, 52.4, 20.2. HRMS (*m*/*z*): calcd. for $C_{11}H_{16}N_2O_3Na$ 247.1053 [M+Na]$^+$; found 247.1054.

***N*-[4-chloro-3-(trifluoromethyl)phenyl]-*N'*-(1,3-dihydroxyprop-2-yl)urea (129).** The product was obtained as a white solid. (750 mg, 80% yield); mp 176–178 ºC. ^{1}H NMR (500 MHz, DMSO-d_6) δ9.06 (s, 1H, N*H*Ar), 8.03 (d, *J* = 2.1 Hz, 1H, Ar), 7.59–7.44 (m, 2H, Ar), 6.2 (d, *J* = 8.2 Hz, 1H, CHN*H*), 4.87 (bs, 2H, OH), 3.51–3.39 (m, 5H, HOCH_2C*H*CH_2OH). ^{13}C NMR (125 MHz, DMSO-d_6) δ 154.7, 139.8, 131.9, 122.3, 121.5, 116.0, 115.9, 60.1, 52.5. HRMS (*m*/*z*): calcd for $C_{11}H_{12}ClN_2F_3ClO_3Na$ 335.0380 [M+Na]$^+$; found 335.0381. Anal. Calcd for $C_{11}H_{12}ClN_2F_3ClO_3$: C, 42.26; H, 3.87; N, 8.68. Found: C, 42.75; H, 3.65; N, 8.68.

***N*-(4-Chlorophenyl)-*N'*-(1,3-dihydroxyprop-2-yl)urea (130)** [118]**.** The compound was obtained as a pure white solid (606 mg, 83% yield); mp 181–184 ºC. ^{1}H NMR (500 MHz, DMSO-d_6) δ8.75 (s, 1H, N*H*Ar), 7.41 (d, *J* = 8.9 Hz, 2H, Ar), 7.26 (d, *J* = 8.7 Hz, 2H, Ar), 6.07 (d, *J* = 7,8 Hz, 1H, CHN*H*), 4.71 (t, *J* = 5,2 Hz, 2H, OH), 3.65–3.59 (m, 1H, CH), 3.53–3.40 (m, 4H, 2CH_2OH). ^{13}C NMR (125 MHz, DMSO-d_6) δ154.7, 139.5, 128.5, 124.3, 118.9, 60.1, 52.4. HRMS (*m*/*z*): calcd for

$C_{10}H_{13}ClN_2O_3Na$ 267.0507 $[M+Na]^+$; found 267.0508. Anal. Calcd for $C_{10}H_{13}ClN_2O_3$: C, 49.09; H, 5.36; N, 11.45. Found: C, 49.47; H, 5.38; N, 11.40.

-General Procedure 5. Acylation reaction of N-(substituted)-N'-(1,3-dihydroxyprop-2-yl)phenylureas from acyl chloride (131-152, 156-158)

*A) O,O'-Diacylation reaction (**131-152**).* To a solution of the urea derivative (**127-130**) (0.54 mmol) in dry DCM (20 mL) and DMAP (1.35 mmol), the appropriate acylating agent (1.1 mmol) in dry DCM (5 mL) was added. The reaction mixture was stirred at rt until TLC showed that all the starting material had reacted (24 h), then was washed with HCl 1N aqueous solution (2 x 20mL), saturated $NaHCO_3$ solution (2 x 20 mL) and brine (20 mL). The organic layer was dried over Na_2SO_4, filtered and evaporated under reduced pressure. The compound was further purified by flash column chromatography on silica gel using the appropriate eluent.

***N*-[1,3-Bis(4-methylbenzoyloxy)prop-2-yl]-*N'*-[4-(trifluoromethyl)phenyl]urea (131).** The product was obtained as a white solid and purified by column chromatography using hexane-ethyl acetate (4:1) as eluent (209 mg; 75% yield); mp 158–162 ºC. ^{1}H NMR (500 MHz, DMSO-d_6) δ 9.03 (s, 1H, N*H*Ar), 7.90 (d, *J* = 8.1 Hz, 4H, Ar), 7.62–7.56 (m, 4H, Ar), 7.32 (d, *J* = 8.1 Hz, 4H, Ar), 6.71 (d, *J* = 8.5 Hz, 1H, CHN*H*), 4.57–4.40 (m, 5H, OCH_2C*H*CH_2O), 2.39 (s, 6H, CH_3). ^{13}C NMR (125 MHz, DMSO-d_6) δ 165.5, 154.5, 143.8, 129.3, 129.2, 126.7, 126.0, 125.9, 121.4, 121.1, 117.4, 63.9, 47.3, 21.1. HRMS (*m*/*z*): calcd for $C_{27}H_{25}F_3N_2O_5Na$ 537.1608 $[M+Na]^+$; found 537.1600. Anal. Calcd for $C_{27}H_{25}F_3N_2O_5$: C, 63.03; H, 4.90; N, 5.44. Found: C, 62.90; H, 4.91; N, 5.46.

***N*-[1,3-Bis(2-methylbenzoyloxy)prop-2-yl]-*N'*-[4-(trifluoromethyl)phenyl]urea (132).** The product was obtained as a white solid and purified by column chromatography using hexane-ethyl acetate (5:1) as eluent (190 mg; 68% yield); mp 158–160 ºC. ^{1}H NMR (500 MHz, DMSO-d_6) δ 9.00 (s, 1H, N*H*Ar), 7.85 (d, *J* = 7.2 Hz, 2H, Ar), 7.61–7.52 (m, 4H, Ar), 7.50–7.43 (m, 2H, Ar), 7.35–7.22 (m, 4H, Ar), 6.66 (d, *J* = 8.0 Hz, 1H, CHN*H*), 4.57–4.40 (m, 5H, OCH_2C*H*CH_2O), 2.50 (s, 6H, CH_3). ^{13}C NMR (125 MHz, DMSO-d_6) δ 166.7, 154.6, 143.5, 139.2, 132.3, 131.6, 130.1, 129.0, 125.9, 117.5, 63.8, 47.3, 20.9. HRMS (*m*/*z*): calcd for $C_{27}H_{25}F_3N_2O_5Na$ 537.1608 $[M+Na]^+$; found 537.1598. Anal. Calcd for $C_{27}H_{25}F_3N_2O_5$: C, 63.03; H, 4.90; N, 5.44. Found: C, 62.85; H, 4.92; N, 5.42.

***N*-[1,3-Bis(4-methoxylbenzoyloxy)prop-2-yl]-*N'*-[4-(trifluoromethyl)phenyl]urea (133).** The product was obtained as a white solid and purified by column chromatography using hexane-ethyl acetate (2:1) as eluent. (199 mg; 67 % yield); mp 118–119ºC. ^{1}H NMR (500 MHz, DMSO-d_6) δ 9.04

(s, 1H, N*H*Ar), 7.94 (d, *J* = 8.4 Hz, 4H, Ar), 7.62–7.52 (m, 4H, Ar), 7.00 (d, *J* = 8.4 Hz, 4H, Ar), 6.71 (d, *J* = 7.1 Hz, 1H, CHN*H*), 4.52–4.35 (m, 5H, OCH_2C*H*CH_2O), 3.81 (s, 6H, OCH_3). ^{13}C NMR (125 MHz, DMSO-d_6) δ 165.2, 163.3, 154.6, 143.9, 131.4, 125.9, 125.6, 123.5, 121.6, 117.4, 113.9, 63.8, 55.5, 47.4. HRMS (*m*/*z*): calcd for $C_{27}H_{25}F_3N_2O_7Na$ 569.1506 $[M+Na]^+$; found 569.1498. Anal. Calcd for $C_{27}H_{25}F_3N_2O_7$: C, 59.34; H, 4.61; N, 5.13. Found: C, 59.12; H, 4.59; N, 5.11.

***N*-[1,3-Bis(4-cyanobenzoyloxy)prop-2-yl]-*N'*-[4-(trifluoromethyl)phenyl]urea (134).** The product was obtained as an amorphous solid and purified by column chromatography using hexane-ethyl acetate (2:1) as eluent. (194 mg, 65% yield); ^{1}H NMR (500 MHz, DMSO-d_6) δ 8.98 (s, 1H, N*H*Ar), 8.10 (d, *J* = 8.4 Hz, 4H, Ar), 7.92 (d, *J* = 8.4 Hz, 4H, Ar), 7.58–7.50 (m, 4H, Ar), 6.75 (d, *J* = 7.7 Hz, 1H, CHN*H*), 4.58–4.47 (m, 5H, OCH_2C*H*CH_2O). ^{13}C NMR (125 MHz, DMSO-d_6) δ164.4, 143.4, 133.2, 132.6, 129.9, 125.9, 117.9, 117.5, 115.5, 64.7, 47.1. HRMS (*m*/*z*): calcd for $C_{27}H_{19}F_3N_4O_5Na$ 559.1200 $[M+Na]^+$; found 559.1193. Anal. Calcd for $C_{27}H_{19}F_3N_4O_5$: C, 60.45; H, 3.57; N, 10.44. Found: C, 60.49; H, 3.59; N, 10.40.

***N*-[1,3-Bis(4-nitrobenzoyloxy)prop-2-yl]-*N'*-[4-(trifluoromethyl)phenyl]urea (135).** The product was obtained as a yellow solid and purified by flash chromatography using hexane-ethyl acetate (2:1) as eluent. (223mg; 71% yield); mp 208–210 ºC. ^{1}H NMR (500 MHz, DMSO-d_6) δ 9.04 (s, 1H, N*H*Ar), 8.27 (d, *J* = 8.5 Hz, 4H, Ar), 8.18 (d, *J* = 8.8 Hz, 4H, Ar), 7.55–7.51 (m, 4 H, Ar), 6.80 (d, *J* = 7.3 Hz, 1H, CHN*H*), 4.61–4.50 (m, 5H, OCH_2C*H*CH_2O). ^{13}C NMR (125 MHz, DMSO-d_6) δ 164.2, 154.7, 150.2, 143.5, 134.7, 130.7, 126.0, 125.9, 123.7, 117.5, 64.9, 47.1. HRMS (*m*/*z*): calcd for $C_{25}H_{19}F_3N_4O_9Na$ 599.0996 $[M+Na]^+$; found 599.0989. Anal. Calcd for $C_{25}H_{19}F_3N_4O_9$: C, 52.05; H, 3.22; N, 9.72. Found: C, 51.95; H, 3.23; N, 9.68.

***N*-[1,3-Bis(2,4-dimethoxylbenzoyloxy)prop-2-yl]-*N'*-[4-(trifluoromethyl)phenyl]urea (136).** The product was obtained as a white solid and purified by column chromatography using hexane-ethyl acetate (1:1) as eluent. (233mg; 70% yield); mp 177–178 ºC. ^{1}H NMR (500 MHz, DMSO-d_6) δ 9.05 (s, 1H, N*H*Ar), 7.74 (d, *J* = 8.7 Hz, 2H, Ar), 7.60–7.54 (m, 4H, Ar), 6.64–6.60 (m, 1H, CHN*H*), 6.57–6.51 (m, 4H, Ar), 4.43–4.29 (m, 5H, OCH_2C*H*CH_2O), 3.84–3.75 (m, 12H, OCH_3). ^{13}C NMR (125 MHz, DMSO-d_6) δ 164.6, 164.1, 160.9, 154.4, 143.9, 133.2, 125.9, 125.6, 123.5, 117.3, 111.4, 105.3, 98.9, 63.2, 55.8, 55.5, 47.3. HRMS (*m*/*z*): calcd for $C_{29}H_{29}F_3N_2O_9Na$ 629.1717 $[M+Na]^+$; found 629.1711. Anal. Calcd for $C_{29}H_{29}F_3N_2O_9$: C, 57.43; H, 4.82; N, 4.62. Found: C, 57.17; H, 4.80; N, 4.60.

***N*-[1,3-Bis(3,4,5-trimethoxylbenzoyloxy)prop-2-yl]-*N'*-[4-(trifluoromethyl)phenyl]urea (137).** The product was obtained as a white solid and purified by column chromatography using hexane-

ethyl acetate (1:2) as eluent. (295 mg; 82% yield); mp 188–189 ºC. ^{1}H NMR (500 MHz, DMSO-d_6) δ 9.05 (s, 1H, N*H*Ar), 7.63–7.56 (m, 4H, Ar), 7.28 (s, 4H, Ar), 6.70 (d, J = 8.80 Hz, 1H, CHN*H*), 4.63-4.55 (m, 1H, C*H*), 4.53–4.42 (m, 4H, OCH_2CHCH_2O), 3.84–3.72 (m, 18H, OCH_3). ^{13}C NMR (125 MHz, DMSO-d_6) δ 165.1, 154.6, 152.7, 143.8, 141.9, 125.9, 125.6, 124.5, 121.7, 121.3, 117.4, 106.8, 64.3, 60.1, 55.9, 47.4. HRMS (*m*/*z*): calcd for $C_{31}H_{32}F_3N_2O_{11}Na$ 689.1929 $[M+Na]^+$; found 689.1920. Anal. Calcd for $C_{31}H_{33}F_3N_2O_{11}$: C, 55.86; H, 4.99; N, 4.20. Found: C, 55.61; H, 4.97; N, 4.22.

***N*-[1,3-Bis(4-methylbenzoyloxy)prop-2-yl]-*N'*-(4-methylphenyl)urea (138).** The product was obtained as a white solid and purified by column chromatography using hexane-ethyl acetate (2:1) as eluent. (165 mg; 66% yield); mp 164–165 ºC. ^{1}H NMR (500 MHz, DMSO-d_6) δ 8.50 (s, 1H, N*H*Ar), 8.00 (d, J = 8.1 Hz, 4H, Ar), 8.21 (d, J = 8.9 Hz, 4H, Ar), 7.44–7.35 (m, 2H, Ar), 7.13 (d, J = 8.3 Hz, 2H, Ar), 6.61 (d, J = 8.1 Hz, 1H, CHN*H*), 4.63–4.50 (m, 5H, OCH_2C*H*CH_2O), 2.49 (s, 6H, CH_3), 2.32 (s, 3H, CH_3). ^{13}C NMR (125 MHz, DMSO-d_6) δ 165.5, 154.9, 143.7, 137.5, 130.1, 129.3, 129.2, 129.0, 126.7, 117.9, 64.0, 47.2, 21.1, 20.2. HRMS (*m*/*z*): calcd for $C_{27}H_{28}N_2O_5Na$ 483.1880 $[M+Na]^+$; found 483.1887. Anal. Calcd for $C_{27}H_{28}N_2O_5$: C, 70.42; H, 6.13; N, 6.08. Found: C, 70.09; H, 6.15; N, 6.10.

***N*-[1,3-Bis(2-methylbenzoyloxy)prop-2-yl]-*N'*-(4-methylphenyl)urea (139).** The product was obtained as a white solid and purified by column chromatography using hexane-ethyl acetate (2:1) as eluent. (230 mg; 92 % yield); mp 122–123 ºC. ^{1}H NMR (500 MHz, DMSO-d_6) δ 8.43 (s, 1H, N*H*Ar), 7.85 (d, J = 7.7 Hz, 2H, Ar), 7.78 (d, J = 7.6 Hz, 2H, Ar), 7.49–7.41 (m, 2H, Ar), 7.33–7.19 (m, 4H, Ar), 7.00 (d, J = 8.2 Hz, 2H, Ar), 6.42 (d, J = 8.5 Hz, CHN*H*), 4.51–4.33 (m, 5H, OCH_2C*H*CH_2O), 2.49 (s, 6H, CH_3), 2.19 (s, 3H, CH_3). ^{13}C NMR (125 MHz, DMSO-d_6) δ 166.6, 154.8, 139.3, 137.5, 132.2, 131.9, 131.5, 130.2, 130.1, 129.9, 129.8, 129.0, 125.9, 117.9, 64.0, 60.4, 47.2, 21.0, 20.2. HRMS (*m*/*z*): calcd for $C_{27}H_{28}N_2O_5Na$ 483.1890 $[M+Na]^+$; found 483.1883. Anal. Calcd for $C_{27}H_{28}N_2O_5$: C, 70.42; H, 6.13; N, 6.08. Found: C, 70.08; H, 6.10; N, 6.06.

***N*-[1,3-Bis(4-methoxylbenzoyloxy)prop-2-yl]-*N'*-(4-methylphenyl)urea (140).** The product was obtained as a white solid and purified by column chromatography using hexane-ethyl acetate (2:1) as eluent. (210 mg; 79% yield); mp 165–166 ºC. ^{1}H NMR (500 MHz, DMSO-d_6) δ 8.49 (s, 1H, N*H*Ar), 7.99–7.94 (m, 4H, Ar), 7.28 (d, J = 8.4 Hz, 2H, Ar), 7.08–6.99 (m, 6H, Ar), 6.49 (d, J = 8.3 Hz, 1H, CHN*H*), 4.52–4.38 (m, 5H, OCH_2C*H*CH_2O), 3.85 (s, 6H, OCH_3), 2.22 (s, 3H, CH_3). ^{13}C NMR (125 MHz, DMSO-d_6) δ 165.2, 163.2, 154.9, 137.5, 131.4, 130.1, 129.8, 121.6, 117.7, 113.9, 63.7, 55.4, 47.3, 20.2HRMS (*m*/*z*): calcd. for $C_{27}H_{28}N_2O_7Na$ 515.1789 $[M+Na]^+$; $]^+$; 515.1782. Anal. Calcd for $C_{27}H_{28}N_2O_7$: C, 65.84; H, 5.73; N, 5.69. Found: C, 65.54; H, 5.71; N, 5.70.

***N*-[1,3-Bis(4-nitrobenzoyloxy)prop-2-yl]-*N'*-(4-methylphenyl)urea (141).** The product was obtained as a light yellow solid and purified by column chromatography using hexane-ethyl acetate (2:1) as eluent. (177 mg; 62% yield); mp 195–196 ºC. ^{1}H NMR (500 MHz, DMSO-d_6) δ 8.48 (s, 1H, N*H*Ar), 8.30 (d, *J* = 8.9 Hz, 4H, Ar), 8.21 (d, *J* = 8.9 Hz, 4H, Ar), 7.25 (d, *J* = 8.4 Hz, 2H, Ar), 7.02 (d, *J* = 8.3 Hz, 2H, Ar), 6.58 (d, *J* = 6.4 Hz, 1H, CHN*H*), 4.59–4.49 (m, 5H, OCH_2C*H*CH_2O), 2.22 (s, 3H, CH_3). ^{13}C NMR (125 MHz, DMSO-d_6) δ 164.1, 154.9, 150.3, 137.5, 134.9, 130.7, 130.1, 129.0, 123.7, 117.9, 64.9, 47.0, 20.2. HRMS (*m/z*): calcd for $C_{25}H_{22}N_4O_9Na$ 545.1279 [M+Na]$^+$; found 545.1272. Anal. Calcd for $C_{25}H_{22}N_4O_9$: C, 57.47; H, 4.24; N, 10.72. Found: C, 57.69; H, 4.26; N, 10.71.

***N*-[1,3-Bis(2,4-dimethoxylbenzoyloxy)prop-2-yl]-*N'*-(4-methylphenyl)urea (142).** The product was obtained as a white solid and purified by column chromatography using hexane-ethyl acetate (1:2) as eluent. (195 mg; 65% yield); mp 158–159 ºC. ^{1}H NMR (500 MHz, DMSO-d_6) δ 8.52 (s, 1H, N*H*Ar), 7.77 (d, *J* = 8.7 Hz, 2H, Ar), 7.3 (d, *J* = 8.4 Hz, 2H, Ar), 7.28 (d, *J* = 8.2 Hz, 2H, Ar), 7.03 (d, *J* = 8.0 Hz, 2H, Ar), 6.69–6.51 (m, 2H, Ar), 6.32 (d, *J* = 7.6 Hz, 1H, CHN*H*), 4.48–4.29 (m, 5H, OCH_2C*H*CH_2O), 3.95–3.85 (m, 12H, OCH_3), 2.22 (s, 3H, CH_3). ^{13}C NMR (125 MHz, DMSO-d_6) δ 164.6, 164.1, 160.9, 154.8, 137.6, 133.2, 130.0, 129.0, 117.8, 111.5, 105.3, 98.9, 63.4, 55.8, 55.5, 47.2, 20.2. HRMS (*m/z*): calcd for $C_{29}H_{32}N_2O_9Na$ 575.2000 [M+Na]$^+$; found 575.1993. Anal. Calcd for $C_{29}H_{32}N_2O_9$: C, 63.04; H, 5.84; N, 5.07. Found: C, 62.74; H, 5.85; N, 5.09.

***N*-[1,3-Bis(3,4,5-trimethoxylbenzoyloxy)prop-2-yl]-*N'*-(4-methylphenyl)urea (143).** The product was obtained as a white solid and purified through column chromatography using hexane-ethyl acetate (1:2) as eluent. (202mg; 61% yield); mp 204–205 ºC. ^{1}H NMR (500 MHz, DMSO-d_6) δ 8.48 (s, 1H, N*H*Ar), 7.31–7.24 (m, 6H, Ar), 7.03 (d, *J* = 8.2 Hz, 2H, Ar), 6.47 (d, *J* = 8.70 Hz, 1H, CHN*H*), 4.60–4.40 (m, 5H, OCH_2C*H*CH_2O), 3.80 (s, 12H, OCH_3), 3.75 (s, 6H, OCH_3), 2.22 (s, 3H, CH_3). ^{13}C NMR (125 MHz, DMSO-d_6) δ 165.1 (2C), 154.9, 152.7, 141.9, 137.5, 130.1, 128.9, 124.5, 117.9, 106.8, 64.5, 60.1, 55.9, 47.2, 20.2. HRMS (*m/z*): calcd for $C_{31}H_{36}N_2O_{11}Na$ 635.2211 [M+Na]$^+$; found 635.2204.

***N*-[1,3-Bis(4-methylbenzoyloxy)prop-2-yl]-*N'*-[4-chloro-3-(trifluoromethyl)phenyl]urea (144)** [118]**.** The product was obtained as a white solid and purified by column chromatography using hexane-ethyl acetate (3.5:1) as eluent. (248 mg; 85% yield); mp 170–173 ºC. ^{1}H NMR (500 MHz, DMSO-d_6) δ 9.07 (s, 1H, N*H*Ar), 7.98 (d, *J* = 1.8 Hz, 1H, Ar), 7.98–7.80 (d, *J* = 8.2 Hz, 4H, Ar), 7.52–7.47 (m, 2H, Ar), 7.26 (d, *J* = 8.1 Hz, 4H, Ar), 6.68 (d, *J* = 8.7 Hz, 1H, CHN*H*), 4.56–4.35 (m, 5H, OCH_2C*H*CH_2O), 2.34 (s, 6H, CH_3). ^{13}C NMR (125 MHz, DMSO-d_6) δ 165.6, 154.7, 143.9, 139.4, 131.8, 129.3, 129.2, 129.0, 126.7, 122.5, 121.6, 116.4, 63.8, 47.5, 21.0. HRMS (*m/z*): calcd

for $C_{27}H_{25}ClF_3N_2O_5$ 549.1399 $[M+H]^+$; found 549.1391. Anal. Calcd for $C_{27}H_{24}ClF_3N_2O_5$: C, 58.08; H, 4.41; N, 5.10. Found: C, 58.18; H, 4.42; N, 5.08.

***N*-[1,3-Bis(2-methylbenzoyloxy)prop-2-yl]-*N'*-[4-chloro-3-(trifluoromethyl)phenyl]urea (145).** The product was obtained as a white solid and purified by column chromatography using hexane-ethyl acetate (3.5:1) as eluent (186 mg; 62% yield); mp 132–136 ºC. ^{1}H NMR (500 MHz, DMSO-d_6) δ 9.06 (s, 1H, N*H*Ar), 8.00 (d, *J* = 2.1 Hz, 1H, Ar), 7.85 (d, *J* = 7.1 Hz, 2H, Ar), 7.55–7.43 (m, 4H, Ar), 7.33–7.21 (m, 4H, Ar), 6.67 (d, *J* = 8.7 Hz, 1H, CHN*H*), 4.54–4.48 (m, 1H, C*H*), 4.45–4.49 (m, 4H, OCH_2CHCH_2O), 2.49 (s, 6H, CH_3). ^{13}C NMR (125 MHz, DMSO-d_6) δ 166.7, 154.6, 139.4, 139.2, 132.2, 131.8, 131.6, 130.1, 129.0, 125.8, 122.6, 63.8, 47.4, 20.9. HRMS (*m*/*z*): calcd for $C_{27}H_{24}ClF_3N_2O_5Na$ 571.1218 $[M+Na]^+$; found 571.1213. Anal. Calcd for $C_{27}H_{24}ClF_3N_2O_5$: C, 58.08; H, 4.41; N, 5.10. Found: C, 58.32; H, 4.39; N, 5.12.

***N*-[1,3-Bis(4-methoxylbenzoyloxy)prop-2-yl]-*N'*-[4-chloro-3-(trifluoromethyl)phenyl]urea (146)** [118]**.** The product was obtained as a white solid and purified by column chromatography using hexane-ethyl acetate (1:2) as eluent. (177 mg; 56% yield); mp 133–134 ºC. ^{1}H NMR (500 MHz, DMSO-d_6) δ 9.19 (s, 1H, N*H*Ar), 8.50 (s, 1H, Ar), 7.95 (d, *J* = 8.5 Hz, 4H, Ar), 7.58–7.53 (m, 2H, Ar), 7.04–6.96 (m, 4H, Ar), 6.80 (d, *J* = 8.2 Hz, 1H, CHN*H*), 4.55–4.38 (m, 5H, OCH_2C*H*CH_2O), 3.82 (s, 6H, OCH_3). ^{13}C NMR (125 MHz, DMSO-d_6) δ 165.2, 163.3, 154.7, 139.8, 131.9, 131.4, 126.5, 123.9, 122.5, 121.7, 121.6, 116.3, 113.9, 63.7, 55.8, 47.5. HRMS (*m*/*z*): calcd for $C_{27}H_{24}ClF_3N_2O_7Na$ 603.1116 $[M+Na]^+$; found 603.1109. Anal. Calcd for $C_{27}H_{24}ClF_3N_2O_7$: C, 55.82; H, 4.16; N, 4.82. Found: C, 55.56; H, 4.15; N, 4.84.

***N*-[1,3-Bis(4-cyanobenzoyloxy)prop-2-yl]-*N'*-[4-chloro-3-(trifluoromethyl)phenyl]urea (147)** [118]**.** The product was obtained as a white solid and purified by column chromatography using hexane-ethyl acetate (2:1) as eluent (218 mg; 70% yield); mp 132–133 ºC. ^{1}H NMR (500 MHz, DMSO-d_6) δ 9.05 (s, 1H, N*H*Ar), 8.1 (d, *J* = 8.3 Hz, 4H, Ar), 7.96–7.90 (m, 5H, Ar), 7.53–7.45 (m, 2H, Ar), 6.76 (d, *J* = 8.0 Hz, 1H, CHN*H*), 4.52 (m, 5H, OCH_2C*H*CH_2O). ^{13}C NMR (125 MHz, DMSO-d_6) δ 164.4, 154.7, 139.3, 133.2, 132.6, 131.8, 129.9, 122.6, 122.0, 117.9, 116.2, 115.4, 64.7, 47.2. HRMS (*m*/*z*): calcd for $C_{27}H_{18}ClF_3N_4O_5Na$ 593.0810 $[M+Na]^+$; found 593.0809. Anal. Calcd for $C_{27}H_{18}ClF_3N_4O_5$: C, 56.80; H, 3.18; N, 9.62. Found: C, 56.75; H, 3.20; N, 9.62.

***N*-[1,3-Bis(4-nitrobenzoyloxy)prop-2-yl]-*N'*-[4-chloro-3-(trifluoromethyl)phenyl]urea (148).** The product was obtained as a yellow solid and purified by column chromatography using hexane-ethyl acetate (2:1) as eluent. (127mg; 68% yield); mp 134–136 ºC. ^{1}H NMR (500 MHz, DMSO-d_6)

δ 9.05 (s, 1H, N*H*Ar), 8.1 (d, *J* = 8.3 Hz, 4H, Ar), 7.55–7.43 (m, 4H, Ar), 7.94–7.91 (m, 1H, Ar), 7.53 (d, *J* = 8.8 Hz, 1H, Ar), 7.47 (dd, *J* = 8.8 Hz, *J* = 2.4 Hz, 1H, Ar), 6.76 (d, *J* = 8.0 Hz, 1H, N*H*CH), 4.52 (m, 5H, OCH_2C*H*CH_2O). ^{13}C NMR (125 MHz, DMSO-d_6) δ 164.4, 154.7, 139.3, 133.2, 132.6, 131.8, 129.9, 122.6, 117.9, 115.4, 64.7, 47.2. HRMS (*m*/*z*): calcd for $C_{25}H_{18}ClF_3N_4O_9Na$ 633.0607 $[M+Na]^+$; found 633.0599. Anal. Calcd for $C_{25}H_{18}ClF_3N_4O_9$: C, 49.15; H, 2.97; N, 9.17. Found: C, 48.99; H, 2.98; N, 9.14.

***N*-[1,3-Bis(2,4-dimethoxylbenzoyloxy)prop-2-yl]-*N'*-[4-chloro-3-(trifluoromethyl)phenyl]urea (149).** The product was obtained as a white solid and purified by column chromatography using hexane-ethyl acetate (1:2) as eluent. (255 mg; 74% yield); mp 178–179 ºC. ^{1}H NMR (500 MHz, DMSO-d_6) δ 9.11 (s, 1H, N*H*Ar), 8.06–8.03 (m, 1H, Ar), 7.74 (d, *J* = 8.7 Hz, 2H, Ar), 7.55–7.52 (m, 2H, Ar), 6.63–6.59 (m, 2H, Ar), 6.56–6.50 (m, 3H, Ar, CHN*H*), 4.43–4.29 (m, 5H, OCH_2C*H*CH_2O), 3.87–3.76 (m, 12H, OCH_3). ^{13}C NMR (125 MHz, DMSO-d_6) δ 164.6, 164.1, 160.9, 154.5, 139.8, 133.2, 131.8, 128.6, 126.5, 126.3, 123.9, 116.3, 111.4, 105.3, 98.9, 63.2, 55.5, 55.4, 47.4. HRMS (*m*/*z*): calcd for $C_{29}H_{28}ClF_3N_2O_9Na$ 663.1328 $[M+Na]^+$; found 663.1321. Anal. Calcd for $C_{29}H_{28}ClF_3N_2O_9$: C, 54.34; H, 4.40; N, 4.37. Found: C, 54.11; H, 4.39; N, 4.35.

***N*-[1,3-Bis(3,4,5-trimethoxylbenzoyloxy)prop-2-yl]-*N'*-[4-chloro-3-(trifluoromethyl)phenyl]urea (150).** The product was obtained as a white solid and purified by column chromatography using hexane-ethyl acetate (2:1) as eluent (287 mg; 76 % yeld); mp 159–160 ºC. ^{1}H NMR (500 MHz, DMSO-d_6) δ 9.12 (s, 1H, N*H*Ar), 8.08 (s, 1H, Ar), 7.53 (s, 2H, Ar), 7.26 (s, 4H, Ar), 6.73 (d, *J* = 8.9 Hz, 1H, CHN*H*), 4.62–4.54 (m, 1H, C*H*), 4.51–4.41 (m, 4H, OCH_2CHCH_2O), 3.83–3.71 (m, 18H, OCH_3). ^{13}C NMR (125 MHz, DMSO-d_6) δ 165.1, 154.7, 152.7, 141.9, 139.7, 131.8, 126.7, 124.4, 123.9, 122.5, 121.8, 121.7, 106.7, 64.3, 60.1, 55.9, 47.5. HRMS (*m*/*z*): calcd for $C_{31}H_{32}ClF_3N_2O_{11}Na$ 723.1539 $[M+Na]^+$; found 723.1524. Anal. Calcd for $C_{31}H_{32}ClF_3N_2O_{11}$: C, 53.11; H, 4.60; N, 4.00. Found: C, 53.20; H, 4.59; N, 4.02.

***N*-[1,3-Bis(4-dimethylaminobenzoyloxy)prop-2-yl]-*N'*-[4-chloro-3-(trifluoromethyl)phenyl]urea (151)** The product was obtained as a white solid and purified by column chromatography using hexane-ethyl acetate (1:1) as eluent. (215mg; 66% yield). ^{1}H NMR (500 MHz, DMSO-d_6) δ 9.10 (s, 1H, N*H*Ar), 8.07 (s, 1H, Ar), 7.80 (d, *J* = 8.9 Hz, 4H, Ar), 7.56 (s, 2H, , Ar), 6.66 (m, 5H, Ar + CHN*H*), 4.45-4.32 (m, 5H, OCH_2CHCH_2O). ^{13}C NMR (125 MHz, DMSO-d_6) δ 165.7 (2C), 154.7, 153.3 (2C), 139.8, 131.8, 130.9, 129.5, 122.4, 121.6, 116.3, 115.4, 110.7, 63.2, 42.7.

***N*-[1,3-Bis(4-methoxylbenzoyloxy)prop-2-yl]-*N'*-(4-chlorophenyl)urea (152).** The product was obtained as a white solid and purified by column chromatography using hexane-ethyl acetate (1:1) as eluent. (239 mg; 86% yield); mp 164–166 ºC. ^{1}H NMR (500 MHz, DMSO-d_6) δ 8.76 (s, 1H, N*H*Ar), 7.96 (d, *J* = 8.8 Hz, 4H, Ar), 7.43 (d, *J* = 8.9 Hz, 2H, Ar), 7.28 (d, *J* = 8.6 Hz, 2H, Ar), 7.03 (d, *J* = 8.8 Hz, 4H, Ar), 6.59 (d, *J* = 8.4 Hz, 1H, CHN*H*), 4.52–4.37 (m, 4H, OCH_2CHCH_2O), 4.11–4.07 (m, 1H, C*H*), 3.84 (s, 6H, OCH_3). ^{13}C NMR (125 MHz, DMSO-d_6) δ 165.2, 163.3, 154.7, 139.1, 131.4, 131.2, 128.5, 124.8, 121.6, 114.0, 63.8, 55.5, 48.6, 47.3. HRMS (*m*/*z*): calcd for $C_{26}H_{25}ClN_2O_7Na$ 535.1242 [M+Na]$^+$; found 535.1238. Anal. Calcd for $C_{26}H_{25}ClN_2O_7$: C, 60.88; H, 4.91; N, 5.46. Found: C, 61.10; H, 4.89; N, 5.43.

*B) Chemoselective O-acylation reaction (**156-158**)* To a cooled solution (–15 °C) of urea derivative (**128** or **129,** 1 mmol) in dry DCM (20 mL) and pyridine (2 mL), a solution of acyl chloride (0.9 mmol) in dry DCM (15 mL) was added. The reaction mixture was stirred at –15 °C for 1 hour, then it was washed with HCl 1N aqueous solution (2 x 15 mL), saturated $NaHCO_3$ (2 x 15 mL) and brine. The organic layer was dried over Na_2SO_4, filtered and evaporated to dryness. The compound was purified through flash column chromatography using the appropriate mixture hexane-ethyl acetate as eluent.

***N*-[4-Chloro-3-(trifluoromethyl)phenyl]-*N'*-[1-hydroxy-3-(4-methoxybenzoyloxy)prop-2-yl]urea (156).** The product was obtained as a white solid and purified by column chromatography using hexane-ethyl acetate (1:2) as eluent. (132 mg; 30% yield); mp 197–198 ºC. ^{1}H NMR (500 MHz, DMSO-d_6) δ 9.10 (s, 1H, N*H*Ar), 8.08–8.03 (m, 1H, Ar), 7.95 (d, *J* = 8.8 Hz, 2H, Ar), 7.58–7. 50 (m, 2H, Ar), 7.02 (d, *J* = 8.8 Hz, 2H, Ar), 6.44 (d, *J* = 8.5 Hz, 1H, CHN*H*), 5.02 (t, *J* = 5.25 Hz, 1H, OH), 4.32 (d, *J* = 5.7 Hz, 2H, OCH_2), 4.12–4.02 (m, 1H, C*H*) 3.83 (s, 3H, OCH_3), 3.67–3.60 (m, 1H, CH_2OH), 3.58–3.51 (m, 1H, CH_2OH). ^{13}C NMR (125 MHz, DMSO-d_6) δ 165.3, 163.2, 154.6, 139.9, 131.9, 131.3, 123.9, 122.3, 121.8, 121.7, 121.5, 116.0, 113.9, 63.6, 60.3, 55.5, 49.9. HRMS (*m*/*z*): calcd for $C_{19}H_{18}ClF_3N_2O_5Na$ 469.0749 [M+Na]$^+$; found 469.0744. Anal. Calcd for $C_{18}H_{18}ClF_3N_2O_5$: C, 51.08; H, 4.06; N, 6.27. Found: C, 51.27; H, 4.04; N, 6.26.

***N*-[1-Hydroxy-3-(2,4-dimethoxybenzoyloxy)prop-2-yl]-*N'*-(4-methylphenyl)urea (157).** The product was obtained as a white solid and purified by column chromatography using hexane-ethyl acetate (1:2) as eluent. (134 mg; 34% yield); mp 176–177 ºC. ^{1}H NMR (500 MHz, DMSO-d_6) δ 8.48 (s, 1H, N*H*Ar), 7.74 (d, *J* = 8.7 Hz, 1H, Ar), 7.25 (d, *J* = 7.6 Hz, 2H, Ar), 7.02 (d, *J* = 8.1 Hz, 2H, Ar), 6.66-6.53 (m, 2H, Ar), 6.13 (d, *J* = 8.3 Hz, 1H, CHN*H*), 4.93 (t, *J* = 5.1 Hz, 1H, OH), 4.27–4.15 (m, 2H, OCH_2), 4.03–3.95 (m, 1H, C*H*), 3.87–3.76 (m, 6H, OCH_3), 3.63–3.56 (m, 1H, CH_2OH),

3.54–3.46 (m, 1H, C*H*$_2$OH), 2.20 (s, 3H, CH$_3$). ^{13}C NMR (125 MHz, DMSO-*d*$_6$) δ 164.6, 164.0, 160.8, 154.8, 137.8, 133.1, 129.8, 129.0, 116.7, 111.8, 105.3, 98.9, 63.3, 60.4, 55.8, 55.5, 49.7, 20.2. HRMS (*m*/*z*): calcd for $C_{20}H_{24}N_2O_6Na$ 411.1527 [M+Na]$^+$; found 411.1520. Anal. Calcd for $C_{20}H_{24}N_2O_6$: C, 61.85; H, 6.23; N, 7.21. Found: C, 61.64; H, 6.22; N, 7.19.

***N*-[1-Hydroxy-3-(3,4,5-trimethoxybenzoyloxy)prop-2-yl]-*N'*-(4-methylphenyl)urea (158).** The product was obtained as a white solid and purified by column chromatography using hexane-ethyl acetate (1:2) as eluent. (117 mg; 28% yield); mp 175–176ºC. ^{1}H NMR (500 MHz, DMSO-*d*$_6$) δ 8.45 (s, 1H, N*H*Ar), 7.32–7.18 (m, 4H, Ar), 6.99 (d, *J* = 8.2 Hz, 2H, Ar), 6.20 (d, *J* = 8.6 Hz, 1H, CHN*H*) 4.99 (t, *J* = 5.2 Hz, 1H, OH), 4.37–4.21 (m, 2H, OC*H*$_2$), 4.14–4.04 (m, 1H, C*H*), 3.83–3.67 (m, 9H, OCH$_3$), 3.65–3.46 (m, 1H, C*H*$_2$OH), 3.55–3.46 (m, 1H, C*H*$_2$OH), 2.20 (s, 3H, CH$_3$). ^{13}C NMR (125 MHz, DMSO-*d*$_6$) δ 165.3, 154.9, 152.7, 141.8, 137.8, 129.8, 128.9, 124.8, 117.7, 106.7, 64.7, 60.6, 60.1, 55.9, 49.5, 20.2. HRMS (*m*/*z*): calcd for $C_{21}H_{26}N_2O_7Na$ 441.1632 [M+Na]$^+$; found 441.1626.

-General Procedure 6. Diacylation reaction of N-(substituted)-N'-(1,3-dihydroxyprop-2-yl)phenylureas from carboxylic acids (153-155). According to a published procedure with some modifications [103], carboxylic acid (2.87 mmol) was dissolved in DCM and EDCI (3.55 mmol) was added. The mixture was stirred for 1 hour at rt (mixture 1). At the same time, to a suspension of urea derivative (**127-129**, 0.78 mmol) in DCM was added DMAP (0.78 mmol) and the mixture was stirred for 1 hour at rt (mixture 2); then the mixture 2 was added dropwise into the mixture 1. The reaction was stirred for 24 hours at rt. The organic layer was washed with saturated NaHCO$_3$ aqueous solution and brine, then it was dried over Na$_2$SO$_4$, filtered and evaporated *in vacuo*. The compound was further purified through flash column chromatography using the appropriate mixture hexane-ethyl acetate as eluent.

***N*-{1,3-Bis[(*E*)-(3,4,5-trimethoxylphenyl)acryloyloxy]prop-2-yl}-*N'*-[4-chloro-3-(trifluoromethyl)phenyl]urea (153).** The product was obtained as a white solid and purified by column chromatography using hexane-ethyl acetate (1:2) as eluent. (340 mg; 57% yield); mp 128–129 ºC. ^{1}H NMR (500 MHz, DMSO-*d*$_6$) δ 9.10 (s, 1H, N*H*Ar), 8.05 (s, 2H, Ar), 7.66–7.48 (m, 4H, C*H*=CHCO, Ar), 7.07–6.96 (m, 3H, Ar), 6.65 (m, 3H, CHN*H*, CH=C*H*CO), 4.38–4.28 (m, 5H, OC*H*$_2$C*H*C*H*$_2$O), 3.78 (s, 12H, OCH$_3$), 3.68 (s, 6H, OCH$_3$). ^{13}C NMR (125 MHz, DMSO-*d*$_6$) δ 166.2, 154.5, 153.1, 145.2, 139.7, 139.6, 131.8, 129.4, 122.5, 121.7, 116.8, 116.3, 106.0, 63.2, 60.0, 56.0, 47.6. HRMS (*m*/*z*): calcd for $C_{35}H_{36}ClF_3N_2O_{11}Na$ 775.1852 [M+Na]$^+$; found 775.1846. Anal. Calcd for $C_{35}H_{36}ClF_3N_2O_{11}$: C, 55.82; H, 4.82; N, 3.72. Found: C, 55.76; H, 4.80; N, 3.71.

***N*-{1,3-Bis[(*E*)-(3,4,5-trimethoxylphenyl)acryloyloxy]prop-2-yl}-*N'*-[4-(trifluoromethyl)phenyl]urea (154).** The product was obtained as a white solid and purified by column chromatography using hexane-ethyl acetate (1:2) as eluent. (348 mg; 61% yield); mp 100–101 ºC. ^{1}H NMR (500 MHz, DMSO-d_6) δ 9.03 (s, 1H, N*H*Ar), 7.67–7.52 (m, 6H, C*H*=CHCO, Ar), 7.06–6.98 (m, 4H, Ar), 6.67 (d, J = 15.9 Hz, 2H, CH=C*H*CO), 6.61 (d, J = 7.5 Hz, 1H, CHN*H*), 4.40–4.30 (m, 5H, OCH_2C*H*CH_2O), 3.79 (s, 12H, OCH_3), 3.69 (s, 6H, OCH_3). ^{13}C NMR (125 MHz, DMSO-d_6) δ 166.2, 154.4, 153.0, 145.2, 143.8, 139.6, 129.5, 129.1, 127.8, 125.6, 123.5, 117.4, 116.8, 106.0, 63.3, 60.0, 56.0, 47.5. HRMS (*m*/*z*): calcd for $C_{35}H_{37}F_3N_2O_{11}Na$ 741.2242 $[M+Na]^+$; found 741.2234. Anal. Calcd for $C_{35}H_{37}F_3N_2O_{11}$: C, 58.49; H, 5.19; N, 3.90. Found: C, 58.35; H, 5.20; N, 3.90.

***N*-{1,3-Bis[(*E*)-(3,4,5-trimethoxylphenyl)acryloyloxy]prop-2-yl}-*N'*-(4-methylphenyl)urea (155).** The product was obtained as a white solid and purified by column chromatography using hexane-ethyl acetate (1:2) as eluent. (332 mg; 64% yield); mp 110–111 ºC. ^{1}H NMR (500 MHz, DMSO-d_6) δ 8.48 (s, 1H, N*H*Ar), 7.63 (d, J = 15.7 Hz, 2H, C*H*=CHCO), 7.32–7.22 (m, 2H, Ar), 7.09–6.95 (m, 6H, Ar), 6.68 (d, J = 15.7 Hz, 2H, CH=C*H*CO), 6.42–6.34 (m, 1H, CHN*H*), 4.40–4.22 (m, 5H, OCH_2C*H*CH_2O), 3.90–3.60 (m, 18H, OCH_3), 2.21 (s, 3H, CH_3). ^{13}C NMR (125 MHz, DMSO-d_6) δ 166.2, 154.7, 153.1, 145.2, 139.6, 137.6, 129.5, 129.0, 117.8, 116.9, 105.9, 63.4, 60.1, 55.9, 47.4, 20.2. HRMS (*m*/*z*): calcd for $C_{35}H_{40}N_2O_{11}Na$ 687.2524 $[M+Na]^+$; found 687.2517.

-General procedure 7. Synthesis of dicarbamate derivatives of N-(substituted)-N'-(1,3-dihydroxyprop-2-yl)phenylureas (159-167)

*A) Synthesis of dicarbamate derivatives from commercial isocyanates (**159**, **161-164**, **166**,**167**)* According to reported procedure [104], urea derivative (**127-129**) (0.64 mmol) and isocyanate (1.47 mmol) were mixed in toluene (10 mL). The resulting suspension was refluxed (110 ºC) for 24 hours; then the reaction mixture was filtered and washed with fresh toluene. The obtained solid was dried at rt and analysed as pure compound or further purify through flash column chromatography using hexane-ethyl acetate as eluent. In the case of 4-nitroisocyanate, the monoderivative was also obtained, after column chromatography of the mixture.

***N*-{1,3-Bis[(4-methylphenyl)aminocarboxy]prop-2-yl}-*N'*-[4-(trifluoromethyl)phenyl]urea (159).** The product was obtained as a white solid and purified by filtration of the reaction mixture with fresh toluene. (233 mg; 66 % yield); mp 218–219 ºC. ^{1}H NMR (500 MHz, DMSO-d_6) δ 9.58 (s, 2H, ArN*H*COO), 9.08 (s, 1H, CON*H*Ar), 7.61–7.52 (m, 4H, Ar), 7.33 (d, J = 7.9 Hz, 4H, Ar), 7.55

(d, J = 8.3 Hz, 4H, Ar), 6.52 (d, J = 6.9 Hz, 1H, CHN*H*), 4.30–4.10 (m, 5H, OC*H*$_2$C*H*CH$_2$O), 2.22 (s, 6H, CH$_3$). ^{13}C NMR (125 MHz, DMSO-d_6) δ 154.4, 153.3, 143.9, 136.4, 131.3, 129.1, 125.9, 123.5, 120.8, 117.3, 63.3, 48.1, 20.3. HRMS (*m*/*z*): calcd for $C_{27}H_{27}F_3N_4O_5Na$ 567.1826 [M+Na]$^+$; found 567.1818. Anal. Calcd for $C_{27}H_{27}F_3N_4O_5$: C, 59.56; H, 5.00; N, 10.29. Found: C, 59.35; H, 4.98; N, 10.26.

***N*-{1,3-Bis[(4-methoxyphenyl)aminocarboxy]prop-2-yl}-*N'*-[4-(trifluoromethyl)phenyl]urea (161).** The product was obtained as a white solid and purified by column chromatography using hexane-ethyl acetate (1.5:1) as eluent. (190 mg; 50% yield); mp 220–221 ºC. ^{1}H NMR (500 MHz, DMSO-d_6) δ 9.52 (s, 2H, ArN*H*COO), 9.08 (s, 1H, CON*H*Ar), 7.62–7.55 (m, 4H, Ar), 7.38 (d, J = 7.6 Hz, 4H, Ar), 7.37 (d, J = 8.8 Hz, 4H, Ar), 6.51 (d, J = 7.1 Hz, 1H, CHN*H*), 4.30–4.15 (m, 5H, OC*H*$_2$C*H*C*H*$_2$O), 3.71 (s, 6H, OCH$_3$). ^{13}C NMR (125 MHz, DMSO-d_6) δ 154.8, 154.4, 153.4, 143.8, 131.9, 125.8, 125.9, 125.6, 123.5, 121.3, 121.1, 119.9, 118.0, 117.3, 113.9, 63.2, 55.1, 48.1. HRMS (*m*/*z*): calcd for $C_{27}H_{27}F_3N_4O_7Na$ 599.1724 [M+Na]$^+$¸ found 599.1718. Anal. Calcd for $C_{27}H_{27}F_3N_4O_7$: C, 56.25; H, 4.72; N, 9.72. Found: C, 56.04; H, 4.70; N, 9.76.

***N*-{1,3-Bis[(4-cyanophenyl)aminocarboxy]prop-2-yl}-*N'*-[4-(trifluoromethyl)phenyl]urea (162).** The product was obtained as a white solid and purified by column chromatography using hexane-ethyl acetate (1:1) as eluent. (218 mg; 60 % yield); mp 223–224. ^{1}H NMR (500 MHz, DMSO-d_6) δ 10.18 (s, 2H, ArN*H*COO), 8.93 (s, 1H, CON*H*Ar), 7.67–7.63 (m, 4H, Ar), 7.59–7.54 (m, 4H, Ar), 7.50–7.46 (m, 4H, Ar), 6.47 (d, J = 7.35 Hz, 1H, CHN*H*), 4.28–4.13 (m, 5H, OC*H*$_2$C*H*C*H*$_2$O). ^{13}C NMR (125 MHz, DMSO-d_6) δ 154.9, 153.5 (2C), 144.3, 143.9, 133.7, 126.4, 123.9, 121.9, 121.6, 119.5, 118.7, 117.9, 104.7, 64.3, 48.4. HRMS (*m*/*z*): calcd for $C_{27}H_{21}F_3N_6O_5Na$ 589.1418 [M+Na]$^+$; found 589.1411.

***N*-{1,3-Bis[(4-nitrophenyl)aminocarboxy]prop-2-yl}-*N'*-[4-(trifluoromethyl)phenyl]urea (163).** The product was obtained as a yellow solid and purified by column chromatography using hexane-ethyl acetate (1:2) as eluent. (196 mg; 50 % yield); mp 220–221 ºC. ^{1}H NMR (500 MHz, DMSO-d_6) δ 10.47 (s, 2H, ArN*H*COO), 9.00 (s, 1H, CON*H*Ar), 8.24–8.15 (m, 4H, Ar), 7.75–7.66 (m, 4H, Ar), 7.60–7.51 (m, 4H, Ar), 6.55 (d, J = 6.4 Hz, 1H, CHN*H*), 4.41–4.22 (m, 5H, OC*H*$_2$C*H*C*H*$_2$O). ^{13}C NMR (125 MHz, DMSO-d_6) δ 154.5, 153.0, 145.6, 145.4, 143.8, 141.7, 141.5, 125.9, 125.0, 124.9, 117.9, 117.7, 117.4, 63.9, 47.9. HRMS (*m*/*z*): calcd for $C_{25}H_{21}F_3N_6O_9Na$ 629.1214 [M+Na]$^+$; found 629.1207. Anal. Calcd for $C_{25}H_{21}F_3N_6O_9$: C, 49.51; H, 3.49; N, 13.86. Found: C, 49.68; H, 3.51; N, 13.84.

***N*-{1,3-Bis[(4-methylphenyl)aminocarboxy]prop-2-yl}-*N'*-[4-chloro-3-(trifluoromethyl)phenyl]urea (164).** The product was obtained as a white solid and purified by

filtration of the reaction mixture with fresh toluene. (298 mg; 80% yield); mp 210–211 ºC. ^{1}H NMR (500 MHz, DMSO-d_6) δ 9.58 (s, 2H, ArN*H*COO), 9.11 (s, 1H, CON*H*Ar), 8.10–8.02 (m, 1H, Ar), 7.58–7.48 (m, 2H, Ar), 7.34 (d, *J* = 7.6 Hz, 4H, Ar), 7.06 (d, *J* = 8.2 Hz, 4H, Ar), 6.48 (d, *J* = 7.0 Hz, 1H, CHN*H*), 4.35–4.10 (m, 5H, OCH_2C*H*CH_2O), 2.12 (s, 6H, CH_3). ^{13}C NMR (125 MHz, DMSO-d_6) δ 154.7, 154.5, 139.7, 137.6, 136.4, 131.3, 130.0, 129.1, 123.9, 122.4, 121.7, 119.6, 118.4, 117.8, 63.2, 48.2, 20.3. HRMS (*m*/*z*): calcd for $C_{27}H_{26}ClF_3N_4O_5Na$ 601.1436 $[M+Na]^+$; found 601.1430. Anal. Calcd for $C_{27}H_{26}ClF_3N_4O_5$: C, 56.01; H, 4.53; N, 9.68. Found: C, 56.21; H, 4.51; N, 9.70.

***N*-{1,3-Bis[(4-nitrophenyl)aminocarboxy]prop-2-yl}-*N'*-[4-chloro-3-(trifluoromethyl)phenyl]urea (166).** The product was obtained as a yellow solid and purified by column chromatography using hexane-ethyl acetate (1.5:2) as eluent. (264 mg; 65% yield); mp 223–224 ºC. ^{1}H NMR (500 MHz, DMSO-d_6) δ 10.48 (s, 2H, ArN*H*COO), 9.11 (s, 1H, CON*H*Ar), 8.24–8.18 (m, 4H, Ar), 8.07–8.05 (m, 1H, Ar), 7.77–7.68 (m, 4H, Ar), 7.57–7.52 (m, 2H, Ar), 6.54 (d, *J* = 7.2 Hz, 1H, CHN*H*), 4.40–4.25 (m, 5H, OCH_2C*H*CH_2O). ^{13}C NMR (125 MHz, DMSO-d_6) δ 154.5, 153.0, 145.4, 141.7, 139.7, 139.1, 131.8, 124.9, 124.8, 122.5, 121.7, 117.8, 63.9, 47.9. HRMS (*m*/*z*): calcd for $C_{25}H_{20}ClF_3N_6O_9Na$ 663.0825 $[M+Na]^+$; found 663.0817. Anal. Calcd for $C_{25}H_{20}ClF_3N_6O_9$: C, 46.85; H, 3.15; N, 13.11. Found: C, 46.78; H, 3.17; N, 13.08.

***N*-{1,3-Bis[(4-methylphenyl)aminocarboxy]prop-2-yl}-*N'*-(4-methylphenyl)urea (167).** The product was obtained as a white solid and purified by filtration of the reaction mixture with fresh toluene. (147 mg; 46% yield); mp 209–210 ºC. ^{1}H NMR (500 MHz, DMSO-d_6) δ 9.58 (s, 2H, ArN*H*COO), 8.48 (s, 1H, CON*H*Ar),7.40–7.29 (d, *J* = 7.90 Hz, 4H, Ar), 7.28–7.21 (d, *J* = 8.35 Hz, 2H, Ar), 7.10–6.97 (m, 6H, Ar), 6.26 (d, *J* = 6.65 Hz, 1H, CHN*H*), 4.35–4.10 (m, 5H, OCH_2C*H*CH_2O), 2.22 (s, 9H, CH_3). ^{13}C NMR (125 MHz, DMSO-d_6) δ 154.7, 153.3, 137.6, 136.4, 131.3, 129.6, 118.4, 117.8, 63.4, 47.9, 20.3. HRMS (*m*/*z*): calcd for $C_{27}H_{30}N_4O_5Na$ 513.2108 $[M+Na]^+$; found 513.2101. Anal. Calcd for $C_{27}H_{30}N_4O_5$: C, 66.11; H, 6.16; N, 11.42. Found: C, 65.99; H, 6.15; N, 11.46.

***N*-{1-Hydroxy-3-[(4-nitrophenyl)aminocarboxy]prop-2-yl}-*N'*-[4-(trifluoromethyl)phenyl]urea (168).** The product was obtained as a light yellow solid and purified by column chromatography using hexane-ethyl acetate (1:2) as eluent (74 mg; 24% yield); mp 100–101 ºC. ^{1}H NMR (500 MHz, DMSO-d_6) δ 10.40 (s, 1H, ArN*H*COO), 9.02 (s, 1H, CON*H*Ar), 8.19 (d, *J* = 9.3 Hz, 2H, Ar), 7.71 (d, *J* = 9.3 Hz, 2H, Ar), 7.61–7.51 (m, 4H, Ar), 6.38 (d, *J* = 6.3 Hz, 1H, CHN*H*), 5.02 (t, *J* = 5.1 Hz, 1H, OH), 4.33–4.10 (m, 2H, OCH_2), 4.04–3.94 (m, 1H, C*H*), 3.64–3.56 (m, 1H, CH_2OH), 3.55–3.46 (m, 1H, CH_2OH). ^{13}C NMR (125 MHz, DMSO-d_6) δ 154.5, 139.9, 153.2, 145.6, 143.9, 141.7, 125.9, 125.6, 124.9, 123.5, 117.7, 117.2, 64.2, 60.3, 49.9. HRMS (*m*/*z*): calcd

for $C_{18}H_{17}F_3N_4O_6Na$ 465.0992 $[M+Na]^+$; found 465.0986. Anal. Calcd for $C_{18}H_{17}F_3N_4O_6$: C, 48.87; H, 4.87; N, 12.67. Found: C, 49.04; H, 4.85; N, 12.64.

*B) Synthesis of dicarbamate derivatives from prepared isocyanate (**160**, **165**).* 1-Isocyanato-2-methylbenzene (**251**) (1 mmol), previously synthesized (**section 6.1.4**) was dissolved in DCM (20 mL), then DMAP (1 mmol) and appropriate urea derivatives (**129** or **129**, 0.42 mmol) were added. The reaction mixture was stirred for 48 h and then concentred under reduced pressure. The crude product was purified through flash column chromatography using hexane-ethyl acetate as eluent.

***N*-{1,3-Bis[(2-methylphenyl)aminocarboxy]prop-2-yl}-*N'*-[4-(trifluoromethyl)phenyl]urea (160).** The product was obtained as a white solid and purified by column chromatography using hexane-ethyl acetate (3.5:1) as eluent (100 mg; 43% yield); mp 198–199 ºC. ^{1}H NMR (500 MHz, DMSO-d_6) δ 9.12–9.07 (m, 1H, CON*H*Ar), 8.91 (s, 2H, ArN*H*COO), 7.72–7.57 (m, 5H, Ar), 7.35 (d, J = 7.8 Hz, 2H, Ar), 7.21–7.04 (m, 5H, Ar), 6.52–6.42 (m, 1H, CHN*H*), 4.36–4.18 (m, 5H, OCH_2C*H*CH_2O), 2.21 (s, 6H, CH_3). ^{13}C NMR (125 MHz, DMSO-d_6) δ 154.4, 154.2, 143.9, 136.2, 131.8, 126.0, 125.7, 123.5, 118.0, 117.3, 63.4, 48.2, 17.7. HRMS (*m*/*z*): calcd for $C_{27}H_{27}F_3N_4O_5Na$ 567.1826 $[M+Na]^+$; found 567.1818. Anal. Calcd for $C_{27}H_{27}F_3N_4O_5$: C, 59.56; H, 5.00; N, 10.29. Found: C, 59.36; H, 5.01; N, 10.28.

***N*-{1,3-Bis[(2-methylphenyl)aminocarboxy]prop-2-yl}-*N'*-[4-chloro-3-(trifluoromethyl)phenyl]urea (165).** The product was obtained as a white solid and purified by column chromatography using hexane-ethyl acetate (3:1) as eluent. (117 mg; 48% yield); mp 200–201 ºC. ^{1}H NMR (500 MHz, DMSO-d_6) δ 9.21–9.12 (m, 1H, CON*H*Ar), 8.91 (s, 2H, ArN*H*COO), 7.67–7.49 (m, 4H, Ar), 7.42–7.28 (m, 2H, Ar), 7.22–7.02 (m, 5H, Ar), 6.51–6.42 (m, 1H, CHN*H*), 4.36–4.16 (m, 5H, OCH_2C*H*CH_2O), 2.21 (s, 6H, CH_3). ^{13}C NMR (125 MHz, DMSO-d_6) δ 154.5, 154.2, 139.8, 136.2, 131.8, 130.2, 129.2, 128.5, 125.9, 124.9, 122.9, 63.4, 48.3, 17.6. HRMS (*m*/*z*): calcd for $C_{27}H_{26}ClF_3N_4O_5Na$ 601.1436 $[M+Na]^+$; found 601.1431. Anal. Calcd for $C_{27}H_{26}ClF_3N_4O_5$: C, 56.01; H, 4.53; N, 9.68. Found: C, 55.45; H, 4.52; N, 9.66.

6.1.3 3-Phenylaminocarbonyl-1,2-propanediol derivatives

-General procedure 8. Synthesis of urea derivatives of 3-amino-1,2-propanediol and allylamine (173-179, 233)

*A) Synthesis of urea derivatives from commerical isocyanates (**173-176**, **178**, **233**).* Compounds were prepared following the general procedure 4, **section 6.1.2**.

***N*-(4-Chlorophenyl)-*N'*-(2,3-dihydroxypropyl)urea (173)** [119]**.** The product was obtained as a white solid (690 mg; 94% yield), mp 160–161 ºC. ^{1}H NMR (500 MHz, DMSO-d_6) δ 8.76 (s, 1H, N*H*Ar), 7.37–7.35 (m, 2H, Ar), 7.25–7.23 (m, 2H, Ar), 6.19 (t, *J* = 5.5 Hz, 1H, CH_2N*H*), 5.01 (d, *J* = 4.9 Hz, 1H. CHO*H*), 4.82 (t, *J* = 5,2 Hz, 1H, CH_2O*H*), 3.56–3.50 (m, 2H, CH_2OH), 3.38–3.30 (m, 2H, CH_2NH), 3.03–2.98 (m, 1H, CH). ^{13}C NMR (125 MHz, DMSO-d_6) δ 155.6, 139.1, 128.4, 124.8, 119.4, 70.5, 63.5, 42.4. HRMS (*m/z*): calcd for $C_{10}H_{13}ClN_2O_3Na$ 267.0507 [M+Na]$^+$; found 267.0501. Anal. Calcd for $C_{10}H_{13}ClN_2O_3$: C, 49.09; H, 5.36; N, 11.45. Found: C, 49.51; H, 5.66; N, 11.34.

***N*-(2,3-Dihydroxypropyl)-*N'*-(4-methylphenyl)urea (174).** The product was obtained as a white solid (615 mg; 91% yield), mp 147–148 ºC. ^{1}H NMR (500 MHz, DMSO-d_6) δ 8.48 (s, 1H, N*H*Ar), 7.26 (d, *J* = 8.5 Hz, 2H, Ar), 7.03 (d, *J* = 8.2 Hz, 2H, Ar), 6.10 (t, *J* = 5.6 Hz, 1H, CH_2N*H*), 4.85 (d, *J* = 4.9 Hz, 1H, CHO*H*), 4.60 (t, *J* = 5.7 Hz, 1H, CH_2O*H*), 3.51 (sex, *J* = 5.6 Hz, 1H, CH), 3.32–3.27 (m, 2H, CH_2OH), 3.01-2.95 (m, 2H, CH_2NH), 2.22 (s, 3H, CH_3). ^{13}C NMR (125 MHz, DMSO-d_6) δ 155.6, 138.1, 129.6, 129.0, 117.6, 70.7, 63.7, 42.5, 20.3. HRMS (*m/z*): calcd for $C_{11}H_{16}N_2O_3Na$ 247.1064 [M+Na]$^+$; found 247.1056. Anal. Calcd for $C_{11}H_{16}N_2O_3$: C, 58.91; H, 7.19; N, 12.49. Found: C, 58.53; H, 7.03; N, 12.16.

***N*-(2,3-Dihydroxypropyl)-*N'*-[4-(trifluoromethyl)phenyl]urea (175).** The product was obtained as a white solid (673 mg; 80% yield) , mp 135–136 ºC ^{1}H NMR (500 MHz, DMSO-d_6) δ 9,04 (s, 1H, N*H*Ar), 7.60–7.57 (m, 4H, Ar), 6.30 (t, *J* = 5,3 Hz, 1H, CH_2N*H*), 4.88 (d, *J* = 5.0 Hz, 1H, CHO*H*), 4.61 (t, *J* = 5,6 Hz, 1H, CH_2O*H*), 3.57–3.51 (m, 1H, CH), 3.35–3.30 (m, 2H, CH_2OH), 3.04–2.99 (m, 2H, CH_2NH). ^{13}C NMR (125 MHz, DMSO-d_6) δ 155.0, 144.2, 125.9, 121.0, 120.8, 117.1, 70.5, 63.7, 42.5. HRMS (*m/z*): calcd for $C_{11}H_{13}F_3N_2O_3Na$ 301.0770 [M+Na]$^+$; found 301,0769. Anal. Calcd for $C_{11}H_{13}F_3N_2O_3$: C, 47.49; H, 4.71; N, 10.07. Found: C, 49.51; H, 5.66; N, 11.34.

***N*-(2,3-Dihydroxypropyl)-*N'*-(4-methoxyphenyl)urea (176).** The product was obtained as a white solid (635 mg; 88% yield), mp 155–156 ºC. ^{1}H NMR (300 MHz, DMSO-d_6) δ 8.39 (s, 1H, N*H*Ar),

7.28 (d, J = 6.8 Hz, 2H, Ar), 6.81 (d, J = 6.8 Hz, 2H, Ar), 6.03 (t, J = 5.5 Hz, 1H, CH_2NH), 4.85 (d, J = 4.8 Hz, 1H, CHO*H*), 4.60 (t, J = 5.7 Hz, 1H, CH_2OH), 3.69 (s, 3H, OCH_3), 3.53–3.44 (m, 1H, CH), 3.38–3.23 (m, 2H, CH_2OH), 3.02–2.92 (m, 2H, CH_2NH). ^{13}C NMR (125 MHz, DMSO-d_6) δ 156.2, 154.1, 134.2, 119.7, 114.3, 71.2, 64.1, 55.6, 43.1.

***N*-[2-Chloro-5-(trifluoromethyl)phenyl]-*N'*-(2,3-dihydroxypropyl)urea (178).** The product was obtained as a white solid (680 mg; 72% yield), mp 129–130 ºC. MS (FAB): *m/z* 403 (65%) $[M+Na]^+$. ^{1}H NMR (500 MHz, DMSO-d_6) δ 8.66 (s, 1H, N*H*Ar), 8.50 (s, 1H, Ar), 7.65 (d, J = 5.3 Hz, 1H, Ar), 7.32-7.26 (m, 2H, Ar + CH_2NH), 4.85 (m, 1H, CHO*H*), 4.58 (t, J = 5.7 Hz, 1H, CH_2OH), 3.58-3.52 (m, 1H, CH), 3.41-3.34 (m, 2H, CH_2OH), 3.05-2.99 (m, 2H, CH_2NH). ^{13}C NMR (125 MHz, DMSO-d_6) δ 154.8, 137.7, 130.2, 128.2, 124.4, 118.2, 116.3, 70.5, 63.7, 42.5.

***N*-Allyl-*N'*-(4-chlorophenyl)urea (233).** The product was obtained as a white solid and purified by column chromatography using dichloromethane-methanol (140:1) as eluent (570 mg; 90% yield). ^{1}H NMR (500 MHz, DMSO-d_6) δ 8.66 (s, 1H, N*H*Ar), 7.46 (d, J = 8.3 Hz, 2H, Ar), 7.30 (d, J = 8.7 Hz, 2H, Ar), 6.32 (t, J = 5.3 Hz, 1H, CH_2NH), 5.91–5.87 (m, 1H, CH_2=C*H*), 5.23–5.18 (m, 1H, CH_2=CH), 5.13–5.08 (m, 1H, CH_2=CH), 3.77 (t, J = 5.4 Hz, 1H, CH_2NH). ^{13}C NMR (125 MHz, DMSO-d_6) δ 154.9, 139.4, 136.2, 128.6, 128.4, 124.5, 119.8, 119.1, 114.7, 41.4. HRMS (*m/z*): calcd for $C_{10}H_{12}ClN_2O$ 211.0633 $[M+H]^+$; found 211.0633. Anal. Calcd for $C_{10}H_{11}ClN_2O$: C, 57.02; H, 5.26; N, 13.30. Found: C, 56.79; H, 5.03; N, 12.86.

*B) Synthesis of urea derivatives from substituted anilines (**177** and **179**).* According to a reported procedure with some modifications [105], a solution of appropriate substituted aniline (1.2 mmol) in DCM (25 mL) was added to a solution of Na_2CO_3 (1.92 mmol) in water (25 mL) and the reaction mixture was vigorously stirred for 5 minutes at rt; then triphosgene (0.39 mmol) was added and the solution was stirred for additional 30 minutes. After this time, 3-amino-1,2-propanediol (1.8 mmol) was added dropwise to the flask and the solution was stirred at rt until TLC showed the full consumption of the starting material (2 hours). The mixture was separated and the inorganic layer was extracted with ethyl acetate (3 x 40 mL). The combined organic layers were dried over $MgSO_4$, filtered and evaporated *in vacuo* to obtain a crude product. The compound was further purified by flash column chromatography on silica gel using the appropriate eluent or by filtration at vacuum.

***N*-(2,3-Dihydroxypropyl)-*N'*-(2-methylphenyl)urea (177).** The product was obtained as a white resin by filtration at *vacuum*. (455 mg; 67% yield). ^{1}H NMR (300 MHz, DMSO-d_6) δ 7.87–7.77 (m, 2H, N*H*Ar, Ar), 7.13–7.04 (m, 1H, Ar), 6.85 (t, J = 7.3 Hz, 2H, Ar), 6.63 (t, J = 5.2 Hz, 1H, CH_2NH),

4.89–4.84 (m, 1H, CHO*H*), 4.63–4.56 (m, 1H, CH_2O*H*), 3.55–3.46 (m, 1H, CH), 3.33–3.25 (m, 2H, C*H*$_2$OH), 3.03-2.93 (m, 2H, C*H*$_2$NH), 2.18 (s, 3H, CH_3). ^{13}C NMR (125 MHz, DMSO-*d*$_6$) δ 156.2, 138.7, 130.5, 127.0, 126.5, 122.2, 120.8, 71.3, 64.1, 42.9, 18.4.

***N*-(2,3-Dihydroxypropyl)-*N'*-(3,4,5-trimethoxyphenyl)urea (179).** The product was obtained as a white solid and purified by flash column chromatography using dichloromethane-methanol (15:1) as eluent. (255 mg; 70% yield), mp 165–166 ºC. ^{1}H NMR (500 MHz, DMSO-*d*$_6$) δ 8.55 (s, 1H, N*H*Ar), 6.73 (s, 2H, Ar), 6.08 (t, *J* = 5.65 Hz, 1H, CH_2N*H*), 4.81 (d, *J* = 4.8 Hz, 1H, CHO*H*), 4.57 (t, *J* = 5.70 Hz, 1H, -CH_2O*H*), 3.73 (s, 6H, OCH_3), 3.60 (s, 3H, OCH_3), 3.54–3.49 (m, 1H, CH), 3.39–3.26 (m, 2H, C*H*$_2$OH), 3.03–2.95 (m, 2H, C*H*$_2$NH). ^{13}C NMR (125 MHz, DMSO-*d*$_6$) δ 155.5, 152.7, 136.7, 131.9, 95.4, 70.6, 63.7, 60.0, 55.6, 42.4. HRMS (*m/z*): calcd for $C_{13}H_{20}N_2O_6Na$ 323.1214 $[M+Na]^+$; found 323.1211.

-General procedure 9. Acylation reaction from acyl chloride (180-209, 212-223)

*A) O,O'-Diacylation reaction of N-(2,3-dihydroxypropyl)-N'-(substituted)phenylureas (**180-209**).* Compounds were prepared following the general procedure 5A **section 6.1.2**.

***N*-[2,3-Bis(benzoyloxy)propyl]-*N'*-(4-chlorophenyl)urea (180).** The product was obtained as a white solid and purified by column chromatography using hexane-ethyl acetate (1:1) as eluent (160 mg; 70% yield), mp 130–131 ºC. NMR (500 MHz, DMSO-*d*$_6$) δ 8.72, (s, 1H, N*H*Ar), 8.02 (d, *J* = 7.5 Hz, 2H, Ar), 7.95 (d, *J* = 7.5 Hz, 2H, Ar), 7.60–7.52 (m, 2H, Ar), 7.55–7.49 (m, 4H, Ar), 7.43 (d, *J* = 8.8 Hz, 2H, Ar), 7.28 (d, *J* = 8.7 Hz, 2H, Ar), 6.50 (t, *J* = 5.9 Hz, 1H, CH_2N*H*), 5.52–5.45 (m, 1H, CH), 4.67 (dd, *J* = 3.4 Hz, *J* = 12.0 Hz, 1H, C*H*$_2$O), 4.52 (dd, *J* = 6.6 Hz, *J* = 12.0 Hz, 1H, C*H*$_2$O), 3.70–3.58 (m, 2H, C*H*$_2$NH). ^{13}C NMR (125 MHz, DMSO-*d*$_6$) δ 165.4, 165.3, 155.2, 139.3, 133.4,129.6, 129.4, 129.3, 129.1, 128.7, 128.6, 128.4, 124.7 119.2, 710.6, 63.7, 39.5. HRMS (*m/z*): calcd for $C_{24}H_{21}ClN_2O_5Na$ 475.1031 $[M+Na]^+$; found 475.1026.

***N*-[2,3-Bis(4-methylbenzoyloxy)propyl]-*N'*-(4-chlorophenyl)urea (181)** [119]**.** The product was obtained as a colourless oil and purified by column chromatography using hexane-ethyl acetate (1.5:1) as eluent (205 mg; 85% yield). MS (FAB): *m/z* 503 (100%) $[M+Na]^+$. ^{1}H NMR (500 MHz, DMSO-*d*$_6$) δ 8.72, (s, 1H, N*H*Ar), 7.89–7.87 (m, 2H, Ar), 7.83–7.81 (m, 2H, Ar), 7.42–7.40 (m, 2H, Ar), 7.33–7.29 (m, 4H, Ar), 7.27–7.25 (m, 2H, Ar), 6.28 (t, *J* = 5.8 Hz, 1H, CH_2N*H*), 5.46–5.41 (m, 1H, CH), 4.61 (dd, *J* = 4.1 Hz, *J* = 12.0 Hz, 1H, C*H*$_2$O), 4.46 (dd, *J* = 6.0 Hz, *J* = 11.6 Hz, 1H, C*H*$_2$O), 3.62–3.54 (m, 2H, C*H*$_2$NH), 2.38 (s, 3H, CH_3), 2.37 (s, 3H, CH_3). ^{13}C NMR (125 MHz, DMSO-*d*$_6$)

δ 165.4, 165.2, 155.1, 143.8, 143.6, 139.3, 129.4, 129.3, 129.2, 129.1, 128.4, 126.8, 124.4, 119.2, 71.3, 65.7, 30.7, 21.2, 21.1. Anal. Calcd for $C_{26}H_{25}ClN_2O_5$: C, 64.93; H, 5.24; N, 5.82. Found: C, 64.82; H, 5.76; N, 5.74.

***N*-[2,3-Bis(2-methylbenzoyloxy)propyl]-*N'*-(4-chlorophenyl)urea (182)** [119]**.** The product was obtained as a colourless oil and purified by column chromatography hexane-ethyl acetate (1.5:1) as eluent (216 mg; 90% yield). MS (FAB): *m/z* 503 (100%) $[M+Na]^+$. ^{1}H NMR (500 MHz, DMSO-d_6) δ 8.72, (s, 1H, N*H*Ar), 7.88–7.86 (m, 1H, Ar), 7.83–7.81 (m, 1H, Ar), 7.50–7.46 (m, 2H, Ar), 7.43–7.41 (m, 2H, Ar), 7.43–7.27 (m, 6H, Ar), 6.48 (t, *J* = 6.0 Hz, 1H, CH_2N*H*), 5.50–5.45 (m, 1H, CH), 4.63 (dd, *J* = 3.4 Hz, *J* = 12.0 Hz, 1H, CH_2O), 4.48 (dd, *J* = 6.5 Hz, *J* = 12.0 Hz, 1H, CH_2O), 3.64–3.55 (m, 2H, CH_2NH), 2.49 (s, 3H, CH_3), 2.48 (s, 3H, CH_3). ^{13}C NMR (125 MHz, DMSO-d_6) δ 167.0, 166.8, 155.6, 139.8, 139.7, 139.6, 132.8, 132.7, 132.1, 132.0, 130.7, 130.6, 129.9, 129.5, 128.9, 126.5, 126.3, 125.2, 119.8, 71.8, 64.1, 31.2, 21.5, 21.4. Anal. Calcd for $C_{26}H_{25}ClN_2O_5$: C, 64.93; H, 5.24; N, 5.82. Found: C, 64.75; H, 5.58; N, 5.60.

***N*-[2,3-Bis(4-methoxybenzoyloxy)propyl]-*N'*-(4-chlorophenyl)urea (183)** [119]**.** The product was obtained as a white solid and purified by column chromatography using hexane-ethyl acetate (1:1) as eluent (190 mg; 74% yield), mp 202–203 ºC. ^{1}H NMR (500 MHz, DMSO-d_6) δ 8.71, (s, 1H, N*H*Ar), 7.96–7.94 (m, 2H, Ar), 7.90–7.88 (m, 2H, Ar), 7.44–7.42 (m, 2H, Ar), 7.27–7.25 (m, 2H, Ar), 7.04–7.01 (m, 4H, Ar), 6.48 (t, *J* = 5.7 Hz, 1H, CH_2N*H*), 5.45–5.41 (m, 1H, CH), 4.59 (dd, *J* = 3.5 Hz, *J* = 12.1 Hz, 1H, CH_2O), 4.46 (dd, *J* = 6.7 Hz, *J* = 11.8 Hz, 1H, CH_2O), 3.63–3.55 (m, 2H, CH_2NH), 3.83 (s, 3H, OCH_3), 3.82 (s, 3H, OCH_3). ^{13}C NMR (125 MHz, DMSO-d_6) δ 165.1, 165.0, 163.3, 163.2, 155.1, 139.3, 131.4, 131.3, 128.4, 124.7, 121.8, 121.5, 119.2, 114.0, 113.9, 71.2, 63.4, 55.5, 55.4, 31.2. HRMS (*m/z*): calcd for $C_{26}H_{25}ClN_2O_7Na$ 535.1242 $[M+Na]^+$; found 535.1247.

***N*-[2,3-Bis(4-cyanobenzoyloxy)propyl]-*N'*-(4-chlorophenyl)urea (184)** [119]**.** The product was obtained as a white solid and purified by column chromatography using hexane-ethyl acetate (1.5:1) as eluent (150 mg; 60% yield), mp 205–206 ºC. ^{1}H NMR (500 MHz, DMSO-d_6) δ 8.70, (s, 1H, N*H*Ar), 8.13–8.12 (m, 2H, Ar), 8.08–8.06 (m, 2H, Ar), 8.01–7.99 (m, 4H, Ar), 7.40–7.38 (m, 2H, Ar), 7.26–7.23 (m, 2H, Ar), 6.51 (t, *J* = 5.7 Hz, 1H, CH_2N*H*), 5.50–5.47 (m, 1H, CH), 4.70 (dd, *J* = 3.3 Hz, *J* = 12.4 Hz, 1H, CH_2O), 4.56 (dd, *J* = 6.6 Hz, *J* = 12.0 Hz, 1H, CH_2O), 3.67-3.60 (m, 2H, CH_2NH). ^{13}C NMR (125 MHz, DMSO-d_6) δ 164.3, 164.2, 155.2, 139.2, 133.5, 133.2, 132.8, 132.7, 129.9, 129.8, 128.4, 124.7, 119.3, 118.0, 117.9, 115.6, 7.23, 64.3. HRMS (*m/z*): calcd for

$C_{26}H_{19}ClN_4O_5Na$ 525.0936 $[M+Na]^+$; found 525.0933. Anal. Calcd for $C_{26}H_{19}ClN_4O_5$: C, 62.09; H, 3.82; N, 11.14. Found: C, 62.25; H, 3.81; N, 11.00.

***N*-[2,3-Bis(4-nitrobenzoyloxy)propyl]-*N'*-(4-chlorophenyl)urea (185)** [119]**.** The product was obtained as a yellow solid and purified by column chromatography using hexane-ethyl acetate (1:1) as eluent (244 mg; 90% yield), mp 216-217 ºC. mp 216–217 ºC. MS (FAB): *m/z* 565 (100%) $[M+Na]^+$. ^{1}H NMR (500 MHz, DMSO-d_6) δ 8.70, (s, 1H, N*H*Ar), 8.35–8.33 (m, 4H, Ar), 8.23–8.21 (m, 2H, Ar), 8.18–8.16 (m, 2H, Ar), 7.41–7.38 (m, 2H, Ar), 7.26–7.23 (m, 2H, Ar), 6.53 (t, *J* = 6.01 Hz, 1H, CH_2N*H*), 5.55–5.51 (m, 1H, CH), 4.74 (dd, *J* = 3.3 Hz, *J* = 12.2 Hz, 1H, C*H*$_2$O), 4.60 (dd, *J* = 6.7 Hz, *J* = 12.2 Hz, 1H, C*H*$_2$O), 3.70–3.60 (m, 2H, C*H*$_2$NH). ^{13}C NMR (125 MHz, DMSO-d_6) δ 164.1, 163.0, 155.2, 150.4, 150.3, 139.2, 134.9, 134.7, 130.8, 130.6, 128.4, 124.7, 123.9, 123.8, 119.2, 72.5, 64.4.

***N*-{2,3-Bis[(4-trifluoromethyl)benzoyloxy]propyl}-*N'*-(4-chlorophenyl)urea (186).** The product was obtained as a white solid and purified by column chromatography using hexane-ethyl acetate (2:1) as eluent (198 mg; 67% yield), mp 156–157 ºC. ^{1}H NMR (500 MHz, DMSO-d_6) δ 8.73, (s, 1H, N*H*Ar), 8.21 (d, *J* = 8.53 Hz, 2H, Ar), 8.16 (d, *J* = 8.62 Hz, 2H, Ar), 7.93–7.88 (m, 4H, Ar), 4.43–4.41 (m, 2H, Ar), 7.28–7.24 (m, 2H, Ar), 6.54 (t, *J* = 5.90 Hz, 1H, CH_2N*H*), 5.57–5.52 (m, 1H, CH), 4.74 (dd, *J* = 3.6 Hz, *J* = 12.3 Hz, 1H, C*H*$_2$O), 4.61 (dd, *J* = 6.6 Hz, *J* = 12.0 Hz, 1H, C*H*$_2$O), 3.72–3.62 (m, 2H, C*H*$_2$NH). ^{13}C NMR (125 MHz, DMSO-d_6) δ 164.4, 164.3, 155.2, 139.2, 133.3, 133.1, 133.0, 132.9, 130.2, 130.0, 128.4, 125.8, 125.7, 125.6, 124.7, 122.6, 122.5, 119.2, 72.2, 64.2. HRMS (*m/z*): calcd for $C_{26}H_{19}Cl\ F_6N_2O_5Na$ 611.0779 $[M+Na]^+$; found 611.0771. Anal. Calcd for $C_{26}H_{19}ClF_6N_2O_5$: C, 53.03; H, 3.25; N, 4.76. Found: C, 52.75; H, 3.36; N, 4.77.

***N*-[2,3-Bis(2,4-dimethoxybenzoyloxy)propyl]-*N'*-(4-chlorophenyl)urea (187)** The product was obtained as a white solid and purified by column chromatography using hexane-ethyl acetate (1:1.5) as eluent (235 mg; 82% yield), mp 113–114 ºC. ^{1}H NMR (500 MHz, DMSO-d_6) δ 8.75, (s, 1H, N*H*Ar), 7.78–7.72 (m, 2H, Ar), 7.45 (d, *J* = 8.5 Hz, 2H, Ar), 7.28 (d, *J* = 8.9 Hz, 2H, Ar), 6.65 (s, 2H, Ar), 6.62–6.57 (m, 2H, Ar), 6.42 (t, *J* = 5.7 Hz, 1H, CH_2N*H*), 5.35–5.30 (m, 1H, CH), 4.47 (dd, *J* = 3.2 Hz, *J* = 12.1 Hz, 1H, C*H*$_2$O), 4.37 (dd, *J* = 6.5 Hz, *J* = 12.2 Hz, 1H, C*H*$_2$O), 3.85 (d, *J* = 3.3 Hz, 6H, OCH_3), 3.80 (d, *J* = 4.5 Hz, 6H, OCH_3), 3.55 (t, *J* = 5.5 Hz, 2H, C*H*$_2$NH). ^{13}C NMR (125 MHz, DMSO-d_6) δ 164.5, 164.1, 164.0, 163.9, 161.0, 160.9, 155.1, 139.3, 133.2, 133.1, 128.4, 124.6, 119.2, 111.6, 111.3, 105.3, 105.2, 98.9, 70.5, 62.9, 55.7, 55.5. HRMS (*m/z*): calcd for $C_{28}H_{29}ClN_2O_9Na$

595.1454 [M+Na]$^+$; found 595.1447. Anal. Calcd for $C_{28}H_{29}ClN_4O_9$: C, 58.69; H, 5.10; N, 4.89. Found: C, 58.25; H, 5.23; N, 4.44.

***N*-[2,3-Bis(3,4,5-trimethoxybenzoyloxy)propyl]-*N'*-(4-chlorophenyl)urea (188)** The product was obtained as a white solid and purified by column chromatography using hexane-ethyl acetate (1:1.5) as eluent (248 mg; 78% yield), mp 163–164 ºC. ^{1}H NMR (500 MHz, DMSO-d_6) δ8.73 (s, 1H, N*H*Ar), 7.41 (d, *J* = 8.7 Hz, 2H, Ar),7.28-7.25 (m, 4H, Ar), 7.22 (s, 2H, Ar), 6.49 (t, *J* = 8.2 Hz 1H, CH_2N*H*), 5.48-5.42 (m, 1H, CH), 4.65 (dd, *J* = 3.4 Hz, , *J* = 11.9 Hz, 1H, C*H*$_2$O), 4.49-4.42 (m, 1H, C*H*$_2$O), 3.81-3.76 (m, 12H, OCH_3) 3.74-3.71 (m, 6H, OCH_3), 3.66-3.55 (m, 2H, C*H*$_2$NH). ^{13}C NMR (125 MHz, DMSO-d_6) δ165.0, 164.9, 155.2, 152.7, 152.6, 141.9, 141.8, 139.2, 129.2, 128.4, 124.7, 124.6, 124.3, 119.2, 106.8, 106.4, 71.7, 63.6, 60.1, 55.9, 55.8. HRMS (*m/z*): calcd. for $C_{30}H_{33}ClN_2O_{11}Na$ 655.1665 [M+Na]$^+$; found 655.1653.

***N*-[2,3-Bis(4-methylbenzoyloxy)propyl]-*N'*-(4-methylphenyl)urea (189).** The product was obtained as a white solid and purified by column chromatography using hexane-ethyl acetate (2.5:1) as eluent (175 mg; 84% yield), mp 95–96 ºC. ^{1}H NMR (500 MHz, DMSO-d_6) δ8.44 (s, 1H, N*H*Ar), 7.89 (d, *J* = 8.2 Hz, 2H, Ar), 7.82 (d, *J* = 8.2 Hz, 2H, Ar), 7.31 (t, *J* = 6.7 Hz, 4H, Ar), 7.27 (d, *J* = 8.4 Hz, 2H, Ar), 7.02 (d, *J* = 8.3 Hz, 2H, Ar), 6.39 (t, *J* = 6.0 Hz, 1H, CH_2N*H*), 5.44 (quint, *J* = 5.2 Hz, 1H, CH), 4.62 (dd, *J* = 3,5 Hz, *J* = 8,6 Hz, 1H, C*H*$_2$O), 4.47 (dd, *J* = 6,8 Hz, J = 5,2 Hz, 1H, C*H*$_2$O), 3.63–3.54 (m, 2H, C*H*$_2$NH), 2.37 (d, *J* = 4,0 Hz, 6H, CH_3), 2.22 (s, 3H, CH_3). ^{13}C NMR (125 MHz, DMSO-d_6) δ165.4, 165.3, 155.3, 143.8, 143.7, 137.7, 129.9, 129.4, 129.3, 129.2, 129.1(2C), 128.9, 126.9, 126.7, 117.9, 71.4, 63.6, 26.8, 21.1, 20.3. HRMS (*m/z*): calcd for $C_{27}H_{28}N_2O_5Na$ 483.1890 [M+Na]$^+$; found 483.1884. Anal. Calcd for $C_{27}H_{28}N_2O_5$: C, 70.42; H, 6.13; N, 6.08. Found: C, 69.40; H, 5.96; N, 5.89.

***N*-[2,3-Bis(2-methylbenzoyloxy)propyl]-*N'*-(4-methylphenyl)urea (190).** The product was obtained as a white solid and purified by column chromatography using hexane-ethyl acetate (2.5:1) as eluent (168 mg; 74% yield), mp 116–117 ºC. ^{1}H NMR (500 MHz, DMSO-d_6) δ8.45 (s, 1H, N*H*Ar), 7.87 (d, *J* = 7.7 Hz, 2H, Ar), 7.83 (d, *J* = 7.7 Hz, 2H, Ar),7.51–7.46 (m, 2H, Ar), 7.34–7.25 (m, 6H, Ar), 7.03 (d, *J* = 8.0 Hz, 2H, Ar), 6.39 (t, *J* = 5.9 Hz, 1H, CH_2N*H*), 5.50–5.44 (m, 1H, CH), 4.63 (dd, *J* = 3.3 Hz, *J* = 12.1 Hz, 1H, C*H*$_2$O), 4.48 (dd, *J* = 6.8 Hz, *J* = 12.1 Hz, 1H, C*H*$_2$O), 3.63–3.53 (m, 2H, C*H*$_2$NH), 2.49 (s, 6H, CH_3), 2.22 (s, 3H, CH_3). ^{13}C NMR (125 MHz, DMSO-d_6) δ166.5, 166.3, 155.3, 139.2, 139.1, 137.7, 132.3, 132.2, 131.6, 131.5, 130.2, 130.1, 129.9, 129.3, 129.1, 129.0, 125.9,

125.8, 117.2, 71.3, 63.5, 21.0, 20.8, 20.2. HRMS (*m/z*): calcd for $C_{27}H_{28}N_2O_5Na$ 483.1890 $[M+Na]^+$; found 483.1886.

***N*-[2,3-Bis(4-methoxybenzoyloxy)propyl]-*N'*-(4-methylphenyl)urea (191).** The product was obtained as a solid and purified by column chromatography using hexane-ethyl acetate (2:1) as eluent (150 mg; 61% yield), mp 144–145 ºC. ^{1}H NMR (500 MHz, DMSO-d_6) δ 8.42 (s, 1H, N*H*Ar), 7.95 (d, *J* = 7.5 Hz, 2H, Ar), 7.89 (d, *J* = 9.1 Hz, 2H, Ar), 7.27 (d, *J* = 8.0 Hz, 2H, Ar), 7.05–7.00 (m, 6H, Ar), 6.37 (t, *J* = 6.0 Hz, 1H, CH_2N*H*), 5.43–5.39 (m, 1H, CH), 4.58 (dd, *J* = 3.8 Hz, *J* = 11.5 Hz, 1H, C*H*$_2$O), 4.45 (dd, *J* = 3.8 Hz, *J* = 11.5 Hz, 1H, C*H*$_2$O), 3.83 (s, 6H, OCH_3), 3.62–3.53 (m, 2H, C*H*$_2$NH), 2.22 (s, 3H, CH_3). ^{13}C NMR (125 MHz, DMSO-d_6) δ 165.1, 164.9, 163.3, 155.3, 137.7, 131.4, 131.3, 129.9, 128.9, 121.8, 121.5, 117.9, 114.0, 113.9, 71.3, 63.5, 55.5, 55.4, 20.2. HRMS (*m/z*): calcd for $C_{27}H_{28}N_2O_7Na$ 515.1789 $[M+Na]^+$; found 515.1783.

***N*-[2,3-Bis(4-cyanobenzoyloxy)propyl]-*N'*-(4-methylphenyl)urea (192).** The product was obtained as a solid and purified by column chromatography using hexane-ethyl acetate (1:1) as eluent (155 mg; 64% yield), mp 181–182 ºC. ^{1}H NMR (500 MHz, DMSO-d_6) δ 8.40 (s, 1H, N*H*Ar), 8.13 (d, *J* = 8.2 Hz, 2H, Ar), 8.07 (d, *J* = 8.2 Hz, 2H, Ar), 8.03–7.98 (m, 4H, Ar), 7.23 (d, *J* = 8.4 Hz, 2H, Ar), 7.02 (d, *J* = 8.3 Hz, 2H, Ar), 6.40 (t, *J* = 6.0 Hz, 1H, CH_2N*H*), 5.51–5.47 (m, 1H, CH), 4.69 (dd, *J* = 3,5 Hz, *J* = 8,6 Hz, 1H, C*H*$_2$O), 4.56 (dd, *J* = 6,8 Hz, *J* = 5,2 Hz, 1H, C*H*$_2$O), 3.66–3.57 (m, 2H, C*H*$_2$NH), 2.22 (s, 3H, CH_3). ^{13}C NMR (125 MHz, DMSO-d_6) δ 164.3, 164.2, 155.3, 137.6, 133.5, 133.2, 129.9, 129.8, 129.0, 117.9, 115.6, 72.4, 64.3, 39.5, 20.2. HRMS (*m/z*): calcd for $C_{27}H_{22}N_4O_5Na$ 505.1482 $[M+Na]^+$; found 505.1476. Anal. Calcd for $C_{27}H_{22}N_4O_5$: C, 67.21; H, 4.60; N, 11.61. Found: C, 66.22; H, 4.47; N, 11.14.

***N*-[2,3-Bis(4-nitrobenzoyloxy)propyl]-*N'*-(4-methylphenyl)urea (193).** The product was obtained as a light yellow solid and purified by column chromatography using hexane-ethyl acetate (2:1) as eluent (162 mg; 62% yield), mp 214–215 ºC. ^{1}H NMR (500 MHz, DMSO-d_6) δ 8.45 (s, 1H, N*H*Ar), 8.38–8.33 (m, 4H, Ar), 8.24 (d, *J* = 8.4 Hz, 2H, Ar), 8.19 (d, *J* = 8.3 Hz, 2H, Ar), 7.26 (d, *J* = 6.0 Hz, 2H, Ar), 7.03 (d, *J* = 7.0 Hz, 2H, Ar), 6.45 (t, *J* = 5 Hz, 1H, CH_2N*H*) 5.56–5.52 (m, 1H, CH), 4.75 (dd, *J* = 3,5 Hz, *J* = 8,6 Hz, 1H, C*H*$_2$O), 4.62 (dd, *J* = 6,8 Hz, *J* = 5,2 Hz, 1H, C*H*$_2$O), 3.71–3.61 (m, 2H, C*H*$_2$NH), 2.24 (s, 3H, CH_3). ^{13}C NMR (125 MHz, DMSO-d_6) δ 164.0, 163.9, 155.3, 150.3, 137.6, 134.9, 134.6, 130.7, 130.6, 129.9, 128.9, 123.8, 117.8, 72.5, 64.4, 39.5, 20.2. HRMS (*m/z*): calcd for $C_{25}H_{22}N_4O_9Na$ 545.1279 $[M+Na]^+$; found 545.1274. Anal. Calcd for $C_{25}H_{22}N_4O_9$: C, 57.47; H, 4.24; N, 10.72. Found: C, 56.99; H, 4.20; N, 10.68.

***N*-{2,3-Bis[4-(trifluoromethyl)benzoyloxy]propyl}-*N'*-(4-methylphenyl)urea (194).** The product was obtained as a white solid and purified by column chromatography using hexane-ethyl acetate (2:1) as eluent (179 mg; 63% yield), mp 137–138 ºC. ^{1}H NMR (500 MHz, DMSO-d_6) δ 8.43 (s, 1H, N*H*Ar), 8.20 (d, *J* = 8.2 Hz, 2H, Ar), 8.15 (d, *J* = 8.2 Hz, 2H, Ar), 7.92 (d, *J* = 7.0 Hz, 4H, Ar), 7.26 (d, *J* = 8.4 Hz, 2H, Ar), 7.04 (d, *J* = 8.3 Hz, 2H, Ar), 6.43 (t, *J* = 6.1 Hz, 1H, CH_2N*H*), 5.55–5.51 (m, 1H, CH), 4.74 (dd, *J* = 3,4 Hz, *J* = 8,7 Hz, 1H, C*H*$_2$O), 4.60 (dd, *J* = 6,7 Hz, *J* = 5,4 Hz, 1H, C*H*$_2$O), 3.70–3.60 (m, 2H, C*H*$_2$NH), 2.24 (s, 3H, CH_3). ^{13}C NMR (125 MHz, DMSO-d_6) δ 164.4, 164.3, 155.4, 137.6, 133.3, 133.1, 133.0, 132.8, 132.6, 130.2, 130.0, 129.9, 129.0, 125.9, 125.8, 125.7, 125.6, 124.7, 122.6, 117.9, 72.3, 64.2, 20.2. HRMS (*m/z*): calcd for $C_{27}H_{22}F_6N_2O_5Na$ 681.4719 $[M+Na]^+$; found 681.4715. Anal. Calcd for $C_{27}H_{22}F_6N_2O_5$: C, 57.05; H, 3.90; N, 4.93. Found: C, 56.80; H, 3.88; N, 4.90.

***N*-[2,3-Bis(2,4-dimethoxybenzoyloxy)propyl]-*N'*-(4-methylphenyl)urea (195).** The product was obtained as a white resin and purified by column chromatography using hexane-ethyl acetate (1:1.5) as eluent (169 mg; 61% yield). ^{1}H NMR (500 MHz, DMSO-d_6) δ 8.45 (s, 1H, N*H*Ar), 7.75 (q, *J* = 8.6 Hz, 2H, Ar), 7.29 (d, *J* = 8.0 Hz, 2H, Ar), 7.04 (d, *J* = 8.1 Hz, 2H, Ar), 6.64 (s, 2H, Ar), 6.59 (t, *J* = 8.5 Hz, 2H, Ar), 6.32–6.28 (m, 1H, CH_2N*H*), 5.36–5.29 (m, 1H, CH), 4.51–4.43 (m, 1H, C*H*$_2$O), 4.37 (dd, *J* = 6.5 Hz, *J* = 9.5 Hz, 1H, C*H*$_2$O), 3.84-3.80 (m, 12H, OCH_3), 3.55–3.50 (m, 2H, C*H*$_2$NH), 2.24 (s, 3H, CH_3). ^{13}C NMR (125 MHz, DMSO-d6) δ 164.1, 164.0, 163.9, 160.9, 155.3, 137.8, 133.2, 133.1, 129.9, 129.0, 117.8, 111.7, 111.4, 105.3, 105.2, 98.9, 98.8, 70.6, 63.0, 55.5, 55.4, 20.2. HRMS (*m/z*): calcd for $C_{29}H_{32}N_2O_9Na$ 575.2000 $[M+Na]^+$; found 575.1993. Anal. Calcd for $C_{29}H_{32}N_2O_9$: C, 63.04; H, 5.84; N, 5.07. Found: C, 62.97; H, 5.81; N, 4.99.

***N*-[2,3-Bis(3,4,5-trimethoxybenzoyloxy)propyl]-*N'*-(4-methylphenyl)urea (196).** The product was obtained as a white solid and purified by column chromatography using hexane-ethyl acetate (1:1.5) as eluent (267 mg; 87% yield), mp 151–152 ºC. ^{1}H NMR (500 MHz, DMSO-d_6) δ 8.43 (s, 1H, N*H*Ar), 7.26–7.24 (m, 4H, Ar), 7.22 (s, 2H, Ar), 7.02 (d, *J* = 8.1 Hz, 2H, Ar), 6.38 (t, *J* = 8.5Hz 1H, CH_2N*H*), 5.47–5.42 (m, 1H, CH), 4.65 (dd, *J* = 3.6 Hz, *J* = 8.5Hz, 1H, C*H*$_2$O), 4.45 (dd, *J* = 3.5 Hz, *J* = 8.4 Hz, 1H, C*H*$_2$O), 3.82-3.72 (m, 18H, OCH_3) 3.63–3.55 (m, 2H, C*H*$_2$NH), 2.22 (s, 3H, CH_3). ^{13}C NMR (125 MHz, DMSO-d_6) δ 165.0, 164.9, 155.4, 152.7, 152.6, 142.0, 141.9, 137.7, 130.0, 128.9, 124.7, 124.4, 117.9, 106.8, 106.6, 71.8, 63.7, 60.1, 55.9, 55.8, 39.5, 20.2. HRMS (*m/z*): calcd for $C_{31}H_{36}N_2O_{11}Na$ 635.2211 $[M+Na]^+$; found 635.2202. Anal. Calcd for $C_{25}H_{22}N_4O_9$: C, 60.78; H, 5.92; N, 4.57. Found: C, 60.90; H, 5.94; N, 4.58.

***N*-[2,3-Bis(4-methylbenzoyloxy)propyl]-*N'*-[4-(trifluoromethyl)phenyl]urea (197).** The product was obtained as a white solid and purified by column chromatography using hexane-ethyl acetate (3:1) as eluent (217 mg; 84%yield), mp 111–112 ºC. ^{1}H NMR (500 MHz, DMSO-d_6) δ 9.00, (s, 1H, N*H*Ar), 7.89 (d, *J* = 8.2 Hz, 2H, Ar), 7.83 (d, *J* = 8.2 Hz, 2H, Ar), 7.61–7.55 (m, 4H, Ar), 7.32–7.29 (m, 4H, Ar), 6.59 (t, *J* = 5.9 Hz, 1H, CH_2N*H*), 5.48–5.44 (m, 1H, CH), 4.63 (dd, *J* = 3.3 Hz, *J* = 12.1 Hz, 1H, C*H*$_2$O), 4.48 (dd, *J* = 6.9 Hz, *J* = 12.1 Hz, 1H, C*H*$_2$O), 3.67–3.58 (m, 2H, C*H*$_2$NH), 2.37, 2.36 (2s, 6H, CH_3). ^{13}C NMR (125 MHz, DMSO-d_6) δ 165.4, 165.2, 154.9, 144.0, 143.8, 143.7, 129.4, 129.3, 129.2, 129.1, 129.0, 126.8, 126.6 125.8, 125.7, 117.3, 71.3, 63.5, 21.1, 21.0. HRMS (*m/z*): calcd for $C_{27}H_{25}F_3N_2O_5Na$: 537.1608 [M+Na]$^+$; found 537.1600 Anal. Calcd for $C_{27}H_{25}F_3N_2O_5$: C, 63.03; H, 4.90; N, 5.44. Found: C, 62.88; H, 4.87; N, 5,38.

***N*-[2,3-Bis(2-methylbenzoyloxy)propyl]-*N'*-[4-(trifluoromethyl)phenyl]urea (198).** The product was obtained as a white solid and purified by column chromatography using hexane-ethyl acetate (2.5:1) as eluent (188 mg; 73% yield), mp 112–113 ºC. ^{1}H NMR (500 MHz, DMSO-d_6) δ 9.05 (s, 1H, N*H*Ar), 7.90 (d, *J* = 8.2 Hz, 1H, Ar), 7.85 (d, *J* = 8.2 Hz, 1H, Ar), 7.61 (q, *J* = 8.7 Hz, 4H, Ar), 7.52–7.47 (m, 2H, Ar), 7.35–7.28 (m, 4H, Ar), 6.63 (t, *J* = 6.1 Hz, 1H, CH_2N*H*), 5.54-5.50 (m, 1H, CH), 4.67 (dd, *J* = 3,5 Hz, *J* = 11,8 Hz, 1H, C*H*$_2$O), 4.52 (dd, *J* = 6,8 Hz, *J* = 11,9 Hz, 1H, C*H*$_2$O), 3.68–3.61 (m, 2H, C*H*$_2$NH), 2.51 (s, 3H, CH_3). ^{13}C NMR (125 MHz, DMSO-d_6) δ 166.5, 166.3, 154.9, 143.9, 139.3, 139.2, 132.3, 132.2, 131.6, 131.5, 130.2, 130.1, 129.3, 128.9, 125.9, 123.5, 121.3, 117.4, 71.2, 63.5, 39.5, 21.0, 20.9. HRMS (*m/z*): calcd for $C_{27}H_{25}F_3N_2O_5Na$ 515.1788 [M+Na]$^+$; found 515.1782. Anal. Calcd for $C_{27}H_{25}F_3N_2O_5$: C, 63.03; H, 4.90; N, 5.44. Found: C, 62.52; H, 4.92; N, 5.49.

***N*-[2,3-Bis(4-methoxybenzoyloxy)propyl]-*N'*-[4-(trifluoromethyl)phenyl]urea (199).** The product was obtained as a white solid and purified by column chromatography using hexane-ethyl acetate (1:1) as eluent (195 mg; 71% yield), mp 128–129 ºC. ^{1}H NMR (500 MHz, DMSO-d_6) δ 9.01 (s, 1H, N*H*Ar), 7.98–7.96 (m, 2H, Ar), 7.94–7.89 (m, 2H, Ar) 7.60 (q, *J* = 8.0 Hz, 4H, Ar), 7.07–7.03 (m, 4H, Ar), 6.60 (t, *J* = 6.9 Hz, 1H, CH_2N*H*), 5.47–5.43 (m, 1H, CH), 4.61 (dd, *J* = 3.6 Hz, *J* = 11.8 Hz, 1H, C*H*$_2$O), 4.48 (dd, *J* = 7.0 Hz, *J* = 11.9 Hz, 1H, C*H*$_2$O), 3.85 (s, 6H, OCH_3), 3.65–3.60 (m, 2H, C*H*$_2$NH). ^{13}C NMR (125 MHz, DMSO-d_6) δ 165.1, 164.9, 163.3, 163.2, 154.9, 143.9, 132.6, 131.4, 131.2, 123.5, 121.7, 121.5, 117.3, 114.1, 114.0, 113.9, 113.8, 71.1, 63.4, 55.5, 39.5. HRMS (*m/z*): calcd for $C_{27}H_{25}F_3N_2O_7Na$ 569.1506 [M+Na]$^+$; found 569.1497. Anal. Calcd for $C_{27}H_{25}F_3N_2O_7$: C, 59.34; H, 4.61; N, 5.13. Found: C, 59.18; H,4.57; N, 5.51.

***N*-[2,3-Bis(4-cyanobenzoyloxy)propyl]-*N'*-[4-(trifluoromethyl)phenyl]urea (200).** The product was obtained as a white solid and purified by column chromatography using hexane-ethyl acetate (2:1) as eluent (205 mg; 76% yield), mp 170–171 ºC. ^{1}H NMR (500 MHz, DMSO-d_6) δ 9.00, (s, 1H, N*H*Ar), 8.14 (d, *J* = 8.2 Hz, 2H, Ar), 8.08 (d, *J* = 8.2 Hz, 2H, Ar), 8.02-7.99 (m, 4H, Ar), 7.56 (m, 4H, Ar), 6.63 (t, *J* = 5.9 Hz, 1H, CH_2N*H*), 5.53–5.49 (m, 1H, CH), 4.71 (dd, *J* = 3.5 Hz, *J* = 12.1 Hz, 1H, C*H*$_2$O), 4.57 (dd, *J* = 6.7 Hz, *J* = 12.1 Hz, 1H, C*H*$_2$O), 3.69–3.62 (m, 2H, C*H*$_2$NH). ^{13}C NMR (125 MHz, DMSO-d_6) δ 164.3, 164.2, 155.0, 143.9, 133.4, 133.2, 132.8, 132.7, 130.0, 129.8, 125.9, 117.9, 117.4, 115.6, 72.2, 64.3. HRMS (*m/z*): calcd for $C_{27}H_{19}F_3N_4O_5Na$: 559.1200 [M+Na]$^+$; found 559.1192 Anal. Calcd for $C_{27}H_{19}F_3N_4O_5$: C, 60.45; H, 3.57; N, 10.44. Found: C, 59.85; H, 3.56; N, 10.42.

***N*-[2,3-Bis(4-nitrobenzoyloxy)propyl]-*N'*-[4-(trifluoromethyl)phenyl]urea (201).** The product was obtained as a yellow solid and purified by column chromatography using hexane-ethyl acetate (1:1) as eluent (195 mg; 68% yield), mp 186–187 ºC. ^{1}H NMR (500 MHz, DMSO-d_6) δ 9.00, (s, 1H, N*H*Ar), 8.35–8.32 (m, 4H, Ar), 8.23 (d, *J* = 8.7 Hz, 2H, Ar), 8.17 (d, *J* = 8.6 Hz, 2H, Ar), 7.56 (m, 4H, Ar), 6.65 (t, *J* = 5.4 Hz, 1H, CH_2N*H*), 5.54 (m, 1H, CH), 4.74 (dd, *J* = 2.8 Hz, *J* = 12.1 Hz, 1H, C*H*$_2$O), 4.61 (dd, *J* = 6.4 Hz, *J* = 12.1 Hz, 1H, C*H*$_2$O), 3.71–3.63 (m, 2H, C*H*$_2$NH). ^{13}C NMR (125 MHz, DMSO-d_6) δ 164.0, 163.9, 155.0, 150.4, 150.3, 134.9, 134.7, 130.8, 130.6, 125.9, 123.9, 123.8, 117.3, 129.1, 129.0, 126.8, 126.6 125.8, 125.7, 117.3, 72.4, 64.4. HRMS (*m/z*): calcd for $C_{25}H_{19}F_3N_4O_9Na$: 599.0996 [M+Na]$^+$; found 599.0988. Anal. Calcd for $C_{25}H_{19}F_3N_4O_9$: C, 52.09; H, 3.32; N, 9.72. Found: C, 51.63; H, 3.22; N, 9.78.

***N*-{2,3-Bis[4-(trifluoromethxyl)benzoyloxy]propyl}-*N'*-[4-(trifluoromethyl)phenyl]urea (202).** The product was obtained as a white solid and purified by column chromatography using hexane-ethyl acetate (2.5:1) as eluent (236 mg; 76% yield), mp 135–136 ºC. ^{1}H NMR (500 MHz, DMSO-d_6) δ 9.01 (s, 1H, N*H*Ar), 8.17 (d, *J* = 8.2 Hz, 2H, Ar), 8.11 (d, *J* = 8.2 Hz, 2H, Ar), 7.90-7.86 (m, 4H, Ar), 7.58-7.52 (m, 4H, Ar), 6.63 (t, *J* = 6.0 Hz, 1H, CH_2N*H*), 5.55–5.50 (m, 1H, CH), 4.52 (dd, *J* = 3.4 Hz, *J* = 12.1 Hz, 1H, C*H*$_2$O), 4.58 (dd, *J* = 6.6 Hz, *J* = 12.2 Hz, 1H, C*H*$_2$O), 3.70–3.61 (m, 2H, C*H*$_2$NH). ^{13}C NMR (125 MHz, DMSO-d_6) δ 164.9, 164.7, 155.5, 144.4, 133.8, 133.6, 133.3, 130.7, 130.5, 127.4, 126.4, 126.3, 126.2, 125.2, 123.9, 117.8, 72.6, 64.7. HRMS (*m/z*): calcd. for $C_{27}H_{19}F_9N_2O_5Na$ 645.1042 [M+Na]$^+$; found 645.1035.

***N*-[2,3-Bis(2,4-dimethoxybenzoyloxy)propyl]-*N'*-[4-(trifluoromethyl)phenyl]urea (203).** The product was obtained as a white solid and purified by column chromatography using hexane-ethyl

acetate (1:1.5) as eluent (169 mg; 56% yield), mp101–102 ºC. ^{1}H NMR (500 MHz, DMSO-d_6) δ 9.04 (s, 1H, N*H*Ar), 7.77 (d, *J* = 8.6 Hz, 1H, Ar), 7.74 (d, *J* = 8.6 Hz, 1H, Ar) 7.61 (q, *J* = 8.0 Hz, 4H, Ar), 6.67–6.64 (m, 2H, Ar), 6.62–6.56 (m, 2H, Ar), 6.53 (t, *J* = 5.5 Hz, 1H, CH_2N*H*), 5.39-5.33 (m, 1H, CH), 4.50 (dd, *J* = 3.5 Hz, *J* = 12.3 Hz, 1H, C*H*$_2$O), 4.39 (dd, *J* = 6.5 Hz, *J* = 12.3 Hz, 1H, C*H*$_2$O), 3.87–3.84 (m, 6H, OCH_3), 3.83–3.78 (m, 6H, OCH_3), 3.59 (t, *J* = 8.6 Hz, 2H, C*H*$_2$NH). ^{13}C NMR (125 MHz, DMSO-d_6) δ 164.4, 164.1, 164.0, 163.8, 160.9, 154.9, 144.0, 133.2, 125.9, 125.7, 123.5, 120.9, 117.3, 111.7, 111.4, 105.3, 105.2, 98.9, 70.4, 63.0, 55.7, 55.5, 26.7. HRMS (*m/z*): calcd for $C_{29}H_{29}F_3N_2O_9Na$ 629.1717 $[M+Na]^+$; found 629.1709. Anal. Calcd for $C_{29}H_{29}F_3N_2O_9$: C, 57.43; H, 4.82; N, 4.62. Found: C, 57.22; H, 4.79; N, 4.55.

***N*-[2,3-Bis(3,4,5-trimethoxybenzoyloxy)propyl]-*N'*-[4-(trifluoromethyl)phenyl]urea (204).** The product was obtained as a white solid and purified by column chromatography using hexane-ethyl acetate (1:1) as eluent (276 mg; 82% yield), mp 185–186 ºC. ^{1}H NMR (500 MHz, DMSO-d_6) δ 9.03 (s, 1H, N*H*Ar), 7.62–7.57 (m, 4H, Ar), 7.28 (s, 2H, Ar), 7.24 (s, 2H, Ar), 6.62 (t, *J* = 5.6 Hz, 1H, CH_2N*H*), 5.50–5.46 (m, 1H, CH), 4.68 (dd, *J* = 3.2 Hz, *J* = 12.2 Hz, 1H, C*H*$_2$O), 4.49 (dd, *J* = 6.4 Hz, 12.2 Hz, 1H, C*H*$_2$O), 3.82-3.73 (m, 18H, OCH_3) 3.67–3.61 (m, 2H, C*H*$_2$NH). ^{13}C NMR (125 MHz, DMSO-d_6) δ 165.0, 155.0, 152.7, 152.6, 143.9, 142.0, 141.9, 127.5, 125.9, 125.8, 124.6, 124.3, 121.0, 117.3, 106.8, 106.6, 71.6, 63.6, 60.1, 55.9, 55.8, 39.5. HRMS (*m/z*): calcd for $C_{31}H_{33}F_3N_2O_{11}Na$: 689.1229 $[M+Na]^+$; found 689.1229. Anal. Calcd for $C_{31}H_{33}F_3N_2O_{11}$: C, 55.86; H, 4.99; N, 4.20. Found: C, 55.41; H, 5.05; N, 4.21.

***N*-[2,3-Bis(2-methylbenzoyloxy)propyl]-*N'*-[2-chloro-5-(trifluoromethyl)phenyl]) (205).** The product was obtained as a white solid and purified by column chromatography using hexane-ethyl acetate (2.5:1) as eluent (223mg; 74% yield), mp 125–126 ºC. ^{1}H NMR (500 MHz, DMSO-d_6) δ 8.59 (s, 1H, N*H*Ar), 8.44 (s, 1H, Ar), 7.88-7.61 (m, 2H, Ar), 7.66 (d, *J* = 8.5 Hz, 2H, Ar), 7.51-7.44 (m, 2H, Ar), 7.35-7.25 (m, 5H, Ar, CH_2N*H*), 5.52-5.47 (m, 1H, CH), 4.64 (dd, *J* = 3.5 Hz, *J* = 12.0 Hz, 1H, C*H*$_2$O), 4.49 (dd, *J* = 7.1 Hz, *J* = 11.9 Hz, 1H, C*H*$_2$O), 3.70-3.59 (m, 2H, C*H*$_2$NH), 2.63-2.50 (m, 6H, CH_3). ^{13}C NMR (125 MHz, DMSO-d_6) δ 166.5, 166.3, 154.8, 139.3, 139.2, 137.4, 132.3, 132.2, 131.6, 131.5, 130.2, 130.0, 129.3, 128.9, 125.9, 125.8, 118.6, 71.0, 63.4, 21.0, 20.87. HRMS (m/z): calcd. for $C_{27}H_{24}ClF_3N_2O_5Na$ 571.1218 $[M+Na]^+$; found 571.1225.

***N*-[2,3-Bis(3,4,5-trimethoxybenzoyloxy)propyl]-*N'*-(2-methylphenyl)urea (206).** The product was obtained as a white solid and purified by column chromatography using hexane-ethyl acetate (1:1) as eluent (254 mg; 77% yield), mp 103–104 ºC. ^{1}H NMR (500 MHz, DMSO-d_6) δ 7.74–7.68 (m, 2H, N*H*Ar, Ar), 7.27 (s, 2H, Ar), 7.23 (s, 2H, Ar), 7.13–7.05 (m, 2H, Ar), 6.90 (t, *J* = 7.4 Hz, 1H,

Ar), 6.77(t, *J* = 5.9 Hz, 1H, CH_2NH), 5.48–5.43 (m, 1H, CH), 4.67 (dd, *J* = 3.6 Hz, *J* = 11.8 Hz, 1H, CH_2O), 4.47 (dd, *J* = 7.3 Hz, *J* = 11.8 Hz, 1H, CH_2O), 3.82–3.72 (m, 18H, OCH_3), 3.64–3.58 (m, 2H, CH_2NH). ^{13}C NMR (125 MHz, DMSO-d_6) δ 165.1, 165.0, 155.6, 152.7, 142.0, 141.9, 137.8, 130.0, 127.4, 125.9, 124.7, 124.4, 122.3, 121.2, 106.8, 71.8, 63.7, 60.1, 55.8, 17.7. HRMS (*m/z*): calcd for $C_{31}H_{36}N_2O_{11}Na$ 635.2211 $[M+Na]^+$; found 635.2207.

***N*-[2,3-Bis(3,4,5-trimethoxybenzoyloxy)propyl]-*N'*-(4-methoxyphenyl)urea (207).** The product was obtained as a white solid and purified by column chromatography using hexane-ethyl acetate (1:1) as eluent (300 mg; 90% yield), mp 137–138 ºC. ^1H NMR (500 MHz, DMSO-d_6) *δ* 8.35 (s, 1H, N*H*Ar), 7.28 (d, *J* = 8.0 Hz, 2H, Ar), 7.23 (s, 4H, Ar), 6.81 (d, *J* = 9.0 Hz, 2H, Ar), 6.33 (t, *J* = 6.1 Hz, 1H, CH_2NH), 5.48–5.42 (m, 1H, CH), 4.66 (dd, *J* = 3.5 Hz, *J* = 11.9 Hz, 1H, CH_2O-), 4.45 (dd, *J* = 7.3 Hz, *J* = 11.9 Hz, 1H, CH_2O), 3.83–3.77 (m, 12H, OCH_3), 3.76–3.69 (m, 9H, OCH_3), 3.65–3.53 (m, 2H, CH_2NH). ^{13}C NMR (125 MHz, DMSO-d_6) δ 165.0, 164.9, 155.5, 154.0, 152.8, 152.7, 142.0, 141.9, 133.3, 124.7, 124.3, 119.6, 113.8, 106.8, 106.6, 71.8, 63.7, 60.1, 55.9, 55.8, 55.1, 36.2. HRMS (*m/z*): calcd for $C_{31}H_{36}N_2O_{12}Na$ 651.2160 $[M+Na]^+$; found 651.2154.

***N*-[2,3-Bis(3,4,5-trimethoxybenzoyloxy)propyl]-*N'*-[2-chloro-5-(trifluoromethyl)phenyl]urea (208).** The product was obtained as a white solid and purified by column chromatography using hexane-ethyl acetate (1.5:1) as eluent (235 mg; 71% yield), mp 115–116 ºC. ^1H NMR (500 MHz, DMSO-d_6) *δ* 8.58 (s, 1H, N*H*Ar),8.42 (s, 1H, Ar) 7.64 (m, 1H, Ar), 7.46 (t, *J* = 6.2 Hz, 1H, Ar), 7.32–7.23 (m, 5H, Ar*H*, CH_2NH), 5.50–5.44 (m, 1H, CH), 4.68 (dd, *J* = 4.5 Hz, *J* = 12.1 Hz, 1H, CH_2O), 4.49 (dd, *J* = 7.3 Hz, *J* = 11.5 Hz, 1H, CH_2O), 3.82–3.70 (m, 18H, OCH_3), 3.69–3.64 (m, 2H, CH_2NH). ^{13}C NMR (125 MHz, DMSO-d_6) *δ* 165.0, 164.9, 154.8, 152.8, 152.7, 142.0, 141.9, 137.3, 130.1, 124.7, 124.6, 124.3, 122.7, 118.6, 116.4, 106.8, 106.6, 71.5, 63.5, 60.1, 55.9, 55.8, 36.2. HRMS (*m/z*): calcd for $C_{31}H_{32}ClF_3N_2O_{11}Na$ 723.1539 $[M+Na]^+$; found 723.1530.

***N*-[2,3-Bis(3,4,5-trimethoxybenzoyloxy)propyl]-*N'*-(3,4,5-trimethoxyphenyl)urea (209).** The product was obtained as a white solid and purified by column chromatography using hexane-ethyl acetate (1:1.5) as eluent (274 mg; 78% yield), mp 105–106 ºC. ^1H NMR (500 MHz, DMSO-d_6) *δ* 8.51 (s, 1H, N*H*Ar), 7.27 (s, 2H, Ar), 7.23 (s, 2H, Ar), 7.73 (s, 2H, Ar), 6.38 (t, *J* = 6.0 Hz, 1H, CH_2NH), 5.48–5.42 (m, 1H, CH), 4.66 (dd, *J* = 3.6 Hz, *J* = 11.9 Hz, 1H, CH_2O), 4.45 (dd, *J* = 7.3 Hz, *J* = 11.9 Hz, 1H, CH_2O), 3.82–3.77 (m, 12H, OCH_3), 3.75–3.70 (m, 12H, OCH_3), 3.66–3.54 (m, 5H, OCH_3, CH_2NH). ^{13}C NMR (125 MHz, DMSO-d_6) *δ* 164.9, 155.2, 152.8, 152.7, 152.6, 142.0, 141.9, 136.4, 132.1, 124.6, 124.3, 106.8, 106.6, 96.6, 71.7, 63.6, 60.1, 60.0, 55.9, 55.8, 55.5. HRMS (*m/z*): calcd for $C_{33}H_{40}N_2O_{14}Na$ 711.2372 $[M+Na]^+$; found 711.2364.

*B) Chemoselective O-acylation reaction of the primary hydroxyl of N-(2,3-dihydroxypropyl)-N'-(substituted)phenylureas (**212-217**).* The urea derivative **173** (0.7 mmol) was suspended in dry DCM (15 mL), then pyridine was added until dissolution (5 mL) and the reaction was cooled to –40 ºC. A solution of the appropriate acylating agent (0.6 mmol) in dry DCM (5 mL) was added dropwise and the reaction mixture was kept with stirring for 2 hours. The reaction mixture was coevaporated with toluene to remove the pyridine residue. The compound was further purified by flash column chromatography on silica gel using the appropriate eluent.

***N*-[3-(Benzoyloxy)-2-hydroxypropyl]-*N'*-(4-chlorophenyl)urea (212).** The product was obtained as a white solid and purified by column chromatography using hexane-ethyl acetate (1.5:1) as eluent (122 mg; 58% yield), mp 155–156 ºC. ^{1}H NMR (500 MHz, DMSO-d_6) δ 8.73, (s, 1H, N*H*Ar) 8.04–8.01 (m, 2H, Ar), 7.70–7.63 (m, 1H, Ar), 7.57–7.52 (m, 2H, Ar), 7.41 (t, *J* = 8.8 Hz, 2H, Ar), 7.28–7.24 (m, 2H, Ar), 6.33 (m, 1H, CH_2N*H*), 5.36 (d, *J* = 4.9 Hz, 1H, OH) 5.08–5.05 (m, 1H, CH), 4.27–4.17 (m, 2H, C*H*$_2$O), 3.45–3.39 (m, 1H, C*H*$_2$NH), 3.23–3.17 (m, 1H, C*H*$_2$NH). ^{13}C NMR (125 MHz, DMSO-d_6) δ 165.7, 155.2, 139.4, 133.3, 129.3, 129.2, 128.7, 128.4, 124.5, 119.1, 119.0, 67.6, 66.6, 42.2. HRMS (*m/z*): calcd for $C_{17}H_{17}ClN_2O_4Na$ 371.0769 $[M+Na]^+$; found 371.0763.

***N*-(4-Chlorophenyl)-*N'*-[2-hydroxy-3-(4-methylbenzoyloxy)propyl]urea (213).** The product was obtained as a white solid and purified by column chromatography using using hexane-ethyl acetate (1:2) as eluent (125mg; 57% yield). mp 155–156 ºC. MS (CI): *m/z* 369 (100%) $[M+Na]^+$. ^{1}H NMR (500 MHz, DMSO-d_6) δ 8.74, (s, 1H, N*H*Ar), 7.93–7.89 (m, 2H, Ar), 7.43–7.39 (m, 2H, Ar), 7.36–7.32 (m, 2H, Ar), 7.27–7.23 (m, 2H, Ar), 6.32 (t, *J* = 5.5 Hz, 1H, CH_2N*H*), 5.35 (d, *J* = 4.9 Hz, 1H, OH), 4.99–4.96 (m, 1H, CH), 4.23–4.20 (m, 2H, C*H*$_2$O), 3.43-3.39 (m, 1H, C*H*$_2$NH), 3.22–3.17 (m, 1H, C*H*$_2$NH), 2.40 (s, 3H, CH_3). ^{13}C NMR (125 MHz, DMSO-d_6) δ 165.8, 155.2, 143.6, 139.5, 129.3, 129.2, 129.1, 128.5, 127.0, 124.4, 119.0, 67.6, 66.4, 42.2, 21.1. Anal. Calcd for $C_{18}H_{19}ClN_2O_4$: C, 59.59; H, 5.28; N, 7.72. Found: C, 59.24; H, 5.25; N, 7.69.

***N*-(4-Chlorophenyl)-*N'*-[2-hydroxy-3-(2-methylbenzoyloxy)propyl]urea (214).** The product was obtained as a white resin and purified by column chromatography using using hexane-ethyl acetate (1:2) as eluent (131 mg; 60% yield). ^{1}H NMR (500 MHz, DMSO-d_6) δ 8.73, (s, 1H, N*H*Ar), 7.92–7.87 (m, 1H, Ar), 7.51–7.38 (m, 3H, Ar), 7.34–7.23 (m, 4H, Ar), 6.35–6.29 (m, 1H, CH_2N*H*), 5.33 (d, *J* = 5.2 Hz, 1H, OH), 5.08–5.03 (m, 1H, CH) 4.23–4.17 (m, 1H, C*H*$_2$O), 3.92–3.87 (m, 1H, C*H*$_2$O), 3.63–3.52 (m, 1H, C*H*$_2$NH), 3.21–3.16 (m, 1H, C*H*$_2$NH), 2.54 (s, 3H, CH_3). ^{13}C NMR (125 MHz, DMSO-d_6) δ 166.8, 155.2, 139.4, 139.0, 132.1, 131.5, 130.2 129.5, 128.4, 125.9, 124.4, 119.2, 74.4,

67.6, 66.4, 60.6, 42.3, 21.1. HRMS (*m/z*): calcd for $C_{18}H_{19}ClN_2O_4Na$ 385.0926 $[M+Na]^+$; found 385.0921.

***N*-(4-Chlorophenyl)-*N'*-{2-hydroxy-3-[4-(trifluoromethyl)benzoyloxy]propyl}urea (215).** The product was obtained as a white solid and purified by column chromatography using hexane-ethyl acetate (1:1.5) as eluent (120 mg; 48% yield), mp 137–138 ºC. ^{1}H NMR (500 MHz, DMSO-d_6) δ 8.74, (s, 1H, N*H*Ar), 8.23–8.18 (m, 2H, Ar), 7.93–7.88 (m, 2H, Ar), 7.43–7.36 (m, 2H, Ar), 7.28–7.23 (m, 2H, Ar), 6.32 (t, *J* = 5.7 Hz, 1H, CH_2N*H*), 5.44 (sb, 1H, OH), 4.33–4.24 (m, 2H, CH_2O), 3.96–3.91 (m, 1H, CH), 3.37–3.31 (m, 1H, CH_2NH), 3.26–3.19 (m, 1H, CH_2NH). ^{13}C NMR (125 MHz, DMSO-d_6) δ164.7, 155.2, 139.4, 133.5, 130.2, 130.1, 128.4, 128.4, 125.7, 124.5, 119.2, 119.1, 67.5, 67.2, 42.1.

***N*-[3-(2-Chloroacetoxy)-2-hydroxypropyl]-*N'*-(4-chlorophenyl)urea (216).** The product was obtained as a white resin (380 mg; 51% yield). MS (FAB): *m/z* 343 (100%) $[M+Na]^+$. ^{1}H NMR (500 MHz, DMSO-d_6) δ8.75, (s, 1H, N*H*Ar), 7.44 (d, *J* = 8.5 Hz, 2H, Ar), 8.16 (d, *J* = 8.6 Hz, 2H, Ar), 6.27 (t, *J* = 5.8 Hz, 1H, CH_2N*H*), 5.30 (d, *J* = 5.1 Hz 1H, OH), 4.44 (s, 2H, ClCH_2), 4.12–4.09 (m, 2H, CH_2O), 3.83–3.79 (m, 1H, CH), 3.30–3.24 (m, 1H, CH_2NH), 3.16–3.10 (m, 1H, CH_2NH). ^{13}C NMR (125 MHz, DMSO-d_6) δ167.3, 155.1, 139.4, 128.5, 124.5, 119.0, 67.4, 67.3, 42.0, 41.1.

***N*-[3-(2-Chloroacetoxy)-2-hydroxypropyl]-*N'*-(4-methylphenyl)urea (217).** The product was obtained as a white resin (540 mg; 49% yield). ^{1}H NMR (500 MHz, DMSO-d_6) δ8.45, (s, 1H, N*H*Ar), 7.27 (d, *J* = 8.3 Hz, 2H, Ar), 7.03 (d, *J* = 8.62Hz, 2H, Ar), 6.16 (t, *J* = 5.7 Hz, 1H, CH_2N*H*), 5.27 (sb, 1H, OH), 4.42 (s, 2H, ClCH_2), 4.12–4.04 (m, 2H, CH_2O), 3.81–3.76 (m, 1H, CH), 3.27-3.21 (m, 1H, CH_2NH), 3.13-3.07 (m, 1H, *CH*$_2$NH). ^{13}C NMR (125 MHz, DMSO-d_6) δ167.3, 155.4, 137.9, 129.7, 129.0, 117.7, 67.5, 67.4, 42.0, 41.3, 20.2. HRMS (*m/z*): calcd for $C_{13}H_{17}ClN_2O_4Na$ 323.0769 $[M+Na]^+$; found 323.0766.

*C) O-Acylation reaction of the secondary hydroxyl of N-[3-(2-Chloroacetoxy)-2-hydroxypropyl]-N'-(substituted)phenylureas (**218-223**).* To a solution of chloroacetyl derivative (**216** or **217**) (0.7 mmol) in dry DCM (10 mL) and DMAP (1.4 mmol), was added a solution of the appropriate acylatin agent (or isocyanate) (1 mmol) in dry DCM (2 mL). The reaction mixture was stirred at rt until TLC showed that the starting material had reacted (12-24 hours). The organic layer was washed with 1 N HCl solution (2 x 20mL), saturated $NaHCO_3$ (2 x 20 mL), brine (20 mL); then, it was dried over $MgSO_4$, filtered and evaporated *in vacuo*. The product was used without further purification.

***N*-[3-(2-Chloroacetoxy)-2-(4-methylbenzoyloxy)propyl]-*N'*-(4-chlorophenyl)urea (218).** The product was obtained as a colourless oil (230 mg; 76% yield). MS (FAB): *m/z* 461 (100%) $[M+Na]^+$. ^{1}H NMR (500 MHz, DMSO-d_6) δ 8.68 (s, 1H, N*H*Ar), 7.91–7.83 (m, 2H, Ar), 7.43–7.39 (m, 2H, Ar), 7.36–7.31 (m, 2H, Ar), 7.28–7.24 (m, 2H, Ar), 6.42 (t, *J* = 6.0 Hz, 1H, CH_2N*H*), 5.32–5.27 (m, 1H, CH), 4.50–4.46 (m, 1H, CH_2O), 4.40–4.32 (m, 3H, ClCH_2, CH_2O), 3.57–3.44 (m, 2H, CH_2NH), 2.41–2.37 (m, 3H, CH_3). ^{13}C NMR (125 MHz, DMSO-d_6) δ 167.2, 165.3, 155.0, 143.8, 139.2, 129.4, 129.1, 128.4, 126.8, 124.6, 119.2, 71.1, 64.3, 40.9, 21.1.

***N*-{3-(2-Chloroacetoxy)-2-[4-(trifluoromethyl)benzoyloxy]propyl}-*N'*-(4-chlorophenyl)urea (219).** The product was obtained as a colourless oil (235 mg; 68% yield). MS (FAB): *m/z* 515 (100%) $[M+Na]^+$. ^{1}H NMR (500 MHz, DMSO-d_6) δ 8.68 (s, 1H, N*H*Ar), 8.20–8.13 (m, 2H, Ar), 7.93–7.87 (m, 2H, Ar), 7.44–7.37 (m, 2H, Ar), 7.28–7.22 (m, 2H, Ar), 6.47 (t, *J* = 5.9 Hz, 1H, CH_2N*H*), 5.38–5.32 (m, 1H, CH), 4.52 (dd, *J* = 3.4 Hz, *J* = 12.2 Hz 1H, CH_2O), 4.45-4.37 (m, 3H, ClCH_2, CH_2O), 3.60–3.48 (m, 2H, CH_2NH). ^{13}C NMR (125 MHz, DMSO-d_6) δ 167.2, 164.2, 155.1, 139.2, 133.3, 130.2, 130.1, 128.4, 125.6, 125.5, 124.7, 119.2, 72.0, 64.2, 40.9. HRMS (*m/z*): calcd. for $C_{20}H_{17}Cl_2F_3N_2O_5Na$ 515.0359 $[M+Na]^+$; found 515.0359.

***N*-[3-(2-Chloroacetoxy)-2-(4-nitrobenzoyloxy)propyl]-*N'*-(4-chlorophenyl)urea (220).** The product was obtained as a light yellow oil (298 mg; 91% yield). ^{1}H NMR (500 MHz, DMSO-d_6) δ 8.69 (s, 1H, N*H*Ar), 8.35 (d, *J* = 8.8 Hz, 2H, Ar), 8.23–8.19 (m, 2H, Ar), 7.46–7.38 (m, 2H, Ar), 7.30–7.23 (m, 2H, Ar), 6.47 (t, *J* = 5.9 Hz, 1H, CH_2N*H*), 5.40–5.33 (m, 1H, CH), 4.53 (dd, *J* = 3.3 Hz, *J* = 12.2 Hz 1H, CH_2O), 4.47–4.36 (m, 3H, ClCH_2, CH_2O), 3.62–3.48 (m, 2H, CH_2NH). ^{13}C NMR (125 MHz, DMSO-d_6) δ 167.2, 163.7, 155.0, 150.3, 139.1, 134.9, 130.7, 128.4, 124.6, 123.7, 119.2, 72.3, 64.2, 40.9, 26.7. HRMS (*m/z*): calcd for $C_{19}H_{17}Cl_2N_3O_7Na$ 492.0336 $[M+Na]^+$; found 492.0331.

***N*-[3-(2-Chloroacetoxy)-2-(3,4,5-trimethoxybenzoyloxy)propyl]-*N'*-(4-chlorophenyl)urea (221).** The product was obtained as a colourless oil (260 mg; 72% yield). ^{1}H NMR (500 MHz, DMSO-d_6) δ 8.74 (s, 1H, N*H*Ar), 7.46–7.39 (m, 2H, Ar), 7.30–7.23 (m, 4H, Ar), 6.47–6.40 (m, 1H, CH_2N*H*), 5.36–5.40 (m, 1H, CH), 4.57–4.52 (m, 1H, CH_2O), 4.47–4.38 (m, 2H, ClCH_2), 4.34–4.28(m, 1H, CH_2O), 3.87–3.80 (m, 6H, OCH_3), 3.78–3.72 (m, 3H, OCH_3), 3.57–3.50 (m, 1H, CH_2NH), 3.48–3.40 (m, 1H, CH_2NH). ^{13}C NMR (125 MHz, DMSO-d_6) δ 167.0, 164.9, 155.1, 152.7, 152.6, 141.9, 139.2, 128.4, 124.7, 124.3, 119.3, 106.9, 106.7, 72.4, 63.7, 60.1, 55.9, 41.2, 40.9. HRMS (*m/z*): calcd for $C_{22}H_{24}ClN_2O_8Na$ 537.0802 $[M+Na]^+$; found 537.0795.

***N*-{3-(2-Chloroacetoxy)-2-[(4-trifluoromethyl)benzoyloxy]propyl}-*N'*-(4-methylphenyl)urea (222).** The product was obtained as a colourless oil (249 mg; 75% yield). ^{1}H NMR (500 MHz, DMSO-d_6) δ 8.43 (s, 1H, N*H*Ar), 8.21–8.50 (m, 2H, Ar), 7.94–7.90 (m, 2H, Ar), 7.29–7.21 (m, 2H, Ar), 7.06–6.99 (m, 2H, Ar), 6.28 (t, *J* = 6.0 Hz, 1H, CH_2N*H*), 5.17–5.12 (m, 1H, CH), 4.52 (dd, *J* = 3.5 Hz, *J* = 12.0 Hz 1H, CH_2O), 4.45–4.34 (m, 3H, ClCH_2, CH_2O), 3.59–3.47 (m, 2H, CH_2NH), 2.22 (s, 3H, CH_3). ^{13}C NMR (125 MHz, DMSO-d_6) δ 167.2, 164.4, 155.3, 137.8, 130.2, 130.1, 129.1, 125.6, 118.0, 72.3, 64.1, 40.1, 40.0, 20.2. HRMS (*m/z*): calcd for $C_{21}H_{20}ClCF_3N_2O_5Na$ 495.0905 $[M+Na]^+$; found 495.0898.

***N*-[3-(2-Chloroacetoxy)-2-(3,4,5-trimethoxybenzoyloxy)propyl]-*N'*-(4-methylphenyl)urea (223).**The product was obtained as a colourless oil (274 mg; 80% yield). ^{1}H NMR (500 MHz, DMSO-d_6) δ 7.98 (s, 1H, N*H*Ar), 7.32–7.21 (m, 4H, Ar), 7.08–6.99 (m, 2H, Ar), 6.40–6.32 (m, 1H, CH_2N*H*), 5.28–5.21 (m, 1H, CH), 4.53–4.48 (m, 1H, CH_2O), 4.45–4.35 (m, 2H, ClCH_2), 4.30-4.25 (m, 1H, CH_2O), 3.89–3.80 (m, 6H, OCH_3), 3.78–3.72 (m, 3H, OCH_3), 3.57–3.44 (m, 2H, CH_2NH), 2.21 (s, 3H, CH_3). ^{13}C NMR (125 MHz, DMSO-d_6) δ 167.3, 162.3, 155.3, 152.7, 141.9, 137.7, 129.9, 129.0, 124.7, 117.9, 107.0, 106.5, 72.3, 64.1, 60.1, 56.0, 35.7, 20.3. HRMS (*m/z*): calcd for $C_{23}H_{27}ClN_2O_8Na$ 517.1348 $[M+Na]^+$; found 517.1341.

-General procedure 10. Diacylation reaction of N-(2,3-dihydroxypropyl)-N'-(substituted)phenylureas from carboxylic acids (210 and 211).

Compounds were prepared following the general procedure 6, **section 6.1.2**.

***N*-{2,3-Bis[(*E*)-(3,4,5-trimethoxyphenyl)acryloxy]prop-2-yl}-*N'*-(4-chlorophenyl)urea (210).** The product was obtained as a white solid and purified by column chromatography using using hexane-ethyl acetate (2:1) as eluent (376 mg; 69% yield), mp 120–121 ºC. ^{1}H NMR (500 MHz, DMSO-d_6) δ 8.73, (s, 1H, N*H*Ar), 7.67–7.58 (m, 2H, C*H*=CHCO), 7.46–7.40 (m, 2H, Ar), 7.28–7.23 (m, 2H, Ar), 7.07 (s, 4H, Ar), 6.62–6.54 (m, 2H, CH=C*H*CO), 6.45 (t, *J* = 5.7 Hz, 1H, CH_2N*H*), 5.29–5.23 (m, 1H, CH), 4.48 (dd, *J* = 3.3 Hz, *J* = 12.0 Hz, 1H, CH_2O), 4.33 (dd, *J* = 6.5 Hz, *J* = 12.2 Hz, 1H, CH_2O), 3.88–3.78 (m, 12H, OCH_3), 3.72–3.68 (m, 6H, OCH_3), 3.58-3.41 (m, 2H, CH_2NH). ^{13}C NMR (125 MHz, DMSO-d_6) δ 166.1, 165.9, 155.1, 153.0, 145.3, 139.7, 139.6, 139.2, 129.4, 128.4, 124.6, 119.2(2C), 117.1, 116.7, 106.1, 106.0, 70.8, 60.0, 56.0, 44.8, 30.6. HRMS (*m/z*): calcd for $C_{34}H_{37}ClN_2O_{11}Na$ 707.1978 $[M+Na]^+$; found 707.1971.

***N*-{2,3-Bis[(*E*)-(3,4,5-trimethoxyphenyl)acryloxy]prop-2-yl}-*N'*-(4-methylphenyl)urea (211).** The product was obtained as a white solid and purified by column chromatography using using

hexane-ethyl acetate (2:1) as eluent (306mg; 60% yield), mp 106–107 ºC. ^{1}H NMR (500 MHz, DMSO-d_6) δ8.44, (s, 1H, N*H*Ar), 7.67–7.59 (m, 2H, C*H*=CHCO), 7.28 (d, *J* = 8.2 Hz, 2H, Ar), 7.10–7.00 (m, 6H, Ar), 6.73–6.64 (m, 2H, CH=C*H*CO), 6.33 (t, *J* = 5.7 Hz, 1H, CH_2N*H*), 5.28–5.22 (m, 1H, CH), 4.47 (dd, *J* = 3.1 Hz, *J* = 12.1 Hz, 1H, CH_2O), 4.32 (dd, *J* = 6.5 Hz, *J* = 12.1 Hz, 1H, CH_2O), 3.85–3.74 (m, 12H, OCH_3), 3.72–3.66 (m, 6H, OCH_3), 3.58–3.52 (m, 1H, CH_2NH), 3.47–3.42 (m, 1H, CH_2NH), 2.22 (s, 3H, CH_3). ^{13}C NMR (125 MHz, DMSO-d_6) δ166.1, 165.9, 155.2, 153.0, 145.3, 139.6, 137.7, 129.9, 129.5, 129.4, 117.8, 117.1, 116.7, 106.1, 106.0, 70.9, 63.1, 60.1, 56.0, 20.2. HRMS (*m/z*): calcd for $C_{35}H_{40}N_2O_{11}Na$ 687.2508 $[M+Na]^+$; found 687.2510.

-General procedure 11. Deprotection reaction of N-[3-(2-Chloroacetoxy)-2-(acetyl)propyl]-N'-(substituted)ureas (225-231). To a solution of chloroacetyl derivative (**218-224**, 0.4 mmol) in acetonitrile-water (3:1, 10 mL), thiourea (1.2 mmol) was added and the reaction mixture was stirred at 60 ºC until TLC showed the full consumption of the starting material (12 hours). After this time, a saturated solution of $NaHCO_3$ was added to the flask and the reaction mixture was the evaporated under reduced pressure. The reaction was extracted with chloroform (2 x 10 mL). The organic layer was washed with brine, dried over $MgSO_4$, filtered and evaporated to dryness to obtain a crude product. The compound was purified by flash column chromatography on silica gel using the appropriate eluent.

***N*-(4-Chlorophenyl)-*N'*-[3-hydroxy-2-(4-methylbenzoyloxy)propyl]urea (225).** The product was obtained as a white solid and purified by column chromatography using hexane-ethyl acetate (2:1) as eluent (110 mg; 76% yield). mp 140-141 ºC. ^{1}H NMR (500 MHz, DMSO-d_6) δ8.67, (s, 1H, N*H*Ar), 7.94–7.88 (m, 2H, Ar), 7.44–7.38 (m, 2H, Ar), 7.37–7.32 (m, 2H, Ar), 7.29–7.22 (m, 2H, Ar), 6.37–6.29 (m, 1H, CH_2N*H*), 5.07–4.98 (m, 2H, CH, OH), 3.62 (t, *J* = 5.5 Hz, 2H, CH_2NH), 3.56–3.50 (m, 1H, CH_2OH), 3.43-3.37 (m, 1H, CH_2OH), 2.39 (s, 3H, CH_3). ^{13}C NMR (125 MHz, DMSO-d_6) δ 165.4, 155.1, 143.5, 139.3, 129.4, 129.1, 128.4, 127.2, 124.5,119.1, 74.4, 60.5, 42.1, 21.1. HRMS (*m/z*): calcd for $C_{18}H_{19}ClN_2O_4Na$ 385.0922 $[M+Na]^+$; found 385.0920.

***N*-(4-Chlorophenyl)-*N'*-{3-hydroxy-2-[(4-trifluoromethyl)benzoyloxy]propyl}urea (226).** The product was obtained as a white solid and purified by column chromatography using hexane-ethyl acetate (1.5:1) as eluent (120 mg; 73% yield). mp 175–176 ºC. ^{1}H NMR (500 MHz, DMSO-d_6) δ 8.73, (s, 1H, N*H*Ar), 8.23–8.18 (m, 2H, Ar), 7.94–7.89 (m, 2H, Ar), 7.43–7.36 (m, 2H, Ar), 7.28–7.22 (m, 2H, Ar), 6.32 (t, *J* = 5.7 Hz, 1H, CH_2N*H*), 5.38 (bs, 1H, OH), 5.13–5.07 (m, 1H, CH), 4.32–4.23 (m, 2H, CH_2NH), 3.69-3.62 (m, 1H, CH_2OH), 3.26-3.19 (m, 1H, CH_2OH). ^{13}C NMR (125 MHz,

DMSO-d_6) δ 164.6, 155.2, 139.4, 139.3, 133.5, 130.2, 130.1, 128.4, 125.7, 124.8, 119.2, 119.0, 75.5, 67.4, 42.1. HRMS (*m/z*): calcd for $C_{18}H_{16}ClF_3N_2O_4Na$ 439.0643 $[M+Na]^+$; found 439.0637.

***N*-(4-Chlorophenyl)-*N'*-[3-hydroxy-2-(4-nitrobenzoyloxy)propyl]urea (227).** The product was obtained as a light yellow resin and purified by column chromatography using hexane-ethyl acetate (1:2) as eluent (116 mg; 73% yield). ^{1}H NMR (500 MHz, DMSO-d_6) δ 8.63, (s, 1H, N*H*Ar), 8.38–8.33 (m, 2H, Ar), 8.27–8.22 (m, 2H, Ar), 7.43–7.37 (m, 2H, Ar), 7.28–7.23 (m, 2H, Ar), 6.38 (t, *J* = 5.9 Hz, 1H, CH_2N*H*), 5.14–5.08 (m, 1H, CH), 5.03 (s, *J* = 5.9 Hz, 1H, OH), 3.71–3.62 (m, 2H, C*H*$_2$NH), 3.59–3.53 (m, 1H, C*H*$_2$OH), 3.47–3.40 (m, 1H, C*H*$_2$OH). ^{13}C NMR (125 MHz, DMSO-d_6) δ 164.0, 155.2, 150.2, 139.4, 133.5, 130.7, 128.4, 124.6, 123.7, 119.2, 75.8, 67.5, 60.4. HRMS (*m/z*): calcd for $C_{17}H_{16}ClN_3O_6Na$ 416.0620 $[M+Na]^+$; found 416.0617.

***N*-(4-Chlorophenyl)-*N'*-[3-hydroxy-2-(3,4,5-trimethoxybenzoyloxy)propyl]urea (228).** The product was obtained as a white solid and purified by column chromatography using hexane-ethyl acetate (1.5:1) as eluent (135 mg; 77% yield). mp 155–156 ºC. ^{1}H NMR (500 MHz, DMSO-d_6) δ 8.67, (s, 1H, N*H*Ar), 7.43–7.38 (m, 2H, Ar), 7.29 (s, 2H, Ar), 7.26–7.23 (m, 2H, Ar), 6.33 (t, *J* = 5.9 Hz, 1H, CH_2N*H*), 5.04–4.98 (m, 2H, CH, OH), 3.83–3.79 (m, 6H, OCH_3), 3.75–3.72 (m, 3H, OCH_3), 3.65–3.61 (m, 2H, C*H*$_2$NH), 3.57-3.52 (m, 1H, C*H*$_2$OH), 3.47–3.41 (m, 1H, C*H*$_2$OH). ^{13}C NMR (125 MHz, DMSO-d_6) δ 165.3, 155.2, 152.7, 141.9, 139.4, 128.4, 125.1, 124.8, 119.1, 106.9, 74.9, 60.4, 60.1, 56.0, 42.2. HRMS (*m/z*): calcd for $C_{20}H_{23}ClN_2O_7Na$ 461.1086 $[M+Na]^+$; found 461.1084.

***N*-{3-Hydroxy-2-[(4-trifluoromethyl)benzoyloxy]propyl}-*N'*-(4-methylphenyl) urea (229).** The product was obtained as a white resin and purified by column chromatography using hexane-ethyl acetate (1.5:1) as eluent (128 mg; 80% yield). ^{1}H NMR (500 MHz, DMSO-d_6) δ 8.48 (s, 1H, N*H*Ar), 8.25–8.20 (m, 2H, Ar), 7.85–7.79 (m, 2H, Ar), 7.29–7.21 (m, 2H, Ar), 7.14–7.00 (m, 2H, Ar), 6.29 (m, 1H, CH_2N*H*), 5.12–5.06 (m, 1H, CH), 5.03 (t, *J* = 5.9 Hz, 1H, OH), 4.32–4.23 (m, 2H, C*H*$_2$NH), 3.69–3.52 (m, 2H, C*H*$_2$OH). ^{13}C NMR (125 MHz, DMSO-d_6) δ 164.6, 155.4, 137.8, 137.7, 130.2, 129.8, 129.7, 128.9, 125.6, 125.5, 117.9, 117.7, 75.6, 60.5, 42.2, 20.2. HRMS (*m/z*): calcd for $C_{19}H_{19}F_3N_2O_4Na$ 419.1240 $[M+Na]^+$; found 419.1237.

***N*-[3-Hydroxy-2-(3,4,5-trimethoxybenzoyloxy)propyl]-*N'*-(4-methylphenyl)urea (230).** The product was obtained as a white solid and purified by column chromatography using hexane-ethyl acetate (1:2) as eluent (123 mg; 73% yield). mp 170–171 ºC. ^{1}H NMR (500 MHz, DMSO-d_6) δ 8.39, (s, 1H, N*H*Ar), 7.33–7.22 (m, 4H, Ar), 7.02 (d, *J* = 8.2 Hz, 2H, Ar), 6.23 (t, *J* = 5.9 Hz, 1H, CH_2N*H*), 5.03–4.98 (m, 2H, CH, OH), 3.88–3.80 (m, 6H, OCH_3), 3.78–3.72 (m, 3H, OCH_3), 3.66–3.61 (m,

2H, C*H*$_2$NH), 3.57–3.51 (m, 1H, C*H*$_2$OH), 3.47–3.40 (m, 1H, C*H*$_2$OH). ^{13}C NMR (125 MHz, DMSO-*d*$_6$) δ 165.2, 155.4, 152.6, 141.8, 137.7, 129.8, 128.9, 125.2, 117.8, 106.9, 75.0, 60.4, 60.1, 56.0, 20.2. HRMS (*m/z*): calcd for $C_{21}H_{26}N_2O_7Na$ 441.1632 $[M+Na]^+$; found 441.1629.

***N*-(4-Chlorophenyl)-*N'*-{3-hydroxy-2-[(4-trifluoromethyl)phenylaminocarboxy]propyl}urea (231).** The product was obtained as an amorphous solid solid and purified by column chromatography using using hexane-ethyl acetate (1:2) as eluent (112 mg; 64% yield). ^{1}H NMR (500 MHz, DMSO-*d*$_6$) δ 10.11 (s, 1H, N*H*COO), 8.70 (s, 1H, N*H*Ar), 8.72–8.62 (m, 4H, Ar), 7.45–7.39 (m, 2H, Ar), 7.29–7.22 (m, 2H, Ar), 6.32 (t, *J* = 5.75 Hz, 1H, CH$_2$N*H*), 4.96 (t, *J* = 5.60 Hz, 1H, OH), 4.86–4.70 (m, 1H, CH), 3.62–3.49 (m, 4H, C*H*$_2$NH, C*H*$_2$OH). ^{13}C NMR (125 MHz, DMSO-*d*$_6$) δ 155.1, 153.1, 142.9, 139.3, 128.4, 126.0, 125.5, 124.6, 122.5, 122.2, 119.1, 119.0, 117.9, 74.5, 67.7, 60.7. HRMS (*m/z*): calcd for $C_{18}H_{17}ClF_3N_3O_4Na$ 454.0752 $[M+Na]^+$; found 454.0748.

-Procedure 12. Olefin oxidation of N-Allyl-N'-(4-chlorophenyl)urea.

N-(4-chlorophenyl)-N'-(2,3-epoxypropyl)urea (234). According to the published procedure [120], a solution of *meta*-chloroperoxybenzoic acid (*m*CPBA), previous dried over $MgSO_4$, (15 mmol) in anhydrous THF (10 mL) was added to a solution (THF, 30 mL) of *N*-allyl-*N'*-(4-chlorophenyl)urea (**233**, 3 mmol) and the reaction mixture was stirred at rt until TLC showed that all the starting material had reacted (24 hours). After that, ethyl acetate (30mL) and a saturated solution of K_2CO_3 was added to the flask and the mixture was stirred for 5 minutes, then the phases were separated. The organic layer was washed with K_2CO_3 (3 x 20 mL) and brine, then dried over $MgSO_4$ and evaporated to dryness. The compound was obtained as a light yellow solid and purified by precipitation in toluene (542mg, 80%). ^{1}H NMR (500 MHz, DMSO-*d*$_6$) δ 8.70 (s, 1H, N*H*Ar), 7.42 (d, *J* = 8.8 Hz, 2H, Ar), 7.27 (d, *J* = 8.4 Hz, 2H, Ar), 6.32 (t, *J* = 5.0 Hz, 1H, CH$_2$N*H*), 3.22–3.17 [m, 2H, C*H*$_2$(O)CH], 3.07–3.04 [m, 1H, CH$_2$(O)C*H*], 2.73 (t, *J* = 4.7 Hz, 1H, C*H*$_2$NH), 2.57–2.55 (m, 1H, C*H*$_2$NH). ^{13}C NMR (125 MHz, DMSO-*d*$_6$) δ 155.0, 139.3, 128.5, 124.6, 119.2, 50.6, 44.6, 40.4. HRMS (*m/z*): calcd for $C_{10}H_{12}ClN_2O_2$ 227.0587 $[M+H]^+$; found 227.0582.

-Procedure 13. Epoxide ring opening of N-(4-chlorophenyl)-N'-(2,3-epoxypropyl)urea in acid condition.

N-(3-Azido-2-hydroxypropyl)-N'-(4-chlorophenyl)urea (235). According to a reported procedure [121], to a suspension of oxirane (**234**, 1 mmol) in ethanol (20 mL), were added sodium azide (1.2 mmol) and NH_4Cl (1.2 mmol) and the mixture was heated at 60 ºC and stirred until TLC showed the

full consumption of the starting material (15 hours). The reaction was washed with water (10 mL) and brine (10 mL), then dried over $MgSO_4$ and evaporated under reduced pressure. The compound was obtained as a light yellow resin and purified by flash column chromatography on silica gel using hexane:ethyl acetate (1:1) as eluent. (215 mg; 79% yield). ^{1}H NMR (500 MHz, DMSO-d_6) δ 8.70 (s, 1H, N*H*Ar), 7.41 (d, *J* = 9.0 Hz, 2H, Ar), 7.27 (d, *J* = 8.5 Hz, 2H, Ar), 6.25 (t, *J* = 5.8 Hz, 1H, CH_2N*H*), 5.40 (d, *J* = 5.1 Hz, 1H, OH), 6.76–6.71 (m, 1H, CH), 3.30–3.26 (m, 2H, C*H*$_2$NH), 3.25–3.17 (m, 1H, N_3C*H*$_2$), 3.11–3.06 (m, 1H, N_3C*H*$_2$). ^{13}C NMR (125 MHz, DMSO-d_6) δ 155.1, 139.4, 128.5, 124.5, 119.1, 69.1, 54.0, 42.8. HRMS (*m/z*): calcd for $C_{10}H_{12}ClN_5O_2Na$ 292.0572 $[M+Na]^+$; found 292.0574.

-Procedure 14. Mesylation reaction of N-[3-(benzoyloxy)-2-hydroxypropyl]-N'-(4-chlorophenyl)urea.

***N*-[3-Benzoyloxy-2-(methylsulfonyloxy)propyl]-*N'*-(4-chlorophenyl)urea (242)** According to the reported procedure with little modifications [122], to a solution of benzoyl derivative **212** (1mmol) and triethylamine (2 mmol) in dry THF (7 mL) was added dropwise the mesyl chloride (2 mmol) at 0 ºC. The reaction mixture was heated to room temperature and stirred for 5 hours, then NH_4Cl (5% water solution) and dichloromethane were added. The phases were separated and the organic layer was washed with saturated $NaHCO_3$, brine and dried over $MgSO_4$; then filtered and evaporated *in vacuo* to give compound as colourless oil, that was used without further modification. (220 mg; 92% yield). ^{1}H NMR (500 MHz, DMSO-d_6) δ 9.01 (s, 1H, *NH*Ar), 8.09-7.99 (m, 2H, Ar), 7.74-7.68 (m,1H, Ar), 7.61-7.52 (m, 2H, Ar), 7.48-7.39 (m, 2H, Ar), 7.30-7.23 (m, 2H, Ar), 6.71-6.64 (m, 1H, CH_2N*H*), 5.08-4.98 (m, 1H, CH), 4.64-4.39 (m, 2H, C*H*$_2$O), 3.60-3.52 (m, 2H, C*H*$_2$NH), 3.26 (s, 3H, CH_3). HRMS (*m/z*): calcd. for $C_{18}H_{19}ClN_2O_6SNa$ 449.0545 $[M+Na]^+$; found 449.0541.

-Procedure 15. Nucleophilic substitution reaction with sodium azide.

***N*-[2-Azido-(3-benzoyloxy)propyl]-*N'*-(4-chlorophenyl)urea (243).** According to the reported procedure [122], to solution of mesyl derivative (**242**, 0.5 mmol) in DMF (3 mL), was added sodium azide (2.5 mmol) at rt and the mixture was heated to 85 ºC and stirred overnight. The reaction was diluted with water and extracted with ethyl acetate. The organic phase was washed with saturated $NaHCO_3$ and brine, then was dried over $MgSO_4$ and filtered. The solvent was removed under reduced pressure to give compounds as colourless oil, that was used without further modification. (150 mg; 80% yield). ^{1}H NMR (500 MHz, DMSO-d_6) δ 8.78 (s, 1H, N*H*Ar), 8.06–7.99 (m, 2H, Ar), 7.73–7.66 (m, 1H, Ar), 7.60–7.51 (m, 2H, Ar), 7.47–7.39 (m, 2H, Ar), 7.31–7.23 (m, 2H, Ar), 6.51 (t, *J* = 5.9

Hz, 1H, CH_2NH), 4.53 (dd, J = 3.5 Hz, J = 11.8 Hz 1H, CH_2O), 4.35 (dd, J = 7.5 Hz, J = 11.9 Hz 1H, CH_2O), 4.12–4.06 (m, 1H, CH), 3.52–3.37 (m, 2H, CH_2NH). ^{13}C NMR (125 MHz, DMSO-d_6) δ 165.4, 155.0, 139.2, 133.5, 129.4, 129.3, 129.2, 128.7, 124.7, 119.3, 64.7, 60.2, 36.2.

-Procedure 16. Deprotection reaction of N-[2-azido-(3-benzoyloxy)propyl]-N'-(4-chlorophenyl)urea.

***N*-(2-Azido-3-hydroxypropyl)-*N'*-(4-chlorophenyl)urea (244).** According to the published procedure [123] with some modifications, ompound **243** (0.5 mmol) was dissolved in methanol and a 0.5 M sodium hydroxide solution (0.65 mmol) was added. The reaction mixture was heated to 55 ºC and stirred for 1 hour (TLC revealed the full consumption of the starting material). The reaction was evaporated to dryness and the residue was crystallized in DCM, filtered and washed with fresh DCM to give compound a white solid. (120, 88% yield). ^1H NMR (500 MHz, DMSO-d_6) δ 9.22 (s, 1H, N*H*Ar), 7.50–7.42 (m, 2H, Ar), 7.30–7.23 (d, 2H, Ar), 6.98–6.89 (m, 1H, CH_2NH), 3.75–3.71 (m, 2H, CH_2NH), 3.63–3.45 (m, 2H, CH_2OH), 3.26–3.15 (m, 1H, CHN_3). ^{13}C NMR (125 MHz, DMSO-d_6) δ 155.4, 139.7, 128.4, 124.4, 119.1, 63.2, 61.8, 42.8. HRMS (*m/z*): calcd for $C_{10}H_{12}ClN_5O_2Na$ 292.0572 $[M+Na]^+$; found 292.0573.

-General procedure 17. Synthesis of 1,2,3 triazole derivative by Cu(I)-catalyzed 1,3-dipolar cycloaddition (CuAAC) reaction (236-241, 245-250). According to the reported procedure with some modifications [124], azide derivative (**235** or **244**, 0.5 mmol) was dissolved in *tert*-butanol-water (1:1, 15 mL). The appropriate acetylene (0.6 mmol), sodium ascorbate (0.20 mmol) and $CuSO_4$ (0.10 mmol) were added to the flask and the mixture was stirring overnight at 55 ºC. The reaction was monitored by TLC until all the starting material had reacted, then was evaporated under *vacuum*. The product was purified by flash column chromatography on silica gel using the appropriate eluent.

***N*-(4-Chlorophenyl)-*N'*-{2-hydroxy-3-[4-(hydroxymethyl)triazolyl]propyl}urea (236).** The product was obtained as a light yellow solid and purified by column chromatography using dichloromethane-methanol (15:1, 0.5 % Et_3N) as eluent (130 mg; 79% yield), mp 131–132 ºC. ^1H NMR (500 MHz, CD_3OD) δ 7.95 (s, 1H, CH triazole), 7.39 (d, J = 9.2 Hz, 2H, Ar), 7.26 (d, J = 8.5 Hz, 2H, Ar), 4.83 (s, 2H, $HOCH_2$), 4.71 (s, 1H, C*H*OH), 4.58–4.53 (m, 1H, NCH_2), 4.43–4.37 (m, 1H, NCH_2), 3.29–3.24 (m, 1H, CH_2NH), 3.21–3.16 (m, 1H, CH_2NH). ^{13}C NMR (125 MHz, CD_3OD) δ 158.2, 139.8, 132.4, 129.7, 128.3, 125.3, 121.4, 70.7, 56.5, 54.9, 47.9. HRMS (*m/z*): calcd for $C_{13}H_{16}ClN_5O_3Na$ 348.0834 $[M+Na]^+$; found 348.0834.

***N*-(4-Chlorophenyl)-*N'*-{2-hydroxy-3-[4-(phtaloylaminomethyl)triazolyl]propyl}urea (237).** The product was obtained as a white solid and purified by column chromatography using hexane-ethyl acetate (1:4, 0.5 % Et_3N) as eluent (146 mg; 82% yield). mp 222–223 ºC. ^{1}H NMR (500 MHz, DMSO-d_6) δ 13.20 (sb, 1H, COO*H*), 8.75 (s, 1H, ArCON*H*CH_2), 8.03 (s, 1H, N*H*Ar), 7.94-7.84 (m, 3H, Ar), 7.79 (s, 1H, CH triazole), 7.60-7.56 (m, 1H, Ar), 7.43-7.39 (m, 2H, Ar), 7.28-7.24 (m, 2H, Ar), 6.22 (t, *J* = 5.6 Hz, 1H, CH_2N*H*), 5.10 (d, *J* = 5.1 Hz, 1H, OH), 4.86 (s, 2H, ArCONHCH_2), 4.49-2.22 (m, 2H, CH_2N), 3.95-3.88 (m, 1H, CH), 3.20-3.05 (m, 2H, , CH_2NH).^{13}C NMR (125 MHz, DMSO-d_6) δ168.4, 167.3, 155.2, 141.9, 139.4, 134.5, 131.6, 130.6, 128.4, 124.5, 123.9, 123.2, 119.1, 68.3, 59.4, 53.3, 42.8. HRMS (*m/z*): calcd. for $C_{21}H_{21}ClN_6O_5Na$ 495.1049 $[M+Na]^+$; found 495.1044.

***N*-(4-Chlorophenyl)-*N'*-{2-hydroxy-3-[4 (diethylphosphonatemethoxymethyl)triazolyl]propyl}urea (238).** The product was obtained as a colourless oil and purified by column chromatography using ethyl acetate-methanol (15:1, 0.5 % Et_3N) as eluent (193 mg; 81% yield). ^{1}H NMR (500 MHz, DMSO-d_6) δ8.78 (s, 1H, N*H*Ar), 8.17 (s, 1H, CH triazole), 7.42 (d, *J* = 8.9 Hz, 2H, Ar), 7.27 (d, *J* = 8.9 Hz, 2H, Ar), 6.33 (t, *J* = 5.7 Hz, 1H, CH_2N*H*), 5.46 (d, *J* = 5.5 Hz, 1H, OH), 4.63 (s, 2H, OCH_2), 4.43 (dd, *J* = 13.9 Hz, *J* = 3.9Hz, 1H, NCH_2), 4.29 (dd, *J* = 13.9 Hz, *J* = 7.5 Hz, 1H, NCH_2), 4.08–4.00 (m, 4H, OC$H_2$$CH_3$), 3.98–3.91 (m, 1H, C*H*OH), 3.85–3.82 (m, 2H, PCH_2O), 3.22–3.17 (m, 1H, CH_2NH), 3.13–3.07 (m, 1H, CH_2NH), 1.27–1.21 (m, 6H, OCH_2CH_3). ^{13}C NMR (125 MHz, DMSO-d_6) δ155.2, 142.6, 139.3, 128.4, 125.1, 124.6, 119.2, 68.6, 65.1, 63.5, 61.8, 53.2, 42.8, 16.2. HRMS (*m/z*): calcd for $C_{18}H_{27}ClN_5O_6PNa$ 498.1280 $[M+Na]^+$; found 498.1271.

***N*-(4-Chlorophenyl)-*N'*-{2-hydroxy-3-[4-(4-fluorophenyl)triazolyl]propyl}urea (239).** The product was obtained as a white solid and purified by column chromatography hexane-ethyl acetate (1:2.5, 0.5 % Et_3N) as eluent (117 mg; 60% yield), mp 230–231 ºC. ^{1}H NMR (500 MHz, DMSO-d_6) δ8.80 (s, 1H, N*H*Ar), 8.52 (s, 1H, CH triazole), 7.92–7.89 (m, 2H, Ar), 7.43 (d, *J* = 9.2 Hz, 2H, Ar), 7.31–7.26 (m, 4H, Ar), 6.36 (t, *J* = 5.9 Hz, 1H, CH_2N*H*), 5.47 (d, *J* = 5.5 Hz, 1H, OH), 4.71 (dd, *J* = 13.2 Hz, *J* = 3.5 Hz, 1H, NCH_2), 4.32 (dd, *J* = 14.0 Hz, *J* = 7.5 Hz, 1H, NCH_2), 4.04–3.97 (m, 1H, C*H*OH), 3.29–3.24 (m, 1H, CH_2NH), 3.17–3.12 (m, 1H, CH_2NH). ^{13}C NMR (125 MHz, DMSO-d_6) δ162.7, 160.7, 155.2, 145.2, 139.4, 128.5, 127.5, 127.1, 124.5, 122.1, 119.1, 115.9, 115.7, 68.7, 53.6, 42.9. HRMS (*m/z*): calcd for $C_{18}H_{18}ClFN_5O_2$ 390.1128 $[M+H]^+$; found 390.1121.

***N*-(4-Chlorophenyl)-*N'*-{2-hydroxy-3-[4-(4-methoxyphenyl)triazolyl]propyl}urea (240).** The product was obtained as a light yellow solid and purified by column chromatography using hexane-

ethyl acetate (1:2, 0.5 % Et_3N) as eluent (140 mg; 71% yield), mp 218–219 ºC. ^{1}H NMR (500 MHz, DMSO-d_6) δ 8.80 (s, 1H, N*H*Ar), 8.41 (s, 1H, CH triazole), 7.79 (d, *J* = 8.8 Hz, 2H, Ar), 7.44 (d, *J* = 8.9 Hz, 2H, Ar), 7.28 (d, *J* = 8.8 Hz, 2H, Ar), 7.02 (d, *J* = 8.8 Hz, 2H, Ar), 6.37 (t, *J* = 6.7 Hz, 1H, CH_2N*H*), 5.47 (d, *J* = 5.5 Hz, 1H, OH), 4.48 (dd, *J* = 13.9 Hz, *J* = 3.8 Hz, 1H, C*H*$_2$N), 4.32 (dd, *J* = 14.3 Hz, *J* = 7.6 Hz, 1H, C*H*$_2$N), 4.04–3.98 (m, 1H, C*H*OH), 3.81 (s, 3H, OCH_3), 3.27–3.20 (m, 1H, C*H*$_2$NH), 3.17–3.11 (m, 1H, C*H*$_2$NH). ^{13}C NMR (125 MHz, DMSO-d_6) δ 158.9, 155.2, 145.9, 139.4, 128.4, 126.4, 124.5, 123.5, 121.2, 119.1, 114.3, 68.7, 55.1, 53.5, 42.8. HRMS (*m/z*): calcd for $C_{19}H_{21}ClN_5O_3Na$ 402.1327 $[M+H]^+$; found 402.1321..

***N*-(4-Chlorophenyl)-*N'*-{2-hydroxy-3-[4-(2-formylphenyl)triazolyl]propyl}urea (241).** The product was obtained as a white solid and purified by column chromatography using hexane-ethyl acetate (1:2, 0.5 % Et_3N) as eluent (122 mg; 62% yield). mp 198–199 ºC. ^{1}H NMR (500 MHz, DMSO-d_6) δ 10.51(s, 1H, CO*H*), 8.87 (s, 1H, N*H*Ar), 8.66 (s, 1H, Ar), 7.94 (d, *J* = 7.5 Hz, 1H, Ar), 7.83–7.78 (m, 2H, Ar, C*H* triazole), 7.62–7.59 (m, 1H, Ar), 7.50–7.45 (m, 2H, Ar), 7.32–7.29 (m, 2H, Ar), 6.43 (t, *J* = 5.8 Hz, 1H, CH_2N*H*), 5.22 (d, *J* = 5.5 Hz, 1H, OH), 4.60 (dd, *J* = 13.9 Hz, *J* = 3.7 Hz, 1H, C*H*$_2$N), 4.42 (dd, *J* = 13.9 Hz, *J* = 7.8 Hz, 1H, C*H*$_2$N), 4.11-4.05 (m, 1H, C*H*N), 3.32–3.28 (m, 1H, C*H*$_2$NH), 3.22–3.18 (m, 1H, C*H*$_2$NH).^{13}C NMR (125 MHz, DMSO-d_6) δ 193.1, 155.7, 143.9, 139.8, 133.8, 133.7, 130.0, 128.9, 128.8, 127.9, 125.9, 125.0, 119.5, 69.1, 54.2, 43.3.

***N*-(4-Chlorophenyl)-*N'*-{3-hydroxy-2-[4-(hydroxymethyl)triazolyl]propyl}urea (245).** The product was obtained as a light yellow solid and purified by column chromatography using dichloromethane-methanol (15:1, 0.5 % Et_3N) as eluent (104 mg; 64% yield). mp 125–126 ºC. ^{1}H NMR (500 MHz, CD_3OD) δ 8.02 (s, 1H, CH triazole), 7.36-7.32 (m, 2H, Ar), 7.28-7.23 (m, 2H, Ar), 4.83 (s, 2H, HOC*H*$_2$), 4.15-4.10 (m, 1H, C*H*N), 4.02–3.97 (m, 2H, C*H*$_2$NH), 4.83 (dd, *J* = 5.1 Hz, *J* =14.3 Hz, 1H, C*H*$_2$OH), 3.74 (dd, *J* = 8.4 Hz, *J* = 14.4 Hz, 1H, C*H*$_2$OH). ^{13}C NMR (125 MHz, CD_3OD) δ 158.2, 148.9, 139.8, 129.7, 128.4, 125.3, 124.2, 121.4, 70.6, 64.7, 56.6, 44.3. HRMS (*m/z*): calcd. for $C_{13}H_{16}ClN_5O_3Na$ 348.0834 $[M+Na]^+$; found 348.0831.

***N*-(4-Chlorophenyl)-*N'*-{3-hydroxy-2-[4-(phtaloylaminomethyl)triazolyl]propyl}urea (246).** The product was obtained as a white solid and purified by column chromatography using hexane-ethyl acetate (1:4, 0.5 % Et_3N) (162 mg; 69% yield), mp 212–213 ºC. ^{1}H NMR (500 MHz, DMSO-d_6) δ 8.65 (s, 1H, , ArCON*H*CH$_2$), 8.10 (s, 1H, N*H*Ar), 7.93-7.87 (m, 5H, Ar, CH triazole), 7.38-7.34 (m, 2H, Ar), 7.28-7.22 (m, 2H, Ar), 6.22 (t, *J* = 5.8 Hz, 1H, CH_2N*H*), 5.10 (t, *J* = 5.4 Hz, 1H, OH), 4.86 (s, 2H, ArCONHC*H*$_2$), 4.71-4.65 (m, 1H, C*H*N), 3.74 (t, *J* = 5.5 Hz, 2H, C*H*$_2$OH), 3.69-3.63 (m,

1H, C*H*$_2$NH), 3.57-3.49 (m, 1H, C*H*$_2$NH).^{13}C NMR (125 MHz, DMSO-*d*$_6$) δ 167.3, 154.9, 141.9, 139.1, 134.5, 131.6, 128.4, 124.6, 123.2, 122.6, 119.1, 69.8, 62.8, 61.5, 33.0. HRMS (*m/z*): calcd. for $C_{21}H_{21}ClN_6O_5Na$ 495.9001 [M+Na]$^+$; found 495.8999.

***N*-(4-Chlorophenyl)-*N'*-{3-hydroxy-2-[4 (diethylphosphonatemethoxymethyl)triazolyl]propyl}urea (247).** The product was obtained as a colourless oil and purified by column chromatography using ethyl acetate-methanol (15:1, 0.5 % Et_3N) as eluent (173 mg; 72% yield). ^{1}H NMR (500 MHz, DMSO-*d*$_6$) δ 8.71 (s, 1H, N*H*Ar), 8.18 (s, 1H, C*H* triazole), 7.38 (d, *J* = 8.9 Hz, 2H, Ar), 7.25 (d, *J* = 8.9 Hz, 2H, Ar), 6.27 (t, *J* = 5.7 Hz, 1H, CH$_2$N*H*), 5.16 (t, *J* = 5.4 Hz, 1H, OH), 4.77-4.68 (m, 1H, C*H*N), 4.63(s, 2H, OC*H*$_2$), 4.08-3.98 (m, 4H, OC*H*$_2$CH$_3$), 3.87-3.82 (m, 2H, PC*H*$_2$O), 3.77 (t, *J* = 5.4 Hz, 2H, C*H*$_2$OH), 4.71-4.64 (m, 1H, C*H*$_2$NH), 4.61-4.53 (m, 1H, C*H*$_2$NH), 1.25-1.20 (m, 6H, OCH$_2$C*H*$_3$). ^{13}C NMR (125 MHz, DMSO-*d*$_6$) δ 155.5, 143.0, 139.7, 128.9, 125.1, 124.4, 119.5, 65.7, 64.0, 63.3, 62.7, 62.2, 62.0, 16.7. HRMS (*m/z*): calcd. for $C_{18}H_{27}ClN_5O_6PNa$ 498.1280 [M+Na]$^+$; found 498.1276.

***N*-(4-Chlorophenyl)-*N'*-{3-hydroxy-2-[4-(4-fluorophenyl)triazolyl]propyl}urea (248).** The product was obtained as a white solid and purified by column chromatography using hexane-ethyl acetate (1:2, 0.5 % Et_3N) as eluent (163 mg; 84% yield), mp 227–228 ºC. ^{1}H NMR (500 MHz, DMSO-*d*$_6$) δ 8.70 (s, 1H, N*H*Ar), 8.65 (s, 1H, C*H* triazole), 7.94–7.88 (m, 2H, Ar), 7.42–7.37 (m, 2H, Ar), 7.33–7.23 (m, 4H, Ar), 6.30 (t, *J* = 5.8 Hz, 1H, CH$_2$N*H*), 5.21 (t, *J* = 5.5 Hz, 1H, OH), 4.69–4.62 (m, 1H, C*H*N), 3.83 (t, *J* = 5.5 Hz, 2H, C*H*$_2$OH), 3.79–3.73 (m, 1H, C*H*$_2$NH), 3.63–3.56 (m, 1H, C*H*$_2$NH).^{13}C NMR (125 MHz, DMSO-*d*$_6$) δ 160.7, 155.0, 145.2, 139.1, 128.4, 127.5, 127.4, 124.6, 120.8, 119.1, 115.8, 115.7, 63.1, 61.6, 40.0. HRMS (*m/z*): calcd for $C_{18}H_{18}ClFN_5O_2Na$ 390.1128 [M+H]$^+$; found 390.1125.

***N*-(4-Chlorophenyl)-*N'*-{3-hydroxy-2-[4-(4-methoxyphenyl)triazolyl]propyl}urea (249).** The product was obtained as a light yellow solid and purified by column chromatography using hexane-ethyl acetate (1:1.5, 0.5 % Et_3N) (104 mg; 64% yield). mp 206–207 ºC. ^{1}H NMR (500 MHz, DMSO-*d*$_6$) δ 8.70 (s, 1H, N*H*Ar), 8.51 (s, 1H, C*H* triazole), 7.81–7.76 (m, 2H, Ar), 7.45–7.37 (m, 2H, Ar), 7.30–7.23 (m, 2H, Ar), 7.06–6.98 (m, 2H, Ar), 6.30 (t, *J* = 5.8 Hz, 1H, CH$_2$N*H*), 5.22 (t, *J* = 5.2 Hz, 1H, OH), 4.78–4.72 (m, 1H, C*H*N), 4.56–4.46 (m, 1H, C*H*$_2$OH), 4.36-4.29 (m, 1H, C*H*$_2$OH), 3.28–3.21 (m, 1H, C*H*$_2$NH), 3.16–3.11 (m, 1H, C*H*$_2$NH).^{13}C NMR (125 MHz, DMSO-*d*$_6$) δ 166.7, 158.8, 155.2, 155.0, 145.9, 139.1, 128.3, 127.3, 126.4, 124.7, 123.5, 121.3, 119.9, 114.2, 68.7, 62.9, 55.1, 43.5. HRMS (*m/z*): calcd. for $C_{19}H_{21}ClN_5O_3$ 402.8890 [M+H]$^+$; found 402.8889.

***N*-(4-Chlorophenyl)-*N'*-{3-hydroxy-2-[4-(2-formylphenyl)triazolyl]propyl}urea (250).** The product was obtained as a white resin and purified by column chromatography using hexane-ethyl acetate (1:2, 0.5 % Et_3N) (120 mg; 60% yield). H NMR (500 MHz, DMSO-d_6) δ 10.37 (s, 1H, CO*H*), 8.82 (s, 1H, N*H*Ar), 8.73 (s, 1H, Ar), 8.62 (s, 1H, CH triazole), 7.92–7.89 (m, 1H, Ar), 7.80–7.73 (m, 1H, Ar), 7.59–7.55 (m, 1H, Ar), 7.45–7.36 (m, 2H, Ar), 7.28–7.23 (m, 2H, Ar), 6.39 (t, *J* = 5.4 Hz, 1H, CH_2N*H*), 5.23 (t, *J* = 5.5 Hz, 1H, OH), 4.53 (dd, *J* = 13.9 Hz, *J* = 3.8 Hz, 1H, C*H*$_2$OH), 4.38 (dd, *J* = 13.9 Hz, *J* = 7.8 Hz, 1H, C*H*$_2$OH), 4.09–4.01(m, 1H, C*H*N), 3.29–3.23 (m, 1H, C*H*$_2$NH), 3.19–3.13 (m, 1H, C*H*$_2$NH). ^{13}C NMR (125 MHz, DMSO-d_6) δ 193.2, 155.7, 143.9, 139.8, 134.4, 133.8, 133.7, 130.0, 128.9, 128.8, 127.9, 125.9, 124.7, 119.5, 69.1, 54.2, 43.3.

6.1.4 Synthesis of reagents

-General procedure 18. Synthesis of phenylisocyanate from substituted aniline (251, 252)

According to a published procedure with some modifications [105], to a solution of appropriate substituted aniline (1.87 mmol) in DCM (20 mL) was added an aqueous solution of Na_2CO_3 (3 mmol, 20mL) and the heterogeneous mixture was vigorously stirred for 5 min at rt. Triphosgene (0.62 mmol) was added to the flask and stirred for 30 min. The phases were manually separated and the organic layer was dried over Na_2SO_4, filtered and evaporated to dryness. The isocyanate was used without further purification in reaction of urea and carbamate formation (sections 6.1.2 and 6.1.3).

1-isocyanato-2-methylbenzene (251). ^{1}H NMR (500 MHz, DMSO-d_6) δ 7.23-7.16 (m, 3H, Ar), 7.02-6.97 (m, 1H, Ar), 2.32 (s, 3H, CH_3). ^{13}C NMR (125 MHz, DMSO-d_6) δ 152.9, 137.5, 130.1, 127.8, 126.0, 122.7, 121.6.

3,4,5-trimethoxyphenyl isocyanate (252). ^{1}H NMR (500 MHz, DMSO-d_6) δ 6.79 (s, 2H, Ar), 3.77 (s, 6H, OCH_3), 3.63 (s, 3H, OCH_3). ^{13}C NMR (125 MHz, DMSO-d_6) δ 152.8, 135.7, 132.6, 96.2, 91.6, 60.0, 55.4. HRMS (*m/z*): calcd for $C_{10}H_{11}NO_4Na$ 210.0761 $[M+Na]^+$; found 210.0757.

-Procedure 19. Synthesis of N-propargylphtalylmonoamide (253) [125]**.** To a stirred solution of propargylamine (2.2 mmol) in THF (4 mL), phthalic anhydride (2 mmol) was added and the mixture was stirred at rt until TLC showed that all the starting material has reacted (18 hours). The formed solid was filtered, dissolved in water and 1 N solution of HCl was added until pH 5. The reaction was

extracted with EtOAc and the organic layer was washed with brine, dried over $MgSO_4$ and filtered. The solvent was removed under reduced pressure to give the compound that was used without further modification. (170 mg; 83% yield). ^{1}H NMR (300 MHz, DMSO-d_6) δ 9.91 (s, 1H, NH), 7.67–7.61 (m, 1H, Ar), 7.58–7.52 (m, 1H, Ar), 7.48–7.38 (m, 2H, Ar), 3.54 (m, 2H, CH_2), 3.90 (t, J = 2.49 Hz, 1H, CH).

-Procedure 20. Synthesis of propargyloxymethylphosphonate (254). A Solution of propargyl alcohol (1.5 mmol) in THF (3 mL) was added slowly to a solution of NaH (1.6 mmol, 60% dispersion in mineral oil) in THF (2mL). The mixture was stirred for 1 hour and then cooled to 0 ºC. Diethyl (tosyloxy)methylphosphonate (2 mmol) was added to the flask and the reaction was stirred for 3 hours at 0 ºC and then for 24 hours at rt. When TLC revealed the full consumption of the starting material, the reaction was evaporated to dryness and the residue was dissolved in ethyl acetate and washed with water (2 x 10 mL). The organic phase was dried over $MgSO_4$, filtered, and the solved was removed under *vacuum* to give compound as a colourless oil. The compound was used without further modification. (230 mg; 74% yield). MS (FAB): *m*/*z* 229 (100%) $[M+Na]^+$. ^{1}H NMR (300 MHz, DMSO-d_6) δ 4.28-3.22 (m, 2H, OCH_2), 4.12-3.95 (m, 4H, OCH_2CH_3), 3.86-3.78 (m, 2H, PCH_2O), 3.33 (S, 1H, CH), 1.30-1.13 (m, 6H, OCH_2CH_3).

6.2 Biological Methods

The evaluation of the antiviral activity, cytotoxicity and mechanistic studies of new described compounds has been carried out in Unit of Infectious Diseases, Microbiology and Preventive Medicine (IBiS) through a collaboration with members of this Institution. Hamster serum stability studies for optimized compounds were carried out in Fundación Medina, Parque Tecnológico de Ciencias de la Salud.

6.2.1. Cells and Virus

Human A549, 293 and MRC-5 cell lines were obtained from the American Type Culture Collection (ATCC, Manassas, VA). The 293β5 stable cell line overexpressing the human β5 integrin subunit was kindly provided by Dr. Glen Nemerow [126]. The cell lines were propagated in Dulbecco's modified Eagle medium (DMEM, Life Technologies/Thermo Fisher) supplemented with 10% fetal bovine serum (FBS) (Omega Scientific, Tarzana, CA), 10 mM HEPES, 4 mM L-glutamine, 100

units/ml penicillin, 100 μg/ml streptomycin, and 0.1 mM non-essential amino acids (complete DMEM).

Wild-type HAdV-5, and HCMV (AD169) were obtained from the ATCC. The HAdV-5-GFP used in this study is a replication-defective virus containing a CMV promoter-driven enhanced green fluorescent protein (eGFP) reporter gene cassette in place of the E1/E3 regions. HAdV were propagated in 293β5 cells and isolated from the cellular lysate by cesium chloride density centrifugation. Virus concentration, in mg/ml, was calculated with the Bio-Rad Protein Assay (Bio-Rad Laboratories) and converted to virus particles/ml (vp/ml) using 4×10^{12} vp/mg.

6.2.2. Cytotoxicity assay

The cytotoxicity of the compounds was evaluated using the AlamarBlue Cell Viability Assay (Invitrogen) according to the manufacturer's instructions. Actively dividing A549 cells were incubated with the thiourea /urea derivatives for 48 h. After the incubation the AlamarBlue reagent was added to the cells (1/10th Alamar Blue reagent in culture medium) for an extra 4 h. The 50% cytotoxic concentration (CC_{50}) of the molecules was calculated according to Cheng *et al* [127]. The selectivity index (SI) was evaluated as the ratio of CC_{50} to IC_{50}, where the IC_{50} was defined as the concentration of compound that inhibits HAdV infection by 50%.

6.2.3. Plaque assay

Compounds were tested in a dose-response assay using 0.06 vp/cell with concentrations ranging from 10 to 0.62 μM. Briefly, 293β5 cells were seeded in 6-well plates at a density of 4 × 105 cells per well in duplicates for each condition. When cells reached 80−90% confluency, they were infected with HAdV5-GFP (0.06 vp/cell) and rocked for 2 h at 37°C. After the incubation the inoculum was removed, and the cells were washed once with PBS. The cells were then carefully overlaid with 2 mL/well of equal parts of 1.6% (water/vol) Difco Agar Noble (Becton, Dickinson & Co., Sparks, MD) and 2× EMEM (Minimum Essential Medium Eagle, BioWhittaker) supplemented with 2×penicillin/streptomycin, 2× L-glutamine, and 10% FBS. The mixture also contained the compounds in concentrations ranging from 10 to 0.62 μM. Following incubation for 7 days at 37°C, plates were scanned in a Typhoon 9410 imager (GE Healthcare Life Sciences), and plaques were quantified with ImageJ [128].

6.2.4. Nuclear-associated HAdV genomes

Nuclear delivery of the HAdV genomes was assessed with real-time PCR following nuclear isolation from infected cells using a previously described protocol with a few modifications [128]. Briefly, 1×106 A549 cells in 6-well plates were infected with HAdV5 wild-type at an MOI of 2,000 vp/cell in the presence of 50 μM of the selected derivatives or the same volume of DMSO. Forty-five min after the infection, A549 cells were trypsinized and collected, and then washed twice with PBS. The cell pellet was resuspended in 500 μL of 1×hypotonic buffer (20 mM Tris-HCl pH 7.4, 10 mM NaCl, 3 mM MgCl2) and incubated for 15 min at 4°C. Then, 25 μL of NP-40 was added, and the samples were vortexed. The homogenates were centrifuged for 10 min at 835g at 4°C. Following the removal of the cytoplasmic fraction (supernatant), DNA was isolated from the nuclear fraction (pellet) using the QIAamp DNA Mini Kit (QIAGEN, Valencia, CA). We also measured the DNA copy number of the cellular housekeeping gene GAPDH in both samples the nucleus and the cytoplasm as a control for the purity of nuclear isolation.

6.2.5. HAdV yield reduction

The effect of the selected derivatives on virus production was evaluated in a burst assay. A549 cells were infected with wildtype HAdV-5, in the presence or absence of 50 μM of the compounds. After 48 h, cells were harvested and subjected to three rounds of freeze/thaw. Serial dilutions of clarified lysates were titrated on A549 cells, and the $TCID_{50}$ values were calculated using an end-point dilution method [129].

6.2.6. DNA and mRNA quantification by real-time PCR

For DNA quantification, A549 cells (1.5 x 105 cells/well in a 24-well plate) were infected with wild-type HAdV5 (100 vp/cell) and incubated for 2 h at 37°C in complete DMEM. After the incubation, the excess virus was removed, and the medium was replaced with 500 μL of complete DMEM containing 50 μM of either compounds or the same volume of DMSO (positive control). All samples were done in triplicates. After 24 h of incubation at 37°C and 5% CO2, DNA was purified from the cell lysate with the QIAamp DNA Mini Kit (QIAGEN, Valencia, CA) following the manufacturer's instructions. TaqMan primers and probes were designed for a region of the HAdV5 hexon with the GenScript Real-Time PCR (TaqMan) Primer Design software (GenScript). Oligonucleotides sequences were AdF, 5′-GACATGACTTTTGAGGTGGA-3′; AdR, 5′-

GTGGCGTTGCCGGCCGAGAA-3′; and AdProbe, 5′-TCCATGGGATCCACCTCAAA-3′. Real-time PCR mixtures consisted of 2 µL of the purified DNA, AdF, and AdR at a concentration of 200 nM each and AdProbe at a concentration of 50 nM in a total volume of 12.5 µL mixed with 12.5 µL of KAPA PROBE FAST qPCR Master Mix (KAPA Biosystems, MA). The PCR cycling protocol was 95°C for 3 min followed by 40 cycles of 95°C for 10 s and 60°C for 30 s.

For the evaluation of RNA expression, same conditions of infection applied for the DNA quantification were used. Six hours after infection, RNA was purified with the miRCURY RNA Isolation Kit (Exiqon Inc., MA) following the manufacturer's instructions. Quantification of RNA copy numbers was performed using primers and conditions previously reported for E1A [130]. The internal control was human glyceraldehyde-3-phosphate dehydrogenase (GAPDH) gene. Oligonucleotides sequences for GAPDH and conditions applied were those previously reported by Rivera *et al* [130]. For the quantification, gene fragments from hexon, and GAPDH were cloned into the pGEM-T Easy vector (Promega). Known concentrations of the template were used to generate a standard curve in parallel for each experiment. All assays were performed in a LightCycler® 96 System (Roche).

6.2.7. Antiviral activity of compound combinations

To assess the compound concentrations required in combination to generate a given effect to the derivative concentration that would be needed individually to achieve that same effect the software packet Calcusyn (BioSoft, Ferguson, MO, USA) was used. A plaque dose-response assay was carried out using all the possible combination of the three piperazine derivatives starting from twice the IC_{50} obtained previously for each compound and the ratio of those concentrations. CalcuSyn software interpolates the compound concentrations needed in combination at the selected ratio to generate effects of 50%, 75% and 90% inhibition and compares these combinations with the concentrations from the three compound's individual dose-response curves required to achieve the same inhibition. The combination effect of the three compounds is reported by the combination index (CI) value, a pharmacological interaction estimation which uses the IC_{50} and the dose-response curve's shape of each individual compound and their combinations. The CI value was interpreted in accordance with Matthews *et al* [88].

6.2.8. Phi29 DNA polymerase amplification efficiency assay

Amplification of a BAC vector containing HAdV DNA genome was performed in the presence of the compounds at a concentration of 50 μM or the same amount of DMSO in triplicates, using the RCA DNA Amplification Kit (MCLAB) following the manufacturer's instructions. To quantify the amplified products, a quantitative real-time PCR was performed using TaqMan primers and probes designed for a region of the HAdV5-wt hexon with GenScript Real-time PCR (TaqMan) First Design software (GenScript). The oligonucleotide sequences were AQ1:5' -GCC ACG GTG GGG TTT CTA AAC TT -3'; AQ2:5' -GCC CCA GTG GTG TTC TTA CAT GCA CAT -3'; and AP: 6-FAM-5' -TGC ACC AGA CCC CGG CTC AGG TAC TCC GA-3' –TAM. Real-time PCR mixtures consisted of 2 μL of the purified DNA, AdF, and AdR at a concentration of 200 nM each and AdProbe at a concentration of 50 nM in a total volume of 12.5 μL mixed with 12.5 μL of KAPA PROBE FAST qPCR Master Mix (KAPABiosystems, MA). The PCR cycling protocol was 95°C for 3 min followed by 40 cycles of 95°C for 10 s and 60°C for 30 s. All assays were conducted on a C1000 ThermalCycler thermal cycler (BioRad). The results represent the mean ± SD of the samples in triplicates from three independent experiments.

6.2.9. Hamster serum stability assay

The test compound solution (1 μM, 0.25% final DMSO concentration) was incubated with Syrian hamster serum (IGHMS-SER, Innovative Grade US Origin Hamster Serum- Syrian Gold) at 37ºC. Serial samples were taken at 0, 15, 30, 60 and 120 min. All samples were added immediately to 3 volumes of methanol in a microtiter plate cooled in dry-ice to halt chemical degradation. All the samples were analyzed by LC-MS/MS. The percentage of parent compound remaining at each time point relative to the 0 min sample was calculated from peak area. The chemical stability assay returns the percent parent compound remaining at each time point for thiourea derivatives. LC/MS/MS conditions were as follow: Analytes were detected by electrospray ionization (ESI) mass spectrometry in positive mode for **616** and **628**, and negative mode for **585**. Identification was obtained using multiple reaction monitoring (MRM) mode of the transitions at *m/z* 352.074/252.100 for **585**, *m/z* 378.285/143.200 for **616**, and *m/z* 399.116/143.100 for **688**. The chromatographic separation was accomplished on a Discovery® C18 column (50 × 2.1 mm, 3 μm) coupled with a Discovery® HS C18 (20 × 2.1 mm, 3 μm) guard column. The mobile phase consisting of water with

0.1% formic acid (A) and acetonitrile with 0.1% formic acid (B). The flow rate was 0.5 ml/min and the run time was 5 minutes using a linear gradient. The volume injection was 5 μL.

6.2.10. Statistical Analyses

Statistical analyses were performed with the GraphPad Prism 5 suite. Unless otherwise indicated, data are presented as the mean of triplicate samples ± standard deviation (SD). P-values are indicated when statistically significant.

CHAPTER 7
CONCLUSION

1. A set of piperazine derivatives was designed and prepared through an optimization process employing the privileged structure-guided scaffold refining strategy starting from prototypes of our previous work:
   a) From pathway A (replacement of the urea function with a thiourea one), SAR analysis showed that active compounds possessed electron-withdrawing groups at the phenyl ring of the thiourea function. Related to the acyl group at N-4 the highest number of active compounds was detected among those compounds having a 2-cyclohexylacetyl moiety. According to their biological data, eight piperazine-thiourea derivatives were preliminary selected (**52**, **67**, **68**, **71**, **73**, **75**, **80** and **92**) from this route**.**
   b) From pathway B (exchange the acyl groups at N-4 with three different 2-substituted acetyl groups), all evaluated 2-substituted acetyl-2-phenylpiperazine urea derivatives were very active (percentage of plaque-formation inhibition > 80%), but only two were selected (**96**, **98**) because of their low cytotoxicity.
   c) From pathway C (replacement of the central core of 2-substituted piperazine with 2,6-dimethylpiperazine and unsubstituted piperazine), in general terms, 2,6-dimethylpiperazine central backbone failed to provide any improvement over the prototypes. However, among the piperazine derivatives, **112** and **114**, that showed high plaque-formation inhibition (> 90%) and CC_{50} (> 100 μM), were selected.
2. These twelve derivatives demonstrated to block HAdV infection in a dose-dependent manner, with IC_{50} values ranging from 0.6 μM to 5.1 μM. The mechanistic studies suggested that for three of them (**96**, **98** and **114)** the antiviral activity was associated with some steps of HAdV entry. Compounds **71**, **73**, **75**, **80**, and **112** inhibited HAdV DNA replication. Finally, for **52**, **67**, **68**, and **92** the mechanism of action may be related to later steps in the HAdV replicative cycle.
3. A small library of serinol derivatives (37 compounds) was designed with the aim to identify novel scaffolds for the development of new effective anti-HAdV agents. The nitrogen was functionalized as phenyl ureas, whereas the hydroxyl groups as aromatic esters or carbamates possessing substituents with different electronic properties. Mono and diacylated derivatives were prepared. The selective mono-acylation reaction was performed by strictly controlling the time, the stoichiometry and the temperature.

4. According to the biological evaluation data serinol-based aromatic diesters resulted to be promising derivatives. Those compounds having electron-withdrawing groups at the phenyl urea function, and electron-donor groups at the benzoic moiety were the most active. Four compounds (**131**, **132**, **145** and **150**) were identified as effective anti-HAdV agents; they dose-dependently reduced HAdV infection, showing IC_{50} values ranging from 2.8 μM to 5.4 μM, much lower than cidofovir (24.1 μM). These four compounds interfered with HAdV DNA replication and three of them (**131**, **132** and **150**) inhibited the E1A early gene expression. Any of them interfered with the early steps of the entry phase of the HAdV viral particles.
5. A collection of 3-amino-1,2-propanediol (55 compounds) derivatives was designed to further explore the potential of aminoalcohol scaffolds in providing effective antiviral agents. Preserving the urea function at the nitrogen, the hydroxyl groups were firstly functionalized as substituted aromatic esters and also they were replaced with triazole groups:
   a) The selective *O*-acylation reaction of primary alcohol group was performed following similar procedure than for serinol; while for the introduction of the ester function on the secondary alcohol, an acyl protection and deprotection strategy was developed.
   b) A multistep synthesis was employed for the introduction of the triazole function at primary or secondary positions of the aminoalcohol skeleton. For the preparation of the azide precursors at primary or secondary position, two different strategies were developed. Once they were obtained, the synthesis of 1,2,3-triazole ring (1,4 adduct) was performed through a click chemistry approach, the copper(I)-catalysed alkyne-azide 1,3-dipolar cycloaddition (CuAAC) reaction by using the appropriate terminal alkyne.
6. In a similar way to serinol-derived aromatic diesters, electron-donating groups on the aromatic acyl moiety afforded most active compounds, while regarding to the urea function, both electron-withdrawing and donating groups on the phenyl ring were present (**182**, **188**, **190**, **196** and **207**) In addition, one monoester derivatives at position 2 presented 100% of inhibition (**226**). These six derivatives demonstrated a significant inhibition of HAdV infection (> 60%) and displayed IC_{50} values at low micromolar concentration (2.47–4.19 μM). At present these compounds are being submitted to further biological assays in order to selected those compounds with suitable selectivity index and explore their potential mechanism of action.
7. In summary, novel scaffolds based on piperazine and aminoglycerol cores were identified as potential tool useful for the development of effective anti-HAdV drugs

CHAPTER 8

HOMODRIMANE SCAFFOLD FOR THE DEVELOPMENT OF SELECTIVE TRPV4 ANTAGONISTS

8.1 Insights into TRPV4 channel and its functions

8.1.1 Structure and localization

TRPVs belong to the superfamily of Transient Receptor Potential (TRP) cation Channels together with TRPC (Canonical), TRPM (Melastatin), TRPP (Polycystin), TRPML (Mucolipin), the TRPA (Ankyrin), and TRPN (NOMP-C). These receptors are expressed in many cells and tissues and are implicated in several homeostatic functions [131]. TRPVs include four groups of receptors, depending on their structure and function: TRPV1/2, TRPV3, TRPV4 and TRPV5/6 [132,133]. TRPV4 is a non-selective vanilloid cation channel with high permeability to Ca^{2+} and an architecture similar to other receptors of the family. It is a homotetramer of 871 amino acids with a transmembrane domain (TMD) that consists of S1-S6 transmembrane α-helices (Figure 30). These segments and the pore loop form the pore channel associated to an S1-S4 bundle in a voltage-sensor like domain (VSLD) [132].

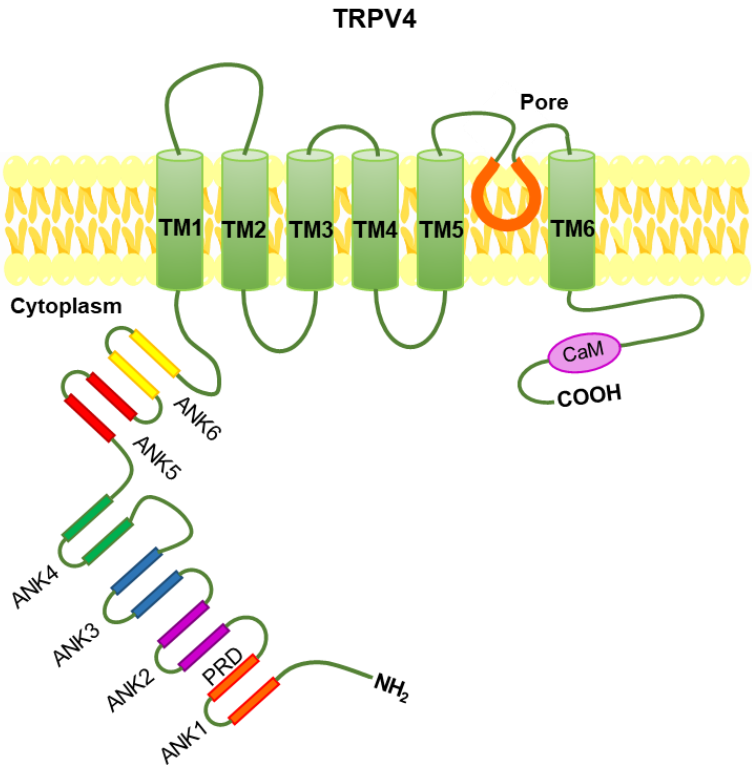

Figure 30. Schematic model of TRPV4 ion channel.

The cytosolic region includes N- and C- terminal domains. N-terminus presents 6 ankyrin (ANK) repeats implicated in protein interaction and in the assembly into a tetrameric structure [134,135]. A proline-rich-domain (PRD) is located closer to the first ANK repeat and regulates mechanosensitive properties of TRPV4 channel; moreover, some central prolines interact with PACSIN 3, a cytoskeleton protein that plays a key role in neurons membrane trafficking and endocytosis [136]. The C-terminus preserves channel protein folding, maturation and interacts with microtubule-associated protein-7. It includes several calmodulin (CaM) binding sites involved in calcium-dependent activation of TRPV4 [137,138] (Figure 30).

TRPV4 is activated by several stimuli such as the hypo-tonicity, temperature (24-27 ºC), pH and UVB radiation. TRPV4 is sensitive to the activation by endocannabinoids anandamide (arachidonoyl-ethanolamide, AEA) and its metabolite arachidonic acid (AA), that activates metabotropic cannabinoid receptors [139]. TRPV4 function is mediated by different signalling mechanisms, such as the Ca^{2+}-dependent modulation. An increase of intracellular calcium levels primary enhance TRPV4 channel activity and then promotes the channel inactivation. This effect is associated to the calmodulin-binding site on C-terminal portion, that is important for the constitutive opening of the channel [140]. TRPV4 is also regulated through the phosphorylation by Src-family tyrosine kinases (SFKs) of tyrosine residues at N- and C-termini [141] Its activation mechanism is also mediated by protein kinase C (PKC), inositol (1,4,5) triphosphate receptor type 3 (IP_3). In fact, PKC inhibitors radically reduced its channel activity[142,143].

TRPV4 is ubiquitously expressed, especially in the lung, brain, kidney, urinary bladder, retina, liver, pancreas and endothelial cells, suggesting its involvement in many physiological processes. TRPV4 in lung and bronchial epithelium is implicated in mucociliary transport and regulation of ciliary beating [131]. TRPV4 is localized also in epithelial cells of the nephron in the kidney [144] in urothelial cells of urethra and urinary bladder, where it is involved in osmoregulation and contributes to the bladder voiding [145]**.** Alteration of the osmolarity in the renal medulla are regulated through tubular reabsorption of Na^+ and water by ATP. Hypotonic conditions stimulate the release of ATP from epithelial cells and it is reported that the activation of TRPV4 also promote an increase of ATP levels, in order to restore the osmotic balance [131]. TRPV4 participates in the regulation of neuronal functions in the peripheral and the central nervous system. In the hypothalamus it is involved in the thermogenesis and detects the temperature modulating the excitability of dopaminergic neurons of the substantia nigra and a population of serotonergic neurons implicated in the behaviour [146]. TRPV4 activity in hippocampal astrocytes is improved after ischemia and hypoxia conditions, and it get involved on the cell death caused by oxidative stress [147]. TRPV4 is also expressed in peripheral

nociceptive neurons in trigeminal and dorsal root ganglia, when it acts as a sensor for mechanical and osmotic stimuli [148]. TRPV4 is highly expressed in the vascular endothelium and in the smooth muscle of pulmonary, aortic and cerebral arteries. It is able to intervene on the vascular tone contributing to cold-induced vasoconstriction and heat-mediated vasodilatation of peripheral blood vessels [149]. TRPV4 regulates also the vascular permeability; in fact, increased pressure in lung capillaries promote the activation of TRPV4 channel and calcium influx, improving the vascular permeability and the synthesis of NO. However, the uncontrolled activation of TRPV4 could alter the normal microvascular permeability causing acute circulatory collapse [131].

8.1.2 Therapeutic opportunities of TRPV4 modulators

The involvement in several physio-pathological conditions prompted the researchers to identify selective TRPV4 modulators, in order to examine how agonists and antagonists could be used in clinical setting. It is reported that TRPV4 is involved in inflammatory lung diseases and urinary bladder dysfunctions [150].

One of the first discovered agonists was bisandrographolide A (BAA, **255**, Figure 31), a dimeric diterpenoid plant from *Andrographis paniculata*, that was able to activate TRPV4 with EC_{50} values in the range between 790 and 950 nM, without any activity against TRPV1, TRPV2, or TRPV3 channels [151]. Also 4R-phorbol-12,13-didecanoate (4α-PDD, **256** Figure 31), a semisynthetic phorbol ester, is able to activate TRPV4 with EC_{50} value of 370 nM, binding in a portion of TM3-TM4 domain. The lipophilic ester moieties influenced the orientation of the diterpenoid core into the binding pocket [152]. GSK1016790A (**257**, Figure 31) is a small molecule hTRPV4 channel agonist (hTRPV4 EC_{50}=2.1 nM) that was employed to investigate the involvement of this receptor in urinary bladder, highlighting its role in bladder voiding [153]. Unfortunately, GSK1016790A causes adverse effects in rats, such as TRPV4-dependent lung edema and circulatory failure [154]. These preliminary studies allow to the development of new synthetic agonists potentially useful in urinary bladder disorders or other TRPV4-mediated diseases. A potent TRPV4 activator based on quinazolin-4(3H)-one scaffold (**258**, Figure 31) was identified by Atobe *et al* as potential useful agent in osteoarthritis. Compound **258** in hydrochloride form reached an excellent EC_{50} value (60 nM), reducing the cartilage degradation as well as the osteoarthritis progression in rat model [155].

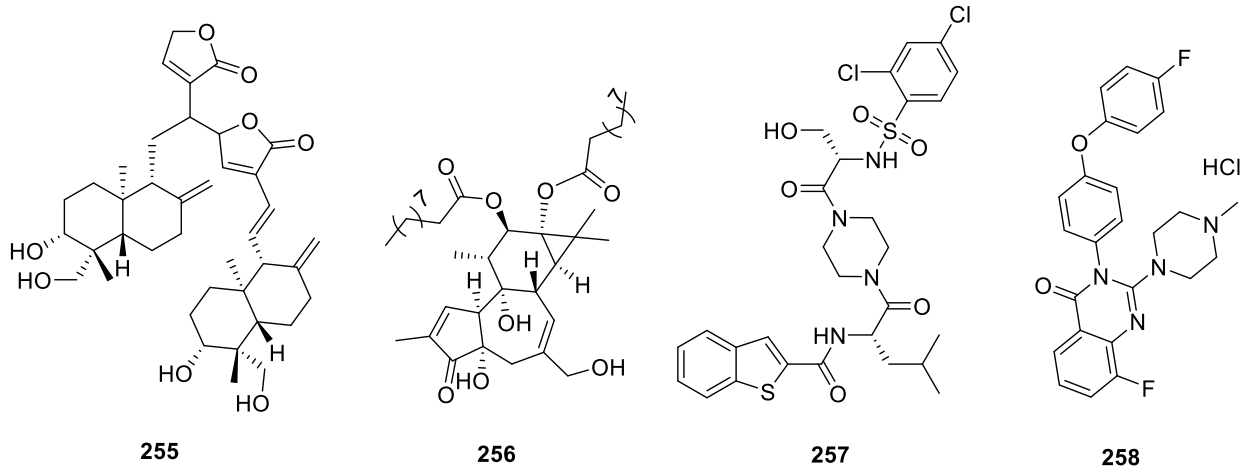

Figure 31. Known TRPV4 agonists.

Instead, TRPV4 antagonism could be useful for the treatment of edema, pain, gastrointestinal and lung diseases. During the years, several structural diversified compounds have been reported as TRPV4 antagonists. HC-067047 (**259**, Figure 32), a pyrrole-3-carboxamide derivative, is considered an historical selective TRPV4 antagonist that has a mitigating effect on painful neuropathy in diabetic mice. In particular, it was able to prevent mechanical allodynia acting on constitutive receptors [156]. Quinoline-carboxamide GSK2193874 (**260**, Figure 32) has been identified as potent and orally active TRPV4 channel antagonist, with IC_{50} value of 40 nM against hTRPV4. It demonstrated to be a suitable candidate for the treatment of pulmonary edema associated with congestive heart failure [157]. Also a series of 1-(4-piperidinyl)-benzimidazole amides (**261**, Figure 32) have been prepared as selective TRPV4 inhibitors useful in pulmonary edema [158].

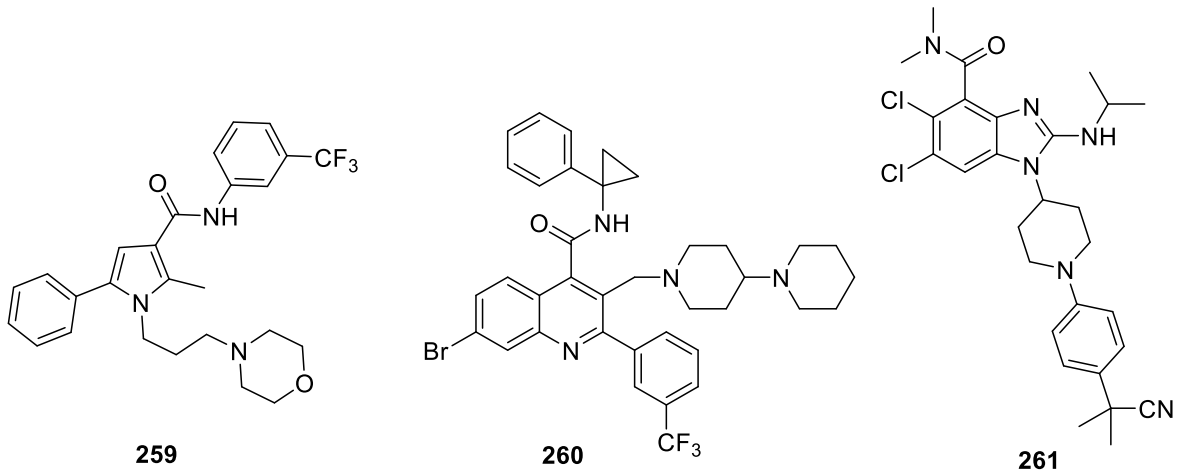

Figure 32. Representative synthetic TRPV4 antagonists part I.

In line with these structures, a typical replacement of amide/ester functions with a sulphonamide one furnished interesting molecules with inhibitory activity in the low nanomolar range. From the GSK family, pyrrolidine sulphonamide derivatives have been investigated by an optimization process. One of them (GSK3527497, **262**, Figure 33) resulted to be a strong inhibitor of TRPV4 (EC_{50} = 12 nM). It showed suitable pharmacokinetic properties that allow intravenous or oral administration and represented a potential candidate for treatment of TRPV4-dependent diseases [159,160]. Also phytochemicals represent interesting tools for the development of TRP channels modulators [161]. In this context, 3-substituted pyridine polyketide onydecalin A (**263**, Figure 33), derived from the fungus *Aioliomyces pyridodomos*, was validated as a TRPV4 antagonist (IC_{50} = 45.9 µM), with a partial activity versus TRPV1 [162]. These compounds and their structural features represented interesting tools for the development of new selective TRPV4 antagonists potentially useful in therapy.

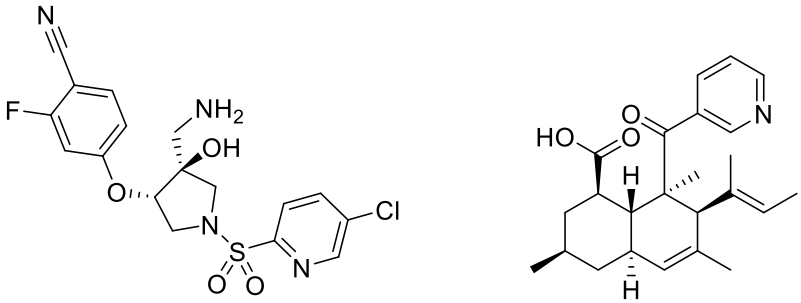

262 **263**

Figure 33. Representative synthetic TRPV4 antagonists part II.

8.2 Design of new homodrimane-based compounds

This study aims to investigate a new potential scaffold for the selective inhibition of TRPV4 channel. The contemporary presence of a *trans*-decalin lipophilic moiety in two TRPV4 modulators from natural source, bisandrographolide A (agonist) and onydecalin A (antagonist), prompted us to employed a natural homodrimane scaffold to generate a set of new suitable TRPV4 antagonists. Based on typical structural features of many reported ligands, several amides, esters and ethers were designed to examine their effect on the interaction with the receptor (Figure 34)

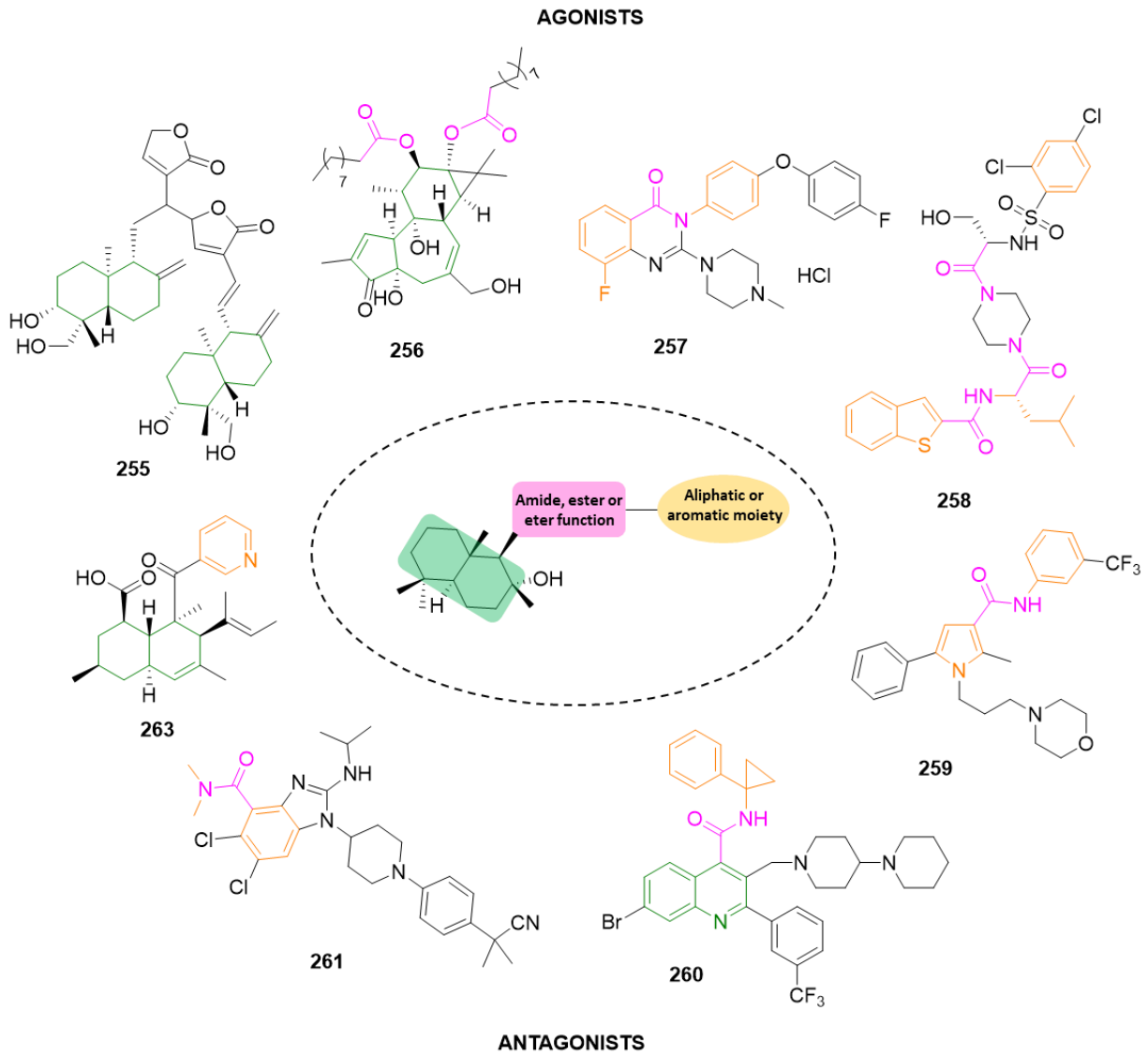

Figure 34. Design of new compounds based on homodrimane scaffold starting from known TRPV4 ligands.

Our attention has been focused on (+)-sclareolide, a sesquiterpene lactone found in *Salvia sclarea* that was employed as a flavour additive in food. (+)-Sclareolide and its alcoholic derivative sclareol demonstrated several biological properties, such as antifungal, antibacterial, anticancer, anti-inflammatory and antiviral ones [163–165].

Since (+)-sclareolide is a lactone condensed with a *trans*-decalin-related drimane scaffold, it was selected as the starting point for the development of a small library of compounds with homodrimane backbone decorated as amide, ester or ether derivatives (Figure 35). Aromatic systems with differences in size, flexibility, and electronic properties were connected to the bicyclic nucleus through the acyl or ether function and a spacer chain of different lengths. The family of homodrimanyl

aliphatic and aromatic amides presented electron-withdrawing or donating groups in several position of the phenyl ring, such as -F, -Cl and -OMe. The effect of pyrrole substituent as well as the presence of imidazole and furan heterocycles were also evaluated. For the most active compounds, the replacement of amide function with the ester one was performed. Homodrimanyl diol esters (reverted esters) were examined in combination with a pyperonylic group, its cinnamic derivative or a thiophene ring. All compounds were then evaluated *in vitro* for their ability to interact with TRPV4 and TRPV1 channels.

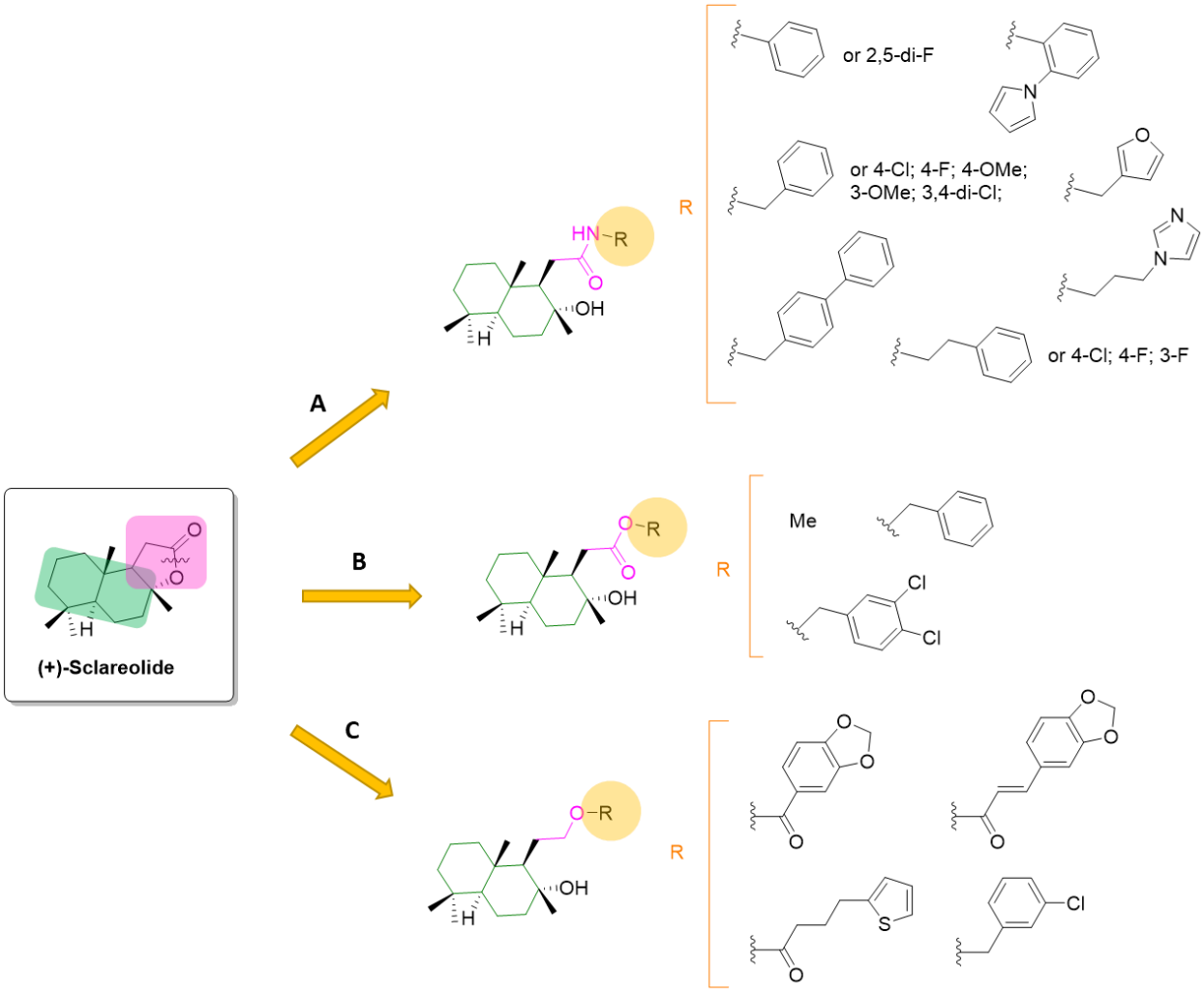

Figure 35. General structures of new designed homodrimanyl amides, esters and ethers from (+)-sclareolide.

8.3 Chemical modification of (+)-sclareolide

From a chemical point of view, all compounds shared the drimane scaffold and differed in the nature of the substituent at position 1 (Figure 34). Aliphatic or aromatic moieties were connected by a spacer to an amide, ester, reverted ester or ether function. With the aim to prepare the designed compounds, we performed several modifications of the (+)-sclareolide scaffold, commercially available, through the opening or the reduction of the lactone ring that provided the drimane sesquiterpene moiety. New synthesized homodrimanyl derivatives were characterized by NMR and through the determination of melting points. Representative resonance assignments from ^{1}H NMR and ^{13}C NMR of some selected compounds were illustrated in the Table 27, 28 and 29).

-Pathway A: Semi-synthesis of homodrymanyl amides (265-280)

Homodrymanyl amide derivatives **265-280** (Table 27) were prepared in high yield through an aminolysis reaction, following two different procedures in accordance with the employed reagent. Compounds derived from aromatic amines (**265-267**) were synthesized through a DIBAL-H assisted amidation. The DIBAL-amine complex was previously generated and used to react with (+)-sclareolide in THF at room temperature. In the presence of aliphatic amines (**268-280**), the lactone ring opening of (+)-sclareolide was carried out by a direct aminolysis, using the amine and THF as co-solvents at 45 ºC (Scheme 13).

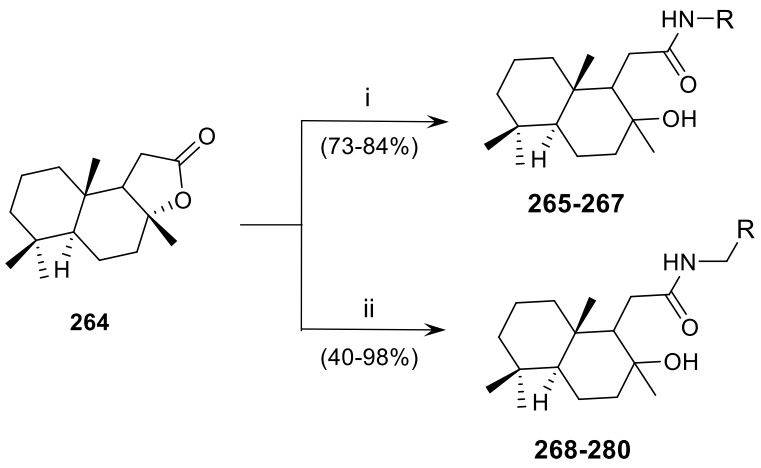

i: Aromatic amine 2.5 eq, DIBAL-H 3 eq, dry THF, rt, 3-5 h

ii: Aliphatic amine, dry THF, 45 ºC, 48 h

Scheme 13. Semi-synthetic pathways for the preparation of homodrymanyl amides (**265-280**).

New synthesized homodrymanyl amides were characterized by NMR, IR Spectroscopy and melting points determination. Representative resonance assignments from ^{1}H NMR and ^{13}C NMR are illustrated in the Table 24.

Table 24. Homodrymanyl amide derivatives and some selected resonance assignments (^{1}H NMR and ^{13}C NMR).

Comp.

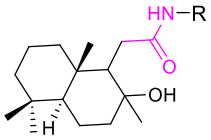

Comp.	R	Yield (%)	^{1}H NMR[a] (ppm)			^{13}C NMR[b] (ppm)		
			CH_2NH	CH_2CO	COH(CH_3)	C=O	Cq-Ar/CH imid[b]	*Cq*-OH(CH_3)
265		84		2.55; 2.22	1.12	174.0	138.4	73.6
266	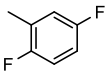	73	-	2.59; 2.26	1.20	173.6	158.7; 148.3; 128.1	74.1
267	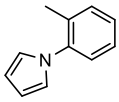	80	-	2.41; 2.11	1.05	173.8	134.8; 130.7	73.4
268	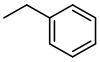	98	4.38-4.21	2.36; 2.09	1.02	175.6	138.4	72.9
269	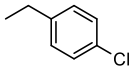	70	4.35-4.21	2.42; 2.16	1.07	175.8	137.1; 132.9	72.9
270	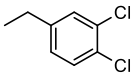	83	4.26; 4.15	2.34; 2.05	0.93	174.6	141.7; 131.3; 130.8	71.6
271	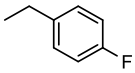	97	4.37; 4.31	2.39; 2.14	1.10	175.2	162.1; 134.3	73.2
272	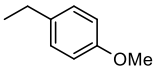	78	4.34; 4.29	2.39; 2.12	1.10	175.1	159.0; 130.5	73.1
273	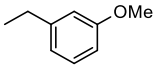	85	4.30; 4.17	2.36; 2.09	1.00	178.9	159.6; 140.1	72.9
274	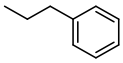	95	3.48-3.32	2.02; 1.85	1.04	175.6	139.0	72.9
275	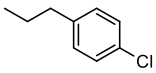	75	3.27-3.20	2.21; 1.95	0.93	174.4	139.1; 131.0	71.6
276	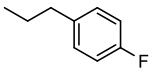	83	3.52-3.37	2.29; 2.04	1.09	175.4	161.6; 134.7	73.1
277	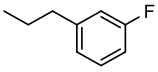	72	3.53-3.32	2.34; 2.06	1.07	175.8	164.5; 161.2	72.9
278		95	4.40; 4.36	2.38; 2.12	1.10	175.1	151.5	73.2

Comp.	R	Yield (%)	^{1}H NMR[a] (ppm)				^{13}C NMR[b] (ppm)	
			C*H*$_2$NH	C*H*$_2$CO	COH(C*H*$_3$)	C=O	Cq-Ar/CH imid[b]	*Cq*-OH(CH$_3$)
279	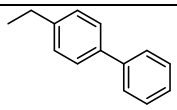	40	4.50-4.36	2.46; 2.17	1.12	175.4	140.7; 140.2; 137.5	73.1
280	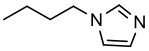	93	3.23-3.11	2.34; 2.12	1.12	175.9	137.2; 129.2; 119.0[b]	73.3

[a]300 or 400 MHz, $CDCl_3$-*d*

[b]125MHz, $CDCl_3$-*d*

-Pathway B: semi-synthesis of homodrymanyl acid esters (282-284)

Homodrimanyl acid esters **282** and **283** (Table 28) were synthesized in two steps (Scheme 14). Firstly, (+)-Sclareolide was hydrolyzed with sodium hydroxide in methanol at room temperature to give the free carboxylic acid **281**. Compound **281** then reacted with corresponding benzyl bromide in basic condition (K_2CO_3) and in dry DMF, affording final compound. On the other hand, the methyl ester **284** was obtained by direct alcoholysis in methanol at 45 C°.

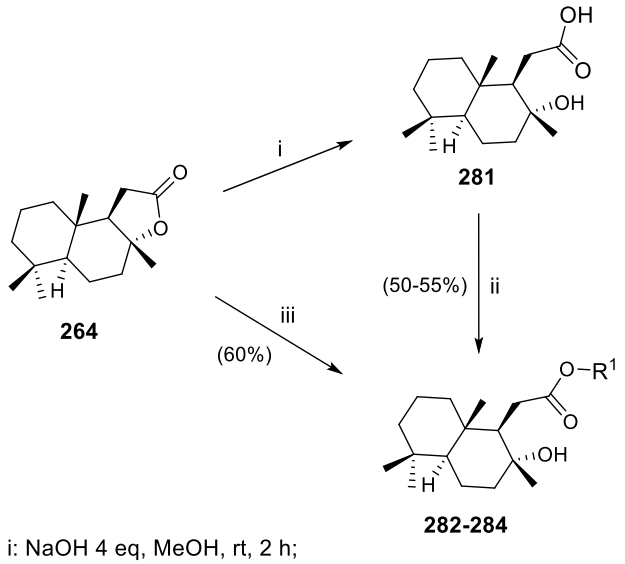

i: NaOH 4 eq, MeOH, rt, 2 h;

ii: Benzyl bromide 1 eq, K_2CO_3 1 eq, dry DMF, rt, 24 h;

iii: MeOH, 45 °C, 72 h

Scheme 14. Semi-synthetic pathways for the preparation homodrymanyl acid esters (**282-284**).

New synthesized homodrymanyl acid esters were characterized by NMR, IR Spectroscopy and melting points determination. Representative resonance assignments from ^{1}H NMR and ^{13}C NMR are illustrated in the Table 25.

Table 25. Homodrymanyl acid ester derivatives and some selected resonance assignments (^{1}H NMR and ^{13}C NMR).

Comp.

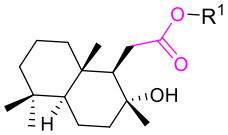

	R	Yield (%)	^{1}H-NMR[a] (ppm)			^{13}C-NMR[b] (ppm)		
			*CH₂*O/COO*CH₃*[b]	*CH₂*CO	COH(*CH₃*)	C=O	Cq-Ar	*Cq*-OH(CH₃)
282	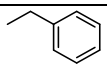	55	5.20-5.10	2.60; 2.38	1.18	175.5	136.0	73.1
283	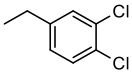	50	5.02	2.52; 2.32	1.12	177.0	141.1; 132.6; 131.4	86.4
284	Me	60	3.71[b]	2.51; 2.27	1.20	175.0	-	73.18

[a]300 or 400 MHz, $CDCl_3$-*d*

[b]125MHz, $CDCl_3$-*d*

-Pathway C: semi-synthesis of homodrymanyl diol esters and ether (286-289)

In the synthetic route for the preparation of reverted esters **286-288** and ether **289** (Table 29), homodrimanyl diol **285** represented the crucial intermediate (Scheme 15). The reduction of carbonyl group of sclareolide lactone, with $LiAlH_4$ in anhydrous THF and at room temperature, afforded the desired compound. Homodrimanyl diol esters **286-288** was obtained by the reaction between diol derivative **285** and the appropriate carboxylic acids in dichloromethane under Steglich conditions (DMAP and EDCI). Finally, ether **289** was synthesized from **285** refluxing it with 3-chlorobenzyl bromide in basic condition (NaOH) and anhydrous THF (Scheme 15).

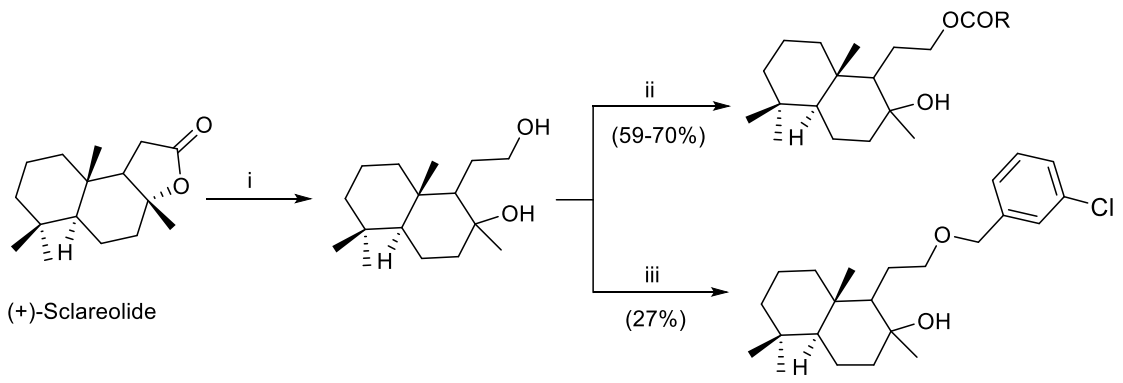

i: $LiAlH_4$ 10 eq, dry THF, rt, 6 h

ii: Carboxylic acid 1 eq, EDCI 1.2 eq, DMAP 0.1 eq, DCM, rt, 48-72 h

iii: NaH 1.1 eq, 3-chlorobenzyl chloride 1.2 eq, dry THF, reflux, 48 h.

Scheme 15. Semi-synthetic pathways for the synthesis of homodrymanyl diol esters and ether (**286-289**).

New synthesized homodrymanyl diol esters and ether were characterized by NMR, IR Spectroscopy and melting points determination. Representative resonance assignments from ^{1}H NMR and ^{13}C NMR are illustrated in the Table 26.

Table 26. Homodrymanyl diol ester and ether derivatives and some selected resonance assignments (^{1}H NMR and ^{13}C NMR).

Comp.

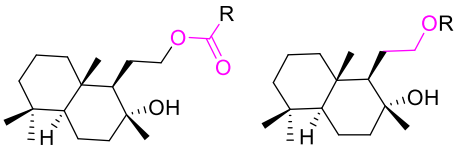

	R	Yield (%)	^{1}H NMR[a] (ppm)			^{13}C NMR[b] (ppm)		
			OCH_2O-/CH thienyl[a]/ CH_2-Ar[b]	CH_2OCO	$COH(CH_3)$	C=O	Cq-Ar	Cq-$OH(CH_3)$
286 (A)	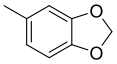	59	6.01	4.36-4.29	1.31-1.10	166.1	151.5; 147.7; 124.6	73.7
287 (A)	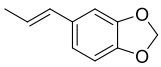	65	5.98	4.28-4.17	1.16	167.3	149.6; 148.4; 128.9	73.6
288 (A)	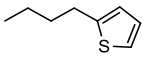	70	6.78[a]	4.17-4.06	1.14	173.4	144.1	73.6
289 (B)	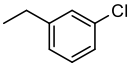	27	4.49[b]	3.68-3.57; 3.41-3.30	1.14	-	139.9; 129.8	72.5

[a]300 or 400 MHz, $CDCl_3$-*d*

[b]125MHz, $CDCl_3$-*d*

8.4 *In vitro* pharmacological characterization

Al compounds from the library of *trans*-decalin-related derivatives, homodrimanyl amide, homodrimanyl acid ester, homodrimanyl diol ester and the ether derivative as well as the intermediate homodrimanyl diol and (+)-sclareolide were tested for their ability to interact with both TRPV4 and TRPV1. The evaluation of changes in intracellular calcium levels were assessed in HEK-293 cell line overexpressing the rat recombinant type-4 (rTRPV4) and the human recombinant type-1 (hTRPV1) channels. The EC_{50} (for activation) and IC_{50} (for antagonism) values were determined and indicated in Table 27.

Among homodrimanyl amides (**265-280**) many derivatives demonstrated to be selective rTRPV4 ligands with an antagonistic activity, whereas no suitable activity was observed towards hTRPV1. Compounds with a spacer of three atoms between the phenyl moiety and the drimane scaffold were not active (unsubstituted and di-fluorien substituted compounds, **265**, **266**), with the exception of compound **267** (2-pyrrol-1-yl derivative), that showed good IC_{50} values against rTRPV4 but resulted poorly effective (Table 27). The majority of benzyl amides, characterized by a four-atom spacer, have the ability to bind the TRPV4 channel. In particular, substituted compounds in *meta* or *para* position on the terminal phenyl ring with electron-withdrawing groups, such as halogens fluorine or chlorine (**269**, **270** and **271**), gave better inhibitory activity compared to derivatives with electron-donating ones (IC_{50} range = 5.3-16-9 vs 18.1-29.7 μM respectively). Compounds **270**, with an addition chlorine atom (3,4-di-chlorine derivative), further increased the activity, afforded the most potent antagonist of this set of drimane-derivatives (IC_{50}= 5.3 μM). On the other hand, compounds presenting a biphenyl system (**279**) or a furan ring (**278**) in the place of benzyl moiety abolished or very decreased the inhibitory activity (IC_{50} > 100 μM and of 53.5 μM respectively). With regard to homodrimanyl amides with a phenylethyl moiety (**274-277**), also in this case the presence of halogens groups in *para*- or *meta*- position (Cl or F, **275-277**) on the aromatic ring improved the activity compared to unsubstituted derivative **274**, displaying IC_{50} values from 7 μM to 11.9 μM vs 15.6 μM. Finally, the presence of an imidazole head and a six-atom spacer (**280**) abolished the activity against rTRPV4 (Table 30). Indeed, compounds with five-atom spacer (**274**, **275**, **277**) reached a better interaction with TRPV4 compared to more shortly spacer analogues (benzylic amides **268**, **269**, **271**, Table 27).

Table 27. TRPV 4 and TRPV1 assays for compounds **265-289**.

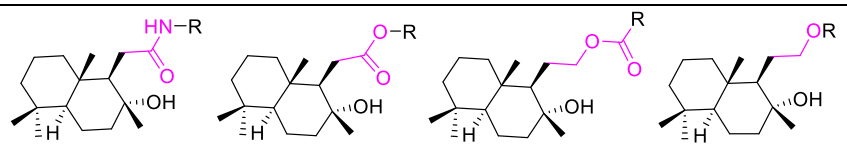

A B C D

Compd.	R	rTRPV4			hTRPV1		
		Efficacy[b] %	Potency EC_{50} (µM)	IC_{50} (µM)[c] inh TRPV4	Efficacy[b] %	Potency EC_{50} (µM)	IC_{50} (µM)[c] inh TRPV4
265 (A)		< 10	NA[d]	> 100	33.6 ± 0.8	45.7 ± 0.5	> 100
266 (A)	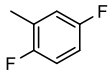	< 10	NA	> 100	< 10	NA	> 100
267 (A)	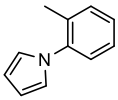	14.6± 1.5[a]	1.1 ± 1.0	6.0 ± 0.1	32.0 ± 1.2	4.7 ± 0,4	> 100
268 (A)	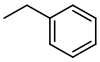	< 10	NA	32.0 ± 0.8	36.8 ± 0.2	30.3 ± 0.4	32.8 ± 0.6
269 (A)	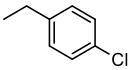	< 10	NA	7.7 ± 0.3	< 10	NA	> 100
270 (A)	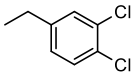	< 10	NA	5.3 ± 0.3	16.9 ± 0.3	> 10	> 100
271 (A)	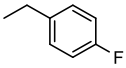	15.8± 0.8	13.4± 2.6	16.9 ± 0.8	24.5± 0.2	9.9 ± 0.1	59.1 ± 1.9
272 (A)	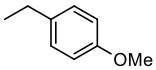	< 10	NA	29.7 ± 0.7	19.7 ± 1.1	41.3 ± 6.7	> 100
273 (A)	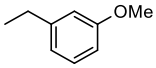	< 10	NA	18.1 ± 0.2	< 10	NA	> 100
274 (A)	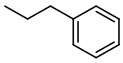	< 10	NA	15.6 ± 0.3	< 10	NA	31.7 ± 0.3
275 (A)	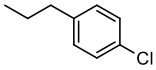	< 10	NA	7.0 ± 0.1	< 10	NA	> 100
276 (A)	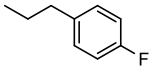	< 10	NA	11.4 ± 0.1	< 10	NA	> 100
277 (A)	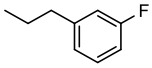	< 10	NA	11.9 ± 0.4	20.8 ± 1.6	11.6 ± 3.4	52.1 ± 0.1
278 (A)		< 10	NA	53.5 ± 1.8	25.2 ± 2.0	> 10	> 100
279 (A)	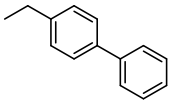	< 10	NA	> 100	< 10	NA	> 100
280 (A)	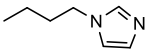	< 10	NA	> 100	< 10	NA	> 100
282 (B)	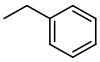	< 10	NA	5.41± 0.07	< 10	NA	38.9 ± 6.3

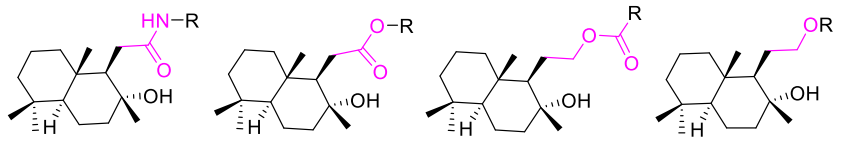

A B C D

Compd.	R	rTRPV4			hTRPV1		
		Efficacy[b] %	Potency EC_{50} (μM)	IC_{50} (μM)[c] inh TRPV4	Efficacy[b] %	Potency EC_{50} (μM)	IC_{50} (μM)[c] inh TRPV4
283 (B)	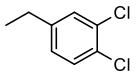	< 10	NA	> 100	17.5 ± 2.7	39.8 ± 11.5	> 100
284 (B)	Me	< 10	NA	> 100	< 10	NA	> 100
285 (C)	H	< 10	NA	> 100	< 10	NA	> 100
286 (C)	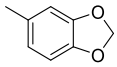	<10	NA	NA	< 10	NA	> 100
287 (C)	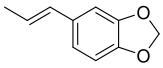	< 10	NA	> 100	< 10	NA	> 100
288 (C)	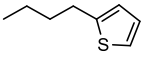	< 10	NA	> 100	< 10	NA	> 100
289 (D)	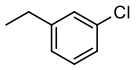	< 10	NA	> 100	32.7 ±	> 10	> 100
Sclareolide	-	11.3± 0.7	> 10	> 100	12.6 ± 0.5	> 10	> 100

[a]Data are means ± SEM of at least $N = 3$ determinations. [b]As percent of the effect of ionomycin (4 μM). Inh = inhibitory activity. [c]Determined against the effect of **GSK1016790A** (10 nM) for TRPV4 assay and **capsaicin** (0.1Mm) for TRPV1, after a 5 min pre-incubation with each compound. [d]NA = not active, if the efficacy is lower than 10% the potency is not calculated

Considering these promising results of some homodrymanil amides, the effect of the amide function replacement with the ester one was assessed for two compounds, furnishing unclear results. The homodrimanyl acid ester **282** (analogue of compound **268**) is one of the most potent antagonist (IC_{50} = 5.41 μM) together with compound **270** (amide). In contrast, the 3,4-dichlorobenzyl ester **283** (analogue of compound **270**) demonstrated to be completely inactive against TRPV4 (IC_{50} > 100 μM). This result could be related to a different receptor sites potentially occupied by amide and ester derivatives, due to the higher flexibility of the ester group that facilitated its accommodation in a different narrow pocket. In this context, the presence of more halogens on the phenyl ring (compound **283**) may be affect the correct binding with receptor. The reverted homodrimanyl diol esters **286-288** and ether **289** resulted inactive against both hTRPV1 and rTRVP4, regardless of the presence of piperonylic or thiophene moiety and the spacer length (IC_{50} > 100 μM, Table 27). Also (+)-sclareolide, the methyl ester **284** and the diol intermediate **285** were not active. For best compounds **270** (amide) and **283** (ester) the dose-response curves are depicted in Figure 36. Further studies are necessary to identify the correct binding sites of these molecules, despite the low resolution of available TRPV4 structures.

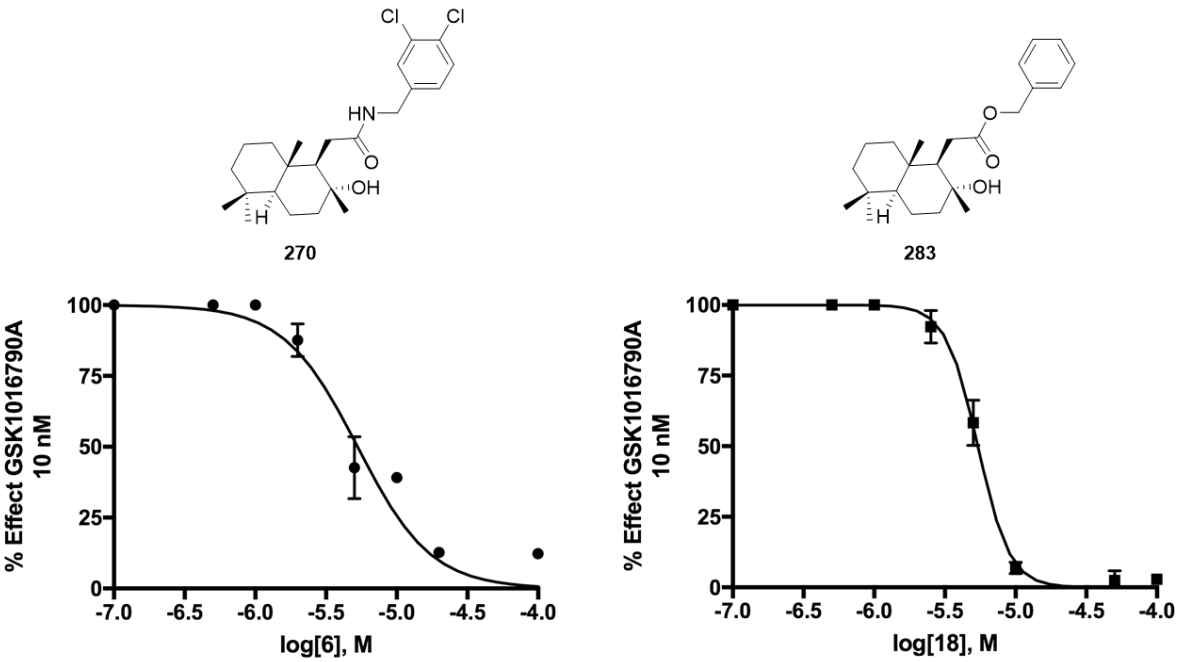

Figure 36. Dose-response curve for best compounds **270** and **283**.

8.5 Conclusion

1. A set of 22 new homodrimanyl amide, esters and ether derivatives were designed, synthesized and tested against hTRPV1 and rTRPV4, identifying a novel class of selective TRPV4 antagonists.
2. Compounds **270** and **283**, homodrimanyl amide and ester respectively, resulted the most potent inhibitors of the series, showing IC_{50} values at low micromolar concentration (5.3 μM and 5.41 μM) and resulting 9-fold more active than onydecalin A. From a structure-activity relationship point of view, the nature of the acyl function directly connected to the drimane scaffold, the length of the spacer chain between the bicyclic system and the terminal phenyl ring seems to be relevant features for the activity on new compounds. The most interesting compounds were included in the amide series, presenting four- or five-atom spacer including the carbonyl group and the aromatic moiety decorated with electronegative substituents as chlorine or fluorine.

3. These promising results highlighted the possibility to employ the drimane skeleton for the development of new interesting TRPV4 modulators and further investigate their efficacy in TRPV4-mediated phatological conditions.
4. In the last few years, the evidence on the role of TRPV4 channel in lung and vascular physiology prompted to investigate this protein as a potential therapeutic target for the treatment of pulmonary edema. Studies on the efficacy of selective TRPV4 inhibitor GSK2798745 on the pulmonary vascular permeability demonstrated that it was able promote a reduction in total protein and neutrophils levels, with subsequently edema regression. The effect of TRPV4 antagonism in lungs could be also useful in the fight against the current COVID-19 pandemic and the severe respiratory syndrome associated with this virus, since TRPV4 also protect and rescue the integrity of the alveolocapillary barrier and could improve patient outcomes [166].

8.6 Experimental part

8.6.1 General chemical methods

All the reagents, solvents and starting materials were purchased from commercial suppliers and were used without further purification. The crude reaction mixtures were concentrated under reduced pressure by removing the organic solvents in a rotary evaporator. Reactions were monitored by thin layer chromatography (TLC) using Kieselgel 60 F254 (Merck, MA, USA) plates and UV detector for visualization. Final products were purified by a flash chromatography system with column chromatography, using Merck 60 silica gel, 230–400 mesh. Melting points were obtained using a Gallenkamp (G) melting point apparatus. The structures of final compounds were unambiguously assessed by ^{1}H NMR and ^{13}C NMR. Spectra were recorded in the indicated solvent at 25 °C on a Bruker 300 MHz spectrometer (Bruker, Milano, Italy) or a Bruker Advance DPX400 employing TMS as internal standard and chemical shifts are expressed in δ values (ppm) and coupling constants (*J*) in hertz (Hz) used as solvents. IR spectra were recorded on a PerkinElmer machine 10.4.00 (PerkinElmer, Milan, Italy). The purity of final compounds was evaluated by C, H and N analysis through Leco Trunspec CHNS Micro elemental system.

***-General procedure 21. Synthesis of homodrimanyl amides through lacton ring opening reaction of* (+)-sclareolide (*265-267*)**

A) DIBAL-H-mediated amidation from substituted anilines. In according with the published procedure [167], to a solution of appropriate substituted aniline (1.0 mmol) in anhydrous THF (1.5 mL) at 0 °C, under argon flux and stirring, a solution of DIBAL–H (1 M in toluene, 3 mmol) was added dropwise. The reaction mixture was warmed to rt and stirred for the next 2 h. The prepared complex was used directly for the aminolysis. (+)-Sclareolide (0.4 mmol) was dissolved in anhydrous THF (1.0 mL) and the DIBAL-H-aniline complex solution was added. The mixture was stirred at rt until TLC showed that all the starting material had reacted (3-5 h). Then, it was cooled to 0 °C, quenched with a 1 M $KHSO_4$ aqueous solution (2.0 mL), and extracted with DCM (3 × 10 mL). The combined organic layers were finally washed with brine, dried over anhydrous Na_2SO_4, filtered and the solvent was removed under reduced pressure. The compound was further purified by flash column chromatography on silica gel using petroleum ether-ethyl acetate as eluent.

2-((1*R*,2*R*,4a*S*,8a*S*)-2-Hydroxy-2,5,5,8a-tetramethyldecahydronaphthalen-1-yl)-*N* phenylacetamide (265) [167]**.** The product was obtained as a white solid and purified by column chromatography using petroleum ether-ethyl acetate (5:1) as eluent (115 mg; 84% yield). ^{1}H NMR (300 MHz, $CDCl_3$) δ: 8.77 (s, 1H, NH), 7.45 (d, J = 7.5 Hz, 2H, Ar), 7.21 (t, J = 7.4 Hz, 2H, Ar), 7.01 (t, J = 7.4 Hz, 1H, Ar), 3.10 (s, 1H, OH), 2.55 (dd, J_1 = 15.3 Hz, J_2 = 4.3 Hz, 1H, CH_2CO), 2.22 (dd, J_1 = 15.5 Hz, J_2 = 4.7 Hz, 1H, CH_2CO), 1.89 (dt, J_1 = 12.3 Hz, J_2 = 2.8 Hz, 1H), 1.77 (t, J = 4.1 Hz, 1H), 1.70-1.18 (m, 9H), 1.12 (s, 3H, CH_3), 1.10-0.85 (m, 1H, CH), 0.80 (s, 3H, CH_3), 0.74 (s, 6H, CH_3). ^{13}C NMR (75 MHz, $CDCl_3$) δ: 174.0, 138.4, 129.8, 127.7, 124.8, 120.7, 118.8, 73.6, 57.8, 55.1, 43.4, 41.7, 38.8, 35.9, 34.9, 33.2, 24.8, 23.3, 22.2, 20.5, 18.2, 143.6. Anal. Calcd. for $C_{22}H_{33}NO_2$: C, 76.92; H, 9.68; N, 4.08. Found: C, 77.05; H, 9.71; N, 4.07.

***N*-(2,5-difluorophenyl)-2-((1*R*,2*R*,4a*S*,8a*S*)-2-hydroxy-2,5,5,8a-tetramethyldecahydronaphthalen-1-yl)acetamide (266)**. The product was obtained as a white solid and purified by column chromatography using petroleum ether-ethyl acetate (8:1) as eluent (112 mg; 73% yield); mp 165–166 °C. ^{1}H NMR (400 MHz, CDCl3) δ (ppm): 8.78 (brs, 2H, NH), 8.24-8.14 (m, 1H, Ar), 6.99-6.91 (m, 1H, Ar), 6.67-6.61 (m, 1H, Ar), 2.59 (dd, J_1 = 15.0 Hz, J_2 = 4.6 Hz, 1H, CH_2CO), 2.26 (dd, J_1 = 15.0 Hz, J_2 = 4.0 Hz, 1H, CH_2CO), 1.92 (dt, J_1 = 12.3 Hz, J_2 = 3.1 Hz, 1H, -CH_2-COH(CH_3)), 1.78 (t, J = 4.2 Hz, 1H, -CH-COH(CH_3)), 1.71-1.66 (m, 2H), 1.60-1.50 (m, 2H), 1.48-1.24 (m, 4H), 1.20 (s, 3H, COH(CH_3)), 1.00-0.89 (m, 2H), 0.85 (s, 3H, CH_3), 0.79 (s, 3H, CH_3), 0.78 (s, 3H, CH_3). ^{13}C NMR (400 MHz, $CDCl_3$) δ (ppm): 173.6 (C=O), 158.7 (d, J = 240 Hz, *Cq*-F),

148.3 (d, *J* = 238 Hz, *Cq*-F), 128.1 (*CqAr*), 114.9 (dd, J_1 = 9.7 Hz, J_2 = 21.9 Hz, *CHAr*), 109.2 (d, *J* = 24.6 Hz, *CHAr*), 108.5 (d, *J* = 36.3 Hz, *CHAr*), 74.1 (*Cq*-OH(CH_3)), 58.2 (*CH*-CH_2CO), 56.0 (CH), 44.2, 41.8, 39.4, 38.9 (*Cq*-(CH_3)$_2$), 34.7, 33.3, 29.7, 24.3, 21.4, 20.5, 18.2, 15.3. IR ν (cm^{-1}): 3266, 2925, 1680, 1630, 1542, 1441, 1189, 754. Anal. Calcd. for $C_{22}H_{31}F_2NO_2$: C, 69.63; H, 8.23; N, 3.69. Found: C, 69.50; H, 8.27; N, 3.68.

***N*-(2-(1*H*-pyrrol-1-yl)phenyl)-2-((1*R*,2*R*,4a*S*,8a*S*)-2-hydroxy-2,5,5,8a-tetramethyldecahydronaphthalen-1-yl)acetamide (267)**. The product was obtained as a light yellow oil and purified by column chromatography using petroleum ether-ethyl acetate (4.5:1) as eluent (131 mg; 80% yield). ^{1}H NMR (400 MHz, $CDCl_3$) δ (ppm): 8.32 (d, *J* = 8.2 Hz, 1H, Ar), 8.10 (brs, 1H), 7.36 (t, *J* = 7.8 Hz, 1H, Ar), 7.21 (d, *J* = 7.4 Hz, 1H, Ar), 7.10 (d, *J* = 7.6 Hz, 1H, Ar), 6.79 (t, *J* = 1.8 Hz, 2H, Pyrrol), 6.36 (t, *J* = 1.8 Hz, 2H, Pyrrol), 2.41 (dd, J_1 = 14.9 Hz, J_2 = 4.5 Hz, 1H, CH_2CO), 2.11 (dd, J_1 = 14.9 Hz, J_2 = 4.1 Hz, 1H, CH_2CO), 1.84 (dt, J_1 = 11.8 Hz, J_2 = 2.9 Hz, 1H, -CH_2-COH(CH_3)), 1.69-1.63 (m, 2H), 1.61-1.48 (m, 2H), 1.45-1.33 (m, 3H), 1.28-1.10 (m, 2H), 1.05 (s, 3H, COH(CH_3)), 0.90-0.89 (m, 2H), 0.86 (s, 3H, CH_3) 0.76 (s, 3H, CH_3), 0.73 (s, 3H, CH_3). ^{13}C NMR (400 MHz, $CDCl_3$) δ (ppm): 173.8 (C=O), 134.8 (*CqAr*), 130.7 (*CqAr*), 129.0 (*CHAr*), 127.3 (*CHAr*), 123.7 (*CHAr*), 122.8 (x2, *CHPyrrol*), 121.8 (*CHAr*), 109.7 (x2, *CHPyrrol*), 73.4 (*Cq*-OH(CH_3)), 59.3 (*CH*-CH_2CO), 56.2 (CH), 43.7, 41.8, 39.4, 38.8 (*Cq*-(CH_3)$_2$), 34.7, 33.3, 33.2, 23.7, 21.4, 20.4, 18.2, 15.2. IR ν (cm^{-1}): 3669, 2970, 1681, 1525, 1451, 1215, 1069, 748, 666. Anal. Calcd. for $C_{26}H_{36}N_2O_2$: C, 76.43; H, 8.88; N, 6.86. Found: C, 76.52; H, 8.91; N, 6.84.

*B) Aminolysis reaction from aliphatic amines (**268-280**).* According to a reported procedure [167] with little modifications, a solution of (+)-sclareolide (0.4 mmol) in opportune amine (0.5 mL) and THF (1.5 mL) was stirred at 45 °C for 48-72 h. The reaction mixture was then concentrated under reduced pressure and dispersed in water (15 mL). The inorganic phase was extracted twice with EtOAc (15 mL) and the collected organic layers were washed with brine (15 mL), dried over anhydrous Na_2SO_4 and filtered. The solvent was removed under vacuum and the crude product was purified by flash chromatography using a mixture of PE/EtOAc as eluent to give the homodrimanyl aliphatic amide in good yield.

***N*-benzyl-2-((1*R*,2*R*,4a*S*,8a*S*)-2-hydroxy-2,5,5,8a-tetramethyldecahydronaphthalen-1-yl)acetamide (268)**. The product was obtained as a colourless oil and purified by column chromatography using petroleum ether-ethyl acetate (1.5:1) as eluent (139 mg; 98% yield). ^{1}H NMR (300 MHz, $CDCl_3$) δ: 7.28-7.14 (m, 4H, Ar), 6.92 (t, *J* = 12.1 Hz, 1H, Ar), 4.38-4.21 (m, 2H, CH_2NH), 3.53 (s, 1H, OH), 2.36 (dd, J_1 = 15.2 Hz, J_2 = 4.5 Hz, 1H, CH_2CO), 2.09 (dd, J_1 = 15.5 Hz, J_2 = 4.7

Hz, 1H, CH_2CO), 1.83 (dt, J_1 = 12.1 Hz, J_2 = 2.7 Hz, 1H), 1.68 (t, J = 4.7 Hz, 1H), 1.62-1.08 (m, 9H, CH_2), 1.02 (s, 3H, CH_3), 0.94-0.85 (m, 1H, CH), 0.80 (s, 3H, CH_3), 0.71 (s, 6H, CH_3). ^{13}C NMR (75 MHz, $CDCl_3$) δ: 175.6, 138.4, 129.1, 128.6, 128.3, 128.1, 72.9, 57.3, 56.6, 55.1, 43.5, 41.7, 38.8, 34.1, 33.2, 32.5, 24.4, 22.9, 22.2, 20.5, 18.3, 16.2, 14.6. IR ν (cm^{-1}): 3014, 2926, 1650, 1214, 748, 666. Anal. Calcd. for $C_{23}H_{35}NO_2$: C, 77.27; H, 9.87; N, 3.92. Found: C, 77.38; H, 9.90; N, 3.93.

***N*-(4-chlorobenzyl)-2-((1*R*,2*R*,4a*S*,8a*S*)-2-hydroxy-2,5,5,8a-tetramethyldecahydronaphthalen-1-yl)acetamide (269)**. The product was obtained as a white solid and purified by column chromatography using petroleum ether-ethyl acetate (2:1) as eluent (110 mg; 70% yield); mp 154–155 °C. ^{1}H NMR (300 MHz, $CDCl_3$) δ: 7.25-7.23(m, 2H, Ar), 7.15-7.13 (m, 2H, Ar), 4.35-4.21 (m, 2H, CH_2NH), 3.69 (brs, 1H, OH), 2.42 (dd, J_1 = 15.4 Hz, J_2 = 4.5 Hz, 1H, CH_2CO), 2.16 (dd, J_1 = 15.4 Hz, J_2 = 4.6 Hz, 1H, CH_2CO), 1.90-1.85 (m, 1H, CH), 1.71-1.20 (m, 10H), 1.07 (s, 3H, CH_3), 0.94-0.90 (m, 1H, CH), 0.86 (s, 3H, CH_3), 0.77 (s, 3H, CH_3), 0.74 (s, 3H, CH_3). ^{13}C NMR (75 MHz, $CDCl_3$) δ: 175.8, 137.1, 132.9, 128.8 (x2), 128.6 (x2), 72.9, 57.9, 55.9, 44.1, 42.8, 41.7, 39.2, 38.7, 33.3, 33.2, 32.5, 23.7, 21.4, 20.4, 18.3, 15.4. IR ν (cm^{-1}): 3279, 2924, 1642, 1492, 1387, 1091, 1015, 938, 800. Anal. Calcd. for $C_{23}H_{34}ClNO_2$: C, 70.48; H, 8.74; N, 3.57. Found: C, 70.22; H, 8.77; N, 3.56.

***N*-(3,4-dichlorobenzyl)-2-((1*R*,2*R*,4a*S*,8a*S*)-2-hydroxy-2,5,5,8a-tetramethyldecahydronaphthalen-1-yl)acetamide (270)**. The product was obtained as a white solid and purified by column chromatography using petroleum ether-ethyl acetate (1:1.5) as eluent (142 mg; 83% yield); mp 149–150 °C. ^{1}H NMR (400 MHz, DMSO) δ (ppm): 8.23 (t, 1H, J = 6.1 Hz, NH), 7.51 (d, J = 8.3 Hz, 1H, Ar), 7.44 (d, J = 1.8 Hz, 1H, Ar), 7.20 (dd, J_1 = 8.3 Hz, J_2 = 1.8 Hz, 1H, Ar), 4.26 (dd, J_1 = 15.5 Hz, J_2 = 6.2 Hz, 1H, CH_2NH), 4.15 (dd, J_1 = 15.5 Hz, J_2 = 5.8 Hz, 1H, CH_2NH), 2.34 (dd, J_1 = 15.4 Hz, J_2 = 2.8 Hz, 1H, CH_2CO), 2.05 (dd, J_1 = 15.4 Hz, J_2 = 7.1 Hz, 1H, CH_2CO), 1.76-1.66 (m, 2H), 1.54-1.02 (mm, 8H), 0.93 (s, 3H, COH(CH_3)), 0.87-0.82 (m, 2H), 0.80 (s, 3H, CH_3), 0.72 (s, 6H, CH_3). ^{13}C NMR (400 MHz, DMSO) δ (ppm): 174.6 (C=O), 141.7 (*CqAr*), 131.3 (*CqAr*), 130.8 (*CHAr*), 129.6 (*CHAr*+*CqAr*), 128.1 (*CHAr*), 71.6 (*Cq*-OH(CH_3)), 56.8 (CH), 56.0 (CH), 44.2, 42.0, 41.6, 39.2, 38.7, 33.7, 33.3, 31.6, 24.6, 21.8, 20.5, 18.3, 15.5. IR ν (cm^{-1}): 3298, 2926, 1642, 1548, 1470, 1388, 1082, 1032, 754. Anal. Calcd. for $C_{23}H_{32}Cl_2NO_2$: C, 64.78; H, 7.80; N, 3.28. Found: C, 65.02; H, 7.77; N, 3.29.

***N*-(4-fluorobenzyl)-2-((1*R*,2*R*,4a*S*,8a*S*)-2-hydroxy-2,5,5,8a-tetramethyldecahydronaphthalen-1-yl)acetamide (271)**. The product was obtained as a white solid and purified by column chromatography using petroleum ether-ethyl acetate (1.5:1) as eluent (147 mg; 97% yield); mp 135–136 °C. ^{1}H NMR (400 MHz, $CDCl_3$) δ (ppm): 7.22-7.19 (m, 2H, Ar), 6.97 (t, J = 8.6 Hz, 2H, Ar),

6.38 (brs, 1H, NH), 4.37 (dd, J_1 = 15.0 Hz, J_2 = 6.0 Hz, 1H, CH_2-NH), 4.31 (dd, J_1 = 15.0 Hz, J_2 = 5.9 Hz, 1H, CH_2-NH), 2.46 (brs, 1H, OH), 2.39 (dd, J_1 = 15.4 Hz, J_2 = 5.2 Hz, 1H, CH_2CO), 2.14 (dd, J_1 = 15.4 Hz, J_2 = 4.1 Hz, 1H, CH_2CO), 1.90 (dt, J_1 = 12.5 Hz, J_2 = 3.0 Hz, 1H, -CH_2-COH(CH_3)), 1.76 (t, J = 4.6 Hz, 1H, -*CH*-COH(CH_3)), 1.68-1.52 (m, 2H), 1.50-1.32 (m, 4H), 1.29-1.12 (m, 2H), 1.10 (s, 3H, COH(CH_3)), 0.97-0.88 (m, 2H), 0.85 (s, 3H, CH_3), 0.76 (s, 3H, CH_3), 0.75 (s, 3H, CH_3). ^{13}C NMR (400 MHz, $CDCl_3$) δ (ppm): 175.2 (C=O), 162.1 (d, J = 267 Hz, *Cq*-F), 134.3 (*CqAr*), 129.4 (x2, J = 7.9 Hz, *CHAr*), 115.5 (x2, J = 21.3 Hz, *CHAr*), 73.2 (*Cq*-OH(CH_3)), 57.9 (CH), 56.0 (CH), 44.3, 43.0, 41.8, 39.4, 38.8 (*Cq*-(CH_3)$_2$), 33.3, 32.6, 29.7, 23.8, 21.4, 20.5, 18.4, 15.5. IR ν (cm^{-1}): 3675, 2987, 2907, 1510, 1214, 1057, 742, 666. Anal. Calcd. for $C_{23}H_{24}FNO_2$: C, 73.56; H, 9.13; N, 3.73. Found: C, 73.76; H, 9.09; N, 3.72.

2-((1*R*,2*R*,4a*S*,8a*S*)-2-hydroxy-2,5,5,8a-tetramethyldecahydronaphthalen-1-yl)-*N*-(4-methoxybenzyl)acetamide (272). The product was obtained as a yellow oil and purified by column chromatography using petroleum ether-ethyl acetate (1:1) as eluent (122 mg, 78% yield). ^{1}H NMR (400 MHz, $CDCl_3$) δ (ppm): 7.17 (d, 2H, J = 8.4 Hz, Ar), 6.83 (d, 2H, J = 8.6 Hz, Ar), 6.23 (brs, 1H, NH), 4.34 (dd, J_1 = 14.8 Hz, J_2 = 5.8 Hz, 1H, CH_2NH), 4.29 (dd, J_1 = 14.8 Hz, J_2 = 5.6 Hz, 1H, CH_2NH), 3.77 (s, 3H, OCH_3), 2.47 (brs, 1H, OH), 2.39 (dd, J_1 = 15.4 Hz, J_2 = 5.2 Hz, 1H, CH_2CO), 2.12 (dd, J_1 = 15.4 Hz, J_2 = 4.0 Hz, 1H, CH_2CO), 1.90 (dt, J_1 = 9.6 Hz, J_2 = 2.9 Hz, 1H, -CH_2-COH(CH_3)), 1.78 (t, J = 4.5 Hz, 1H, -*CH*-COH(CH_3)), 1.68-1.45 (mm, 4H), 1.42-1.12 (mm, 4H), 1.10 (s, 3H, COH(CH_3)), 0.97-0.93 (m, 2H), 0.85 (s, 3H, CH_3), 0.76 (s, 3H, CH_3), 0.75 (s, 3H, CH_3). ^{13}C NMR (400 MHz, $CDCl_3$) δ (ppm): 175.1 (C=O), 159.0 (*CqAr*), 130.5 (*CqAr*), 129.1 (x2, *CHAr*), 114.1 (x2, *CHAr*), 73.1 (*Cq*-OH(CH_3)), 57.8 (CH), 56.0 (CH), 55.3 (OCH_3), 44.3, 43.3, 41.8, 39.4, 38.8 (*Cq*-(CH_3)$_2$), 33.3, 33.2, 32.5, 23.7, 21.4, 20.5, 18.4, 15.5. IR ν (cm^{-1}): 3675, 3289, 2920, 1512, 1214, 1038, 748, 666. Anal. Calcd. for $C_{24}H_{37}NO_3$: C, 74.38; H, 9.62; N, 3.61. Found: C, 74.42; H, 9.66; N, 3.62.

2-((1*R*,2*R*,4a*S*,8a*S*)-2-hydroxy-2,5,5,8a-tetramethyldecahydronaphthalen-1-yl)-*N*-(3 methoxybenzyl)acetamide (273). The product was obtained as a yellow oil and purified by column chromatography using petroleum ether-ethyl acetate (1:1) as eluent (132 mg; 85% yield). ^{1}H NMR (300 MHz, CDCl3) δ: 7.15-7.07 (m, 1H, Ar), 6.74-6.68 (m, 3H, Ar), 4.30-4.17 (m, 2H, CH_2NH), 3.68 (s, 3H, CH_3O), 2.36 (dd, J_1 = 15.4 Hz, J_2 = 4.4 Hz, 1H, CH_2CO), 2.09 (dd, J_1 = 15.3 Hz, J_2 = 4.7 Hz, 1H, CH_2CO), 1.95-1.79 (m, 1H, CH), 1.67 (t, J = 4.5 Hz, 1H), 1.57-1.03 (m, 9H, CH_2), 1.00 (s, 3H, CH_3), 0.87-0.81 (m, 1H, CH), 0.78 (s, 3H, CH_3), 0.69 (s, 6H, CH_3). ^{13}C NMR (75 MHz, CDCl3) δ: 178.9, 159.6, 140.1, 129.5, 119.7, 112.9, 112.7, 72.9, 57.8, 55.9, 44.1, 43.4, 41.7, 39.2, 38.7, 33.3,

33.2 (x2), 32.4, 23.6, 21.4, 20.4, 18.3, 15.3. IR ν (cm^{-1}): 3291, 2945, 1642, 1264, 1214, 1051, 746, 666. Anal. Calcd. for $C_{24}H_{37}NO_3$: C, 74.38; H, 9.62; N, 3.61. Found: C, 74.48; H, 9.65; N, 3.60.

2-((1*R*,2*R*,4a*S*,8a*S*)-2-hydroxy-2,5,5,8a-tetramethyldecahydronaphthalen-1-yl)-*N*-phenethylacetamide (274). The product was obtained as a light yellow oil and purified by column chromatography using petroleum ether-ethyl acetate (1:1) as eluent (141 mg; 95% yield). ^{1}H NMR (300 MHz, CDCl3) δ: 7.29-7.19 (m, 2H, Ar), 7.18-7.10 (m, 2H, Ar), 6.60-6.51 (m, 1H, Ar), 3.54 (s, 1H, OH), 3.48-3.32 (m, 2H, CH_2NH), 2.74 (t, J = 6.6 Hz, 2H, CH_2Ar), 2.02 (dd, J_1 = 14.5 Hz, J_2 = 3.4 Hz, 1H, CH_2CO), 1.85 (dd, J_1 = 12.3 Hz, J_2 = 5.0 Hz, 1H, CH_2CO), 1.91-1.80 (m, 1H), 1.65-1.10 (m, 10H), 1.04 (s, 3H, CH_3), 0.92-0.85 (m, 1H, CH), 0.80 (s, 3H, CH_3), 0.70 (s, 6H, CH_3). ^{13}C NMR (75 MHz, CDCl3) δ: 175.6, 139.0, 129.8, 129.6, 127.8, 127.5, 125.3, 72.9, 57.2, 55.1, 40.7, 38.7, 35.5, 33.2, 32.6, 24.5, 23.1, 22.2, 20.5, 19.8, 19.1, 18.3, 16.2, 14.6. IR ν (cm^{-1}): 3021, 2930, 1655, 1214, 748, 666. Anal. Calcd. for $C_{24}H_{37}NO_2$: C, 77.58; H, 10.04; N, 3.77. Found: C, 77.60; H, 10.07; N, 3.77.

***N*-(4-chlorophenethyl)-2-((1*R*,2*R*,4a*S*,8a*S*)-2-hydroxy-2,5,5,8a-tetramethyldecahydronaphthalen-1-yl)acetamide (275)**. The product was obtained as a white solid and purified by column chromatography using petroleum ether-ethyl acetate (1:1) as eluent (122 mg; 75% yield); mp 168–169 °C. ^{1}H NMR (400 MHz, DMSO) δ (ppm): 7.68 (m, 1H, NH), 7.31-7.28 (m, 2H, Ar), 7.22-7.19 (m, 2H, Ar), 4.23 (s, 1H, OH), 3.27-3.20 (m, 2H, CH_2NH), 2.69-2.64 (m, 2H, CH_2-Ar), 2.21 (d, J = 15.4 Hz, 1H, CH_2CO), 1.95 (dd, J_1 = 15.3 Hz, J_2 = 6.1 Hz, 1H, CH_2CO), 1.71-1.60 (m, 4H), 1.53-1.40 (m, 2H), 1.37-1.12 (m, 4H), 1.08-1.01 (m, 2H), 0.93 (s, 3H, COH(CH_3)), 0.82 (s, 3H, CH_3), 0.73 (s, 3H, CH_3), 0.69 (s, 3H, CH_3). ^{13}C NMR (400 MHz, DMSO) δ (ppm): 174.4 (C=O), 139.1 (*CqAr*), 131.0 (x2, *CHAr*+*CqAr*), 128.6 (x2, *CHAr*), 71.6 (*Cq*-OH(CH_3)), 56.8 (CH), 56.0 (CH), 44.2, 42.0, 39.4 (under DMSO), 38.9, 38.7 (*Cq*-(CH_3)$_2$), 34.7, 33.8, 33.3, 31.8, 24.6, 21.8, 20.5, 18.4, 15.5. IR ν (cm^{-1}): 3298, 2977, 2914, 1634, 1214, 1056, 749, 666 cm^{-1}. Anal. Calcd. for $C_{24}H_{36}ClNO_2$: C, 71.00; H, 8.94; N, 3.45. Found: C, 71.12; H, 8.97; N, 3.46.

***N*-(4-fluorophenethyl)-2-((1*R*,2*R*,4a*S*,8a*S*)-2-hydroxy-2,5,5,8a-tetramethyldecahydronaphthalen-1-yl)acetamide (276).)**. The product was obtained as a white solid and purified by column chromatography using petroleum ether-ethyl acetate (1:1) as eluent (128; 83% yield); mp 114–115 °C. ^{1}H NMR (400 MHz, $CDCl_3$) δ (ppm): 7.15-7.12 (m, 2H, Ar), 6.96 (t, 2H, J = 8.2 Hz, Ar), 6.03 (brs, 1H, NH), 3.52-3.37 (m, 2H, CH_2NH), 2.76 (t, J = 6.1 Hz, 2H, CH_2-Ar), 2.47 (brs, 1H, OH), 2.29 (dd, J_1 = 15.3 Hz, J_2 = 5.2 Hz, 1H, CH_2CO), 2.04 (dd, J_1 = 15.3 Hz, J_2 = 3.9 Hz, 1H, CH_2CO), 1.89 (dt, J_1 = 12.5 Hz, J_2 = 3.1 Hz, 1H, -CH_2-COH(CH_3)), 1.68-1.62 (m, 1H), 1.56-1.51 (m, 2H), 1.42-1.32 (m, 4H), 1.27-1.14 (m, 2H), 1.09 (s, 3H, COH(CH_3)), 0.93-0.90 (m,

2H), 0.85 (s, 3H, CH_3), 0.75 (s, 3H, CH_3), 0.73 (s, 3H, CH_3). ^{13}C NMR (400 MHz, $CDCl_3$) δ (ppm): 175.4 (C=O), 161.6 (d, *J* = 244 ppm, *Cq*-F), 134.7 (*CqAr*), 130.3 (x2, *J* = 7.5 Hz, *CHAr*), 115.4 (x2, *J* = 21.2 Hz, *CHAr*), 73.1 (*Cq*-OH(CH_3)), 57.9 (CH), 56.0 (CH), 44.3, 41.8, 40.7, 39.3, 38.7 (*Cq*-(CH_3)$_2$), 34.8, 33.3, 33.2, 32.6, 23.8, 21.4, 20.5, 18.3, 15.4. IR ν (cm^{-1}): 3298, 2970, 2933, 1642, 1509, 1215, 1057, 748, 666. Anal. Calcd. for $C_{24}H_{36}FNO_2$: C, 74.00; H, 9.32; N, 3.60. Found: C, 73.88; H, 9.36; N, 3.59.

***N*-(3-fluorophenethyl)-2-((1*R*,2*R*,4a*S*,8a*S*)-2-hydroxy-2,5,5,8a-tetramethyldecahydronaphthalen-1-yl)acetamide (277)**. The product was obtained as an amorphous solid and purified by column chromatography using petroleum ether-ethyl acetate (1:1) as eluent (113 mg; 72% yield). ^{1}H NMR (300 MHz, CDCl3) δ: 7.27-7.18 (m, 1H, Ar), 7.00-6.84 (m, 2H, Ar), 6.66 (t, *J* = 5.4 Hz, 1H, Ar), 3.53-3.32 (m, 2H, CH_2NH), 2.77 (t, *J* = 6.9 Hz, 2H, CH_2), 2.34 (dd, J_1 = 15.3 Hz, J_2 = 4.6 Hz, 1H, CH_2), 2.06 (dd, J_1 = 15.3 Hz, J_2 = 5.3 Hz, 1H, CH_2), 1.91-1.86 (m, 1H, CH), 1.65-1.10 (m, 10H), 1.07 (s, 3H, CH_3), 0.95-0.87 (m, 1H, CH), 0.85 (s, 3H, CH_3), 0.73 (s, 6H, CH_3). ^{13}C NMR (75 MHz, CDCl3) δ: 175.8, 164.5, 161.2, 141.6, 128.9, 125.6, 123.5, 114.8, 112.3, 72.9, 57.2, 56.6, 55.1, 40.5, 38.7, 35.2, 32.6, 31.7, 23.3, 20.9, 18.2, 16.2, 14.9, 14.5. IR ν (cm^{-1}): 3685, 3310, 2977, 1642, 1215, 1057, 747, 666. Anal. Calcd. for $C_{24}H_{36}FNO_2$: C, 74.00; H, 9.32; N, 3.60. Found: C, 73.90; H, 9.34; N, 3.61.

***N*-(furan-2-ylmethyl)-2-((1*R*,2*R*,4a*S*,8a*S*)-2-hydroxy-2,5,5,8a-tetramethyldecahydronaphthalen-1-yl)acetamide (278)**. The product was obtained as a yellow oil and purified by column chromatography using petroleum ether-ethyl acetate (1:1) as eluent (132 mg; 95% yield). ^{1}H NMR (400 MHz, $CDCl_3$) δ (ppm): 7.31 (s, 1H, Fur), 6.32 (brs, 1H, NH), 6.28 (t, *J* = 1.3 Hz, 1H, Fur), 6.18 (d, *J* = 2.7 Hz, 1H, Fur), 4.40 (dd, J_1 = 15.5 Hz, J_2 = 5.5 Hz, 1H, CH_2NH), 4.36 (dd, J_1 = 15.5 Hz, J_2 = 5.4 Hz, 1H, CH_2NH), 2.92 (brs, 1H, OH), 2.38 (dd, J_1 = 15.4 Hz, J_2 = 5.1 Hz, 1H, CH_2CO), 2.12 (dd, J_1 = 15.4 Hz, J_2 = 4.2 Hz, 1H, CH_2CO), 1.90 (d, *J* = 12.5 Hz, 1H, -CH_2-COH(CH_3)), 1.76 (t, *J* = 4.5 Hz, 1H, -*CH*-COH(CH_3)), 1.67-1.51 (m, 2H), 1.49-1.31 (m, 4H), 1.29-1.19 (m, 2H), 1.10 (s, 3H, COH(CH_3)), 0.98-0.89 (m, 2H), 0.84 (s, 3H, CH_3), 0.76 (s, 6H, CH_3). ^{13}C NMR (400 MHz, $CDCl_3$) δ (ppm): 175.1 (C=O), 151.5 (*CqAr*), 142.1 (*CHFur*), 110.4 (*CHFur*), 107.2 (*CHFur*), 73.2 (*Cq*-OH(CH_3)), 57.8 (CH), 55.9 (CH), 44.3, 41.8, 39.3, 38.7 (*Cq*-(CH_3)$_2$), 36.8, 33.3, 33.2, 32.5, 23.7, 21.4, 20.5, 18.4, 15.5. IR ν (cm^{-1}): 3306, 2926, 1648, 1214, 746, 666. Anal. Calcd. for $C_{21}H_{33}NO_3$: C, 72.58; H, 9.57; N, 4.03. Found: C, 72.70; H, 9.61; N, 4.03.

***N*-((1,1'-biphenyl)-4-ylmethyl)-2-((1*R*,2*R*,4a*S*,8a*S*)-2-hydroxy-2,5,5,8a-tetramethyldecahydronaphthalen-1-yl)acetamide (279)**. The product was obtained as an amorphous solid and purified by column chromatography using petroleum ether-ethyl acetate (2:1)

as eluent (71 mg; 40% yield). ^{1}H NMR (300 MHz, $CDCl_3$) δ: 7.58-7.52 (m, 4H, Ar), 7.46-7.41 (m, 2H, Ar), 7.37-7.31 (m, 2H, Ar), 6.60 (t, *J* = 5.2 Hz, 1H, Ar), 4.5-4.36 (m, 2H, *CH*$_2$NH), 3.15 (brs, 1H, OH), 2.46 (dd, J_1 = 15.4 Hz, J_2 = 4.9 Hz, 1H, CH_2CO), 2.17 (dd, J_1 = 15.4 Hz, J_2 = 4.3 Hz, 1H, CH_2CO), 1.94-1.89 (m, 1H), 1.81 (t, *J* = 4.6 Hz, 1H), 1.73-1.21 (m, 9H, CH_2), 1.12 (s, 3H, CH_3), 1.00-0.96 (m, 1H), 0.86 (s, 3H, CH_3), 0.77 (s, 6H, CH_3). ^{13}C NMR (75 MHz, $CDCl_3$) δ: 175.4, 140.7, 140.2, 137.5, 128.8 (x2), 128.1, 127.3 (x2), 127.0, 73.1, 57.8, 55.9, 44.2, 43.4, 41.7, 39.3, 38.7, 33.3, 33.2, 32.6, 31.6, 23.7, 22.7, 21.4, 20.5, 18.4, 15.5, 14.2. IR ν (cm^{-1}): 3288, 2924, 1637, 1548, 1386, 1123, 938, 759, 696. Anal. Calcd. for $C_{29}H_{39}NO_2$: C, 80.33; H, 9.07; N, 3.23. Found: C, 80.55; H, 9.11; N, 3.24.

***N*-(3-(1*H*-imidazol-1-yl)propyl)-2-((1*R*,2*R*,4a*S*,8a*S*)-2-hydroxy-2,5,5,8a-tetramethyldecahydronaphthalen-1-yl)acetamide (280)**. Without any further purification, the product was obtained as a light yellow solid (140 mg, 93% yield), mp 83–84 °C. ^{1}H NMR (400 MHz, $CDCl_3$) δ (ppm): 7.47 (s, 1H, imid), 7.00 (s, 1H, imid), 6.90 (s, 1H, imid), 6.79 (brt, *J* = 5.3 Hz, 1H, NH), 3.95 (t, *J* = 6.9 Hz, 2H, *CH*$_2$-Nimid), 3.23-3.11 (m, 2H, *CH*$_2$-NH), 2.72 (brs, 1H, OH), 2.34 (dd, J_1 = 15.2 Hz, J_2 = 5.3 Hz, 1H, *CH*$_2$CO), 2.12 (dd, J_1 = 15.2 Hz, J_2 = 4.0 Hz, 1H, *CH*$_2$CO), 1.97-1.88 (m, 3H), 1.69 (t, *J* = 4.6 Hz, 1H, -*CH*-COH(CH_3)), 1.66-1.32 (mm, 6H), 1.28-1.18 (m, 2H), 1.12 (s, 3H, COH(*CH*$_3$)), 0.95-0.89 (m, 2H), 0.84 (s, 3H, CH_3), 0.75 (s, 3H, CH_3), 0.74 (s, 3H, CH_3). ^{13}C NMR (400 MHz, $CDCl_3$) δ (ppm): 175.9 (C=O), 137.2 (*CHimid*), 129.2 (*CHimid*), 119.0 (*CHimid*), 73.3 (*Cq*-OH(CH_3)), 58.2 (CH), 56.1 (CH), 44.6, 44.3, 41.8, 39.5, 38.8 (*Cq*-(CH_3)$_2$), 36.6, 33.3, 33.2, 32.7, 31.0, 23.8, 21.4, 20.5, 18.4, 15.4. IR ν (cm^{-1}): 3291, 2926, 1644, 1390, 1214, 1082, 747, 666. Anal. Calcd. for $C_{22}H_{37}N_3O_2$: C, 70.36; H, 9.93; N, 11.19. Found: C, 70.24; H, 9.97; N, 11.24.

***-General procedure 22. Synthesis of homodrimanyl acid ester through lacton ring opening reaction of* (+)-sclareolide (*282 and 283*).** According with a reported procedure [167], (+)-sclareolide (0.4 mmol) was dissolved in hot (60 °C) methanol (1 mL) and sodium hydroxide (1.6 mmol) was added under stirring. The result-ing mixture was stirred for 2 hours at 60 °C and then cooled to rt. Diluted HCl was then added until pH 5-6 and the formed precipitate was filtered under vacuum.21 For the next esterification reaction, the obtained intermediate was dissolved in anhydrous DMF (2 mL); then, the appropriate benzyl bromide (0.4 mmol) and solid K_2CO_3 (0.4 mmol) were added. The reaction mixture was stirred at rt for 24 hours and then quenched by addition of water (5 mL). The inorganic phase was extracted with ethyl acetate (3 x 10 mL) and the combined organic layers were washed with water (20 mL) and brine (20 mL). The whole organic phase was dried over anhydrous Na_2SO_4,

filtered, and evaporated to dryness. The crude product was purified by flash chromatography on silica gel using the mixture petroleum ether-ethyl acetate.

Benzyl 2-((1*R*,2*R*,4a*S*,8a*S*)-2-hydroxy-2,5,5,8a-tetramethyldecahydronaphthalen-1-yl)acetate (282). The product was obtained as a colourless oil and purified by column chromatography using petroleum ether-ethyl acetate (6:1) as eluent (78 mg; 55% yield). ^{1}H NMR (300 MHz, $CDCl_3$) δ: 7.45-7.30 (m, 5H, Ar), 5.20-5.10 (m, 2H, CH_2O), 4.72 (brs, 1H, OH), 2.60 (dd, J_1 = 15.2 Hz, J_2 = 4.4 Hz, 1H, CH_2CO), 2.38 (dd, J_1 = 15.4 Hz, J_2 = 4.6 Hz, 1H, CH_2CO), 1.99 (m, 2H), 1.62-1.08 (m, 8H, CH_2), 1.18 (s, 3H, CH_3), 1.09-0.98 (m, 1H, CH), 0.90 (s, 3H, CH_3), 0.81 (s, 6H, CH_3). ^{13}C NMR (75 MHz, $CDCl_3$) δ: 175.5, 136.0, 129.3, 129.2 (x2), 127.4 (x2), 73.1, 66.5, 57.7, 54.9, 43.1, 41.6, 38.5, 33.2, 32.5, 30.6, 29.7, 23.7, 22.3, 20.6, 18.3, 14.5. IR ν (cm^{-1}): 3014, 2939, 1718, 1214, 907, 748, 730, 666. Anal. Calcd. for $C_{23}H_{34}O_3$: C, 77.05; H, 9.56. Found: C, 77.16; H, 9.60.

3,4-dichlorobenzyl 2-((1*R*,2*R*,4a*S*,8a*S*)-2-hydroxy-2,5,5,8a-tetramethyldecahydronaphthalen-1-yl)acetate (283). The product was obtained as a colourless oil and purified by column chromatography using petroleum ether-ethyl acetate (6:1) as eluent (86 mg; 50% yield). ^{1}H NMR (400 MHz, $CDCl_3$) δ: 7.44 (s, 1H, Ar), 7.40 (d, *J* = 8.2 Hz, 1H, Ar), 7.17 (d, *J* = 8.2 Hz, 1H, Ar), 5.02 (ABq, *J* = 12.8 Hz, 2H, CH_2O), 2.52 (dd, *J* = 16.2 Hz, *J* = 5.8 Hz, 1H, CH_2CO), 2.32 (dd, *J* = 16.2 Hz, *J* = 5.1 Hz, 1H, CH_2CO), 1.92 (dt, *J* = 12.4 Hz, *J* = 2.9 Hz, 1H, -CH_2-COH(CH_3)), 1.84 (t, *J* = 5.4 Hz, 1H, -*CH*-COH(CH_3)), 1.69-1.52 (m, 2H), 1.48-1.23 (mm, 6H), 1.12 (s, 3H, COH(CH_3)), 0.99-0.91 (m, 2H), 0.86 (s, 3H, CH_3), 0.77 (s, 6H, CH_3). ^{13}C NMR (400 MHz, $CDCl_3$) δ: 177.0 (C=O), 141.1 (*CqAr*), 132.6 (*CqAr*), 131.4 (*CqAr*), 130.5 (*CHAr*), 128.8 (*CHAr*), 126.0 (*CHAr*), 86.4 (*Cq*-OH(CH_3)), 63.9 (OCH_2-Ar), 59.1 (CH), 56.7 (CH), 42.2, 39.5, 38.7 (*Cq*-(CH_3)$_2$), 33.2 (x2), 28.7, 21.6 (x2), 20.9, 20.6, 18.1, 15.1.

-General procedure 23. Synthesis of homodrimanyl methyl ester derivative through lacton ring opening reaction of* (+)-sclareolide *(284). A well stirred methanolic solution of (+)-sclareolide (0.5 mmol, 3 mL) was heated at 45 °C for 72 h. After that, the mixture was evaporated to dryness and the pure compound obtained was firther purified through flash column chromatography using petroleum ether-ethyl acetate as eluent. The compound was isolated as a white solid (85 mg; 60% yield); mp 72–73 °C. NMR data are in agreement with those reported [168]. Anal. Calcd. for $C_{17}H_{30}O_3$: C, 72.30; H, 10.71. Found: C, 72.56; H, 10.75.

-Procedure 24. Lactone ring reduction reaction of (+)-sclareolide.

(1R,2R,4aS,8aS)-1-(2-hydroxyethyl)-2,5,5,8a-tetramethyldecahydronaphthalen-2-ol (homodrimanyl diol) (285). (+)-Sclareolide (1.2 mmol) was dissolved in dry THF (50 mL) under argon and cooled to 0 °C. Then, $LiAlH_4$ (12.0 mmol) was added to the solution. The reaction mixture was stirred at rt for 6 h, then quenched with ethyle acetate (30 mL) and evaporated to dryness. The residue was dissolved in DCM (50 mL) and the organic phase washed twice with 1 N HCl (30 mL), with staturated aqueous $NaHCO_3$ (30 mL), and brine (30 mL). The organic phase was finally dried over anhydrous Na_2SO_4, filtered and concentrated under vacuum to give homodrimanyl diol **21** as a white crystalline solid in quantitative yield; mp 129.5–130.5 °C. ^{1}H-NMR data are in agreement with those reported [169]. Anal. Calcd. for $C_{17}H_{30}O_3$: C, 72.30; H, 10.71. Found: C, 72.56; H, 10.75.

-General procedure 25. Synthesis of homodrimanyl diol esters (286-289). According to a published procedure [169], homodrimanyl diol **285** (0.31 mmol) was dissolved in anhydrous DCM (2 mL) under an inert atmosphere. The appropriate carboxylic acid (0.34 mmol), EDCI (0.37 mmol) and DMAP (0.031 mmol) was added under stirring to the solution. The mixture was stirred at rt, checking the reaction by TLC, until the starting material disappeared (48-72 h). The reaction was quenched by the addition of water (5 mL) and the inorganic layer was extracted with DCM (2 x 10 mL). The combined organic layers were washed with water (20 mL) and brine (20 mL), dried over anhydrous Na_2SO_4, and filtered. The solvent was removed under reduced pressure and the resulting residue was purified by flash chromatography on silica gel using the mixture petroleum ether-ethyl acetate as eluent.

2-((1*R*,2*R*,4a*S*,8a*S*)-2-Hydroxy-2,5,5,8a-tetramethyldecahydronaphthalen-1-yl)ethyl Benzo[*d*][1,3]dioxole-5-carboxylate (286). The product was obtained as a white solid and purified by column chromatography using petroleum ether-ethyl acetate (4:1) as eluent (74 mg; 59% yield); mp 155–156 °C. ^{1}H NMR (400 MHz, $CDCl_3$) δ (ppm): 7.63 (d, *J* = 8.0 Hz, 1H, Ar), 7.45 (s, 1H, Ar), 6.81 (d, *J* = 8.1 Hz, 1H, Ar), 6.01 (s, 2H, OCH_2O), 4.36-4.29 (m, 2H, CH_2-OCO), 1.91-1.81 (m, 2H), 1.77-1.59 (m, 4H), 1.45-1.34 (m, 3H), 1.31-1.10 (m, 7H), 0.97-0.90 (m, 2H), 0.85 (s, 3H, CH_3), 0.79 (s, 3H, CH_3), 0.78 (s, 3H, CH_3). ^{13}C NMR (400 MHz, $CDCl_3$) δ (ppm): 166.1 (C=O), 151.5 (*CqAr*), 147.7 (*CqAr*), 125.3 (*CHAr*), 124.6 (*CqAr*), 109.6 (*CHAr*), 108.0 (*CHAr*), 101.8 (OCH_2O), 73.7 (*Cq*-OH(CH_3)), 67.1 (CH_2-O), 58.1 (CH), 56.1 (CH), 44.5, 41.9, 39.8, 38.8 (*Cq*-$(CH_3)_2$), 33.4, 33.3, 24.7, 24.0, 21.5, 20.5, 18.4, 15.3. IR ν (cm^{-1}): 3675, 2977, 2901, 1705, 1441, 1258, 1214, 1076, 1041, 750, 666. Anal. Calcd for $C_{24}H_{34}O_5$: C, 71.61; H, 8.51. Found: C, 71.87; H, 8.55.

2-((1*R*,2*R*,4a*S*,8a*S*)-2-hydroxy-2,5,5,8a-tetramethyldecahydronaphthalen-1-yl)ethyl (E)-3-(benzo[*d*][1,3]dioxol-5-yl)acrylate (287). The product was obtained as a white solid and purified by column chromatography using petroleum ether-ethyl acetate (4:1) as eluent (87 mg; 65% yield); mp 115–116 °C. ^{1}H NMR (400 MHz, $CDCl_3$) δ (ppm): 7.57 (d, *J* = 15.9 Hz, 1H, CH=*CH*-Ar), 7.00 (s, 1H, Ar), 6.98 (d, *J* = 8.0 Hz, 1H, Ar), 6.78 (d, *J* = 8.0 Hz, 1H, Ar), 6.22 (d, *J* = 15.9 Hz, 1H, *CH*=CH-Ar), 5.98 (s, 2H, OCH_2O), 4.28-4.17 (m, 2H, CH_2-OCO), 1.88 (dt, *J* = 12.3 Hz, *J* = 2.9 Hz, 1H, -CH_2-COH(CH_3)), 1.83-1.53 (m, 4H), 1.46-1.34 (m, 4H), 1.31-1.20 (m, 2H), 1.16 (s, 3H, COH(CH_3)), 1.14-1.09 (m, 2H), 0.95-0.90 (m, 2H), 0.85 (s, 3H, CH_3), 0.79 (s, 3H, CH_3), 0.77 (s, 3H, CH_3). ^{13}C NMR (400 MHz, $CDCl_3$) δ (ppm): 167.3 (C=O), 149.6 (*CqAr*), 148.4 (*CqAr*), 144.5 (=*CH*-Ar), 128.9 (*CqAr*), 124.4 (*CHAr*), 116.2 (*CH*=CHAr), 108.6 (*CHAr*), 106.6 (*CHAr*), 101.6 (OCH_2O), 73.6 (*Cq*-OH(CH_3)), 66.6 (CH_2-O), 58.1 (CH), 56.1 (CH), 44.4, 41.9, 39.7, 38.8 (*Cq*-$(CH_3)_2$), 33.4, 33.3, 24.7, 24.0, 21.5, 20.5, 18.4, 15.3. IR ν (cm^{-1}): 2983, 2901, 1214, 1057, 744, 668. Anal. Calcd for $C_{26}H_{36}O_5$: C, 72.87; H, 8.47. Found: C, 73.01; H, 8.49.

2-((1*R*,2*R*,4a*S*,8a*S*)-2-hydroxy-2,5,5,8a-tetramethyldecahydronaphthalen-1-yl)ethyl 4-(thiophen-2-yl)butanoate (288). The product was obtained as a colourless oil and purified by column chromatography using petroleum ether-ethyl acetate (3:1) as eluent (88 mg; 70% yield). ^{1}H NMR (400 MHz, $CDCl_3$) δ (ppm): 7.10 (d, *J* = 5.0 Hz, 1H, *thienyl*), 6.90 (t, *J* = 4.2 Hz, 1H, *thienyl*), 6.78 (d, *J* = 2.4 Hz, 1H, *thienyl*), 4.17-4.06 (m, 2H, CH_2-OCO), 2.86 (t, *J* = 7.5 Hz, 2H, $COCH_2$-CH_2-CH_2), 2.34 (t, *J* = 7.5 Hz, 2H, COCH_2-CH_2-CH_2), 2.03-1.95 (m, 2H, $COCH_2$-CH_2-CH_2), 1.87 (d, *J* = 12.3 Hz, 1H, -CH_2-COH(CH_3)), 1.77-1.69 (m, 1H), 1.67-1.52 (mm, 6H), 1.43-1.35 (m, 3H), 1.30-1.19 (m, 1H), 1.14 (s, 3H, COH(CH_3)), 1.12-1.07 (m, 1H), 0.92-0.88 (m, 2H), 0.86 (s, 3H, CH_3), 0.77 (s, 6H, CH_3). ^{13}C NMR (400 MHz, $CDCl_3$) δ (ppm): 173.4 (C=O), 144.1 (*Cqthienyl*), 126.8 (*CHthienyl*), 124.5 (*CHthienyl*), 123.2 (*CHthienyl*), 73.6 (*Cq*-OH(CH_3)), 66.6 (CH_2-O), 58.0 (CH), 56.1 (CH), 44.4, 41.9, 39.7, 38.8 (*Cq*-$(CH_3)_2$), 33.5, 33.4, 33.3, 29.2, 26.8, 24.5, 24.0, 21.5, 20.5, 18.4, 15.3. IR ν (cm^{-1}): 3675, 2958, 1724, 1390, 1214, 1082, 748, 692, 667. Anal. Calcd for $C_{24}H_{38}O_3S$: C, 70.89; H, 9.42. Found: C, 70.75; H, 9.44.

-Procedure 26. Synthesis of homodrimanyl diol ether.

(1*R*,2*R*,4a*S*,8a*S*)-1-(2-((3-Chlorobenzyl)oxy)ethyl)-2,5,5,8a-tetramethyldecahydronaphthalen-2-ol (289). Homodrimanyl diol **20** (0.35 mmol) was dissolved in anhydrous THF (10 mL) under inert atmosphere and NaH, previously purified, (0.4 mmol) was added. The reaction mixture was refluxed for 30 min and then, after cooling at rt, 3-chlorobenzyl chloride (0.42 mmol) was added. The mixture was still heated to reflux for 48 h, cooled to rt and quenched with water and saturated NH_4Cl solution

(pH 7). Afterward, the aqueous layer was extracted with ethyl acetate (3 x 15 mL) and the combined organic phases were washed with water (30 mL) and brine (30 mL), dried over anhydrous Na_2SO_4, filtred and evaporated to dryness to obtain the final homodrimanyl diol ether. The product was obtained as a light yellow oil and purified by column chromatography using petroleum ether-ethyl acetate (8:1) as eluent (37 mg; 27% yield). ^{1}H NMR (300 MHz, $CDCl_3$) δ: 7.39-7.18 (m, 4H), 4.49 (s, 2H, CH_2-Ar), 3.68-3.57 (m, 1H), 3.41-3.30 (m, 1H), 3.19 (brs, 1H, OH), 1.96-1.85 (m, 1H), 1.83-1.70 (m, 1H), 1.69-1.48 (m, 3H), 1.44-1.17 (m, 8H), 1.14 (s, 3H, CH_3), 0.96-0.90 (m, 1H), 0.88 (s, 3H, CH_3), 0.78 (s, 6H, CH_3). ^{13}C NMR (75 MHz, $CDCl_3$) δ: 139.9, 129.8, 127.8, 127.8, 126.5, 125.7, 72.5, 72.3, 72.2, 59.0, 56.0, 43.9, 41.8, 39.5, 38.9, 33.4, 33.2, 25.2, 24.3, 21.5, 20.4, 18.4, 15.3. IR ν (cm^{-1}): 2926, 1214, 1077, 750, 667. Anal. Calcd for $C_{23}H_{35}ClO_2$: C, 72.89; H, 8.31. Found: C, 72.56; H, 8.34.

8.6.2 Biological methods

-TRPV1 and TRPV4 channel assays.

Compound effects on intracellular Ca^{2+} concentration ($[Ca^{2+}]_i$) were determined using the selective intracellular fluorescent probe for Ca^{2+} Fluo-4 and assays were performed as described [170]. Briefly, human embryonic kidney (HEK-293) cells, stably transfected with recombinant rat TRPV4 or human TRPV1 (selected by Geneticin 600 μg mL^{-1}) or not transfected, were cultured in EMEM + 2 mM Glutamine + 1 % Non-Essential Amino Acids + 10 % FBS and maintained at 37 °C with 5 % CO_2. On the day of the experiment the cells were loaded in the dark at room temperature for 1 h with Fluo-4 AM (4 μM in DMSO containing 0.02% Pluronic F-127). After that the cells were rinsed and resuspended in Tyrode's solution (145 mM NaCl, 2.5 mM KCl, 1.5 mM $CaCl_2$, 1.2 mM $MgCl_2$, 10 mM *d*-glucose, and 10 mM HEPES, pH 7.4) then transferred to a quartz cuvette of a spectrofluorimeter (Perkin-Elmer LS50B; λ_{EX} = 488 nm, λ_{EM} = 516 nm) under continuous stirring. Cell fluorescence before and after the addition of various concentrations of test compounds was measured normalizing the effects against the response to ionomycin (4 μM). The values of the effect on $[Ca^{2+}]_i$ in HEK-293 cells not transfected are used as a baseline and subtracted from the values obtained from transfected cells. The potency of the compounds (EC_{50} values) is determined as the concentration required to produce half-maximal increases in $[Ca^{2+}]_i$. Antagonist behavior is evaluated against the agonist of the TRPV4 GSK1016790A (10 nM)[24] and analyzed by adding the compounds

directly in the quartz cuvette 5 min before stimulation of cells with the agonist. IC_{50} is expressed as the concentration exerting a half-maximal inhibition of agonist effect, taking as 100% the effect on $[Ca^{2+}]_i$ exerted by GSK1016790A (10 nM) alone. Similarly, for TRPV1 using agonist capsaicin 0.1 μM. Dose-response curve fitting (sigmoidal dose-response variable slope) and parameter estimation were performed with Graph-Pad Prism8® (GraphPad Software Inc., San Diego, CA, USA). All determinations were performed at least in triplicate.

REFERENCES

[1] C.H. Hoke, C.E. Snyder, History of the restoration of adenovirus type 4 and type 7 vaccine, live oral (Adenovirus Vaccine) in the context of the Department of Defense acquisition system, Vaccine. 31 (2013) 1623–1632. https://doi.org/10.1016/j.vaccine.2012.12.029.

[2] T.G.W. Wallace P. Rowe, Robert J. Huebner, Loretta K. Gilmore, Robert H. Parrott, Isolation of a Cytopathogenic Agent from Human Adenoids LTndergoing Spontaneous Degeneration in Tissue Culture., Exp. Biol. Med. 84 (1952) 570–753.

[3] A. Dhingra, E. Hage, T. Ganzenmueller, S. Böttcher, J. Hofmann, K. Hamprecht, P. Obermeier, B. Rath, F. Hausmann, T. Dobner, A. Heim, Molecular Evolution of Human Adenovirus (HAdV) Species C, Sci. Rep. 9 (2019) 1–13. https://doi.org/10.1038/s41598-018-37249-4.

[4] T. Lion, Adenovirus infections in immunocompetent and immunocompromised patients, Clin. Microbiol. Rev. 27 (2014) 441–462. https://doi.org/10.1128/CMR.00116-13.

[5] C.M. Robinson, G. Singh, J.Y. Lee, S. Dehghan, J. Rajaiya, E.B. Liu, M.A. Yousuf, R.A. Betensky, M.S. Jones, D.W. Dyer, D. Seto, J. Chodosh, Molecular evolution of human adenoviruses, Sci. Rep. 3 (2013) 1–7. https://doi.org/10.1038/srep01812.

[6] G. Paul Thomas, M.B. Mathews, DNA replication and the early to late transition in adenovirus infection, Cell. 22 (1980) 523–533. https://doi.org/10.1016/0092-8674(80)90362-1.

[7] S.M. Frisch, J.S. Mymryk, Adenovirus-5 E1A: Paradox and paradigm, Nat. Rev. Mol. Cell Biol. 3 (2002) 441–452. https://doi.org/10.1038/nrm827.

[8] P.H. Gallimore, A.S. Turnell, Adenovirus E1A: Remodelling the host cell, a life or death experience, Oncogene. 20 (2001) 7824–7835. https://doi.org/10.1038/sj/onc/1204913.

[9] A.N. Blackford, R.J.A. Grand, Adenovirus E1B 55-Kilodalton Protein: Multiple Roles in Viral Infection and Cell Transformation, J. Virol. 83 (2009) 4000–4012. https://doi.org/10.1128/jvi.02417-08.

[10] C. Caravokyri, K.N. Leppard, Human adenovirus type 5 variants with sequence alterations flanking the E2A gene: Effects on E2 expression and DNA replication, Virus Genes. 12 (1996) 65–75. https://doi.org/10.1007/BF00370002.

[11] E.J. Parker, C.H. Botting, A. Webster, R.T. Hay, Adenovirus DNA polymerase: Domain organisation and interaction with preterminal protein, Nucleic Acids Res. 26 (1998) 1240–1247. https://doi.org/10.1093/nar/26.5.1240.

[12] A.E. Tollefson, A. Scaria, T.W. Hermiston, J.S. Ryerse, L.J. Wold, W.S. Wold, The adenovirus death protein (E3-11.6K) is required at very late stages of infection for efficient cell lysis and release of adenovirus from infected cells., J. Virol. 70 (1996) 2296–2306. https://doi.org/10.1128/jvi.70.4.2296-2306.1996.

[13] M.S. Horwitz, Function of adenovirus E3 proteins and their interactions with immunoregulatory cell proteins, J. Gene Med. 6 (2004) 172–183. https://doi.org/10.1002/jgm.495.

[14] M.D. Weitzman, FUNCTIONS OF THE ADENOVIRUS E4 PROTEINS AND THEIR IMPACT ON VIRAL VECTORS, Front. Biosci. 10 (2005) 1106–1117.

[15] D.C. Farley, J.L. Brown, K.N. Leppard, Activation of the Early-Late Switch in Adenovirus Type 5 Major Late Transcription Unit Expression by L4 Gene Products, J. Virol. 78 (2004) 1782–1791. https://doi.org/10.1128/jvi.78.4.1782-1791.2004.

[16] S.J. Morris, G.E. Scott, K.N. Leppard, Adenovirus Late-Phase Infection Is Controlled by a Novel L4 Promoter, J. Virol. 84 (2010) 7096–7104. https://doi.org/10.1128/jvi.00107-10.

[17] B. Saha, C.M. Wong, R.J. Parks, The adenovirus genome contributes to the structural stability of the virion, Viruses. 6 (2014) 3563–3583. https://doi.org/10.3390/v6093563.

[18] W.I. W., Q. W., Management of Adenovirus in Children after Allogeneic Hematopoietic Stem Cell Transplantation, Adv. Hematol. 2013 (2013). http://www.embase.com/search/results?subaction=viewrecord&from=export&id=L370372870%0Ahttp://dx.doi.org/10.1155/2013/176418%0Ahttp://sfx.library.uu.nl/utrecht?sid=EMBASE&issn=16879104&id=doi:10.1155/2013/176418&atitle=Management+of+Adenovirus+in+Children+.

[19] H. Liu, L. Jin, S.B.S. Koh, I. Atanasov, S. Schein, L. Wu, Z.H. Zhou, Atomic structure of human adenovirus by Cryo-EM reveals interactions among protein networks, Science (80-.). 329 (2010) 1038–1043. https://doi.org/10.1126/science.1187433.

[20] J. Vellinga, S. Van der Heijdt, R.C. Hoeben, The adenovirus capsid: Major progress in minor proteins, J. Gen. Virol. 86 (2005) 1581–1588. https://doi.org/10.1099/vir.0.80877-0.

[21] P. Ostapchuk, M. Suomalainen, Y. Zheng, K. Boucke, U.F. Greber, P. Hearing, The adenovirus major core protein VII is dispensable for virion assembly but is essential for lytic infection, PLoS Pathog. 13 (2017) 1–24. https://doi.org/10.1371/journal.ppat.1006455.

[22] J. Perez-Vargas, R.C. Vaughan, C. Houser, K.M. Hastie, C.C. Kao, G.R. Nemerow, Isolation and Characterization of the DNA and Protein Binding Activities of Adenovirus Core Protein V, J. Virol. 88 (2014) 9287–9296. https://doi.org/10.1128/jvi.00935-14.

[23] C.S. Martín, Latest insights on adenovirus structure and assembly, Viruses. 4 (2012) 847–877. https://doi.org/10.3390/v4050847.

[24] C. Lyle, F. McCormick, Integrin αvβ5 is a primary receptor for adenovirus in CAR-negative cells, Virol. J. 7 (2010) 1–13. https://doi.org/10.1186/1743-422X-7-148.

[25] P. Moreau, A. Cournac, G.A. Palumbo, M. Marbouty, S. Mortaza, A. Thierry, S. Cairo, M. Lavigne, R. Koszul, C. Neuveut, Tridimensional infiltration of DNA viruses into the host genome shows preferential contact with active chromatin, Nat. Commun. 9 (2018). https://doi.org/10.1038/s41467-018-06739-4.

[26] J.W. Flatt, S.J. Butcher, Adenovirus flow in host cell networks, Open Biol. 9 (2019). https://doi.org/10.1098/rsob.190012.

[27] T.J. Wickham, E.J. Filardo, D.A. Cheresh, G.R. Nemerow, Integrin αvβ5 selectively promotes adenovirus mediated cell membrane permeabilization, J. Cell Biol. 127 (1994) 257–264. https://doi.org/10.1083/jcb.127.1.257.

[28] T. Komatsu, H. Haruki, K. Nagata, Cellular and viral chromatin proteins are positive factors in the regulation of adenovirus gene expression, Nucleic Acids Res. 39 (2011) 889–901. https://doi.org/10.1093/nar/gkq783.

[29] M.A. Prusinkiewicz, J.S. Mymryk, Metabolic reprogramming of the host cell by human adenovirus infection, Viruses. 11 (2019) 1–21. https://doi.org/10.3390/v11020141.

[30] H. Zhao, F. Granberg, L. Elfineh, U. Pettersson, C. Svensson, Strategic Attack on Host Cell Gene Expression during Adenovirus Infection, J. Virol. 77 (2003) 11006–11015. https://doi.org/10.1128/jvi.77.20.11006-11015.2003.

[31] Y.S. Ahi, S.K. Mittal, Components of adenovirus genome packaging, Front. Microbiol. 7 (2016) 1–15. https://doi.org/10.3389/fmicb.2016.01503.

[32] W.F. Mangel, C.S. Martín, Structure, function and dynamics in adenovirus maturation, Viruses. 6 (2014) 4536–4570. https://doi.org/10.3390/v6114536.

[33] L.N. Liesbeth Lenaerts, Erik De Clercq, Clinical features and treatment of adenovirus infections, Rev. Med. Virol. 19 (2009) 57–64. https://doi.org/10.1002/rmv.

[34] A. Ronchi, C. Doern, E. Brock, L. Pugni, P.J. Sánchez, Neonatal adenoviral infection: A seventeen year experience and review of the literature, J. Pediatr. 164 (2014). https://doi.org/10.1016/j.jpeds.2013.11.009.

[35] S. Khanal, P. Ghimire, A.S. Dhamoon, The repertoire of adenovirus in human disease: The innocuous to the deadly, Biomedicines. 6 (2018).

https://doi.org/10.3390/biomedicines6010030.
[36] T. Kojaoghlanian, P. Flomenberg, M.S. Horwitz, The impact of adenovirus infection on the immunocompromised host, Rev. Med. Virol. 13 (2003) 155–171. https://doi.org/10.1002/rmv.386.
[37] A. Keyes, M. Mathias, F. Boulad, Y.J. Lee, M.A. Marchetti, A. Scaradavou, B. Spitzer, G.A. Papanicolaou, I. Wieczorek, K.J. Busam, Cutaneous involvement of disseminated adenovirus infection in an allogeneic stem cell transplant recipient, Br. J. Dermatol. 174 (2016) 885–888. https://doi.org/10.1111/bjd.14369.
[38] K.L. Schwartz, S.E. Richardson, D. MacGregor, S. Mahant, K. Raghuram, A. Bitnun, Adenovirus-Associated Central Nervous System Disease in Children, J. Pediatr. 205 (2019) 130–137. https://doi.org/10.1016/j.jpeds.2018.09.036.
[39] S. Jobran, R. Kattan, J. Shamaa, H. Marzouqa, M. Hindiyeh, Adenovirus respiratory tract infections in infants: a retrospective chart-review study, Lancet (London, England). 391 (2018) S43. https://doi.org/10.1016/S0140-6736(18)30409-4.
[40] D.M. Musher, How contagious are common respiratory tract infections? [4], N. Engl. J. Med. 349 (2003) 95. https://doi.org/10.1056/NEJMc031032.
[41] M.K. Scott, C. Chommanard, X. Lu, D. Appelgate, L. Grenz, E. Schneider, S.I. Gerber, D.D. Erdman, A. Thomas, Human Adenovirus Associated with Severe Respiratory Infection , Emerg. Infect. Dis. 22 (2016) 2013–2014.
[42] Z. Bhatti, A. Dhamoon, Fatal adenovirus infection in an immunocompetent host, Am. J. Emerg. Med. 35 (2017) 1034.e1-1034.e2. https://doi.org/10.1016/j.ajem.2017.02.008.
[43] D. Garcia-Zalisnak, C. Rapuano, J.D. Sheppard, A.R. Davis, Adenovirus Ocular Infections: Prevalence, Pathology, Pitfalls, and Practical Pointers, Eye Contact Lens. 44 (2018) 1–7. https://doi.org/10.1097/ICL.0000000000000226.
[44] C. Celik, M.G. Gozel, H. Turkay, M.Z. Bakici, A.S. Güven, N. Elaldi, Rotavirus and adenovirus gastroenteritis: Time series analysis, Pediatr. Int. 57 (2015) 590–596. https://doi.org/10.1111/ped.12592.
[45] K. Nanmoku, N. Ishikawa, A. Kurosawa, T. Shimizu, T. Kimura, A. Miki, Y. Sakuma, T. Yagisawa, Clinical characteristics and outcomes of adenovirus infection of the urinary tract after renal transplantation, Transpl. Infect. Dis. 18 (2016) 234–239. https://doi.org/10.1111/tid.12519.
[46] S.M.C. Lopez, M.G. Michaels, M. Green, Adenovirus infection in pediatric transplant recipients: Are effective antiviral agents coming our way?, Curr. Opin. Organ Transplant. 23 (2018) 395–399. https://doi.org/10.1097/MOT.0000000000000542.
[47] S. Cesaro, M. Berger, G. Tridello, M. Mikulska, K.N. Ward, P. Ljungman, S. Van Der Werf, D. Averbuch, J. Styczynski, A survey on incidence and management of adenovirus infection after allogeneic HSCT, Bone Marrow Transplant. 54 (2019) 1275–1280. https://doi.org/10.1038/s41409-018-0421-0.
[48] D.F. Florescu, J.M. Schaenman, Adenovirus in solid organ transplant recipients: Guidelines from the American Society of Transplantation Infectious Diseases Community of Practice, Clin. Transplant. 33 (2019) 1–8. https://doi.org/10.1111/ctr.13527.
[49] M.M.Y. Waye, C.W. Sing, Anti-viral drugs for human adenoviruses, Pharmaceuticals. 3 (2010) 3343–3354. https://doi.org/10.3390/ph3103343.
[50] L. Lenaerts, L. Naesens, Antiviral therapy for adenovirus infections, Antiviral Res. 71 (2006) 172–180. https://doi.org/10.1016/j.antiviral.2006.04.007.
[51] B. Ying, A.E. Tollefson, J.F. Spencer, L. Balakrishnan, S. Dewhurst, C. Capella, R.M.L. Buller, K. Toth, W.S.M. Wold, Ganciclovir inhibits human adenovirus replication and pathogenicity in permissive immunosuppressed syrian hamsters, Antimicrob. Agents Chemother. 58 (2014) 7171–7181. https://doi.org/10.1128/AAC.03860-14.

[52] K. Schaar, C. Röger, T. Pozzuto, J. Kurreck, S. Pinkert, H. Fechner, Biological antivirals for treatment of adenovirus infections, Antivir. Ther. 21 (2016) 559–566. https://doi.org/10.3851/IMP3047.

[53] R.A.B. Jeffrey M. Chamberlain, Katherine Sortino, Phiroze Sethna, Andrew Bae, Randall Lanier, S. Dewhursta, Cidofovir Diphosphate Inhibits Adenovirus 5 DNA Polymerase via both Nonobligate Chain Termination and Direct Inhibition, and Polymerase Mutations Confer Cidofovir Resistance on Intact Virus Jeffrey, 63 (2019) 1–13.

[54] U. Yusuf, G.A. Hale, J. Carr, Z. Gu, E. Benaim, P. Woodard, K.A. Kasow, E.M. Horwitz, W. Leung, D.K. Srivastava, R. Handgretinger, R.T. Hayden, Cidofovir for the treatment of adenoviral infection in pediatric hematopoietic stem cell transplant patients, Transplantation. 81 (2006) 1398–1404. https://doi.org/10.1097/01.tp.0000209195.95115.8e.

[55] G. Lugthart, M.A. Oomen, C.M. Jol-van der Zijde, L.M. Ball, D. Bresters, W.J.W. Kollen, F.J. Smiers, C.L. Vermont, R.G.M. Bredius, M.W. Schilham, M.J.D. van Tol, A.C. Lankester, The Effect of Cidofovir on Adenovirus Plasma DNA Levels in Stem Cell Transplantation Recipients without T Cell Reconstitution, Biol. Blood Marrow Transplant. 21 (2015) 293–299. https://doi.org/10.1016/j.bbmt.2014.10.012.

[56] A.E. Caruso Brown, M.N. Cohen, S. Tong, R.S. Braverman, J.F. Rooney, R. Giller, M.J. Levin, Pharmacokinetics and safety of intravenous cidofovir for life-threatening viral infections in pediatric hematopoietic stem cell transplant recipients, Antimicrob. Agents Chemother. 59 (2015) 3718–3725. https://doi.org/10.1128/AAC.04348-14.

[57] D.F. Florescu, M.A. Keck, Development of CMX001 (Brincidofovir) for the treatment of serious diseases or conditions caused by dsDNA viruses, Expert Rev. Anti. Infect. Ther. 12 (2014) 1171–1178. https://doi.org/10.1586/14787210.2014.948847.

[58] T.K. Tippin, M.E. Morrison, T.M. Brundage, H. Momméja-Marin, Brincidofovir is not a substrate for the human organic anion transporter 1: A mechanistic explanation for the lack of nephrotoxicity observed in clinical studies, Ther. Drug Monit. 38 (2016) 777–786. https://doi.org/10.1097/FTD.0000000000000353.

[59] V.K.P. and D.M.C. Claire J Detweiler, Sarah B Mueller, Anthony D Sung, Jennifer L Saullo, Brincidofovir (CMX001) Toxicity Associated with Epithelial Apoptosis and Crypt Drop Out in a Hematopoietic Cell Transplant Patient: Challenges in Distinguishing Drug Toxicity from GVHD Claire, HHS Public Access. 40 (2018) e364–e368.

[60] S. Voigt, J. Hofmann, A. Edelmann, A. Sauerbrei, J.S. Kühl, Brincidofovir clearance of acyclovir-resistant herpes simplex virus-1 and adenovirus infection after stem cell transplantation, Transpl. Infect. Dis. 18 (2016) 791–794. https://doi.org/10.1111/tid.12582.

[61] S. Chen, X. Tian, Vaccine development for human mastadenovirus, J. Thorac. Dis. 10 (2018) S2280–S2294. https://doi.org/10.21037/jtd.2018.03.168.

[62] P. Martínez-Aguado, A. Serna-Gallego, J.A. Marrugal-Lorenzo, I. Gómez-Marín, J. Sánchez-Céspedes, Antiadenovirus drug discovery: potential targets and evaluation methodologies, Drug Discov. Today. 20 (2015) 1235–1242. https://doi.org/10.1016/j.drudis.2015.07.007.

[63] C.C. Colpitts, L.M. Schang, A Small Molecule Inhibits Virion Attachment to Heparan Sulfate- or Sialic Acid-Containing Glycans, J. Virol. 88 (2014) 7806–7817. https://doi.org/10.1128/jvi.00896-14.

[64] R. Ferrari, D. Gou, G. Jawdekar, S.A. Johnson, M. Nava, T. Su, A.F. Yousef, N.R. Zemke, M. Pellegrini, S.K. Kurdistani, A.J. Berk, Adenovirus small E1A employs the lysine acetylases p300/CBP and tumor suppressor RB to repress select host genes and promote productive virus infection, Cell Host Microbe. 16 (2014) 663–676. https://doi.org/10.1016/j.chom.2014.10.004.

[65] R.J.P. Bratati Saha, Histone Deacetylase Inhibitor Suberoylanilide Hydroxamic Acid Suppresses Human Adenovirus Gene Expression and Replication, J. Virol. 93 (2019) 1–18.

[66] M.C. Patel, K.A. Shirey, L.M. Pletneva, M.S. Boukhvalova, A. Garzino-Demo, S.N. Vogel,

J.C.G. Blanco, Novel drugs targeting Toll-like receptors for antiviral therapy, Future Virol. 9 (2014) 811–829. https://doi.org/10.2217/fvl.14.70.

[67] X. Wang, Q. Zhang, Z. Zhou, M. Liu, Y. Chen, J. Li, L. Xu, J. Guo, Q. Li, J. Yang, S. Wang, Retinoic acid receptor β a potential therapeutic target in the inhibition of adenovirus replication, Antiviral Res. 152 (2018) 84–93. https://doi.org/10.1016/j.antiviral.2018.01.014.

[68] N. Höti, W. Chowdhury, J.T. Hsieh, M.D. Sachs, S.E. Lupold, R. Rodriguez, Valproic Acid, a Histone Deacetylase Inhibitor, Is an Antagonist for Oncolytic Adenoviral Gene Therapy, Mol. Ther. 14 (2006) 768–778. https://doi.org/10.1016/j.ymthe.2006.07.009.

[69] F. Grosso, P. Stoilov, C. Lingwood, M. Brown, A. Cochrane, Suppression of Adenovirus Replication by Cardiotonic Steroids, J. Virol. 91 (2017) 1–16. https://doi.org/10.1128/jvi.01623-16.

[70] J.A. Marrugal-Lorenzo, A. Serna-Gallego, L. González-González, M. Buñuales, J. Poutou, J. Pachón, M. Gonzalez-Aparicio, R. Hernandez-Alcoceba, J. Sánchez-Céspedes, Inhibition of adenovirus infection by mifepristone, Antiviral Res. 159 (2018) 77–83. https://doi.org/10.1016/j.antiviral.2018.09.011.

[71] J.A. Marrugal-Lorenzo, A. Serna-Gallego, J. Berastegui-Cabrera, J. Pachón, J. Sánchez-Céspedes, Repositioning salicylanilide anthelmintic drugs to treat adenovirus infections, Sci. Rep. 9 (2019) 1–10. https://doi.org/10.1038/s41598-018-37290-3.

[72] L. Naesens, L. Lenaerts, G. Andrei, R. Snoeck, D. Van Beers, A. Holý, J. Balzarini, E. De Clercq, Antiadenovirus activities of several classes of nucleoside and nucleotide analogues, Antimicrob. Agents Chemother. 49 (2005) 1010–1016. https://doi.org/10.1128/AAC.49.3.1010-1016.2005.

[73] C.B. Hartline, K.M. Gustin, W.B. Wan, S.L. Ciesla, J.R. Beadle, K.Y. Hostetler, E.R. Kern, Ether Lipid-Ester Prodrugs of Acyclic Nucleoside Phosphonates: Activity against Adenovirus Replication In Vitro, J. Infect. Dis. 191 (2005) 396–399. https://doi.org/10.1086/426831.

[74] Y. Kumaki, J.D. Woolcott, J.P. Roth, T.Z. Mclean, D.F. Smee, D.L. Barnard, N. Valiaeva, J.R. Beadle, K.Y. Hostetler, Inhibition of adenovirus serotype 14 infection by octadecyloxyethyl esters of (S)-[(3-hydroxy-2-phosphonomethoxy)propyl]- nucleosides in vitro, Antiviral Res. 158 (2018) 122–126. https://doi.org/10.1016/j.antiviral.2018.08.004.

[75] I. Alexeeva, L. Nosach, L. Palchykovska, L. Usenko, O. Povnitsa, Synthesis and Comparative Study of Anti-Adenoviral Activity of 6-Azacytidine and Its Analogues, Nucleosides, Nucleotides and Nucleic Acids. 34 (2015) 565–578. https://doi.org/10.1080/15257770.2015.1034363.

[76] N.A. Nikitenko, E.S. Gureeva, A.A. Ozerov, A.I. Tukhvatulin, F.M. Izhaeva, V.S. Prassolov, P.G. Deryabin, M.S. Novikov, D.Y. Logunov, 1-(4-Phenoxybenzyl) 5-aminouracil derivatives and their analogues - novel inhibitors of human adenovirus replication, Acta Naturae. 10 (2018) 58–64. https://doi.org/10.32607/20758251-2018-10-2-58-64.

[77] C.T. Öberg, M. Strand, E.K. Andersson, K. Edlund, N.P.N. Tran, Y.F. Mei, G. Wadell, M. Elofsson, Synthesis, biological evaluation, and structure-activity relationships of 2-[2-(benzoylamino)benzoylamino]benzoic acid analogues as inhibitors of adenovirus replication, J. Med. Chem. 55 (2012) 3170–3181. https://doi.org/10.1021/jm201636v.

[78] J. Xu, J. Berastegui-Cabrera, H. Chen, J. Pachón, J. Zhou, J. Sánchez-Céspedes, Structure-Activity Relationship Studies on Diversified Salicylamide Derivatives as Potent Inhibitors of Human Adenovirus Infection, J. Med. Chem. 63 (2020) 3142–3160. https://doi.org/10.1021/acs.jmedchem.9b01950.

[79] D. Zhang, Qian; Xiang, Dehu; Zhang, Ling; Wang, Xia; Li, Application of aromatic ester compounds in preparing drugs for resisting Adenovirus-7 (ADV-7), CN 2017-11446779, 2018. https://scifinder--cas--org.us.debiblio.com/scifinder/view/scifinder/scifinderExplore.jsf.

[80] N.A. Hamdy, W.M. El-Senousy, Synthesis and antiviral evalution of some novel pyrazoles and pyrazolo[3,4-d]pyridazines bearing 5,6,7,8-tetrahydronaphthalene, Acta Pol. Pharm. - Drug Res. 70 (2013) 99–110.

[81] A. Mac Sweeney, P. Grosche, D. Ellis, K. Combrink, P. Erbel, N. Hughes, F. Sirockin, S. Melkko, A. Bernardi, P. Ramage, N. Jarousse, E. Altmann, Discovery and structure-based optimization of adenain inhibitors, ACS Med. Chem. Lett. 5 (2014) 937–941. https://doi.org/10.1021/ml500224t.

[82] D. Kang, H. Zhang, Z. Zhou, B. Huang, L. Naesens, P. Zhan, X. Liu, First discovery of novel 3-hydroxy-quinazoline-2,4(1H,3H)-diones as specific anti-vaccinia and adenovirus agents via 'privileged scaffold' refining approach, Bioorganic Med. Chem. Lett. 26 (2016) 5182–5186. https://doi.org/10.1016/j.bmcl.2016.09.071.

[83] J. Sanchez-Cespedes, C.L. Moyer, L.R. Whitby, D.L. Boger, G.R. Nemerow, Inhibition of adenovirus replication by a trisubstituted piperazin-2-one derivative, Antiviral Res. 108 (2014) 65–73. https://doi.org/10.1016/j.antiviral.2014.05.010.

[84] J. Sánchez-Céspedes, P. Martínez-Aguado, M. Vega-Holm, A. Serna-Gallego, J.I. Candela, J.A. Marrugal-Lorenzo, J. Pachón, F. Iglesias-Guerra, J.M. Vega-Pérez, New 4-Acyl-1-phenylaminocarbonyl-2-phenylpiperazine Derivatives as Potential Inhibitors of Adenovirus Infection. Synthesis, Biological Evaluation, and Structure-activity Relationships, J. Med. Chem. 59 (2016) 5432–5448. https://doi.org/10.1021/acs.jmedchem.6b00300.

[85] S. Sánchez Céspedes, Javier; Pachón Ibáñez , María Eugenia; Pachón Díaz, Jerónimo; Martínez Aguado, Pablo; Cebrero Cangueiro, Tania; Vega Pérez, José Manuel; Iglesias Guerra, Fernando; Vega Holm, Margarita; Candela Lena, Ignacio; Mazzotta, Piperazine Derivatives as Antiviral Agents with Increased Therapeutic Activity, US 2019 / 0308956, 2019. https://patents.google.com/patent/US20190308956A1/en.

[86] Q. Hong, R.K. Bakshi, J. Dellureficio, S. He, Z. Ye, P.H. Dobbelaar, I.K. Sebhat, L. Guo, J. Liu, T. Jian, R. Tang, R.N. Kalyani, T. MacNeil, A. Vongs, C.I. Rosenblum, D.H. Weinberg, Q. Peng, C. Tamvakopoulos, R.R. Miller, R.A. Stearns, D. Cashen, W.J. Martin, A.S. Chen, J.M. Metzger, H.Y. Chen, A.M. Strack, T.M. Fong, E. MacLntyre, L.H.T. Van Der Ploeg, M.J. Wyvratt, R.P. Nargund, Optimization of privileged structures for selective and potent melanocortin subtype-4 receptor ligands, Bioorganic Med. Chem. Lett. 20 (2010) 4483–4486. https://doi.org/10.1016/j.bmcl.2010.06.038.

[87] B. Chardonnet, Yvette; Gazzolo, Louis; Pogo, Effect of a-Amanitin on Adenovirus 5 Multiplication, Virology. 48 (1972) 300–304.

[88] H. Matthews, J. Deakin, M. Rajab, M. Idris-Usman, N.J. Nirmalan, Investigating antimalarial drug interactions of emetine dihydrochloride hydrate using CalcuSyn-based interactivity calculations, PLoS One. 12 (2017) 1–19. https://doi.org/10.1371/journal.pone.0173303.

[89] H. Kubinyi, Drug research:myths, hype and reality, Nat. Rev. Drug Discov. Vol. 2 (2003) 665–668.

[90] Z. Lv, W. He, X. Tian, J. Kang, Y. Liu, Y. Peng, L. Zheng, Q. Wang, W. Yu, J. Chang, Design, synthesis, and biological evaluation of new N 4-Substituted 2′-deoxy-2′-fluoro-4′-azido cytidine derivatives as potent anti-HBV agents, Eur. J. Med. Chem. 101 (2015) 103–110. https://doi.org/10.1016/j.ejmech.2015.06.030.

[91] A. Daina, O. Michielin, V. Zoete, SwissADME: A free web tool to evaluate pharmacokinetics, drug-likeness and medicinal chemistry friendliness of small molecules, Sci. Rep. 7 (2017) 1–13. https://doi.org/10.1038/srep42717.

[92] A. Daina, V. Zoete, A BOILED-Egg To Predict Gastrointestinal Absorption and Brain Penetration of Small Molecules, ChemMedChem. (2016) 1117–1121. https://doi.org/10.1002/cmdc.201600182.

[93] S. Mazzotta, J.A. Marrugal-Lorenzo, M. Vega-Holm, A. Serna-Gallego, J. Álvarez-Vidal, J.

Berastegui-Cabrera, J. Pérez del Palacio, C. Díaz, F. Aiello, J. Pachón, F. Iglesias-Guerra, J.M. Vega-Pérez, J. Sánchez-Céspedes, Optimization of piperazine-derived ureas privileged structures for effective antiadenovirus agents, Eur. J. Med. Chem. 185 (2020). https://doi.org/10.1016/j.ejmech.2019.111840.

[94] S. Freeman, J.M. Gardiner, Acyclic Nucleosides as Antiviral Compounds, Appl. Biochem. Biotechnol. - Part B Mol. Biotechnol. 5 (1996) 125–137. https://doi.org/10.1007/BF02789061.

[95] F. Tramutola, M.F. Armentano, F. Berti, L. Chiummiento, P. Lupattelli, R. D'Orsi, R. Miglionico, L. Milella, F. Bisaccia, M. Funicello, New heteroaryl carbamates: Synthesis and biological screening in vitro and in mammalian cells of wild-type and mutant HIV-protease inhibitors, Bioorganic Med. Chem. 27 (2019) 1863–1870. https://doi.org/10.1016/j.bmc.2019.03.041.

[96] M. Bassetto, S. Ferla, P. Leyssen, J. Neyts, M.M. Yerukhimovich, D.N. Frick, R. O'Donnell, A. Brancale, Novel symmetrical phenylenediamines as potential anti-hepatitis C virus agents, Antivir. Chem. Chemother. 24 (2015) 155–160. https://doi.org/10.1177/2040206616676353.

[97] J.L. Romine, D.R. St. Laurent, J.E. Leet, S.W. Martin, M.H. Serrano-Wu, F. Yang, M. Gao, D.R. O'Boyle, J.A. Lemm, J.H. Sun, P.T. Nower, X. Huang, M.S. Deshpande, N.A. Meanwell, L.B. Snyder, Inhibitors of HCV NS5A: From iminothiazolidinones to symmetrical stilbenes, ACS Med. Chem. Lett. 2 (2011) 224–229. https://doi.org/10.1021/ml1002647.

[98] M. Zając, I. Muszalska, A. Sobczak, A. Dadej, S. Tomczak, A. Jelińska, Hepatitis C – New drugs and treatment prospects, Eur. J. Med. Chem. 165 (2019) 225–249. https://doi.org/10.1016/j.ejmech.2019.01.025.

[99] M. Ahmed, A. Pal, M. Houghton, K. Barakat, A comprehensive computational analysis for the binding modes of Hepatitis C virus NS5A inhibitors: The question of symmetry, ACS Infect. Dis. 2 (2016) 872–881. https://doi.org/10.1021/acsinfecdis.6b00113.

[100] E. Rivero-Buceta, P. Carrero, E.G. Doyagüez, A. Madrona, E. Quesada, M.J. Camarasa, M.J. Peréz-Pérez, P. Leyssen, J. Paeshuyse, J. Balzarini, J. Neyts, A. San-Félix, Linear and branched alkyl-esters and amides of gallic acid and other (mono-, di- and tri-) hydroxy benzoyl derivatives as promising anti-HCV inhibitors, Eur. J. Med. Chem. 92 (2015) 656–671. https://doi.org/10.1016/j.ejmech.2015.01.033.

[101] S. Saul, S.Y. Pu, W.J. Zuercher, S. Einav, C.R.M. Asquith, Potent antiviral activity of novel multi-substituted 4-anilinoquin(az)olines, Bioorganic Med. Chem. Lett. 30 (2020) 127284. https://doi.org/10.1016/j.bmcl.2020.127284.

[102] Z. Zhao, H. Song, J. Xie, T. Liu, X. Zhao, X. Chen, X. He, S. Wu, Y. Zhang, X. Zheng, Research progress in the biological activities of 3,4,5-trimethoxycinnamic acid (TMCA) derivatives, Eur. J. Med. Chem. 173 (2019) 213–227. https://doi.org/10.1016/j.ejmech.2019.04.009.

[103] M.A. Brimble, C. Brocke, Efficient synthesis of the azabicyclo[3.3.1]nonane ring system in the alkaloid methyllycaconitine using bis(alkoxymethyl)alkylamines as aminoalkylating agents in a double Mannich reaction, European J. Org. Chem. (2005) 2385–2396. https://doi.org/10.1002/ejoc.200500003.

[104] Ö. Demir-Ordu, H. Şimşir, K. Alper, Synthesis of bis[N-(p-aryl)-carbamoyloxy]alkanes as new low-molecular weight organogelators, Tetrahedron. 71 (2015) 1529–1539. https://doi.org/10.1016/j.tet.2015.01.042.

[105] B.M. Minrovic, D. Jung, R.J. Melander, C. Melander, New Class of Adjuvants Enables Lower Dosing of Colistin Against Acinetobacter baumannii, ACS Infect. Dis. 4 (2018) 1368–1376. https://doi.org/10.1021/acsinfecdis.8b00103.

[106] F. Morfin, S. Dupuis-Girod, S. Mundweiler, D. Falcon, D. Carrington, P. Sedlacek, M. Bierings, P. Cetkovsky, A.C.M. Kroes, M.J.D. Van Tol, D. Thouvenot, In vitro susceptibility of adenovirus to antiviral drugs is species-dependent, Antivir. Ther. 10 (2005) 225–229.

[107] M. Krečmerová, R. Pohl, M. Masojídková, J. Balzarini, R. Snoeck, G. Andrei, N4-Acyl derivatives as lipophilic prodrugs of cidofovir and its 5-azacytosine analogue, (S)-HPMP-5-azaC: Chemistry and antiviral activity, Bioorganic Med. Chem. 22 (2014) 2896–2906. https://doi.org/10.1016/j.bmc.2014.03.031.

[108] L. Chiummiento, M. Funicello, P. Lupattelli, F. Tramutola, F. Berti, F. Marino-Merlo, Synthesis and biological evaluation of novel small non-peptidic HIV-1 PIs: The benzothiophene ring as an effective moiety, Bioorganic Med. Chem. Lett. 22 (2012) 2948–2950. https://doi.org/10.1016/j.bmcl.2012.02.046.

[109] J.K. Sahu, S. Ganguly, A. Kaushik, Triazoles: A valuable insight into recent developments and biological activities, Chin. J. Nat. Med. 11 (2013) 456–465. https://doi.org/10.1016/S1875-5364(13)60084-9.

[110] A. Lauria, R. Delisi, F. Mingoia, A. Terenzi, A. Martorana, G. Barone, A.M. Almerico, 1,2,3-Triazole in Heterocyclic Compounds, Endowed With Biological Activity, Through 1,3-Dipolar Cycloadditions, European J. Org. Chem. 2014 (2014) 3289–3306. https://doi.org/10.1002/ejoc.201301695.

[111] E. Tatar, G. Küçükgüzel, S. Karakuş, E. de Clercq, G. Andrei, R. Snoeck, C. Pannecouque, S. Öktem Okullu, N. Ünübol, T. Kocagöz, S. Kalayci, F. Şahİn, İ. Küçükgüzel, Synthesis and biological evaluation of some new 1,3,4-thiadiazole and 1,2,4-triazole derivatives from L-methionine as antituberculosis and antiviral agents, Marmara Pharm. J. 19 (2015) 88–102. https://doi.org/10.12991/mpj.2015199639.

[112] M. Lukáč, D. Hocková, D.T. Keough, L.W. Guddat, Z. Janeba, Novel nucleotide analogues bearing (1H-1,2,3-triazol-4-yl)phosphonic acid moiety as inhibitors of Plasmodium and human 6-oxopurine phosphoribosyltransferases, Tetrahedron. 73 (2017) 692–702. https://doi.org/10.1016/j.tet.2016.12.046.

[113] I.E. Głowacka, J. Balzarini, A.E. Wróblewski, The synthesis, antiviral, cytostatic and cytotoxic evaluation of a new series of acyclonucleotide analogues with a 1,2,3-triazole linker, Eur. J. Med. Chem. 70 (2013) 703–722. https://doi.org/10.1016/j.ejmech.2013.10.057.

[114] S.G. Agalave, S.R. Maujan, V.S. Pore, Click chemistry: 1,2,3-triazoles as pharmacophores, Chem. - An Asian J. 6 (2011) 2696–2718. https://doi.org/10.1002/asia.201100432.

[115] L. Liang, D. Astruc, The copper(I)-catalyzed alkyne-azide cycloaddition (CuAAC) “click” reaction and its applications. An overview, Coord. Chem. Rev. 255 (2011) 2933–2945. https://doi.org/10.1016/j.ccr.2011.06.028.

[116] L. Zhu, C.J. Brassard, X. Zhang, P.M. Guha, R.J. Clark, On the Mechanism of Copper(I)-Catalyzed Azide–Alkyne Cycloaddition, Chem. Rec. (2016) 1501–1517. https://doi.org/10.1002/tcr.201600002.

[117] Y.C. Duan, Y.C. Ma, E. Zhang, X.J. Shi, M.M. Wang, X.W. Ye, H.M. Liu, Design and synthesis of novel 1,2,3-triazole-dithiocarbamate hybrids as potential anticancer agents, Eur. J. Med. Chem. 62 (2013) 11–19. https://doi.org/10.1016/j.ejmech.2012.12.046.

[118] Lorente Guarnido collaborated in the preparation of this compound to be employed as antibacterial agent. Degree Thesis: “Ureas derivadas de 2-amino-1,3-propanodiol y 1,3-diamino-2-propanol con potencial actividad antibacteriana. Síntesis y caracterización estructural” (2017). Supervisors: J.M. Vega Pérez and M. Vega Holm. Laboratory supervisor: S. Mazzotta.

[119] G. Molina Ríos collaborated in the preparation of these compounds for their evaluation as antibacterial agents. Degree Thesis: “Nuevos compuestos derivados del 3-amino- 1,2-propanodiol con actividad contra Acinetobacter baumannii resistente a Colistina. Diseño, síntesis y evaluación in Vitro” (2016). Supervisors: J.M. Vega Pérez and M. Vega Holm. Laboratory supervisor: S. Mazzotta.

[120] C. Fehr, Diastereoface-selective epoxidations: Dependency on the reagent electrophilicity,

Angew. Chemie - Int. Ed. 37 (1998) 2407–2409. https://doi.org/10.1002/(SICI)1521-3773(19980918)37:17<2407::AID-ANIE2407>3.0.CO;2-W.
[121] B. Zhao, Z. Gao, Y. Zheng, C. Gao, Scalable Synthesis of Positively Charged Sequence-Defined Functional Polymers, J. Am. Chem. Soc. (2019) 1–52. https://doi.org/10.1021/jacs.9b00172.
[122] E.W. Sugandhi, J.O. Falkinham, R.D. Gandour, Synthesis and antimicrobial activity of symmetrical two-tailed dendritic tricarboxylato amphiphiles, Bioorganic Med. Chem. 15 (2007) 3842–3853. https://doi.org/10.1016/j.bmc.2007.03.017.
[123] J. Nieschalk, S. Laboratories, S. Road, A short synthesis of (1S,2R)- and (1R,2R)-[1-ZH]-glycerols, 8 (1997) 2325–2330.
[124] M. Martínez-Bailén, A.T. Carmona, E. Moreno-Clavijo, I. Robina, D. Ide, A. Kato, A.J. Moreno-Vargas, Tuning of β-glucosidase and α-galactosidase inhibition by generation and in situ screening of a library of pyrrolidine-triazole hybrid molecules, Eur. J. Med. Chem. 138 (2017) 532–542. https://doi.org/10.1016/j.ejmech.2017.06.055.
[125] L. Liu, C. Li, S. Cochran, S. Jimmink, V. Ferro, Synthesis of a Heparan Sulfate Mimetic Library Targeting FGF and VEGF via Click Chemistry on a Monosaccharide Template, ChemMedChem. 7 (2012) 1267–1275. https://doi.org/10.1002/cmdc.201200151.
[126] E.K. Nguyen, G.R. Nemerow, J.G. Smith, Direct Evidence from Single-Cell Analysis that Human α-Defensins Block Adenovirus Uncoating To Neutralize Infection, J. Virol. 84 (2010) 4041–4049. https://doi.org/10.1128/jvi.02471-09.
[127] H.Y. Cheng, C.C. Lin, T.C. Lin, Antiherpes simplex virus type 2 activity of casuarinin from the bark of Terminalia arjuna Linn., Antiviral Res. 55 (2002) 447–455. https://doi.org/10.1016/S0166-3542(02)00077-3.
[128] C.A. Schneider, W.S. Rasband, K.W. Eliceiri, NIH Image to ImageJ: 25 years of image analysis, Nat. Methods. 9 (2012) 671–675. https://doi.org/10.1038/nmeth.2089.
[129] H.M. L. J. Reed, A Simple Method Of Estimating Fifty Per Cent Endpoints, Am. J. Hyg. 27 (1938) 546–558. https://doi.org/10.7723/antiochreview.72.3.0546.
[130] A.A. Rivera, M. Wang, K. Suzuki, T.G. Uil, V. Krasnykh, D.T. Curiel, D.M. Nettelbeck, Mode of transgene expression after fusion to early or late viral genes of a conditionally replicating adenovirus via an optimized internal ribosome entry site in vitro and in vivo, Virology. 320 (2004) 121–134. https://doi.org/10.1016/j.virol.2003.11.028.
[131] W. Everaerts, B. Nilius, G. Owsianik, The vanilloid transient receptor potential channel TRPV4: From structure to disease, Prog. Biophys. Mol. Biol. 103 (2010) 2–17. https://doi.org/10.1016/j.pbiomolbio.2009.10.002.
[132] C.D. Benham, J.B. Davis, A.D. Randall, Vanilloid and TRP channels: A family of lipid-gated cation channels, Neuropharmacology. 42 (2002) 873–888. https://doi.org/10.1016/S0028-3908(02)00047-3.
[133] B. Nilius, R. Vennekens, G. Owsianik, Vanilloid Transient Receptor Potential Cation Channels: An Overview, Curr. Pharm. Des. 14 (2008) 18–31. https://doi.org/10.2174/138161208783330763.
[134] S.G. Sedgwick, S.J. Smerdon, The ankyrin repeat: A diversity of interactions on a common structural framework, Trends Biochem. Sci. 24 (1999) 311–316. https://doi.org/10.1016/S0968-0004(99)01426-7.
[135] R. Gaudet, A primer on ankyrin repeat function in TRP channels and beyond, Mol. Biosyst. 4 (2008) 372–379. https://doi.org/10.1039/b801481g.
[136] M.P. Cuajungco, C. Grimm, K. Oshima, D. D'Hoedt, B. Nilius, A.R. Mensenkamp, R.J.M. Bindels, M. Plomann, S. Heller, PACSINs bind to the TRPV4 cation channel: PACSIN 3 modulates the subcellular localization of TRPV4, J. Biol. Chem. 281 (2006) 18753–18762. https://doi.org/10.1074/jbc.M602452200.

[137] Z. Deng, N. Paknejad, G. Maksaev, M. Sala-Rabanal, C.G. Nichols, R.K. Hite, P. Yuan, Cryo-EM and X-ray structures of TRPV4 reveal insight into ion permeation and gating mechanisms, Nat. Struct. Mol. Biol. 25 (2018) 252–260. https://doi.org/10.1038/s41594-018-0037-5.
[138] A. Garcia-Elias, I.M. Lorenzo, R. Vicente, M.A. Valverde, IP3 receptor binds to and sensitizes TRPV4 channel to osmotic stimuli via a calmodulin-binding site, J. Biol. Chem. 283 (2008) 31284–31288. https://doi.org/10.1074/jbc.C800184200.
[139] H. Kumar, S.H. Lee, K.T. Kim, X. Zeng, I. Han, TRPV4: a Sensor for Homeostasis and Pathological Events in the CNS, Mol. Neurobiol. 55 (2018) 8695–8708. https://doi.org/10.1007/s12035-018-0998-8.
[140] R. Strotmann, G. Schultz, T.D. Plant, Ca2+-dependent potentiation of the nonselective cation channel TRPV4 is mediated by a C-terminal calmodulin binding site, J. Biol. Chem. 278 (2003) 26541–26549. https://doi.org/10.1074/jbc.M302590200.
[141] F. Xu, E. Satoh, T. Iijima, Protein kinase C-mediated Ca 2+ entry in HEK 293 cells transiently expressing human TRPV4, Br. J. Pharmacol. 140 (2003) 413–421. https://doi.org/10.1038/sj.bjp.0705443.
[142] X. Gao, L. Wu, R.G. O'Neil, Temperature-modulated diversity of TRPV4 channel gating: Activation by physical stresses and phorbol ester derivatives through protein kinase C-dependent and -independent pathways, J. Biol. Chem. 278 (2003) 27129–27137. https://doi.org/10.1074/jbc.M302517200.
[143] W.G. Darby, M.S. Grace, S. Baratchi, P. McIntyre, Modulation of TRPV4 by diverse mechanisms, Int. J. Biochem. Cell Biol. 78 (2016) 217–228. https://doi.org/10.1016/j.biocel.2016.07.012.
[144] W. Tian, M. Salanova, H. Xu, J.N. Lindsley, T.T. Oyama, S. Anderson, S. Bachmann, D.M. Cohen, Renal expression of osmotically responsive cation channel TRPV4 is restricted to water-impermeant nephron segments, Am. J. Physiol. - Ren. Physiol. 287 (2004) 17–24. https://doi.org/10.1152/ajprenal.00397.2003.
[145] T. Yamada, S. Ugawa, T. Ueda, Y. Ishida, K. Kajita, S. Shimada, Differential localizations of the transient receptor potential channels TRPV4 and TRPV1 in the mouse urinary bladder, J. Histochem. Cytochem. 57 (2009) 277–287. https://doi.org/10.1369/jhc.2008.951962.
[146] A.D. Güler, M.C. Hyosang Lee, Tohko Iida, Isao Shimizu, Makoto Tominaga, Heat-Evoked Activation of the Ion Channel, TRPV4, J. Neurosci. 22 (2002) 6408–6414. https://doi.org/10.1016/S0003-2670(01)85240-5.
[147] J.Z. Bai, J. Lipski, Involvement of TRPV4 channels in Aβ40-induced hippocampal cell death and astrocytic Ca2+ signalling, Neurotoxicology. 41 (2014) 64–72. https://doi.org/10.1016/j.neuro.2014.01.001.
[148] N. Alessandri-Haber, J.J. Yeh, A.E. Boyd, C.A. Parada, X. Chen, D.B. Reichling, J.D. Levine, Hypotonicity induces TRPV4-mediated nociception in rat, Neuron. 39 (2003) 497–511. https://doi.org/10.1016/S0896-6273(03)00462-8.
[149] J. Yin, W.M. Kuebler, Mechanotransduction by TRP channels: General concepts and specific role in the vasculature, Cell Biochem. Biophys. 56 (2010) 1–18. https://doi.org/10.1007/s12013-009-9067-2.
[150] F. Vincent, M. A.J. Duncton, TRPV4 Agonists and Antagonists, Curr. Top. Med. Chem. 11 (2011) 2216–2226. https://doi.org/10.2174/156802611796904861.
[151] P.L. Smith, K.N. Maloney, R.G. Pothen, J. Clardy, D.E. Clapham, Bisandrographolide from Andrographis paniculata activates TRPV4 channels, J. Biol. Chem. 281 (2006) 29897–29904. https://doi.org/10.1074/jbc.M605394200.
[152] T.K. Klausen, A. Pagani, A. Minassi, A. Ech-Chahad, J. Prenen, G. Owsianik, E.K. Hoffmann, S.F. Pedersen, G. Appendino, B. Nilius, Modulation of the transient receptor potential vanilloid channel TRPV4 by 4α-phorbol esters: A structure-activity study, J. Med. Chem. 52

(2009) 2933–2939. https://doi.org/10.1021/jm9001007.
[153] K.S. Thorneloe, A.C. Sulpizio, Z. Lin, D.J. Figueroa, A.K. Clouse, G.P. McCafferty, T.P. Chendrimada, E.S.R. Lashinger, E. Gordon, L. Evans, B.A. Misajet, D.J. DeMarini, J.H. Nation, L.N. Casillas, R.W. Marquis, B.J. Votta, S.A. Sheardown, X. Xu, D.P. Brooks, N.J. Laping, T.D. Westfall, GSK1016790A, a Novel and Potent TRPV4 Channel Agonist Induces Urinary Bladder Contraction and Hyperactivity: Part I, J. Pharmacol. Exp. Ther. 326 (2008) 432–442. https://doi.org/10.1124/jpet.108.139295.
[154] R.N. Willette, W. Bao, S. Nerurkar, T.I. Yue, C.P. Doe, G. Stankus, G.H. Turner, H. Ju, H. Thomas, C.E. Fishman, A. Sulpizio, D.J. Behm, S. Hoffman, Z. Lin, I. Lozinskaya, L.N. Casillas, M. Lin, R.E.L. Trout, B.J. Votta, K. Thorneloe, E.S.R. Lashinger, D.J. Figueroa, R. Marquis, X. Xu, Systemic activation of the transient receptor potential vanilloid subtype 4 channel causes endothelial failure and circulatory collapse: Part 2, J. Pharmacol. Exp. Ther. 326 (2008) 443–452. https://doi.org/10.1124/jpet.107.134551.
[155] M. Atobe, T. Nagami, S. Muramatsu, T. Ohno, M. Kitagawa, H. Suzuki, M. Ishiguro, A. Watanabe, M. Kawanishi, Discovery of Novel Transient Receptor Potential Vanilloid 4 (TRPV4) Agonists as Regulators of Chondrogenic Differentiation: Identification of Quinazolin-4(3 H)-ones and in Vivo Studies on a Surgically Induced Rat Model of Osteoarthritis, J. Med. Chem. 62 (2019) 1468–1483. https://doi.org/10.1021/acs.jmedchem.8b01615.
[156] F.C. Dias, V.S. Alves, D.O. Matias, C.P. Figueiredo, A.L.P. Miranda, G.F. Passos, R. Costa, The selective TRPV4 channel antagonist HC-067047 attenuates mechanical allodynia in diabetic mice, Eur. J. Pharmacol. 856 (2019) 172408. https://doi.org/10.1016/j.ejphar.2019.172408.
[157] M. Cheung, W. Bao, D.J. Behm, C.A. Brooks, M.J. Bury, S.E. Dowdell, H.S. Eidam, R.M. Fox, K.B. Goodman, D.A. Holt, D. Lee, T.J. Roethke, R.N. Willette, X. Xu, G. Ye, K.S. Thorneloe, Discovery of GSK2193874: An Orally Active, Potent, and Selective Blocker of Transient Receptor Potential Vanilloid 4, ACS Med. Chem. Lett. 8 (2017) 549–554. https://doi.org/10.1021/acsmedchemlett.7b00094.
[158] M.A. Hilfiker, T.H. Hoang, J. Cornil, H.S. Eidam, D.S. Matasic, T.J. Roethke, M. Klein, K.S. Thorneloe, M. Cheung, Optimization of a novel series of TRPV4 antagonists with in vivo activity in a model of pulmonary edema, ACS Med. Chem. Lett. 4 (2013) 293–296. https://doi.org/10.1021/ml300449k.
[159] C.A. Brooks, L.S. Barton, D.J. Behm, E.J. Brnardic, M.H. Costell, D.A. Holt, L.J. Jolivette, J.M. Matthews, J.J. McAtee, B.W. McCleland, J.R. Patterson, J.E. Pero, R.A. Rivero, T.J. Roethke, R.M. Sanchez, R. Shenje, L.R. Terrell, B.G. Lawhorn, Discovery of GSK3527497: A Candidate for the Inhibition of Transient Receptor Potential Vanilloid-4 (TRPV4), J. Med. Chem. 62 (2019) 9270–9280. https://doi.org/10.1021/acs.jmedchem.9b01247.
[160] E.J. Brnardic, G. Ye, C. Brooks, C. Donatelli, L. Barton, J. McAtee, R.M. Sanchez, A. Shu, K. Erhard, L. Terrell, G. Graczyk-Millbrandt, Y. He, M.H. Costell, D.J. Behm, T. Roethke, P. Stoy, D.A. Holt, B.G. Lawhorn, Discovery of Pyrrolidine Sulfonamides as Selective and Orally Bioavailable Antagonists of Transient Receptor Potential Vanilloid-4 (TRPV4), J. Med. Chem. 61 (2018) 9738–9755. https://doi.org/10.1021/acs.jmedchem.8b01317.
[161] L.S. Premkumar, Transient receptor potential channels as targets for phytochemicals, ACS Chem. Neurosci. 5 (2014) 1117–1130. https://doi.org/10.1021/cn500094a.
[162] Z. Lin, S. Phadke, Z. Lu, S. Beyhan, M.H. Abdel Aziz, C. Reilly, E.W. Schmidt, Onydecalins, Fungal Polyketides with Anti- Histoplasma and Anti-TRP Activity, J. Nat. Prod. 81 (2018) 2605–2611. https://doi.org/10.1021/acs.jnatprod.7b01067.
[163] P. Filomena, F. Luca, H. Ian, B. Matteo, E. magboub Asma, F. Angela, G. Charles, A. Francesca, A.J. David, Naturally occurring sesquiterpene lactones and their semi-synthetic

derivatives modulate PGE2 levels by decreasing COX2 activity and expression, Heliyon. 5 (2019) e01366. https://doi.org/10.1016/j.heliyon.2019.e01366.

[164] A. Coricello, A. El-Magboub, M. Luna, A. Ferrario, I.S. Haworth, C.J. Gomer, F. Aiello, J.D. Adams, Rational drug design and synthesis of new α-Santonin derivatives as potential COX-2 inhibitors, Bioorganic Med. Chem. Lett. 28 (2018) 993–996. https://doi.org/10.1016/j.bmcl.2018.02.036.

[165] Q. Chen, K. Tang, Y. Guo, Discovery of sclareol and sclareolide as filovirus entry inhibitors, J. Asian Nat. Prod. Res. 22 (2020) 464–473. https://doi.org/10.1080/10286020.2019.1681407.

[166] T. Rosenbaum, M. Benítez-Angeles, R. Sánchez-Hernández, S.L. Morales-Lázaro, M. Hiriart, L.E. Morales-Buenrostro, F. Torres-Quiroz, Trpv4: A physio and pathophysiologically significant ion channel, Int. J. Mol. Sci. 21 (2020). https://doi.org/10.3390/ijms21113837.

[167] D. Li, S. Zhang, Z. Song, G. Wang, S. Li, Bioactivity-guided mixed synthesis accelerate the serendipity in lead optimization: Discovery of fungicidal homodrimanyl amides, Eur. J. Med. Chem. 136 (2017) 114–121. https://doi.org/10.1016/j.ejmech.2017.04.073.

[168] R.M.C. and H.C. DEET, DITERPENOIDS. XXVIIL. THE SYNTHESIS OF a-ONOCERADIENE FROM ABIENOL, Aust. J. Chem. 24 (1971) 1099–1102.

[169] T. Koga, Y. Aoki, T. Hirose, H. Nohira, Resolution of sclareolide as a key intermediate for the synthesis of Ambrox®, Tetrahedron Asymmetry. 9 (1998) 3819–3823. https://doi.org/10.1016/S0957-4166(98)00404-2.

[170] K.S. Thorneloe, A.C. Sulpizio, Z. Lin, D.J. Figueroa, A.K. Clouse, G.P. McCafferty, T.P. Chendrimada, E.S.R. Lashinger, E. Gordon, L. Evans, B.A. Misajet, D.J. DeMarini, J.H. Nation, L.N. Casillas, R.W. Marquis, B.J. Votta, S.A. Sheardown, X. Xu, D.P. Brooks, N.J. Laping, T.D. Westfall, N-((1S)-1-{[4-((2S)-2-{[(2,4-dichlorophenyl)sulfonyl]amino} -3-hydroxypropanoyl)-1-piperazinyl]carbonyl}-3-methylbutyl)-1-benzothiophene-2-carboxamide (GSK1016790A), a novel and potent transient receptor potential vanilloid 4 channel agonist induces urin, J. Pharmacol. Exp. Ther. 326 (2008) 432–442. https://doi.org/10.1124/jpet.108.139295.

LIST OF FIGURES

LIST OF SCHEMES

LIST OF TABLES